

Geostatistical Estimation of Reserves in the Abu-Tartur Phosphate Deposits Western Desert, Egypt

by

Ali Ahmed Abdul-Latif

A Thesis Presented to the

FACULTY OF THE COLLEGE OF GRADUATE STUDIES

KING FAHD UNIVERSITY OF PETROLEUM & MINERALS

DHAHRAN, SAUDI ARABIA

In Partial Fulfillment of the
Requirements for the Degree of

MASTER OF SCIENCE

In

EARTH SCIENCES

January, 1987

INFORMATION TO USERS

This manuscript has been reproduced from the microfilm master. UMI films the text directly from the original or copy submitted. Thus, some thesis and dissertation copies are in typewriter face, while others may be from any type of computer printer.

The quality of this reproduction is dependent upon the quality of the copy submitted. Broken or indistinct print, colored or poor quality illustrations and photographs, print bleedthrough, substandard margins, and improper alignment can adversely affect reproduction.

In the unlikely event that the author did not send UMI a complete manuscript and there are missing pages, these will be noted. Also, if unauthorized copyright material had to be removed, a note will indicate the deletion.

Oversize materials (e.g., maps, drawings, charts) are reproduced by sectioning the original, beginning at the upper left-hand corner and continuing from left to right in equal sections with small overlaps. Each original is also photographed in one exposure and is included in reduced form at the back of the book.

Photographs included in the original manuscript have been reproduced xerographically in this copy. Higher quality 6" x 9" black and white photographic prints are available for any photographs or illustrations appearing in this copy for an additional charge. Contact UMI directly to order.

U·M·I

University Microfilms International
A Bell & Howell Information Company
300 North Zeeb Road, Ann Arbor, MI 48106-1346 USA
313/761-4700 800/521-0600

Order Number 1355693

**Geostatistical estimation of reserves in the Abu-Tartur
phosphate deposits Western Desert, Egypt**

Abdul-Latif, Ali Ahmed, M.S.

King Fahd University of Petroleum and Minerals (Saudi Arabia), 1987

U·M·I
300 N. Zeeb Rd.
Ann Arbor, MI 48106

**GEOSTATISTICAL ESTIMATION OF RESERVES IN
THE ABU-TARTUR PHOSPHATE DEPOSITS
WESTERN DESERT, EGYPT**

**BY
ALI AHMED ABDUL-LATIF**

**A Thesis Presented to the
FACULTY OF THE COLLEGE OF GRADUATE STUDIES
KING FAHD UNIVERSITY OF PETROLEUM & MINERALS
DHAHRAN, SAUDI ARABIA**

**In Partial Fulfillment of the
Requirements for the Degree of**


**MASTER OF SCIENCE
In**

EARTH SCIENCES

JANUARY 1987

KING FAHD
UNIVERSITY OF PETROLEUM AND MINERALS
DHAHRAN, SAUDI ARABIA.

This thesis, written by Ali Ahmed Abdul-Latif under the direction of his Thesis Committee, and approved by all its members, has been presented to and accepted by the Dean, College of Graduate Studies, in partial fulfillment of the requirements for the degree of Master of Science in Earth Sciences.

 Abdul-Aziz Al-Jabir
Dean, College of Graduate Studies
Date: 15/12/1987
M. Mhamdi
Department Chairman
Dr. Mustafa A. Ukayli

THESIS COMMITTEE

Ali Sahin
Dr. Ali Sahin, Chairman

Z.R. El-Naggar
Prof. Dr. Z.R. El Naggar, Member

Saif 16/12/87
Dr. Saiful-Islam Saif, Member

بِسْمِ اللَّهِ الرَّحْمَنِ الرَّحِيمِ

In the Name of God, Most Gracious, Most Merciful

LIBRARY
KING FARD UNIVERSITY OF PETROLEUM & MINERALS
Dhahran - 31261. SAUDI ARABIA

This thesis is dedicated to my family

ACKNOWLEDGEMENTS

The present work was carried out under the supervision of Dr. Ali Sahin, Prof. Dr. Z.R. El-Naggar and Dr. S.I. Saif of the Department of Earth Sciences, KFUPM. To Dr. Sahin the thesis committee Chairman, the writer is indebted for laying out the research plan, correcting the manuscript, as well as capable advice and helpful discussions throughout all phases of the work.

Special thanks are also due to Prof. El-Naggar, suggesting the problem, obtaining the data, and for critically reading the manuscript. Also, thanks are due to Dr. S.I. Saif, for his valuable suggestions and critical reading of the manuscript.

I would also like to express my deep appreciation to both Dr. A.M. Niazy and Dr. M.A. Ukayli former and current chairmen of the Department of Earth Sciences for their encouragement and for providing the necessary facilities for research.

Both Eng. Bahi El-Deen Ahmed and Geologist Hafiz Abdeen Badwy were instrumental in providing the basic data for the present work and a special word of thanks is here extended for both of them.

The work has consumed an enormous number of computing hours, at the Data Processing Center, KFUPM, and I would like to thank all those who provided assistance in computing, particularly Mr. Amin R. Ghaleb and Mr. Abdul Salam Al-Traiki.

A word of appreciation should also be recorded here to my two colleagues Mr. S. Kamel and Mr. Abdul-Wahab Z. Ali, whose continued encouragement never failed me, to Mr. Mohammed Khalid Butt, of the Department of Electrical Engineering for typing the manuscript, and to my family, for their moral support throughout all phases of this work.

Finally, acknowledgement is due to the King Fahd University of Petroleum and Minerals for providing academic and research facilities without which this work could have never been achieved.

TABLE OF CONTENTS

	<u>Page</u>
List of Tables	ix
List of Illustrations	x
Abstract (English)	xii
Abstract (Arabic)	xiii
1. Introduction	1
1.1 General	1
1.2 Location and geological setting	3
1.3 Previous work	4
1.4 Data sets	5
2. Geology	6
2.1 Introduction	6
2.2 The Late Cretaceous–Early Paleogene Succession in Egypt	7
2.2.1 The Nubia Group	7
2.2.2 The Esna Group	9
2.2.3 Libyan Desert Group	12
2.3 Geology of Abu Tartur Area	13
2.3.1 The Sibaiya Formation	15
2.3.2 Structure of Abu Tartur Area	16
2.3.3 Mineralogy	19

	<u>Page</u>
3. Review of Classical Reserve Estimation Methods	23
3.1 Introduction	23
3.2 Average Factors and Area Methods	23
3.3 Mining Blocks Method	24
3.4 Cross-Section Methods	25
3.5 Analytical Methods	27
3.5.1 Random Stratified Grid	27
3.5.2 Polygonal Method	29
3.5.3 Triangular Method	29
3.6 Disadvantages of the Classical Methods	30
4. Data Set and Preliminary Statistical Analysis	32
4.1 Data Sets	32
4.2 Composite Files	33
4.3 Contour Maps	33
4.4 Preliminary Statistical Analysis	34
4.5 Histograms	38
4.6 Cumulative Frequency Plots	43
5. Spatial Distribution in Abu Tartur Deposit	47
5.1 Introduction	47
5.2 Critical Review of Data	47
5.3 Variograms	48

	<u>Page</u>
5.4 Estimation Variances	51
5.5 Variogram Modelling	52
5.6 Variograms for Abu Tartur Deposit	54
5.6.1 Vertical variogram for 1-m composites	56
5.6.2 Horizontal variograms	57
5.7 Summary	66
6. Global Estimation	67
6.1 Introduction	67
6.2 Description of Method	67
6.2.1 Estimation of tonnage	68
6.2.2 Estimation of phosphate content	71
6.2.3 Estimation of mean grade	73
6.3 Application to Abu Tartur Phosphate deposit	74
6.4 Final remarks	79
7. Local Estimation (Kriging)	81
7.1 Introduction	81
7.2 Block Kriging	81
7.3 Block Kriging for Abu Tartur Deposit	85
7.4 Grade-Tonnage Relationship	93
7.4.1 General	93
7.4.2 Results for Abu Tartur deposit	94
7.5 Combining Kriged Estimates	97

	<u>Page</u>
8. General Summary and Conclusions	100
References	104
Appendices	
Appendix A: An excerpt from master file	112
Appendix B: An excerpt from the composite file	113
Appendix C: Directional variograms	114
Appendix D: Results of block kriging for P_2O_5 %	115

LIST OF TABLES

	<u>Page</u>
2.1 Correlation of various lithostratigraphic subdivisions for Late Cretaceous–Early Paleogene Succession in Egypt	8
4.1 Summary of statistical parameters (Abu Tartur Phosphate deposit)	42
6.1 Variogram parameters	75
6.2 Summary of global estimation for Abu Tartur deposit	80
7.1 Grade–Tonnage relationship	95

LIST OF ILLUSTRATIONS

	<u>Page</u>
1.1 Sketch map showing phosphate occurrences in Egypt	2
2.1 Stratigraphic column in Abu Tartur area	14
2.2 Structure and contour map at the bottom of phosphate bed	18
3.1 Cross-section methods	26
3.2 Analytical methods of ore reserve estimation	28
4.1 Topographic map	35
4.2 Isopach map	36
4.3 Isograde map based on sample values	37
4.4 Frequency distribution and histogram for P_2O_5 % values	39
4.5 Frequency distribution and histogram for thickness values	40
4.6 Frequency distribution and histogram for accumulation values	41
4.7 Cumulative frequency plot for P_2O_5 %	44
4.8 Cumulative frequency plot for thickness	45
4.9 Cumulative frequency plot for accumulation	46
5.1 Behaviour of variograms near origin	50
5.2 Spherical variogram illustrating transition phenomenon	53
5.3 Direction and regularized angles	55
5.4 Abu Tartur-vertical variogram and fitted model (P_2O_5 % - 1m composites)	58
5.5 Abu Tartur-horizontal variogram and fitted model (P_2O_5 % - 1m composites)	60

	<u>Page</u>
5.6 Abu Tartur-horizontal variogram and fitted model (P_2O_5 %)	62
5.7 Abu Tartur-horizontal variogram and fitted model (thickness)	63
5.8 Abu Tartur-horizontal variogram and fitted model (accumulation)	65
6.1 400 m x 400 m square RSG fitted to Abu Tartur phosphate deposit	70
6.2 Two-dimensional F-function, $F(h/a, \ell/a)$, for spherical model	71
7.1 Results of block kriging for level 113	87
7.2 Results of block kriging (based on average P_2O_5 % values)	89
7.3 Isograde map based on block kriged estimates	90
7.4 Contour map of relative kriging standard deviation x 100	91
7.5 Contour map of kriging standard deviation	92
7.6 Grade-tonnage relationship	96

ABSTRACT

The Abu Tartur Plateau lies between the Kharga and Dakhla Oases in the Western Desert of Egypt and contains the largest phosphate deposit in the country. The phosphates are found in two main horizons within the late Campanian, Sibaiya Formation. The estimation of the reserves in the lower phosphate horizon is the main objective of this study.

The basic data for this study was derived from a drilling program conducted by the Egyptian Geological Survey and included the phosphate grade ($P_2O_5\%$) and the thickness data from 347 vertical holes drilled on a regular grid of 400m x 400m dimensions.

Preliminary statistical analysis of the data was carried out to determine the sampling distributions of the variables, $P_2O_5(\%)$, thickness (m) and accumulation (%m). These distributions are characterized by slight skews, negative for $P_2O_5\%$ and positive for both thickness and accumulation.

The results of variogram modelling indicate that spherical models can appropriately be fitted to all experimental variograms. A compound spherical model was fitted to the horizontal variogram for $P_2O_5\%$, and simple spherical models to the horizontal variograms of both thickness and accumulation.

Fitting a random stratified grid to the drill-hole intersections, the estimates for the total tonnage, the total phosphate content and the mean grade within the central part of the lower phosphate horizon have been obtained. The estimation variances associated with each estimate were derived using model variograms. The confidence intervals for the estimates at 95% confidence level are as follows: tonnage = 308.36 ± 13.56 Mt; total phosphate content = 80.05 ± 0.15 Mt; and mean grade = $26.00 \pm 0.19\%$.

The two dimensional block kriging of the deposit was carried out to obtain estimates for blocks of 400m x 400m x 1m dimensions. The kriged estimates and the corresponding relative kriging standard deviation for a total of 3752 blocks were computed. The kriging standard deviations are relatively small, indicating the reliability of the kriged estimates.

Finally, using the distribution of kriged block estimates, a grade-tonnage curve based on the selective mining units of 25m x 25m x 1m dimensions was constructed. The tonnage of phosphate corresponding to a given cut-off grade can be read off this curve.

بِسْمِ اللَّهِ الرَّحْمَنِ الرَّحِيمِ

**تقدير مخزون رواسب الفوسفات
بمنطقة أبو طرطور بالصحراء الغربية
بجمهورية مصر العربية
بإستخدام الإحصاء الجيولوجي**

موجز

يهتم هذا البحث بالتقدير الإحصائي لمخزون رواسب الفوسفات للطبقة السفلى بمنطقة هضبة أبو طرطور الواقعة جنوبي الصحراء الغربية بجمهورية مصر العربية بين الواحات الداخلة والخارجة . وقد تكونت هذه الرواسب أثناء العصر الطباشيري المتأخر (العهد الكامباني) ضمن متكون السباعية وهي تتألف من طبقتين ، أثبتت الدراسات الجيولوجية الأولية أن الطبقة السفلى منهما هي الطبقة الاقتصادية ، ويقوم هذا البحث بتقدير مخزون هذه الطبقة من الخام اعتماداً على بيانات الآبار التي تم حفرها بواسطة هيئة المساحة الجيولوجية المصرية ، وتشمل هذه البيانات كلاً من درجة تركيز الفوسفات (قو ٢ أو ٥ ٪) ، وسك الطبقة الاقتصادية بالمتر ضمن شبكة منتظمة من الآبار أبعادها ٤٠٠ متر X ٤٠٠ متر بعدد إجمالي ٣٤٧ بئراً .

وقبل تطبيق طرق الإحصاء الجيولوجي ، تم إجراء تحليل إحصائي أولي لثلاثة متغيرات هي : درجة تركيز الفوسفات (قو ٢ أو ٥ ٪) ، وسك الطبقة (متر) ، وتجمع تركيز الفوسفات (٪ متر) ، وذلك لمعرفة نوع التوزيع الإحصائي لهذه المتغيرات ، وقد دلت النتائج الأولية على أن هذه الدوال هي دوال توزيع طبيعية وليست لوغاريتمية ، مما يمكن من تقدير هذه المتغيرات بطرق الحساب العادية .

ومن ثم فقد تلى ذلك تحليل إحصائي جيولوجي لنفس هذه المتغيرات الثلاث بإستخدام دالة التباين البيانية (الفاريوجرام) لدراسة المتغيرات وإتضح أن الشكل العام للدوال الناتجة يتفق مع النموذج الكروي الذي يظهر مع أغلب الصخور الرسوبية ، هذا وقد تم تصميم نموذج كروي مركب لدالة درجة تركيز الفوسفات (قو ٢ أو ٥ ٪) المحسوبة في الاتجاه الأفقي ، أما بالنسبة لسك الطبقة السفلى (متر) وتجمع تركيز الخام بها (٪ متر) المحسوبة في نفس الاتجاه فقد صمم لكل منها نموذج كروي بسيط .

وقد تم تطبيق شبكة من المربعات (٤٠٠ متر X ٤٠٠ متر) حول مواقع الآبار في وسط الطبقة محل البحث فقط بطريقة الشبكة الطبقة العشوائية لتقدير مخزون الفوسفات بالطريقة الشاملة لكل من مخزون الفوسفات (طن) وكمية تركيز الفوسفات (طن) وكذلك متوسط درجة تركيز الفوسفات (٪) ، كذلك فقد صاحب هذه التقديرات حساب التباين التقديري لكل منها بإستخدام نتائج نماذج دوال التباين البيانية للمتغيرات ، وقد كانت حدود الثقة لتقدير المتغيرات عند ٩٥ ٪ كالآتي : -

$$\begin{aligned} \text{المخزون} &= ٣.٨٣٦ \pm ١٣.٥٦ \text{ مليون طن} \\ \text{كمية تركيز الفوسفات} &= ٨.٠٥ \pm ١٥ \text{ مليون طن} \\ \text{متوسط درجة تركيز الفوسفات} &= ٢٦.٠٠ \pm ٠.١٩ \text{ ٪} \end{aligned}$$

هذا وقد إستخدمت طريقة كريج (Kriging) وهي طريقة للتقديرات المحلية كوسيلة أخرى لتقدير مخزون الفوسفات حيث تم تقسيم المنطقة إلى كتل ذات أبعاد ٤٠٠ متر X ٤٠٠ متر X ١ متر ، وقد تم تحديد التقديرات المحلية مع معدل الإلتحاف المعياري ل ٣٧٥٢ كتلة . هذا وقد تم تقدير كل من متوسط درجة تركيز الخام ٪ ، ومعدل الإلتحاف المعياري وعدد العينات لكل من هذه الكتل ، وقد لوحظ أن معدل الإلتحاف المعياري صغير نسبياً مما يؤكد الثقة في التقديرات المحلية .

وأخيراً ، تم رسم العلاقة بين درجة تركيز الفوسفات وكميته بملايين الأطنان وذلك بإستخدام كتل ذات أبعاد ٢٥ متر X ٢٥ متر X ١ متر بإستخدام توزيع التقديرات المحلية السابق حسابها وعليه فقد وجد أن مخزون الفوسفات بمنطقة أبو طرطور هو ١٤١.٠٧ مليون طن مع متوسط درجة تركيز تبلغ ٢٦.٤ ٪ لخامس أكسيد الفوسفور .

Chapter 1

INTRODUCTION

1.1 GENERAL

The Egyptian phosphate deposits, which represent a part of the Late Cretaceous succession, were deposited in a vast interplatform trough that extended for more than 700 km, from the Red Sea coast to the west of the Dakhla Oasis (Fig. 1.1).

In the Western Desert of Egypt (Kharga-Dakhla region), the phosphate deposits were briefly described by both Zittle (1883) and Beadnell (1901a), and were treated later in more detail by several workers.

The Abu Tartur phosphate deposits, located at about 50 km west of Kharga town, were first described in 1959 by the geologists of the Egyptian Geological Survey (Hermina and others 1961). An exploration drilling program, carried out in the Abu Tartur area between the years 1968 and 1976, led to an estimate of 1000 Mt. of phosphate reserves over an area of 1200 km². This estimate was based on the sampling information derived from the 1600 m x 1600 m, 800 m x 800 m and 400 m x 400 m drilling grids, and obtained using ordinary statistical methods (El-Tahlawy and others 1977). Sofremines (Societe' Francaise d'Etudes Minieres, France) and Alusuisse (Swiss Aluminum Ltd., Switzerland) added more drill-holes and conducted an evaluation study using geostatistical method (Sofremines and Alusuisse, 1977). However, no

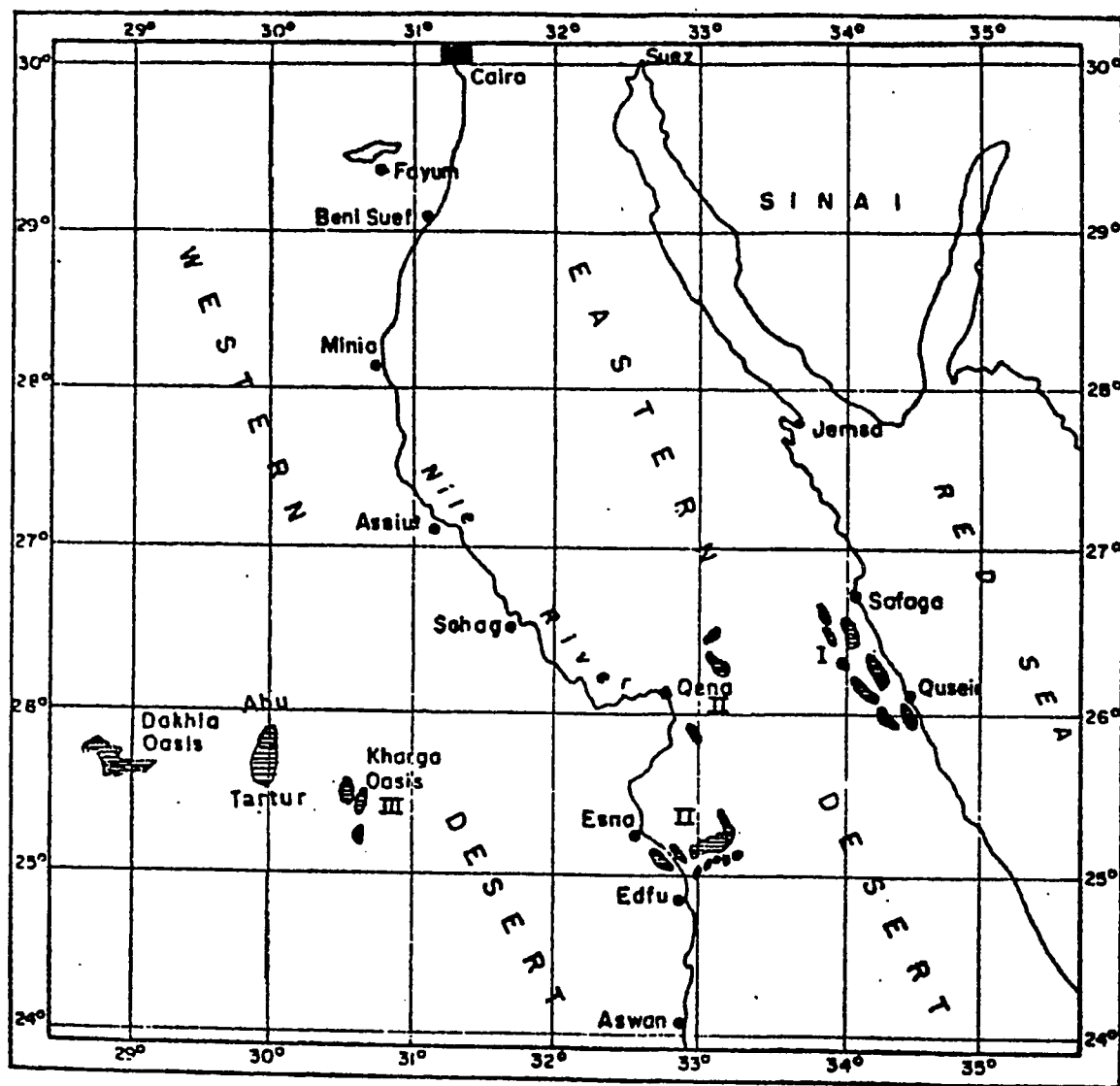


Fig. 1.1 Sketch map showing the phosphorite occurrences in Egypt.

attempt has, yet, been made for the global estimation of the reserves in the Abu Tartur area, using more elaborate geostatistical methods. Consequently, the purpose of the present work is to carry out a detailed geostatistical study for the Abu Tartur phosphate deposit. This study includes the following main steps:

- (a) Initial statistical treatment of the data.
- (b) Computation of horizontal and vertical variograms.
- (c) Fitting theoretical models to the computed variograms.
- (d) Global estimation.
- (e) Local estimation (kriging).

The global estimation involves the computation of the total tonnage, the total phosphate (P_2O_5 %) content and the mean grade estimates of reserves together with the associated estimation variances whereas the local estimation (kriging) provides estimates for the deposit on a block by block basis.

1.2 LOCATION AND GEOLOGICAL SETTING

The Abu Tartur phosphate area is located at the intersection of $25^{\circ}25'N$ latitude and $30^{\circ}04'E$ longitude. It is situated at about 50 km west of Kharga Town which is connected with Assiut city in the Nile Valley by a 225 km asphalt road (see Fig. 1.1).

The Abu Tartur plateau, which covers an area of approximately 1200 km^2 , is semi-oval in outline with an opening to the north west. The rocks of Late Cretaceous-Early Paleogene age crop out in the area. The Late

Cretaceous rocks, which include the Qusair Formation and the overlying Sibaiya Formation and Sharawna Shales, are deeply bisected in the southern edge of the plateau. The Early Paleogene rocks cover the plateau in the form of a thick limestone cap that forms the low hills and ridges in the eastern part of the area.

The Sibaiya Formation which is considered to be of Late Campanian age (El-Naggar, 1966a, 1966b, El-Naggar & Ashour, 1983) is composed of two main phosphate horizons, separated by shaly and marly intercalations. The main phosphate beds which range in thickness between 0.3 and 8.0 m are confined to the lower phosphate horizon and has an average phosphate (P_2O_5) grade of 26%. The upper horizon is of a minor economic value, with an average grade of 17% and a thickness ranging between 0.2 and 4.0 m.

1.3 PREVIOUS WORK

Beadnell (1901) was the first to point out the distribution of phosphorites in the northern part of the Kharga Oasis. He established a company to extract the deposit, but did not succeed to mine it.

In 1959, the Egyptian Geological Survey teams surveyed the area to the east of the Dakhla Oasis, including the Abu Tartur plateau (Hermina and others 1961). Since then extensive geological investigations in the area were carried out (Hermina, 1967, 1973; El-Tahlawy, 1973; Awad and Ghobrial, 1966; Ghobrial and Issawi & others, 1961).

The Egyptian Geological Survey and Mining Authority, together with the Soviet specialists, began a detailed exploratory work including drilling in 1968. The first stage of exploration, employed a grid pattern of 1600 m x 1600 m dimensions and resulted in 39 holes drilled to an average depth of 175 m. The second stage of exploration using a grid pattern of 800 m x 800 m dimensions, resulted in 45 holes drilled to an average depth of 206.1 m. The third stage exploration, using a smaller grid of 400 m x 400 m dimensions in an area of 3.2 km x 2.4 km was completed in 1976. This work was followed by further drilling program using 200 m x 200 m grid within a small area of about 3 km².

In 1976, a joint venture by the Sofremines and Allusuisse companies won a contract from the Egyptian Ministry of Industry and Mineral Wealth for the evaluation of the Abu Tartur phosphate deposits. This company prepared an overall appraisal report, based on all studies carried out between November 1977 and September 1981.

1.4 DATA SETS

The data for the present study were collected during the Summer of 1984 from the Iron and Steel Complex of the Arab Republic of Egypt. These consist of all the available information from 347 holes drilled in the Abu Tartur area, and included the X, Y and Z coordinates for each drill hole, the thickness of each penetrated phosphate bed, and the P_2O_5 % of samples taken along the holes. Further details about the collected data and their preliminary statistical analysis are given in Chapter 4.

Chapter 2

GEOLOGY

2.1 INTRODUCTION

Rocks of Late Cretaceous- Early Paleogene age in Egypt cover about one third of the total surface area of the country and have been met with in practically all wells dug in the north (El-Naggar 1970). Added to these, a dominantly arenaceous group of rock units (the Nubia Group) that covers about 15% of the total surface area, is generally assigned to the Cretaceous age, despite the fact that its rocks are almost devoid of fossils. Both the richly and the poorly fossiliferous sequences cover vast tracts in each of the four main geographical units of Egypt, namely: the Western Desert, the Nile Valley, the Eastern Desert and the Sinai Peninsula, but the poorly fossiliferous facies is mainly developed towards the south.

Many geologists studied the Late Cretaceous- Early Paleogene succession in Egypt. Table 2.1 summarizes the most important works carried out between 1883 and 1983.

2.2 THE LATE CRETACEOUS- EARLY PALEOGENE SUCCESSION IN EGYPT

The subdivision of the Late-Cretaceous-Early Paleogene succession in Egypt into three groups and five formations suggested by El-Naggar (1966a, 1966b, 1970) and followed by El-Naggar and Ashor (1978, 1983) is adopted here. The groups, which are briefly described in the following paragraphs, include from bottom to top the Nubia, Esna and Libyan Desert Groups (Table 2.1).

2.2.1 The Nubia Group

The Nubia Group in its type region is naturally divisible into five distinct formations (El-Naggar, 1970), from the base upwards as follows: the Abu-Aggag Sandstone, the Timsah Clay, The Um-Barmil sandstone (\approx The Taref sandstone), The Quseir Variegated Shale and the Sibaiya Phosphate.

However, only the uppermost part of this group outcrops in the Abut Tartur area and hence our discussion will be restricted to the Quseir and Sibaiya formations.

The Quseir Formation

This formation represents the basal part of the succession in the Abu Tartur area and is composed mainly of sandstones intercalated with shale bands. It is underlain in the subsurface by about 1500 m of sandstones down to basement complex and is conformably overlain by the Sibaiya Phosphate.

TABLE 2.1. Correlation of Various Lithostratigraphic Subdivisions Proposed for the Late Cretaceous-Early Paleogene Succession in Egypt.

LITHOSTRATIGRAPHIC UNITS										TIME ROCK UNITS	
Zittle 1883	Beadnell 1901	Said 1960	Herm ina and others. 1961	Issawi 1972	ElNaggar 1970 and ElNaggar & Ashour 1983	Chron	Age	Epoch	Period	Era	
Numulitic Limestone	Numulitic Limestone	Thebes Limestone	Thebes Limestone	Thebes Limestone Member	Thebes L m. Member	Luxor Formation	Libya Group	Owaina Formation	Qurnah Calc. Sh. Member	Thebes L m. Member	
Shales	Esna Shale	Esna Shale	Esna Shale	Esna Shale Member	Esna Shale	Owaina Formation	Libya Group	Kilabiya Chalk Member	Upper Owaina Sh. Member	Thebes L m. Member	
Clays with Exogyra + Phosphatic beds	Shales, marls and Chalks	Dakhla Shale	Kukur Formation	Tarwan Formation	White L.m. Member	Owaina Formation	Libya Group	Lower Owaina Shale	Kilabiya Chalk Member	Thebes L m. Member	
Variegated Shales + Nubia S. S.	Phosphatic beds + Variegated Shales + Nubia S. S.	Phosphatic beds + Nubia S. S.	Mudstone beds with shale + Red Ferruginous Exogyra Shales + Phosphatic beds	Dakhla Formation	Hamama Member	Sharawna Formation	Libya Group	Upper Sharawna Sh. Member	Middle Sharawna Sh. Member	Lower Sharawna Sh. Member	
Senonian	Maastrichtian	Danian	Heersian	Landenian	Ypresian	Owaina Formation	Libya Group	Kilabiya Chalk Member	Upper Owaina Sh. Member	Thebes L m. Member	
LATE CRETACEOUS	CRETACEOUS	Maastrichtian	Maastrichtian	Dakhla Formation	Hamama Member	Sharawna Formation	Libya Group	Upper Sharawna Sh. Member	Middle Sharawna Sh. Member	Lower Sharawna Sh. Member	
Paleocene	Paleocene	Danian	Heersian	Landenian	Ypresian	Owaina Formation	Libya Group	Kilabiya Chalk Member	Upper Owaina Sh. Member	Thebes L m. Member	
Paleogene	Paleogene	Danian	Heersian	Landenian	Ypresian	Owaina Formation	Libya Group	Kilabiya Chalk Member	Upper Owaina Sh. Member	Thebes L m. Member	
Cretaceous	Cretaceous	Maastrichtian	Maastrichtian	Dakhla Formation	Hamama Member	Sharawna Formation	Libya Group	Upper Sharawna Sh. Member	Middle Sharawna Sh. Member	Lower Sharawna Sh. Member	
Mesozoic	Mesozoic	Maastrichtian	Maastrichtian	Dakhla Formation	Hamama Member	Sharawna Formation	Libya Group	Upper Sharawna Sh. Member	Middle Sharawna Sh. Member	Lower Sharawna Sh. Member	

The Quseir Formation is generally unfossiliferous except for rare plant and vertebrate remains of Campanian age in its upper part. Consequently, the formation was considered by El-Naggar (1970) to be of Senonian (Santonian? – Campanian) age.

This formation was deposited in shallow marine waters bordered by a high relief land area scoured by rather young rivers. The land area was lowered several times to such a degree that only fine clastics were deposited. Consequently the formation was considered to mark the early transgressive phase of an advancing sea (El-Naggar & Ashor, 1983).

The Sibaiya Formation

This formation outcrops in a narrow belt running from both the Dakhla and Kharga Oases to the Red Sea coast, traversing both the Nile Valley and the Eastern Desert. It is composed of several phosphate beds (with a total maximum thickness of 50 m) separated by shaly and marly intercalations and capped by a 2m-thick, silicified limestone bed. This formation, which is considered to be of Late Campanian age (El-Naggar 1966a, 1966b, 1970), is overlain conformably by the strata of Early Maastrichtian age (the Sharawna Shale) and underlain by the Senonian "Quseir Formation".

2.2.2 The Esna Group

The type section of the Esna Group is in the Jabal Owina area located in the south of the town of Esna in the Nile Valley. The group is widely

distributed in Egypt, extending from the type section westwards to the Barqah-Kurkur-Kharga and Dakhla Scarp, southward to a point Kharga Scarp between Faris and El-Halfaya, near Komombo and northward to near Qena. It has also been recorded along the Red sea coast, in the Sinai Peninsula and in the subsurface of both the eastern and the western deserts of Egypt. The Esna Group in the type section is represented by a 237 m thick shale section intercalated with marl and chalk beds. The group is of Maasatrichtian - Paleocene age and traversed by a marked unconformity separating rocks of these ages. The Esna Group is subdivided into two formations which are described briefly in the following paragraphs.

The Sharawna Formation

The formation was introduced by El-Naggar (1963) and later described by the same author (El-Naggar 1966a, 1966b, 1970) and by El-Naggar & Ashor (1983). It was reported to overlies conformably the Sibaiya Formation, underlies disconformably the Owaina Shale and to include three members known as Lower Sharawna Shale Member, Middle Sharawna Marl Member and Upper Sharawna Shale Member.

The Lower Sharawna Shale Member is about 50 m thick and mainly composed of dark-grey shales, calcareous-clayey siltstones and calcareous clays. It was considered by El-Naggar (1966a, 1966b, 1970) to be of Early Maastrichtian age.

The Middle Sharawna Marl Member is composed of about 12 m-thick marl and clay section containing pale yellowish to pale grayish, locally

ferruginous marly clay, clayey marl and marl bands and is full of small dwarfed limonitic megafauna. It is considered to be of Early Middle Maastrichtian age (El-Naggar, op. cit.).

The Upper Sharawna Shale Member is composed of about 60 m of iron-stained, locally ferruginous, dark gray to grayish black shale, and is considered to be of Middle-Late Maastrichtian age (El-Naggar 1966a, 1966b, 1970).

The Owaina Formation

This formation consists of about 120 m of shales and intercalated marly and chalky beds that disconformably overlie the Sharawna Shale and conformably underlie the Luxor Formation. The base of the formation is marked by an obvious hiatus and a conglomeratic band that separates it from the underlying Sharawna Shale (El-Naggar op. cit.). The formation passes westwards into reefal limestones of the Kurkur Formation (25-100 m in thickness). It is considered to be Paleocene age and has been subdivided into three members known as Lower Owaina Shale Member, Kilabiya Chalk Member and Upper Owaina Shale Member from the base upwards as follows:

The Lower Owaina Shale Member is composed of about 40 m thick, iron-stained, light gray shales with limonitic fossils, ferruginous concretions and a yellowish gray, glauconitic, conglomeratic, marly bed at the base. The shales, which are considered to be of Early-Middle Paleocene age (El-Naggar & Ashor 1978, 1983) on the basis of planktonic microfossils, pass upwards into the overlying chalk and contain thin chalky bands near the top. Towards the

western scarp that borders the Nile Valley and extends into the Western Desert Oases (Kharga, Dakhla, etc.) the shale facies changes laterally into reefal limestones (the Kurkur Formation) which are well-developed in the Abu Tartur area.

The Kilabiya Chalk Member is composed mainly of chalk (about 25 m in thickness) with chalky, marly and clayey intercalations. Locally, this member takes over a granular texture and grades laterally into a true calcarenite. It is characterized by a flood of planktonic microfossils which prove its early Landenian age (El-Naggar, 1966a, 1966b, 1970, El-Naggar & Ashor 1978, 1983).

The Upper Owaina Shale Member is composed of about 60 m of iron-stained, light gray, locally ferruginous shale, containing thin gypsum and anhydrite bands as well as ferruginous concretions with rare limonitic megafossils. It is also flooded by both planktonic and benthonic foraminiferid remains which prove its late Landenian age.

2.2.3 The Libyan Desert Group

The Libyan Desert Group is characterized by the succession of calcareous shales and limestones overlying the Esna Group and underlying the Moqattam Group. The group includes two distinctive formations, Luxor Formation and Drunka Formation from bottom to top respectively. The Luxor Formation is considered to be of Early Eocene age, while the Drunka Formation is considered to be of Early Middle Eocene Age (El-Naggar, 1970) in

the Abu Tartur area only the basal members of the Luxor Formation outcrop. Therefore, our discussion will be limited to this formation.

The Luxor Formation

This formation overlies the "Owaina Shale" and underlies the alveolinid limestones of the Drunka Formation and is considered to be of Early Eocene age (El-Naggar, 1966a, 1966b, 1970). It is about 360 m thick and subdivided into a lower member of calcareous shales and an upper member of limestones.

The Qurnah Calcareous Shale Member is composed of about 60 m of dark gray to greenish or even black, thinly bedded, calcareous shales, locally iron stained, with intercalating marly bands.

The Thebes Limestone Member is the upper member of the Luxor Formation and is composed of about 300 m of chalky limestones with flint bands as well as marly and siliceous intercalations.

2.3 GEOLOGY OF ABU-TARTUR AREA

Similar to the succession in the Nile Valley, the outcropping rocks in Abu Tartur area can be subdivided into a lower, Nubia Group, a middle, Esna Group and an upper Libyan Desert Group. The descriptions of these groups have already been given earlier and need not be repeated here. It should, however, be added that some outcropping members in the Nile Valley are not distinguishable in the Abu Tartur area and the variations in thickness are recorded due to lateral change of facies (Fig. 2.1).

STRATIGRAPHIC COLUMN IN ABU TARTUR AREA

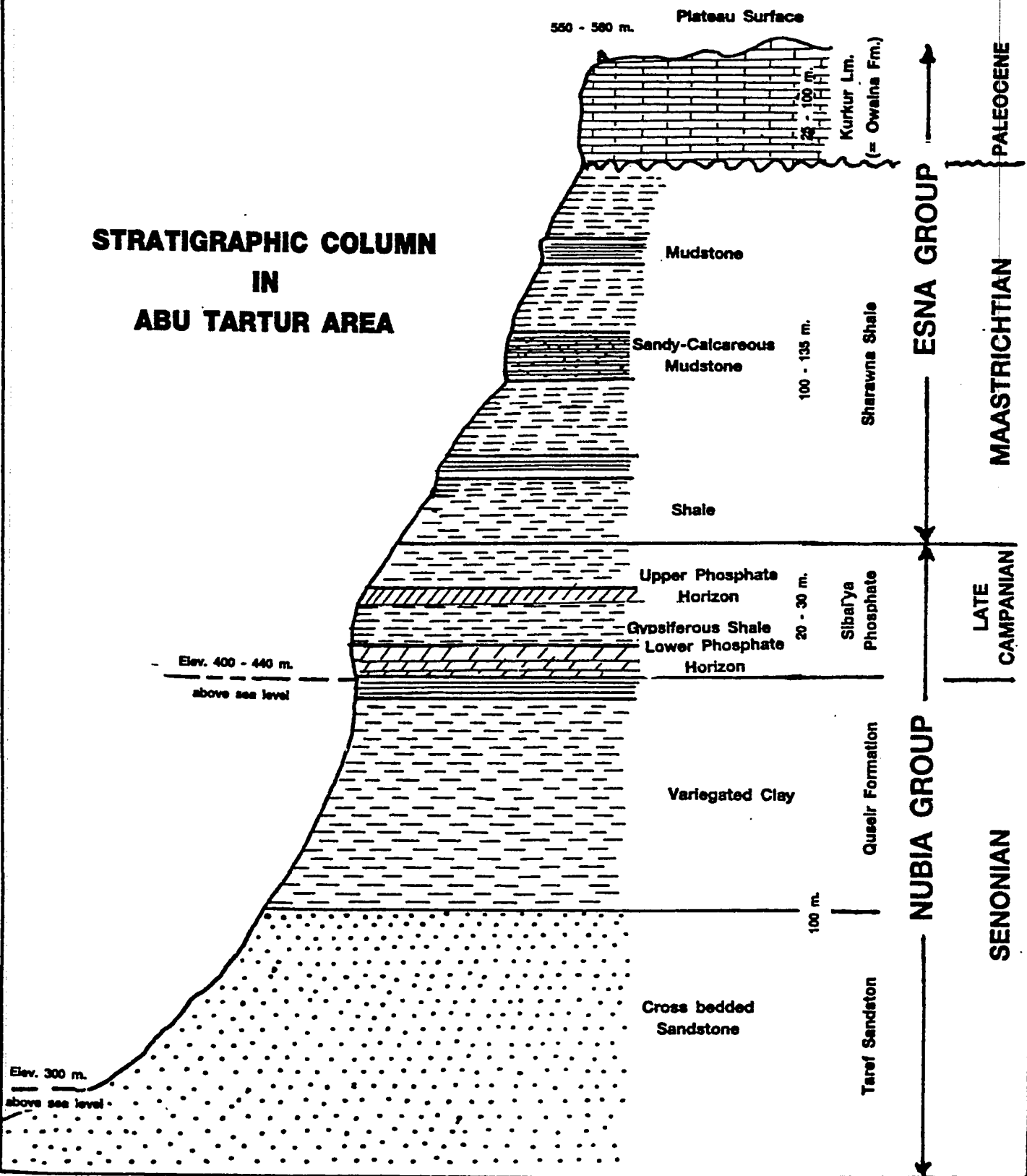


Fig. 2.1 Stratigraphic column in Abu Tartur area.

The Sibaiya Formation in the Abu Tartur area contains the bulk of the phosphate beds, the reserve estimation of which constitutes the main goal of the present thesis. Therefore, the following section will be devoted to the description of this formation.

2.3.1 The Sibaiya Formation in Abu Tartur Area

Rocks of the Sibaiya Formation in Abu Tartur area represent a part of the shallow-water sediments that were deposited in the southernmost fringes of the Late-Companian transgressive sea over the Egyptian territory. This shallow water belt is mainly represented by the Qusair Formation and the overlying Sibaiya Phosphate. The latter formation is composed mainly of phosphate and phosphatic beds intercalating with shaly, clayey, marly and limy bands. The phosphorite beds are generally grouped into a lower and an upper phosphate horizons. Lenses and thin layers of bone breccia are commonly recorded in the phosphate beds, in the layers separating them and in the upper part of the underlying Qusair Variegated Shales (see Fig. 2.1).

The Lower Phosphate Horizon

The lower phosphate horizon lies disconformably on top of the eroded surface of the Quseir Formation. The total thickness of this highly economic phosphate horizon (average grade of 26% P_2O_5) varies between 1.8 m and 8.0 m increasing generally from north to south-west. The dip is not uniform, varying from $0^{\circ}30'$ to $3^{\circ}00'$ in the same direction and decreasing again further

to the west. The phosphorite bed was apparently subjected to a number of diagenetic changes evidenced by abundant forms of replacement which transformed rich phosphorites into poorer ones and vice versa. The lower phosphate horizon in the Abu Tartur area belongs to the first cycle of phosphate deposition which is known in both the Nile Valley and the Red Sea coastal regions. The enclosing rocks in the three areas are dominated by clays and sandy clays with intercalations of silty glauconitic sandstones and subordinate layers of calcareous mudstones, with significant lateral and vertical variations.

The Upper Phosphate Horizon

The upper phosphate horizon with an overall thickness ranging between 0.4 m and 7.3 m, consists mainly of phosphorite beds, intercalated by shales and phosphatic clays. This horizon has an average grade of 17% P_2O_5 and is overlain conformably by the lower Sharawna Shale Member. This horizon is collectively equivalent to the upper phosphate horizon in both the Nile Valley and the Red Sea coast regions, and hence, is considered to be of Late Campanian age. Gypsiferous clays with rare intercalating layers of calcareous mudstones and sandstones are the principal rock types which enclose the upper phosphate horizon in the Abu Tartur area.

2.3.2 Structure of Abu Tartur Area

The structure of Abu Tartur plateau is simple with only local dips varying between $0^{\circ}25'$ and 2° . The dips generally increase from the northeast

to the southwest, but decrease towards the west (Hermína, 1973). Nevertheless, a number of folds and faults, which are described in the following sections, could be identified in this almost flat plateau.

Folding

Three main structures can be identified in the area. The first structure is the eastern anticline, which represents a gentle anticlinal structure plunging at $0^{\circ}30'$ to the SSE with about 1° dip. The western boundary of this anticline is almost marked by N1-7, NE5 and A5 drill-holes as shown in Fig. 2.2.

The second structure is the central homocline which has an average dip of about $0^{\circ}30'$ towards the west. It is locally interrupted by plunging anticlines and synclines, that trend NNE-SSW, diagonal to the main folds and die out approximately along the drilling grid line 11 (Fig. 2.2).

The third structure is the western homocline, occupies the extension beyond line 11 (Fig. 2.2) and displays a gentle, homoclinal bend with dips up to 2° between bore-holes A2 and A15, that flattens again to less than $0^{\circ}30'$ towards A1 in the extreme western part of the drilling area (Fig. 2.2).

Faulting

A fault line trending NE-SW with a total length of about 3 km and a throw of about 50-60 m towards the northwest cuts the plateau in its southwestern part (Fig. 2.2).

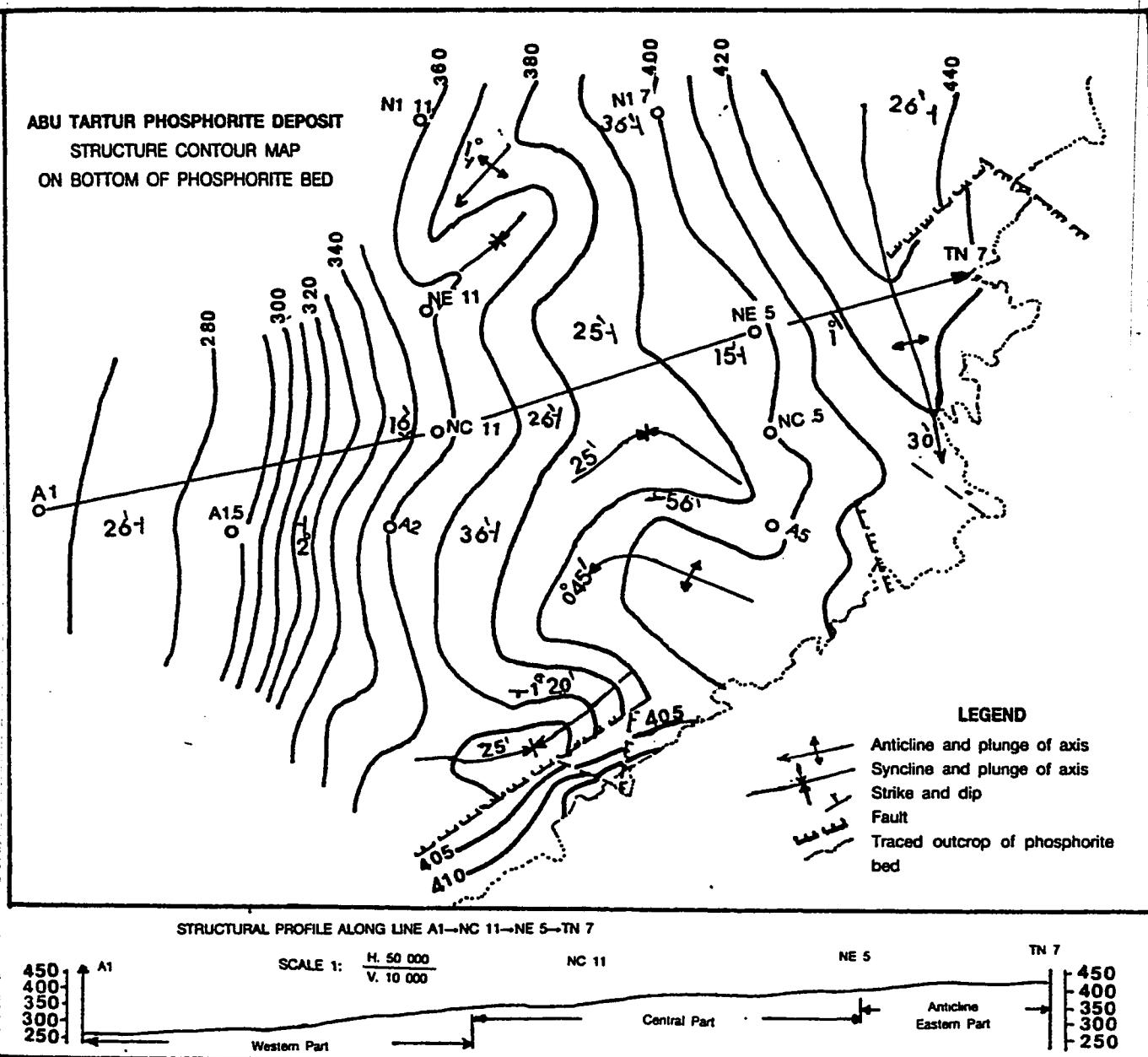


Fig. 2.2 Abu Tartur phosphorite deposit structure contour map on bottom of phosphorite bed. (after Hermina, 1974)

Several other minor faults having NE-SW, NNE-SSW and NNW-SSE trends affect the phosphate beds along the scarp face. All observed faults are of the normal type with throws not exceeding 50 m.

2.3.3 Mineralogy

Tobia and Fekry (1964), Zaghloul and Mabrouk (1964), El-Naasan and Afonin (1970), El-Mabrouk (1975) and Kamel and Hilmy (1977) carried out chemical and mineralogical analyses of the phosphate rocks in the Kharga-Dakhla region in general and in Abu Tartur area in particular. Both El-Kammar (1974) and El-Mabrouk (1975) provided the rare-earth analysis for some phosphate samples from the Abu Tartur deposits. Two main groups of minerals, namely phosphate and non-phosphate minerals are described in the following paragraphs:

Phosphate minerals

The phosphate minerals are essentially represented by an isotropic mineral, forming grains, pellets and coprolites, and a holocrystalline mineral pseudomorphing the bony parts. Three phosphate mineral groups were identified as follows:

Carbonate-fluorapatite group: carbonate-fluorapatites are the dominant minerals in Abu Tartur phosphorites (Kamel 1977). These include francolite and dahillite. The former is an apatite containing appreciable

quantities of CO_2 , more than 1%F, and the OH group the latter a carbonate-hydroxyl-apatite with a small content of F. Sub-microcrystalline collophane was found to be the main constituent of the observed pellets, ovulitic grains, olitic bodies, nodules and coprolites, while bone and shell fragments were described as rare (Kamel and others, 1977). Collophane, which constitutes approximately 60-80% of the phosphate rock, is usually dark gray or even black, and commonly translucent, with opaque inclusions due to the presence of carbonaceous matter. In the oxidized parts, the granules are cracked and filled with cement. The pellets contain about 33% P_2O_5 .

Wavellite group: minerals of the wavellite group are usually observed surrounding and particularly invading different phosphate pellets and bone fragments. They are commonly associated with montmorillonite and have a yellow of brown colour with weak pleochroism changing from pale brown to yellowish brown.

Manganapatite group: manganapatite is rarely encountered in Abu Tartur phosphorites. This mineral has green to dirty green colour. The identification of the mineral is mainly based on its form, colour and presence of Mn(0.3 - 0.4%) in the phosphate pellets.

Nonphosphate minerals

These minerals are present in Abu Tartur phosphorites as cement and/or matrix. The main nonphosphate minerals include dolomite,

montmorillonite, gypsum, anhydrite, pyrite and quartz. In addition to these some glauconite, carbonaceous matter and iron oxides have been observed.

Dolomite: dolomite is mainly present as a cement in dolomitic phosphorites and usually observed in the form of well-developed rhombohedral crystals. It often displays a zonal texture, and may contain rounded carbonate grains. The pure mineral is either colourless or has different colours of grey, pale, yellow, reddish or even dark.

Montmorillonite minerals: these minerals occur mainly in the form of matrix, especially in the clayey phosphorites, and usually have deep yellow, brown, dark brown and sometimes black colours. The brown colour is mostly due to the presence of pigments of organic matter and/or iron oxides, while the black colour seems to be related to fine-grained, dispersed pyrite.

Gypsum and anhydrite: these minerals are commonly present as cementing material (filling intergranular spaces, pores and cavities). They are usually colorless, but when admixed with iron oxides, are coloured and can impart yellowish and brownish colours to the cement. Both the gypsum and anhydrite may also be impregnated by pyrite, as well as by clayey, calcareous and/or carbonaceous matter.

Pyrite: pyrite is usually admixed with the phosphate pellets, scattered around bone fragments or impregnated in the clayey matrix. It is usually

accompanied by marcasite, which may form small aggregates (5% of the rock). The presence of both pyrite and marcasite are essentially responsible for the black colouration of the phosphate rock.

Quartz: quartz is represented by grains and fragments showing subangular to angular outlines. The mineral is commonly embedded in the groundmass, but may be included in the core of some phosphate pellets. Quartz form 10-15% of the main phosphate bed in its lower part and 5-10% in its upper part. It has a milky white, yellow or a light grey colour.

Chapter 3

REVIEW OF RESERVE ESTIMATION METHODS

3.1 INTRODUCTION

The reserve estimation involves the determination of both the quality (grade) and quantity (tonnage) of the mineral deposit. The grade estimation is carried out to determine composite value for samples taken within lengths of drill hole or designated widths of channel, whereas the tonnage estimations are mainly concerned with both the volume and the density of the deposit. Several classical reserve estimation methods were described in the literature (Baxter 1957, Popoff 1966, Peters 1978). These may be classified into four main groups as follows:

- a. Average factors and area methods.
- b. Mining blocks methods.
- c. Cross-section methods.
- d. Analytical methods.

3.2 AVERAGE FACTORS AND AREA METHODS

This group of reserve estimation methods has been described as arithmetic average, weighted average, average depth and area, geological blocks, and general outline. These methods are based on the assumption that

certain segments or blocks of the deposit considered are similar in geology and technology to sections previously studied.

The reserves of uniform bedded deposits such as coal, phosphate rock and clay have been estimated by such methods. The areas are usually measured by a planimeter, computed or scaled from maps. The estimates can be made for individual blocks, panels, levels, or for the entire orebody, and such techniques can generally provide quick and approximate estimates for the reserves.

3.3 MINING BLOCKS METHOD

The mining block methods are used at the final stages of detailed exploration, when blocks have already been outlined on three or four sides by exploration openings, and when all the blocks have been explored to approximately the same degree. The area of the deposit is divided into separate blocks, the height of which equal to the average thickness of the orebody. The volume of ore within each outlined block is calculated as the product of its surface area multiplied by its weighted thickness. Next the volumes of individual blocks are combined to give the total volume. Finally, the ore tonnage is determined as a product of both the volume and weight factors and the metal tonnage as a product of both the ore tonnage and the average grade. Such methods are flexible and may be used in all types of mineral deposits as computations are relatively simple and speedy.

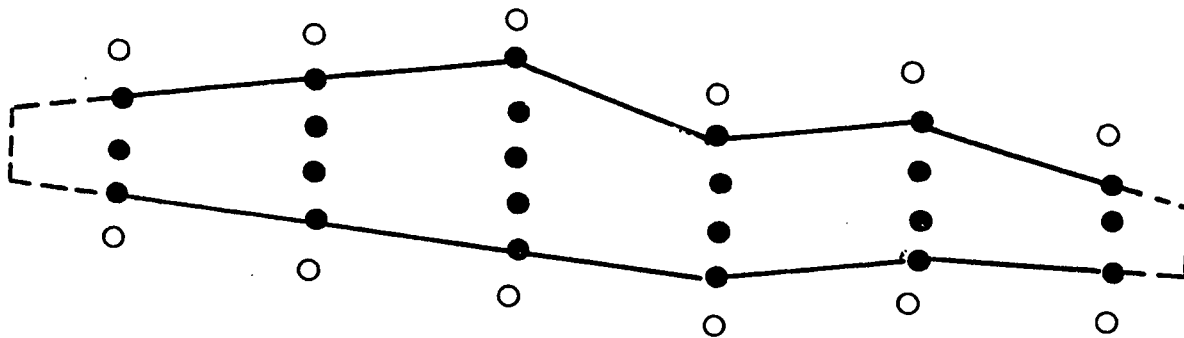
3.4 CROSS-SECTION METHODS

The basis of the cross-section methods is to divide the orebody into blocks by constructing geological sections. The interval between the sections may be constant or may vary depending on the geologic and mining considerations. These methods include the standard linear and isoline methods.

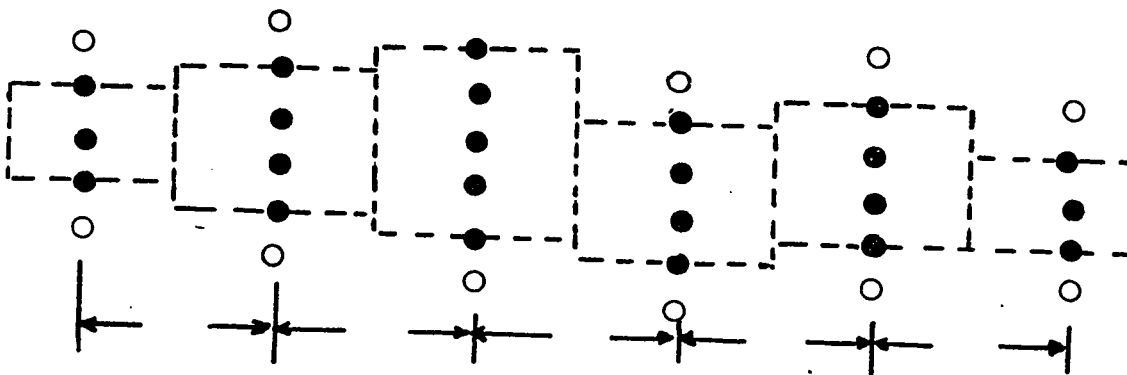
The standard method is based on the rule of gradual changes (Fig. 3.1a). Each internal block is confined by two sections and by an irregular lateral surface, and each end block by a single section and by a lateral surface. Sections may be parallel or nonparallel, vertical, horizontal, or inclined.

The linear method is based on the rule of the nearest points (Fig. 3.1b). Each block is defined by a section and a length equal to one-half the distance to the adjoining sections.

The isoline method is also based on the rule of the gradual changes. The method includes, among numerous lines of equal values, isopach, isochemical and isograde contours. It is used in the geological exploration to show the variability in shape, grade and other properties of the orebodies. The areas bounded by appropriate isolines are usually measured by the planimeter.



PLAN
(a)



PLAN
(b)

Fig. 3.1 Cross-section methods (after Popoff, 1966)

- (a) Laying out blocks according to the rule of gradual changes. (standard method)
- (b) Laying out blocks according to the rule of nearest points (linear method)

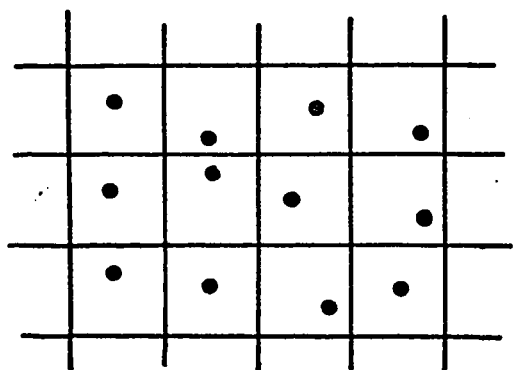
● - Vertical drill-holes crossing ore
○ - Blank vertical drill-holes.

3.5 ANALYTICAL METHODS

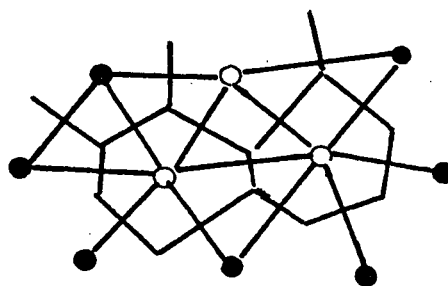
In this group of methods, the deposit is divided into blocks of simple geometric forms, using random stratified grid, polygons or triangles. The factors controlling each block are determined directly and are computed as an arithmetic average or in other ways.

3.5.1 The Random Stratified Grid (RSG)

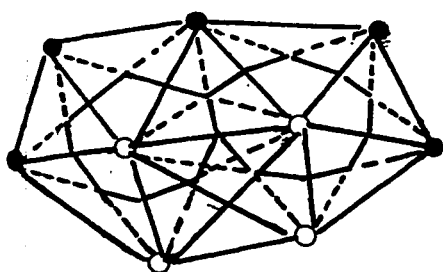
The random stratified grid (RSG) provides a simple method of dividing the deposit into blocks. It can be fitted about the sample points so that the samples occupy random positions within the grid panels and with respect to one another (Fig. 3.2a). Each grid panel can encompass a single sample, but some panels may have two or even more samples and others may have no samples at all. Where two or more samples are located within one RSG panel, the mean value of the samples are computed and assigned to the panel. This can overcome the problem of clustered samples, as these more or less occupy the same influence zone. Where RSG panels without any samples lie within the deposit, surrounded by apparently payable panels, there is no reason to suppose that the ore does not continue through them, and hence these are included in the reserves. The estimated mean value of the deposit is the mean of all the panel values.



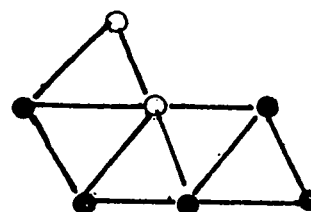
(a)



(b)



(c)



(d)

Fig. 3.2 The analytical methods of ore reserve estimation (after Patterson, 1959)

- (a) Random stratified grid
- (b) Polygonal blocks (constructed by perpendiculars at midpoints between samples)
- (c) Polygonal blocks (constructed by angular bisectors)
- (d) Triangular blocks.

3.5.2 Polygonal Method

In this method, the deposit is divided into a number of polygons. To construct these polygons, each sample point is connected by straight lines with all the samples nearest to it and perpendiculars are drawn from the middle of the connecting lines until they intersect each other (Fig. 3.2b). The angular bisectors may also be used to construct polygons as shown in Fig. 3.2c (Patterson, 1959).

The area of each polygon is measured by the planimeter, and both the thickness and the accumulation of the samples in each polygon are assumed to extend over the whole of the polygon.

The polygonal method is used in computing reserves of tabular deposits, such as sedimentary beds of coal, phosphate rock, oil shales, etc. The accuracy of the results increases with the increase in sampling density.

3.5.3 Triangular Method

In this method, the surface area of the orebody is divided into triangles by connecting the sample points (Fig. 3.2d). The value given to each triangle is the arithmetic mean of the sample values lying at its corners. Thus, the individual triangles tend to be estimated with greater accuracy than the polygons.

The triangular method is applicable to most sedimentary deposits, as the mineralizations of such deposits are consistent with the rule of the gradual

changes. The errors of computations may vary depending on the methods of sampling and the spatial behaviour of the variables under consideration.

3.6 DISADVANTAGES OF CLASSICAL METHODS

The classical methods of ore reserves estimation, have long been in use. However there are several fundamental objections to these methods.

- a) The construction and measurement of some methods are costly in both time and money (Royle 1977). For instance, in the polygonal or triangle methods the areas are generally unequal leading to lengthy calculations. Moreover, the addition of more data needs re-constructing and re-measuring of the several polygons or triangles.
- b) The zone of influence of samples is taken quite arbitrarily as the half-way distance between the drill-holes. It is not considered to be a function of the geological characteristics of mineralization.
- c) The procedures for assigning values to the blocks are quite arbitrary and without a sound theoretical basis. Such methods are a function of geometry, which simplifies the calculations, but not a function of the nature of mineralization. Thus, the

estimates can be biased and there is no way to ensure that they are free of bias.

- d) The classical estimation methods do not usually provide means for determining the precision of the estimates. No confidence limits can be attached to the estimates as theoretical error variance cannot be calculated (Sahin, 1977).

Taking the geological characteristics of deposits fully into account, the geostatistical methods successfully overcome the above-stated problems in reserve estimation. Consequently, the following chapters of this work will be devoted to the geostatistical methods and their application to the Abu Tartur Phosphate deposit.

Chapter 4

DATA SET AND PRELIMINARY STATISTICAL ANALYSIS

4.1 DATA SETS

On the basis of the geological descriptions and mining considerations, two horizons of phosphate deposit were recognized in Abu Tartur area. These are referred to as the Upper and Lower phosphate horizons. The basic data for this study were derived from 400 m x 400 m drilling campaign and consisted of phosphate thicknesses of the lower phosphate horizon in 347 vertical drill-hole sites (see plate 1), and phosphate grade ($P_2O_5\%$) of some 1683 samples taken from these holes. In addition to the thickness and grade data; X, Y and Z coordinates of the collar of each drill-hole, the depth from the collar to the top and the bottom of each core sample were, also, available.

The data were put into a master computer file and used to produce other files for specific uses including the production of the bore-hole location maps, contour maps and the computation of variograms. An excerpt from this master file is given in Appendix A. The first line has the drill-hole name, X, Y, and Z coordinates of collar, azimuth (0.00 degree) and dip (-90.0 degrees) at the collar. The other lines have the drill-hole name, from, to, phosphate grade (%) and sample thickness.

4.2 COMPOSITE FILES

The original data consisted of samples having different lengths (i.e. supports). This necessitated regrouping of the samples to provide equal length samples before starting to the geostatistical study. Such core sample regrouping is commonly referred to as "compositing" and the regrouped samples as "composites". The composites were produced in our case using the FORTRAN program COMPOS of the GEOSTAT package (1984). Selecting appropriate options in this program, two composite files were produced. One of these contains 1-m composites and the other the average grade and thickness data for drill-holes. An example list of the 1-m composite file is given in Appendix B. In addition to the number of drill-holes, this file includes X, Y and Z coordinates of the center of the composited samples and the corresponding composited phosphate grades. A simple FORTRAN program was written to read the average grade and thickness data for drill-holes and to calculate the accumulation (%m) which is the product of the average grade and thickness for each drill-hole.

4.3 CONTOUR MAPS

To view the spatial distributions of variables within the deposit, several contour maps (including topographic, isopach and isograde maps) have been plotted. The computer program ISOPOLY which is designed to contour 2 directional gridded data was used for generating these maps.

The topographic map for Abu Tartur plateau shown in Fig. 4.1 indicates a moderate relief, with 600 m elevation above the sea level. There are several locations on the map with circular depressions. These depressions, which are concentrated in the southern and northwestern part of the area, have depths ranging from 50 to 100 metres.

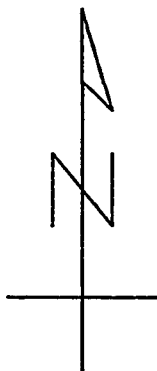
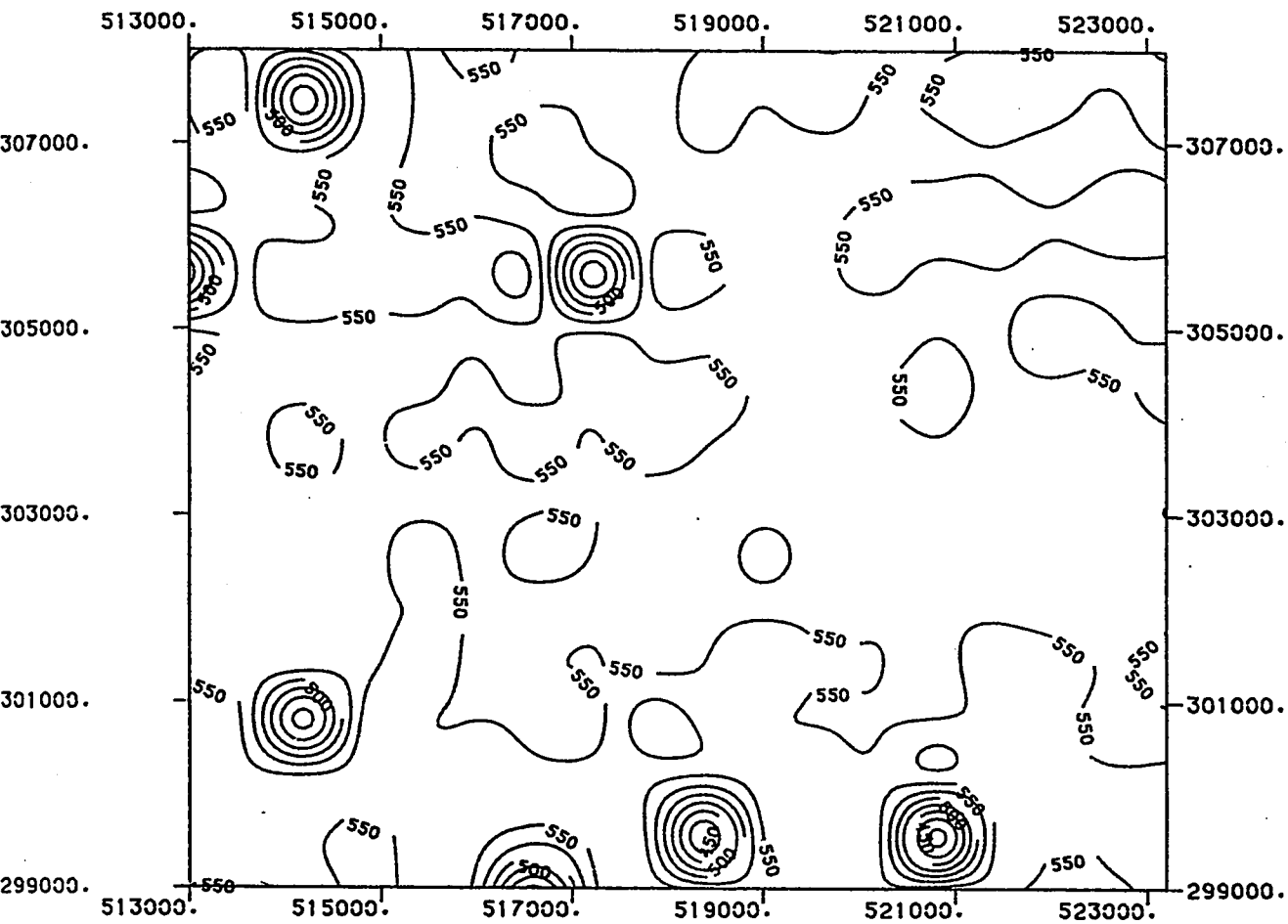
The isopach map for the main phosphate horizon in Abu Tartur plateau is illustrated in Fig. 4.2. This map shows that the thickness of the horizon ranges from about 100 cm to about 500 cm with very small and gradual changes in most parts of the area. The relatively thicker and thinner parts appear to have developed circular to semicircular pattern.

The isograde map illustrated in Fig. 4.3 indicates that P_2O_5 % varies between about 18% and about 28% in a fairly gradual manner. There are several relatively low grade areas in the southern, and south-eastern parts of the plateau. The lowest isograde value in these areas, which are generally circular in shape, is 18%. Throughout most of the northern half of the area, the isograde of 24% P_2O_5 or above, is the rule.

4.4 PRELIMINARY STATISTICAL ANALYSIS


To determine various characteristics of a mineral deposit, the usual practice is to take samples, analyze the properties of samples and infer the characteristics from such properties using statistical methods (Rendu, 1978).

A preliminary statistical analysis for Abu Tartur phosphate deposit has been carried out, using the P_2O_5 (%), the thickness (m) and the accumulation

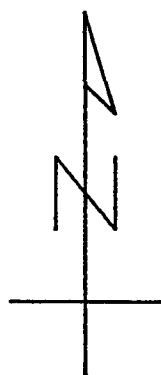
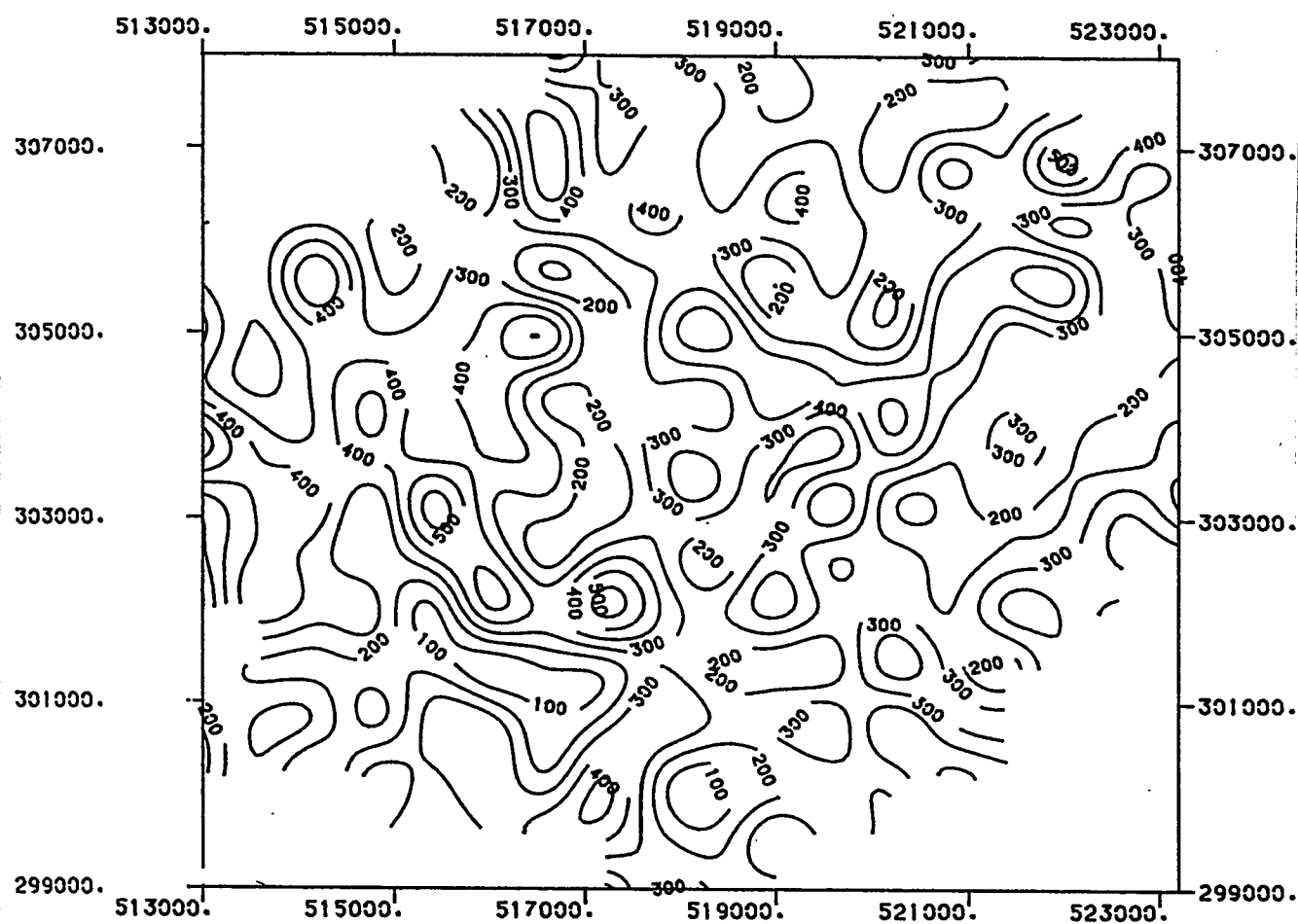


*** ABU TARTUR PHOSPHATE DEPOSIT ***

FIG. 4.1: TOPOGRAPHIC MAP (METERS)

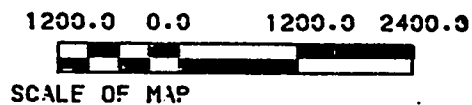
1200.0 0.0 1200.0 2400.0

 SCALE OF MAP

DATA PROCESSED FOR: A. A. ABDELLATIF, MS. UPM.
 SOFTWARE BY : GEOSTAT SYSTEMS, MONTREAL

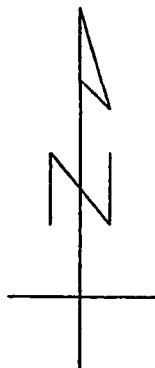
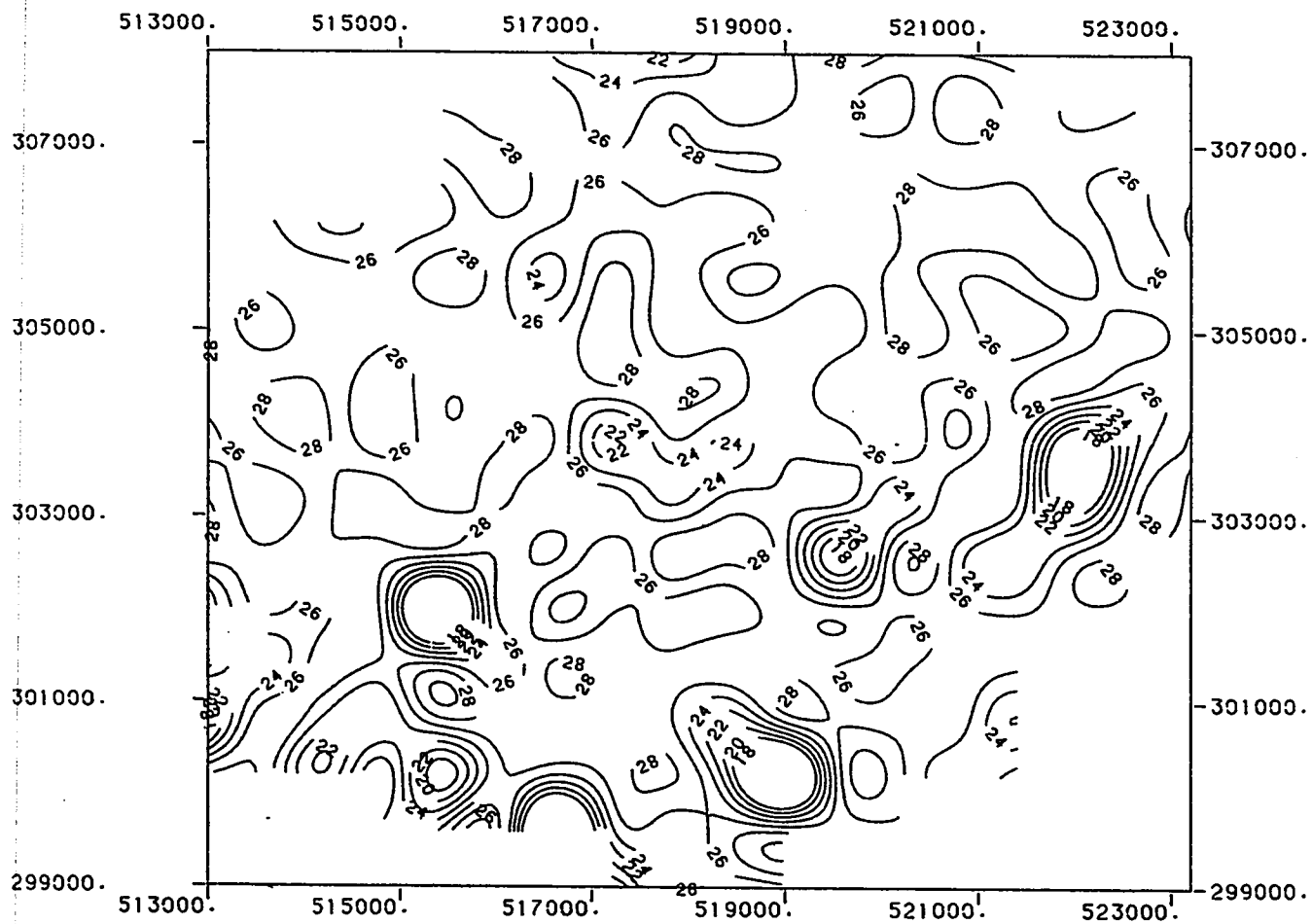


*** ABU TARTUR PHOSPHATE DEPOSIT ***

FIG. 4.2 ISOPACH MAP (CENTIMETERS)



DATA PROCESSED FOR: A. A. ABDELLATIF, MS. UPM.
SOFTWARE BY : GEOSTAT SYSTEMS, MONTREAL



*** ABU TARTUR PHOSPHATE DEPOSIT ***

FIG. 4.3: ISOGRADE MAP BASED ON

SAMPLE VALUES

1200.0 0.0 1200.0 2400.0



SCALE OF MAP

DATA PROCESSED FOR: A. A. ABDELLATIF, MS. UPM.
SOFTWARE BY : GEOSTAT SYSTEMS, MONTREAL

(%m) data. For each variable the mean, variance, standard deviation and the coefficient of variation were calculated and listed in Table 4.1. In addition to of these statistics, the histograms and cumulative frequency distribution curves for the same variables have also been constructed.

4.5 HISTOGRAMS

To plot the histogram of variable values ($P_2O_5\%$, thickness and accumulation), the values are grouped into classes with specified widths, and the number of samples in each class are counted. Next, the rectangles whose heights proportion to the number of samples are constructed.

The histogram is a valuable tool in determining the type of the sampling distribution, and in detecting possible outliers, i.e. sample values that are abnormally high or low (Rendu, 1978). The histogram of most geological variables are very often asymmetrically distributed on both sides of the mean value (i.e. skewed). However, the logarithms of the values are normally distributed, hence the name lognormal distribution.

The histograms for the variable values from Abu Tartur deposit are illustrated in Fig. 4.4 to Fig. 4.6. The histogram for $P_2O_5\%$ values shows slight negative skew whereas the histograms for both thickness and accumulation show slight positive skew.

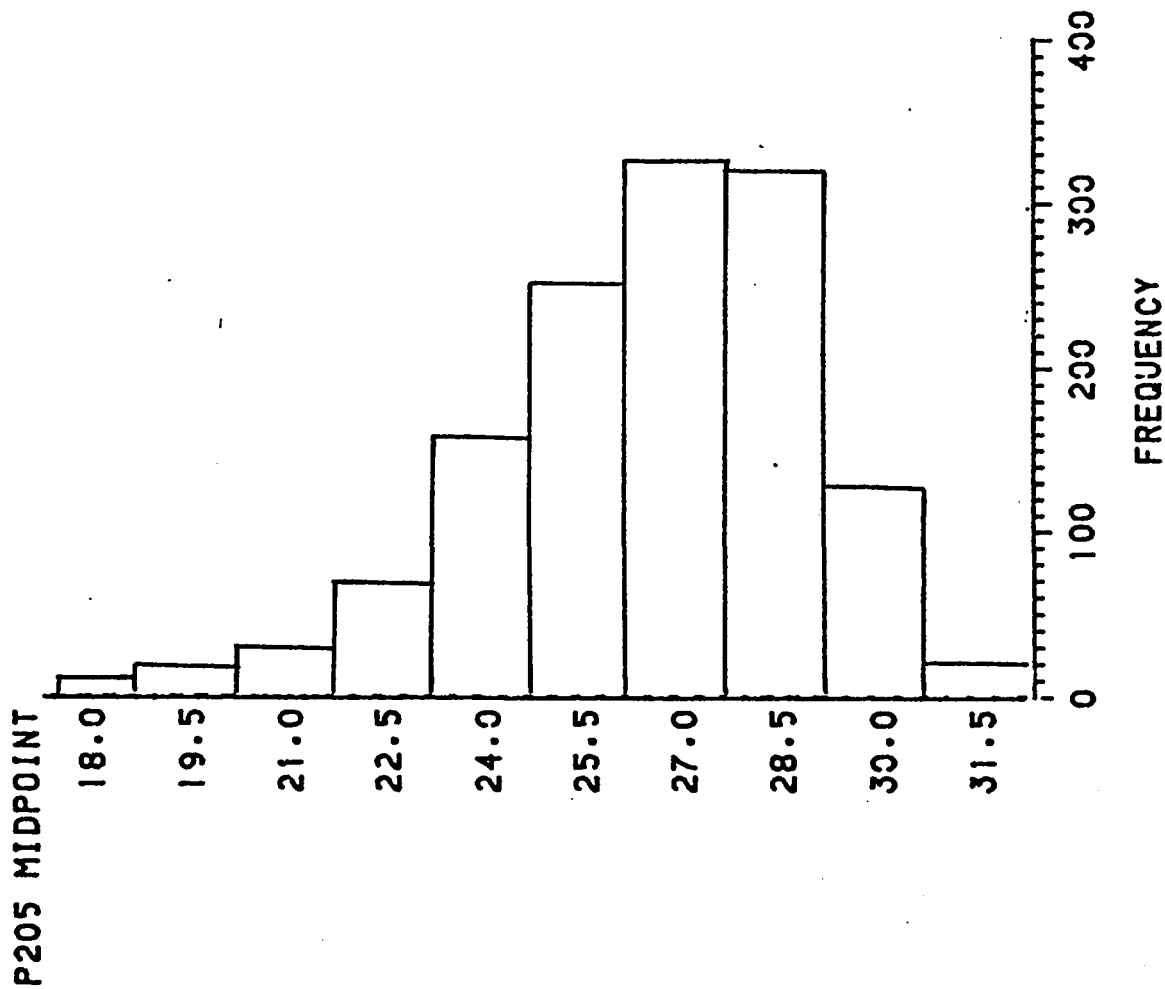


Fig. 4.4 Frequency distribution and histogram for P_{205} values.

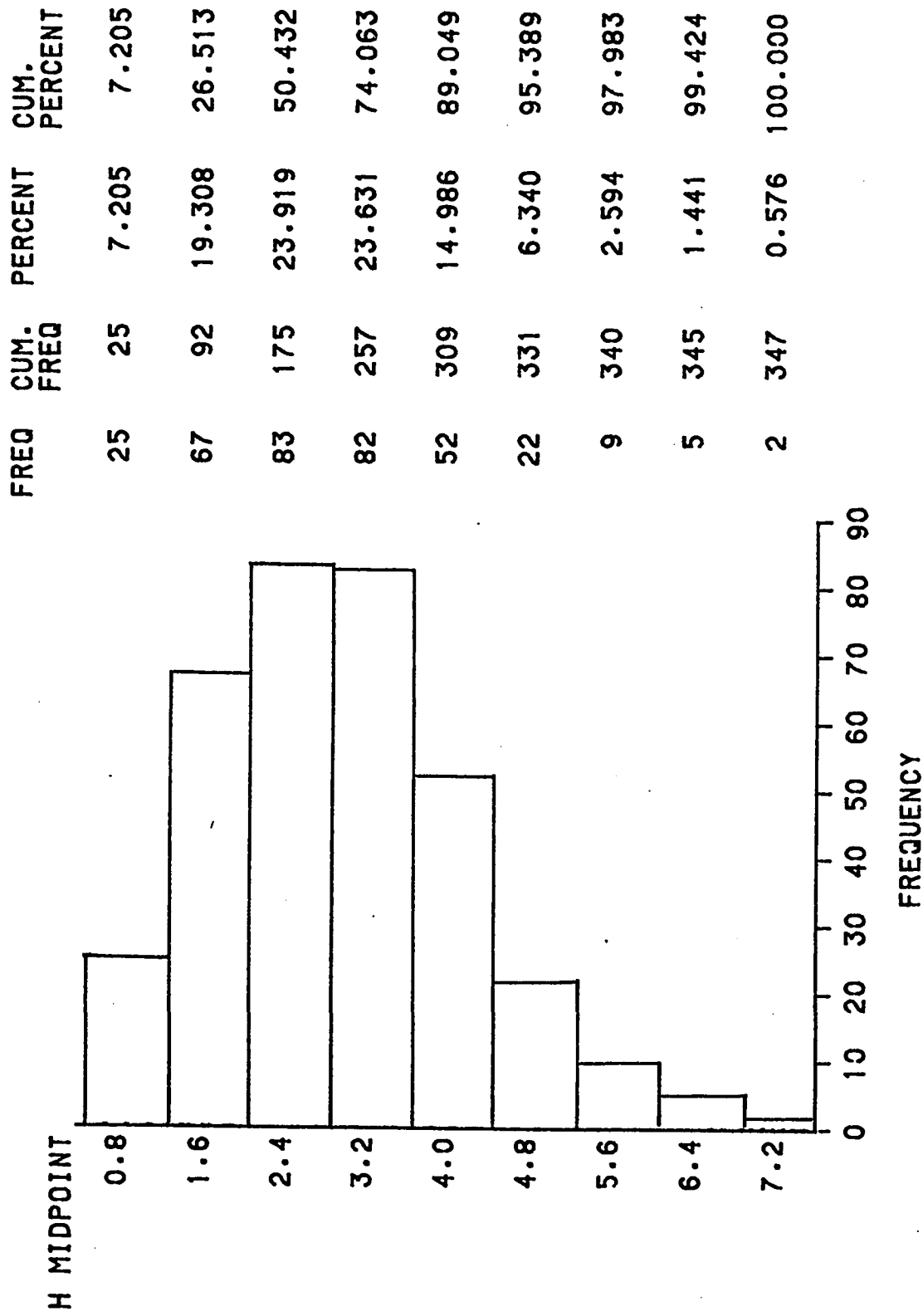


Fig. 4.5 Frequency distribution and histogram for thickness values (m).

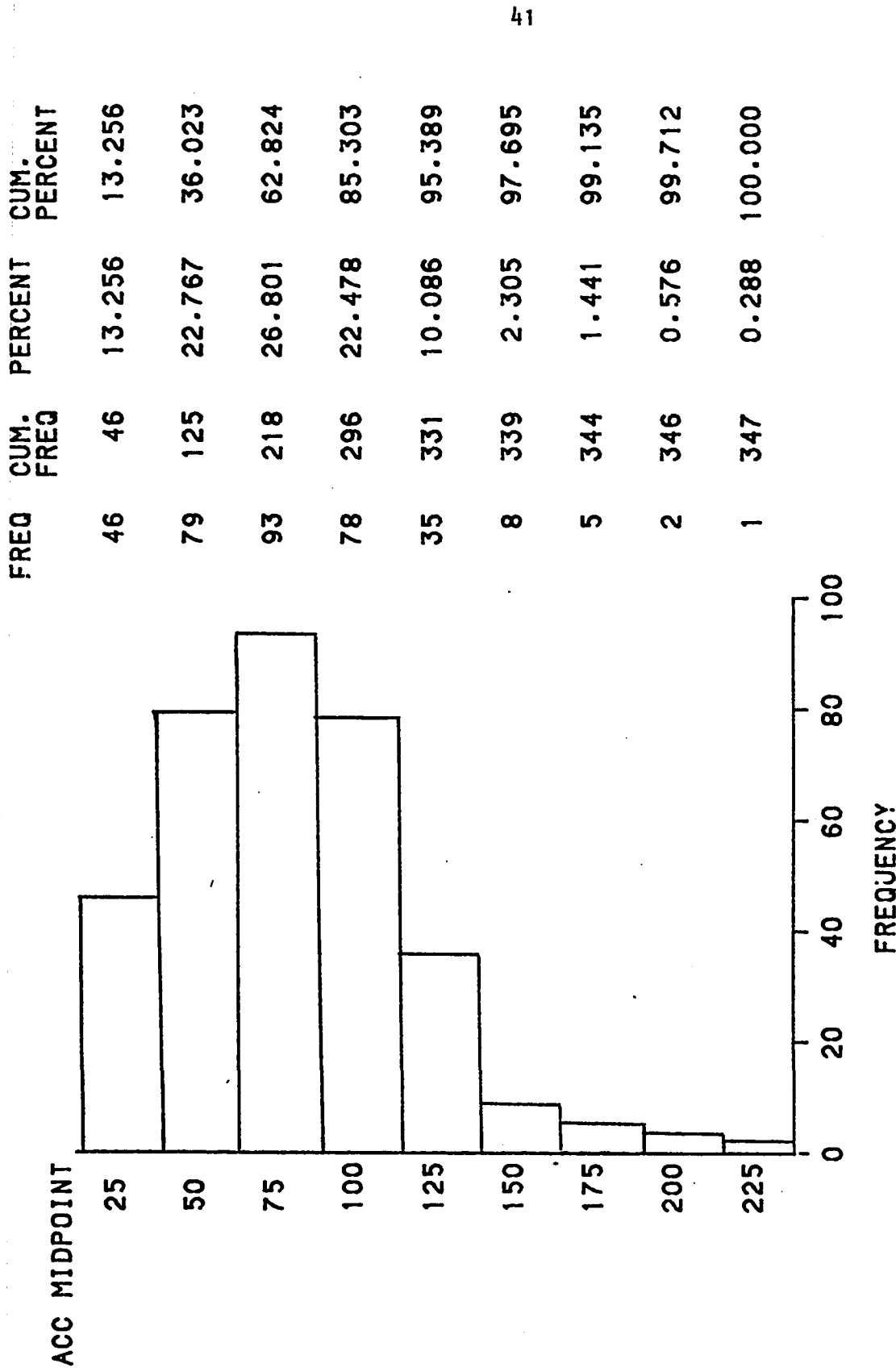


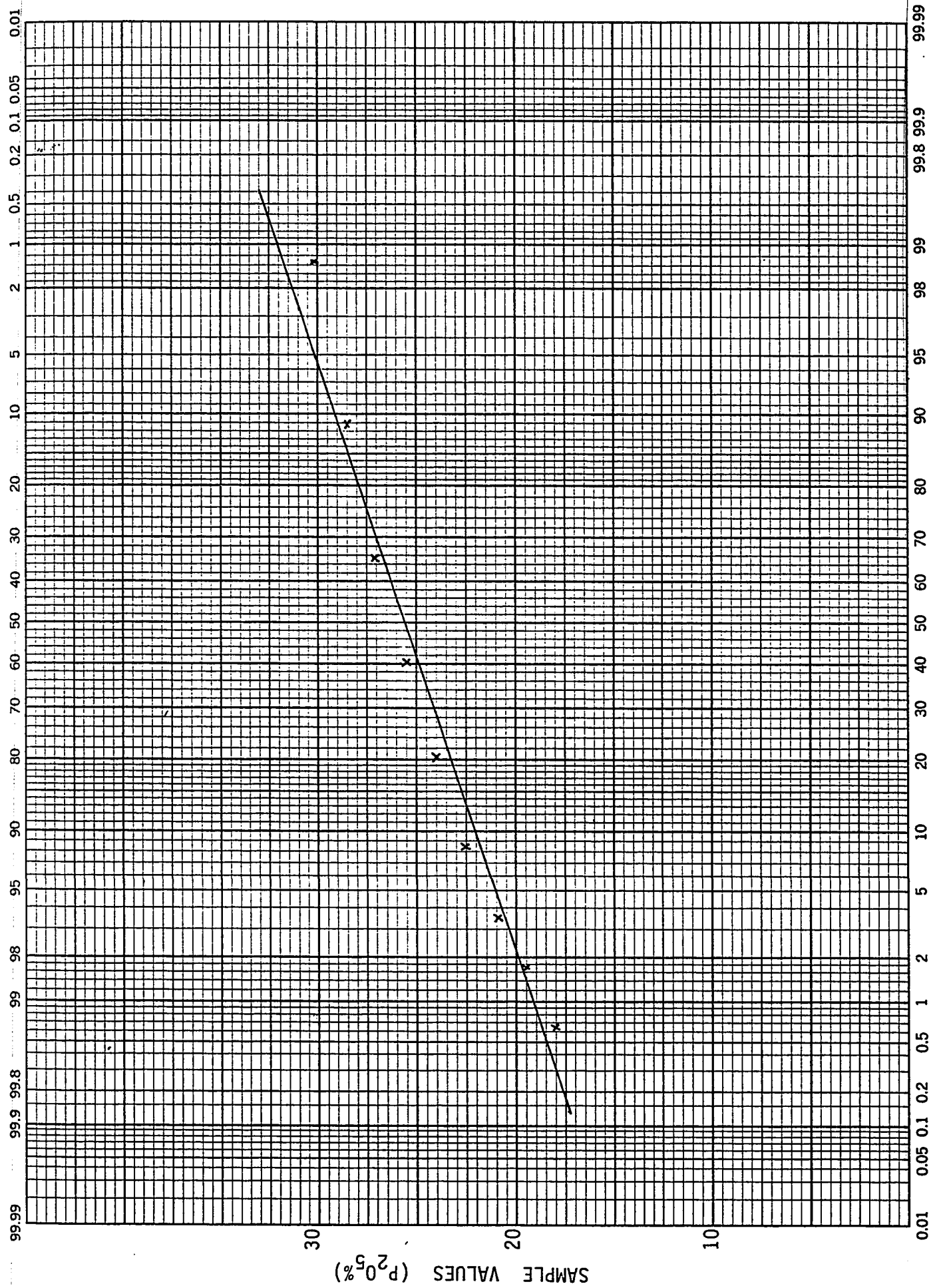
Fig. 4.6 Frequency distribution and histogram for accumulation values.

TABLE 4.1. Summary of Statistical Parameters.
(Abu Tartur Phosphate Deposit).

Variables	Number of samples (n)	Mean (\bar{X})	Variance (S^2)	Standard deviation (S)	Coefficient of variation (S/ \bar{X})
P ₂ O ₅ %	1297	26.58	5.59	2.36	0.089
Thickness (m)	347	2.95	1.61	1.27	0.430
Accumulation (% m)	347	76.58	1292.73	35.95	0.469

4.6 CUMULATIVE FREQUENCY PLOTS

The nature of the skew in the histograms suggested that they may all be approximated by normal distributions. To confirm this the cumulative distribution of the values of each variable has been plotted on the normal-probability graph paper. The resulting plots are presented in Fig. 4.7 to Fig. 4.9. The visual inspection of these plots will reveal that the straight lines can approximately be fitted through the points in each case confirming the approximate normal nature of distributions.

Fig. 4.7 Cumulative frequency plot for $P_{2O_5}\%$

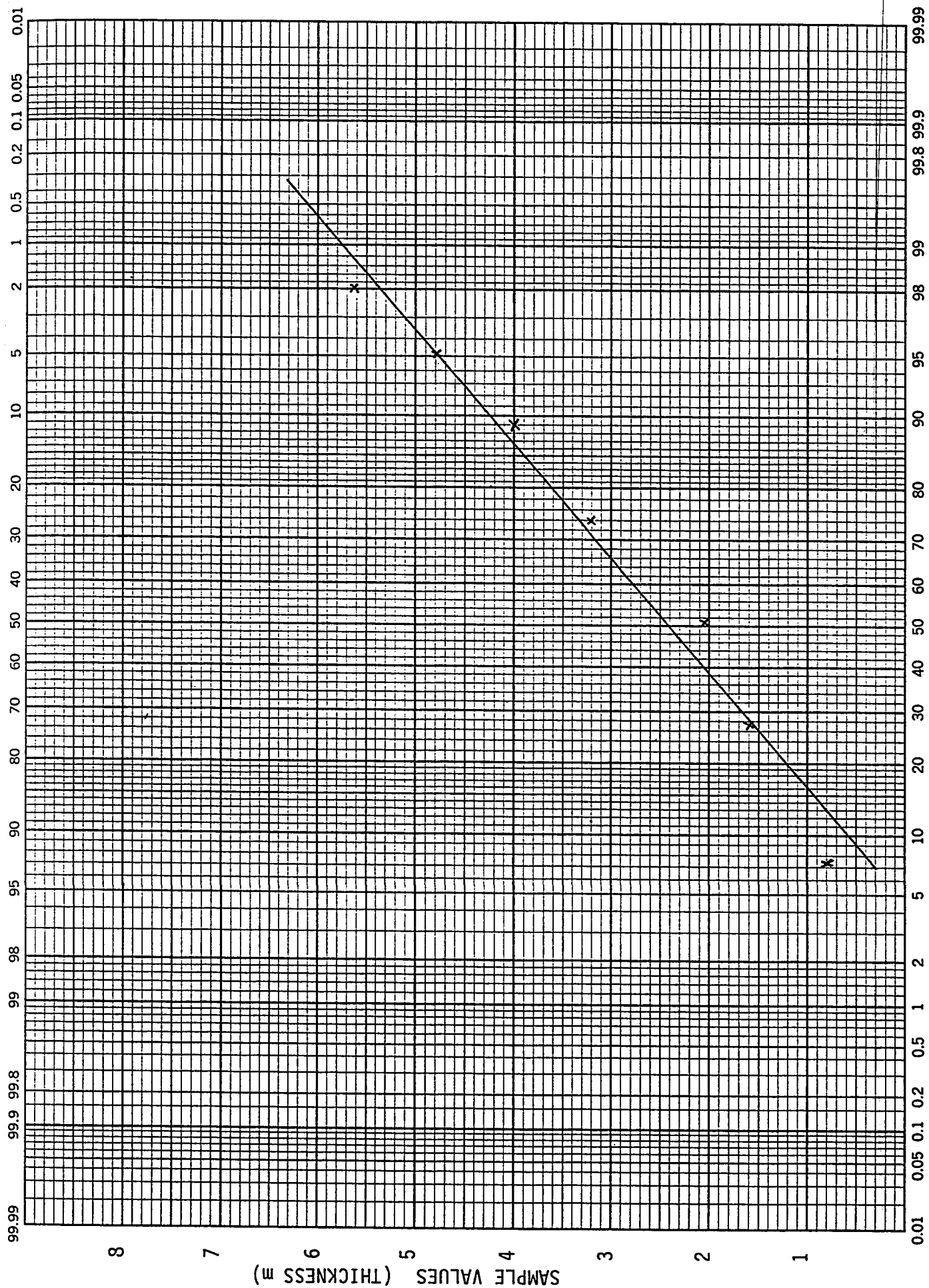


Fig. 4.8 Cumulative frequency plot for thickness

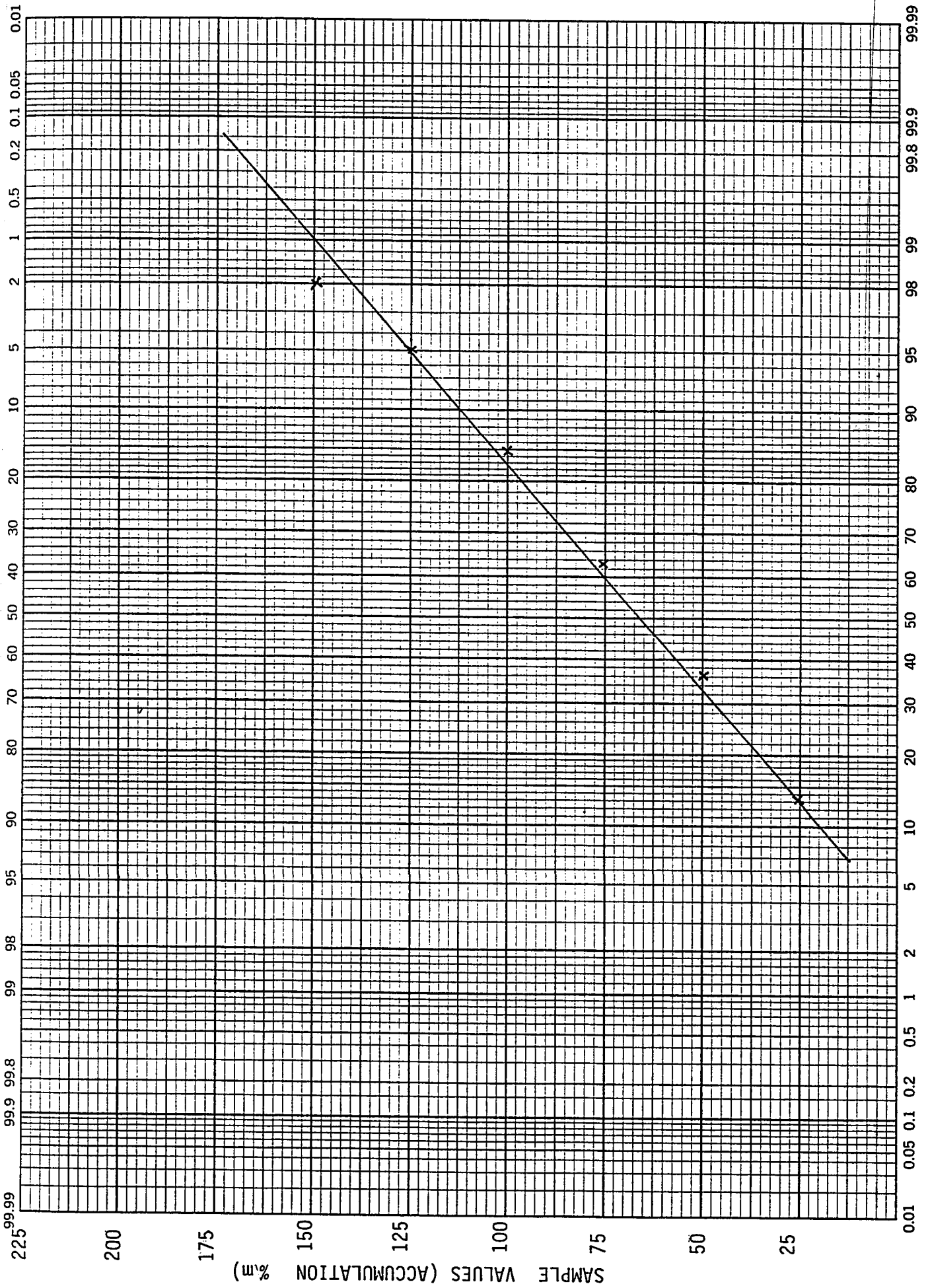


Fig. 4.9 Cumulative frequency plot for accumulation

Chapter 5

SPATIAL DISTRIBUTIONS IN ABU TARTUR DEPOSIT

5.1 INTRODUCTION

The geostatistical estimation involves the following main steps:

- a. Critical review of data,
- b. Construction and interpretation of variograms,
- c. Global estimation of ore reserves,
- d. Local estimation of ore reserves (kriging).

A brief critical review of data from Abu Tartur phosphate deposit is given in the next section. The remaining parts of this chapter are devoted to the construction and interpretation of the experimental variograms including theoretical models fitted to these variograms. The results of the variogram analysis form the basis of the global and local estimations. These estimations will be described and the results discussed in the following chapters (Chapters 6 and 7).

5.2 CRITICAL REVIEW OF DATA

The data used in this study are fully described in the previous chapter (Chapter 4). The techniques employed in sampling and grading are acceptable standard procedures carried out by the qualified Egyptian geological personnel. Thus, there is no reason to question the representativeness of the data.

The variables selected for the study include P_2O_5 (%), thickness (m) and the accumulation (%m). The results of initial statistical treatment of these variables are presented in Chapter 4. The spatial distributions of these variables are determined using variogram.

5.3 VARIOGRAMS

The variogram is the fundamental tool in geostatistics. The experimental variograms are determined for each regionalized variable under consideration using the following expression:

$$\gamma(h) = \frac{\sum_{i=1}^n [Z(x_i) - Z(x_i+h)]^2}{2n} \quad (5.1)$$

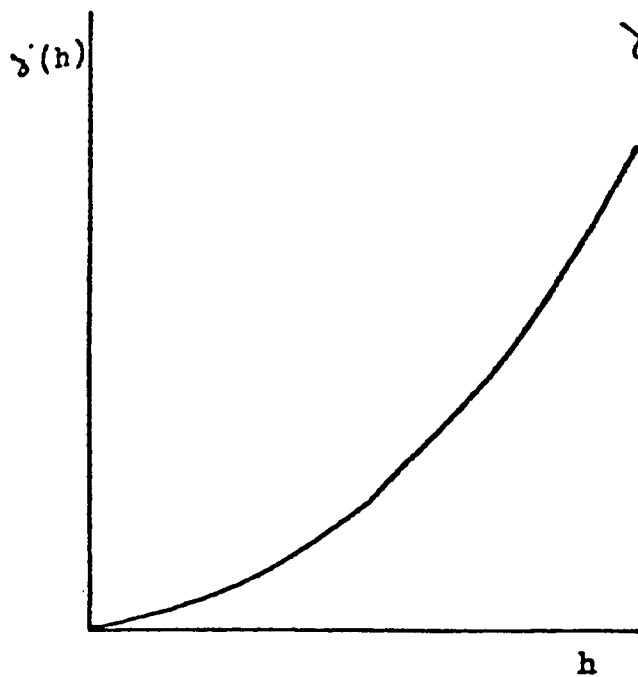
where $Z(x_i)$ and $Z(x_i+h)$ are sample values at location x_i and x_i+h separated by a vector h and n is the total number of sample pairs. Although it is more appropriate to use the term semivariogram for $\gamma(h)$ defined above, many authors shorten this term to variogram for convenience. This approach has also been adopted in this thesis. The experimental variogram is usually calculated using computer. This is because, as the number of samples increases, the sample pairs to be considered becomes unmanageable manually.

The variogram provides both qualitative and quantitative information about the geological characteristics of the regionalized variable. The characteristics revealed by variogram includes the continuity, the anisotropy and the zone of influence.

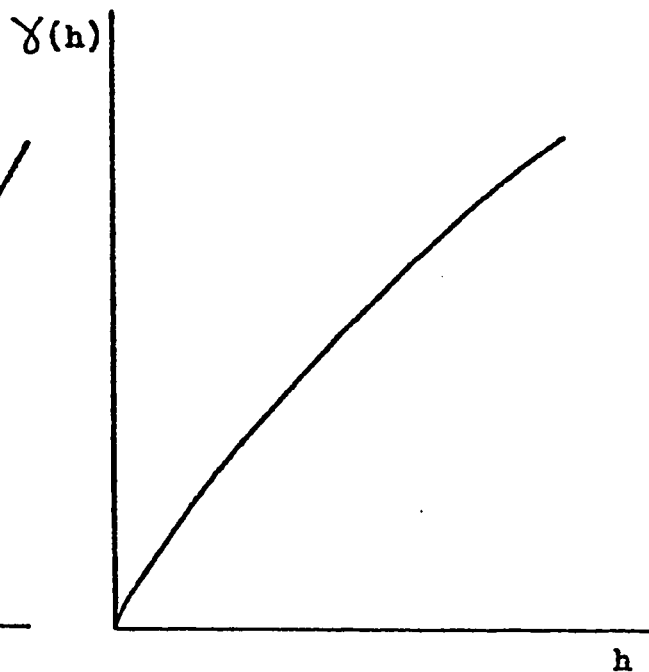
The continuity of a regionalized variable is detected by the behaviour of the variogram near the origin. As shown in Fig. 5.1, it is possible to distinguish four types of behaviour near the origin (Sahin 1977). The first type is recognized with a parabolic behaviour near the origin and indicates a regionalized variable with high continuity. The second type has oblique tangent near the origin and indicates moderate continuity. Many metal deposits are known to give variograms of this type (Royle 1979). The third type is characterized by discontinuity at the origin and corresponds a variable presenting nugget effect. The fourth type is characterized by purely random behaviour. The sample values, in this case, are independent of each other whatever the sampling interval chosen.

The variograms are commonly prepared for samples aligned in several directions to test for the anisotropy. Two types of anisotropy exist. The geometrical anisotropy is revealed by different ranges in different directions. It is due to the presence of structures that have unequal dimensions. The zonal anisotropy is characterized by different sill values in different directions. However, if the variograms are, more or less identical in all directions, the phenomenon under study is said to be isotropic.

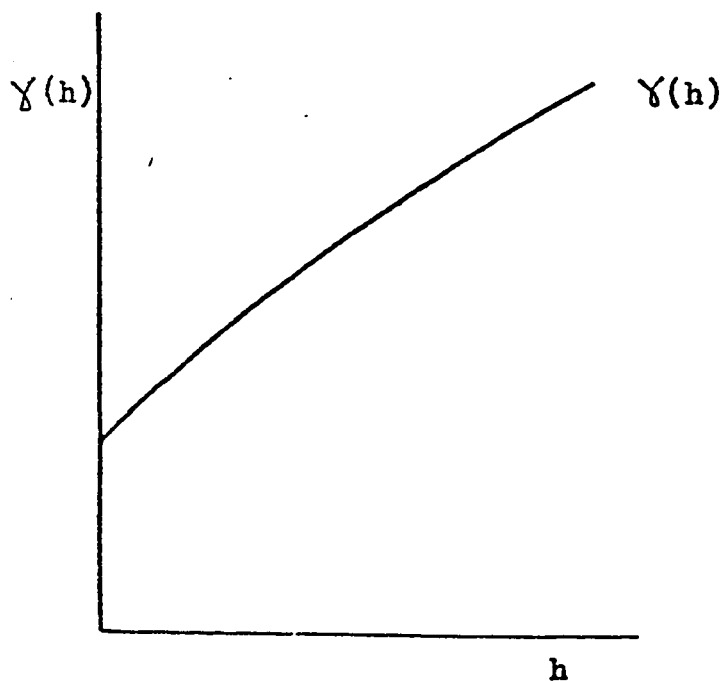
It is common, in practice, to have variogram values increasing up to a certain distance and becoming more or less stable around a sill value. This phenomenon is known as transition phenomenon. The distance after which the $\gamma(h)$ becomes stable is known as the range or the zone of influence of samples.



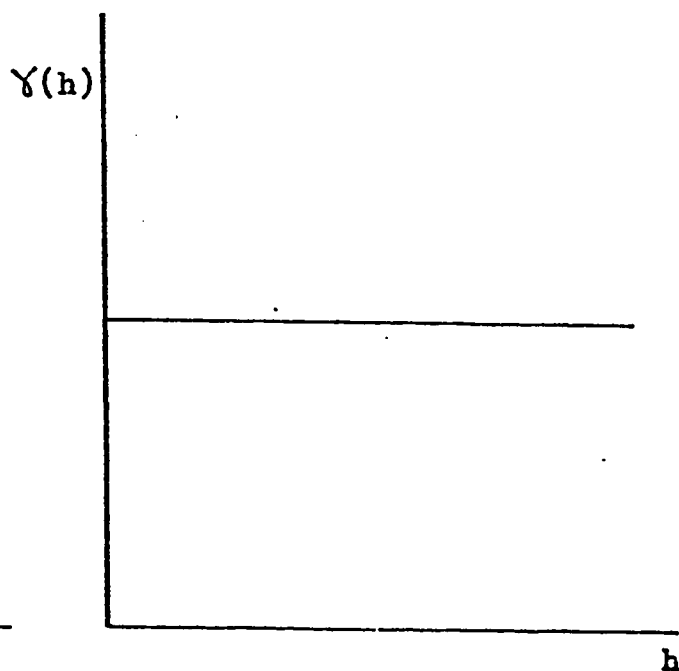
i) Continuous type



ii) Linear type



iii) Nugget type



iv) Random type

Fig.5.1 Behaviour of variograms near origin (after Sahin, 1977)

5.4 ESTIMATION VARIANCES

Besides revealing the above geological characteristics, the variogram can be used to compute the estimation variances. Any estimation procedure is associated with an error. This error, which is known as the estimation error is expressed as $r = Z - Z^*$, where Z is the actual value and Z^* is the estimated value of the variable under consideration. The mean squared error of estimation is known as the estimation variance and can be expressed as:

$$\sigma_E^2 = E [Z - Z^*]^2 \quad (5.2)$$

The estimation variance, which is a measure of the precision of the estimate, can be computed using variogram. Considering two sample grades $Z(x)$ and $Z(x+h)$ separated by vector h , the variogram, for these samples is given by

$$2\gamma(h) = [Z(x) - Z(x+h)]^2 \quad (5.3)$$

Now, assuming $Z(x+h)$ is unknown, the variance of the error when $Z(x+h)$ is estimated by $Z(x)$ is estimated using the following expression:

$$\sigma_E^2 = [Z(x) - Z(x+h)]^2 \quad (5.4)$$

From the Equations (5.3) and (5.4) the relationship between the variogram and the estimation variance, in this simple case, can be expressed as:

$$\sigma_E^2 = 2\gamma(h) \quad (5.5)$$

The general expression for the estimation variance in terms of variogram is given as follows:

$$\sigma_E^2 = 2\bar{\gamma}(V,v) - \bar{\gamma}(V,V) - \bar{\gamma}(v,v) \quad (5.6)$$

where $\bar{\gamma}(V,v)$ for instance represents the mean value of $\gamma(h)$ when one extremity of the vector h describes the volume V and the other extremity independently describes the volume v .

5.5 VARIOGRAM MODELLING

For the purpose of estimation, it is essential to have mathematical equations fitted to the experimental variograms. A variety of mathematical models or schemes have been described in geostatistical literature (David 1977, Journel and Huijbregts 1978). Among these models the spherical or Matheron model which describes transition phenomenon, has been found to give good fits to the variograms of variables from many different mineral deposits. This model, illustrated in Fig. 5.2, is characterized by gradual increase of $\gamma(h)$ as h increases up to a certain value known as the range. Beyond the range, $\gamma(h)$ fluctuates about a line parallel to h axis. In its simplest form, the spherical model is defined by an equation containing three parameters, called the nugget variance (C_0), the sill (C) and the range (a) i.e.

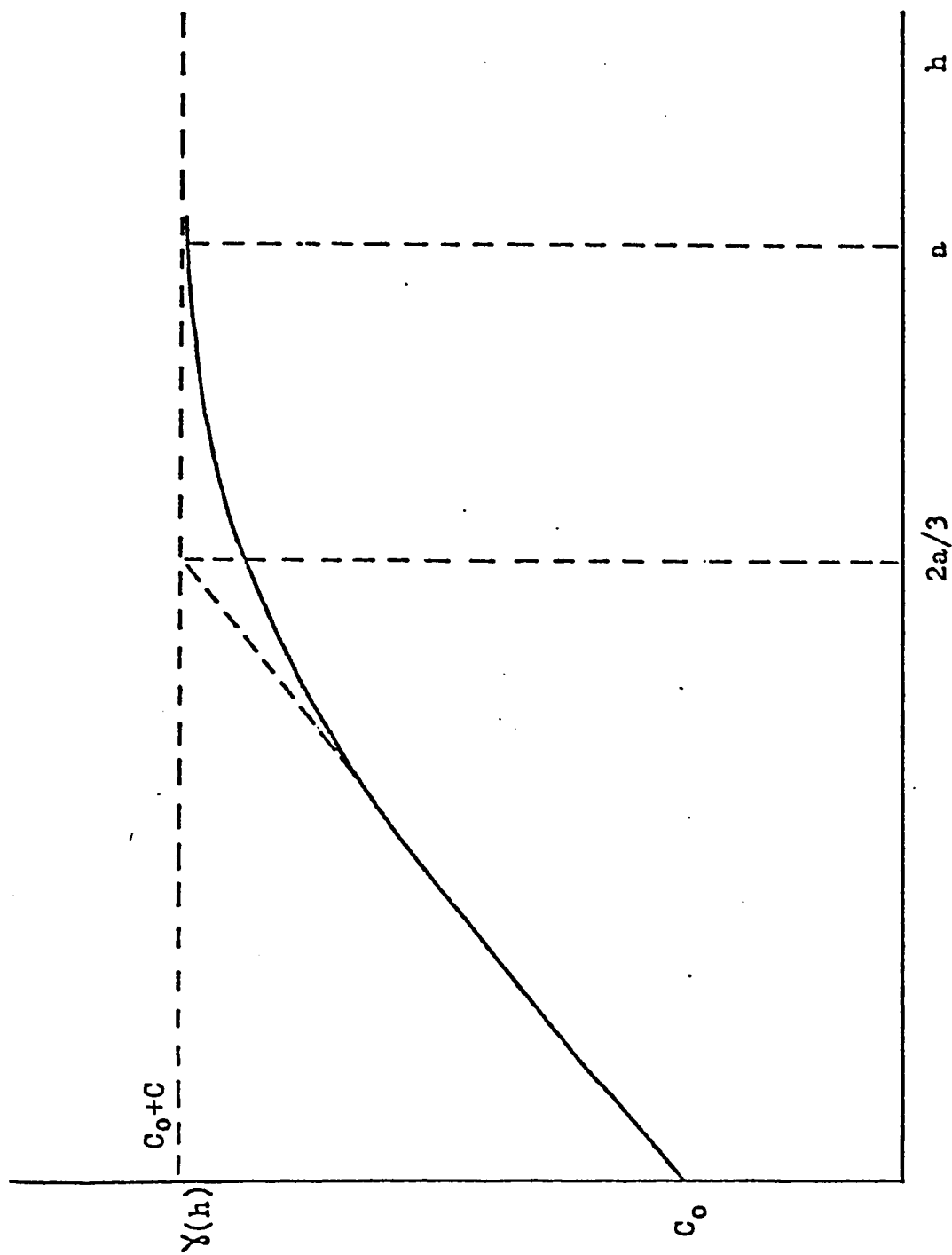


Fig. 5.2 Spherical model illustrating transition phenomenon.

$$\left. \begin{aligned} \gamma(h) &= C_0 + C(3/2 h/a - 1/2 h^3/a^3) && \text{for } h < a \\ \gamma(h) &= C_0 + C && \text{for } h > a \end{aligned} \right\} \quad (5.7)$$

Compound spherical models having the following general expression have also been used

$$\left. \begin{aligned} \gamma(h) &= C_0 + C_1(3/2 h/a_1 - 1/2 h^3/a_1^3) + C_2(3/2 h/a_2 - 1/2 h^3/a_2^3) && \text{for } h < a_1 \\ \gamma(h) &= C_0 + C_1 + C_2(3/2 h/a_2 - 1/2 h^3/a_2^3) && \text{for } a_1 < h < a_2 \\ \gamma(h) &= C_0 + C_1 + C_2 && \text{for } h \geq a_2 \end{aligned} \right\} \quad (5.8)$$

5.6 VARIOGRAMS FOR ABU TARTUR DEPOSIT

The experimental variograms for variables from Abu Tartur phosphate deposit were computed using program VARIO3. This program designed by Geostat Systems Inc. (1984) can handle problems in two or three dimensions and compute variograms for several variables in a single run as well as print and plot the results. In the case of irregularly distributed data, to compute variograms in a particular direction, a regularization angle must be specified (see Fig. 5.3). This angle should be centered on the angular direction, so that any pair falling within the angular sector thus defined is taken as being on the

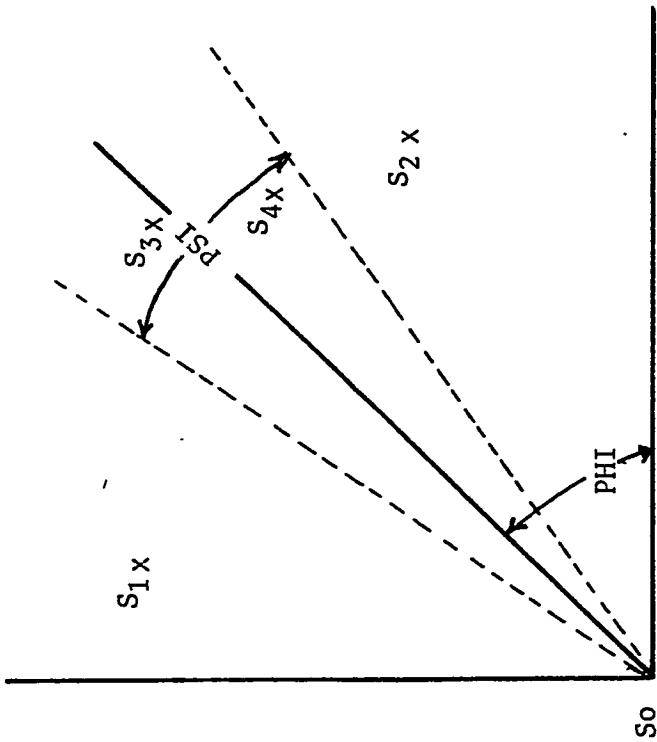


Fig. 5.3 S_0 =reference sample - S_1 and S_2 are rejected -
 S_3 and S_4 are accepted.

PSI =regularization angle

BHI =directional angle

actual direction. If the regularization angle is 180 degrees, all possible pairs of points will be used in the computation of the variogram resulting in the isotropic variogram over the whole plane. When the directional variograms, are required, as far as the data configuration allows a relatively small angle of regularization must be specified.

When the distance (h) separating the points of sample pairs falling within each angular sector are not multiples of the elementary distance, the grouping into distance classes is also required. This is done by specifying a unit distance equal approximately to the average drilling grid size or sub-multiple of it. The variogram is computed for all pairs falling within multiples of this unit distance and assigned to a point situated at a distance corresponding to the average h of all contributing pairs.

The results of the variogram study on Abu Tartur deposit are presented in the following sections. The vertical variogram was computed only for $P_2O_5\%$ of 1-m composites. The horizontal variogram computations on the other hand, were made for $P_2O_5\%$ (1-m composites and mean $P_2O_5\%$ values of drill-holes) as well as thickness and accumulation.

5.6.1 Vertical Variogram for 1-m Composites

The vertical variograms based on $P_2O_5\%$ of 1-m composites were computed for each drill-hole. These variograms were then combined to give the average vertical variogram for the whole deposit using the following expression:

$$\gamma(h) = \frac{\sum_i n_i(h) \gamma_i(h)}{\sum_i n_i(h)} \quad (5.9)$$

Where $\gamma_i(h)$ is the variogram value in i th drill-hole for lag(h) and $n_i(h)$ is the number of data pairs used to calculate $\gamma_i(h)$.

The vertical variogram for $P_2O_5\%$ and the fitted model are illustrated in Fig. 5.4. Considering the general behaviour of the experimental variogram, a simple spherical model with the following parameters has been fitted.

$$C_0 = 0.0 (\%)^2$$

$$C = 9.5 (\%)^2$$

and $a = 2.5 \text{ (m)}$

As the vertical variogram values start at smaller distances, the value of C_0 is fixed fairly accurately from the vertical variogram. Considering the fact that the horizontal and vertical variograms are based on the same data, the value of C_0 fixed from the vertical variogram may be used as an additional data for fitting model to the corresponding horizontal variogram.

5.6.2 Horizontal Variograms

The horizontal variograms in four main directions (E-W, NE-SW, N-S, NW-SE corresponding 0° , 45° , 90° and 135° respectively in program VARIO3) were computed. The angle of regularization was kept 20° for P_2O_5 1-m composites and 45° for other variables. For each variable the directional variograms revealed similar structure with minor variations, only in some cases, in the sill values. They have general spherical behaviour with zero

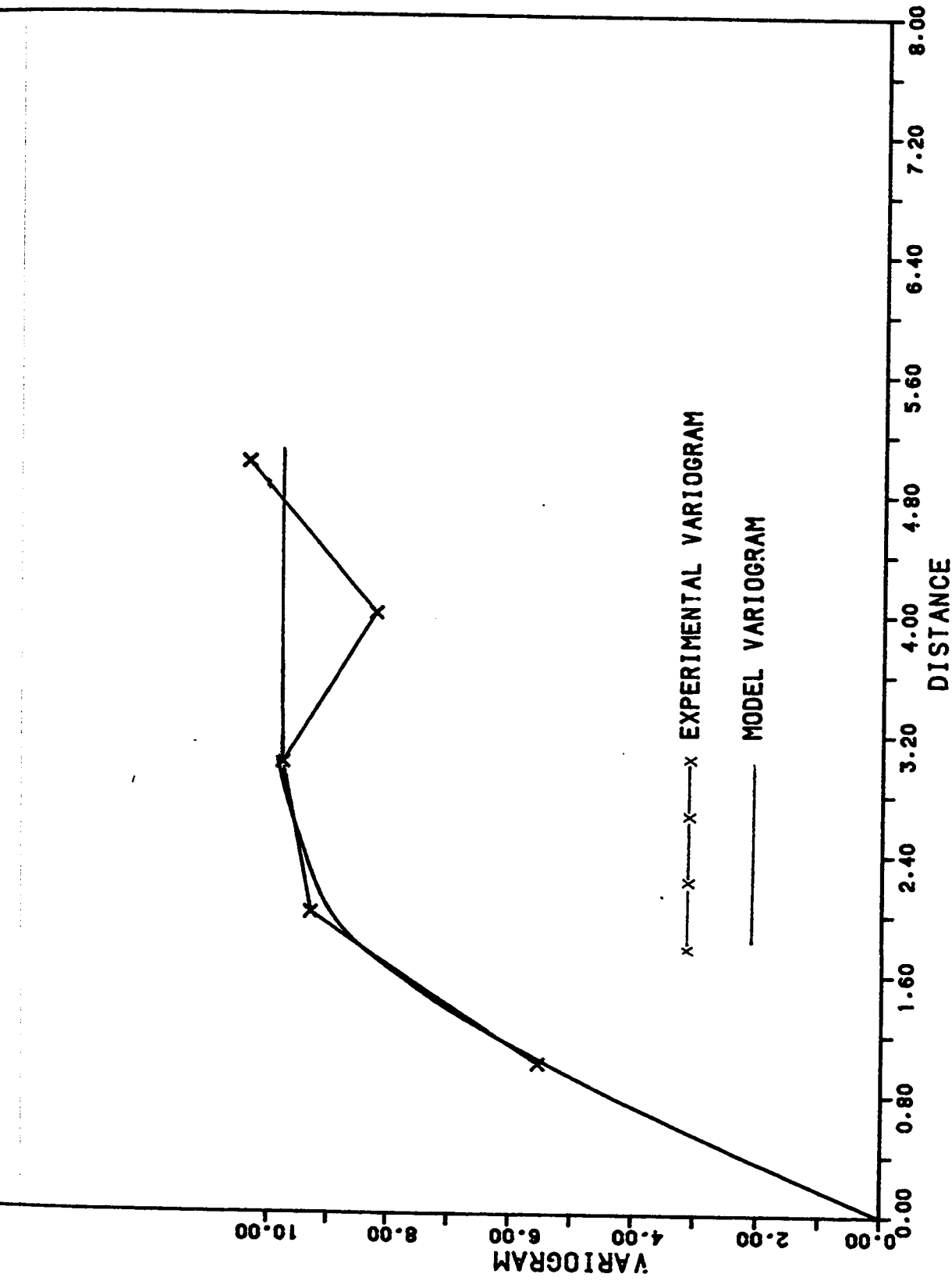


Fig. 5.4 ABU TARTUR - VERTICAL VARIOGRAM AND FITTED MODEL (P205 %- -1M COMPOSITES)

nugget variances. Considering the similarities in the behaviour of these directional variograms, they were combined to give average horizontal variograms for the whole deposit. The directional variograms are illustrated in Appendix 3 and average variograms within the text. Both the direction and the regularization angles are shown on the directional variogram plots. The top number refers to the direction and the bottom to the regularization angle. For instance, the variogram in Appendix 3.1 belongs E-W (i.e. 0°) direction and has been computed with an angular regularization of 20° .

Horizontal variogram for 1-m composites

The horizontal variogram for $P_2O_5\%$ based on 1354 1-m composite samples has been computed. The average isotropic variogram and fitted model are shown in Fig. 5.5. The first point on this variogram, which lies at 55 m from the origin, was estimated with 35 data pairs and the following eleven points were estimated with pairs ranging from 153 to 716. This ensures the reliability of the experimental variogram. Considering the general behaviour of the variogram and the nugget variance fixed from the corresponding vertical variogram ($C_0 = 0$), it can be seen that variogram values increase up to about 80 m, at a greater rate and between 80 m and 700 m at a somewhat slower rate. A compound spherical model with the following parameters gave a good fit to the experimental variogram:

$$C_0 = 0.0 (\%)^2$$

$$C_1 = 2.4 (\%)^2$$

$$C_2 = 2.1 (\%)^2$$

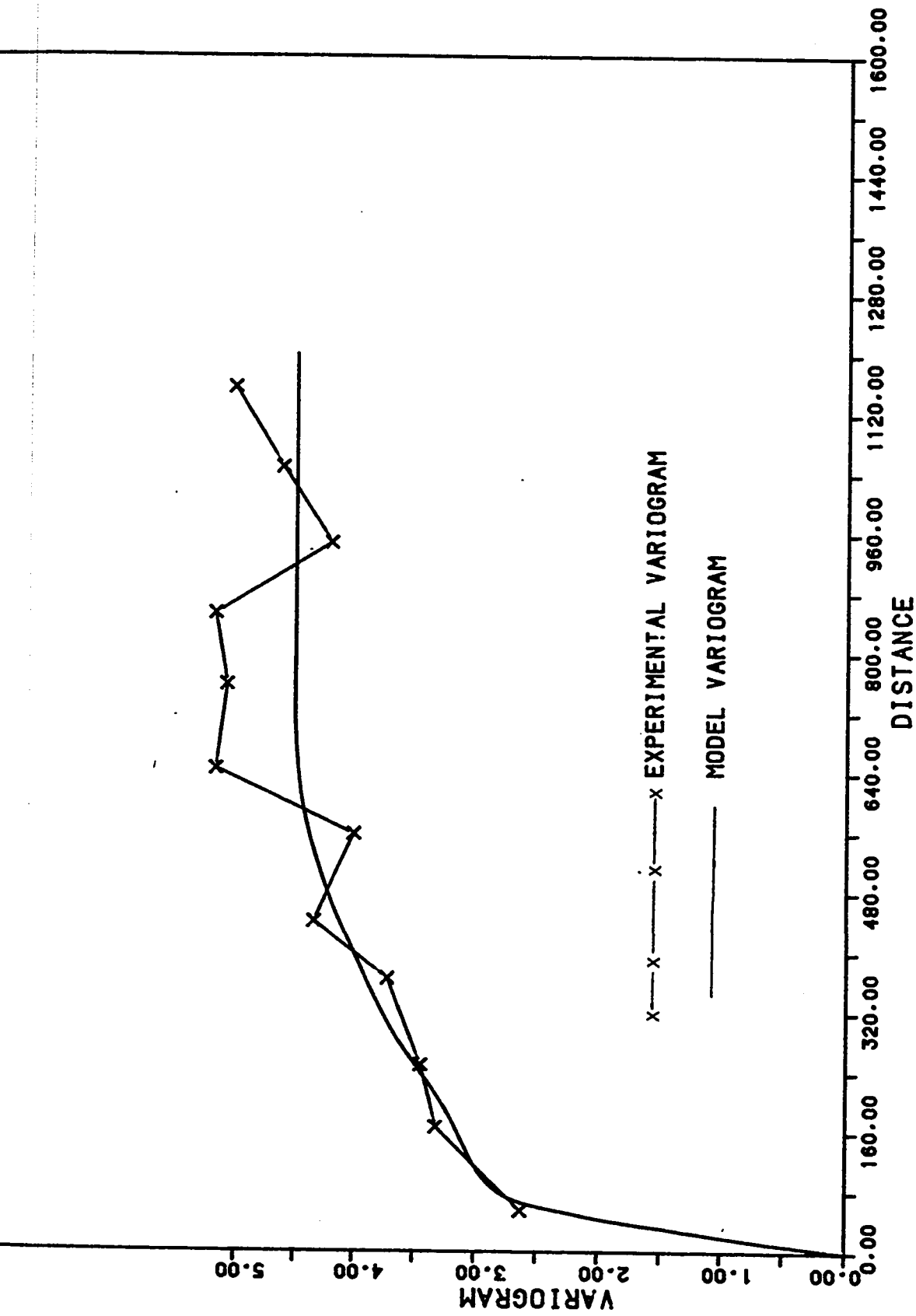


Fig. 5.5 ABO TARTUR - HORIZONTAL VARIOGRAM AND FITTED MODEL (P205 % -1M COMPOSITES)

$$a_1 = 80 \text{ m}$$

and $a_2 = 700 \text{ m}.$

Horizontal variogram for average $P_2O_5\%$

The data from 347 drill-holes were used to compute the horizontal variograms for $P_2O_5\%$. The general behaviour of these variograms are very similar to those of $P_2O_5\%$ from 1-m composites and suggest the applicability of the compound spherical models. The first point on the experimental average variogram illustrated in Fig. 5.6 with fitted model has been estimated with 110 data pairs. The following twelve points were based on far greater number of pairs indicating the reliability of variogram estimates. A compound spherical model with the following parameters has been fitted to the experimental variogram:

$$C_0 = 0 (\%)^2$$

$$C_1 = 3.5 (\%)^2$$

$$C_2 = 3.5 (\%)^2$$

$$a_1 = 175 \text{ m}$$

and

$$a_2 = 800 \text{ m}.$$

Horizontal variogram for thickness

Phosphate thickness data from 347 drill-holes allowed the computation of horizontal variograms for thickness. The average isotropic variogram is shown in Fig. 5.7 together with the fitted model. The first point on the

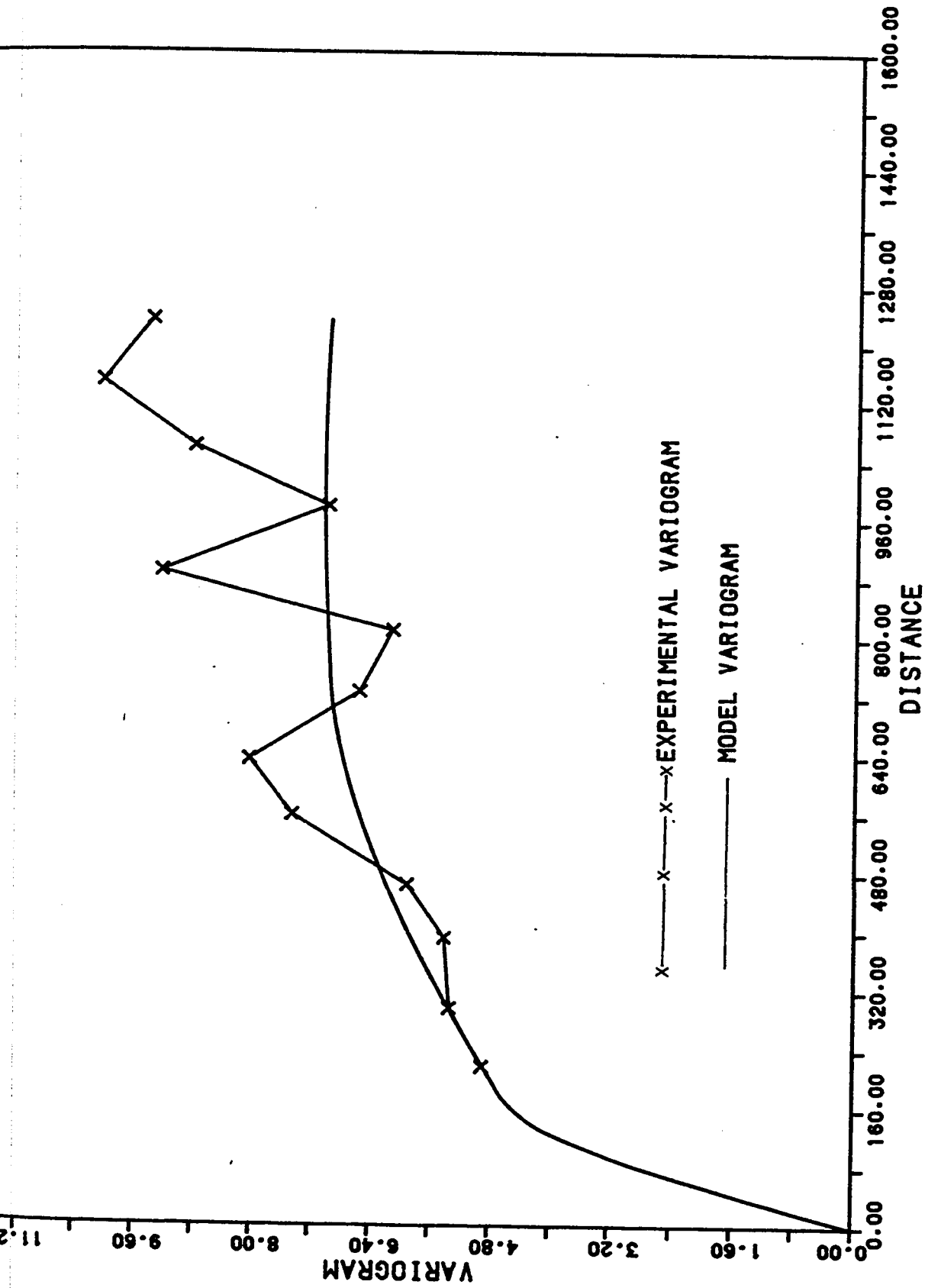


Fig. 5.6 ABU TARTUR - HORIZONTAL VARIOGRAM AND FITTED MODEL (P205 %)

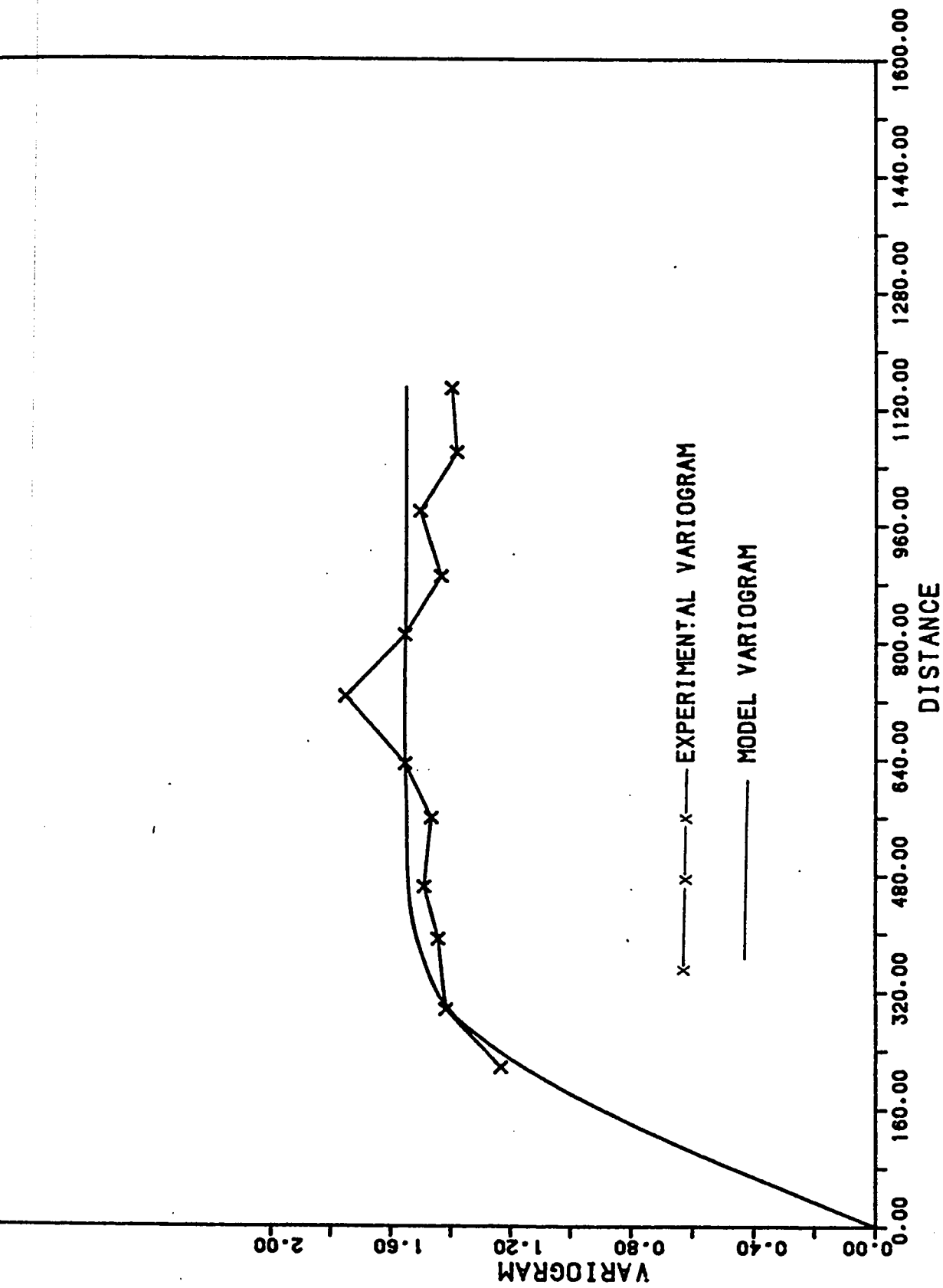


Fig. 5.7 ABU TARTUR - HORIZONTAL VARIOGRAM AND FITTED MODEL (THICKNESS)

experimental isotropic variogram has been estimated with 112 pairs. The other points have been estimated with pairs ranging from 134 to 669. The isotropic variogram indicates that the $\gamma(h)$ values increase regularly up to 375 m, and become more or less stable around $\gamma(h) = 1.5 \text{ (m)}^2$. Considering the behaviour of experimental variogram a simple spherical model with the following parameters has been fitted,

$$C_0 = 0.0 \text{ (m)}^2$$

$$C = 1.5 \text{ (m)}^2$$

and

$$a = 375 \text{ m.}$$

Horizontal variogram for accumulation

The horizontal variogram for accumulation has been computed using the data from 344 drill holes. The average isotropic variogram and fitted model are shown in Fig. 5.8. The first point on this variogram was estimated with 107 pairs. While the other points were estimated with pairs ranging between 133 and 613. The general behaviour of the accumulation variogram is similar to that of the thickness variogram. A simple spherical model with the following parameters has been fitted

$$C_0 = 0.0 \text{ (\%m)}^2,$$

$$C = 1020 \text{ (\%m)}^2$$

and

$$a = 350 \text{ (m).}$$

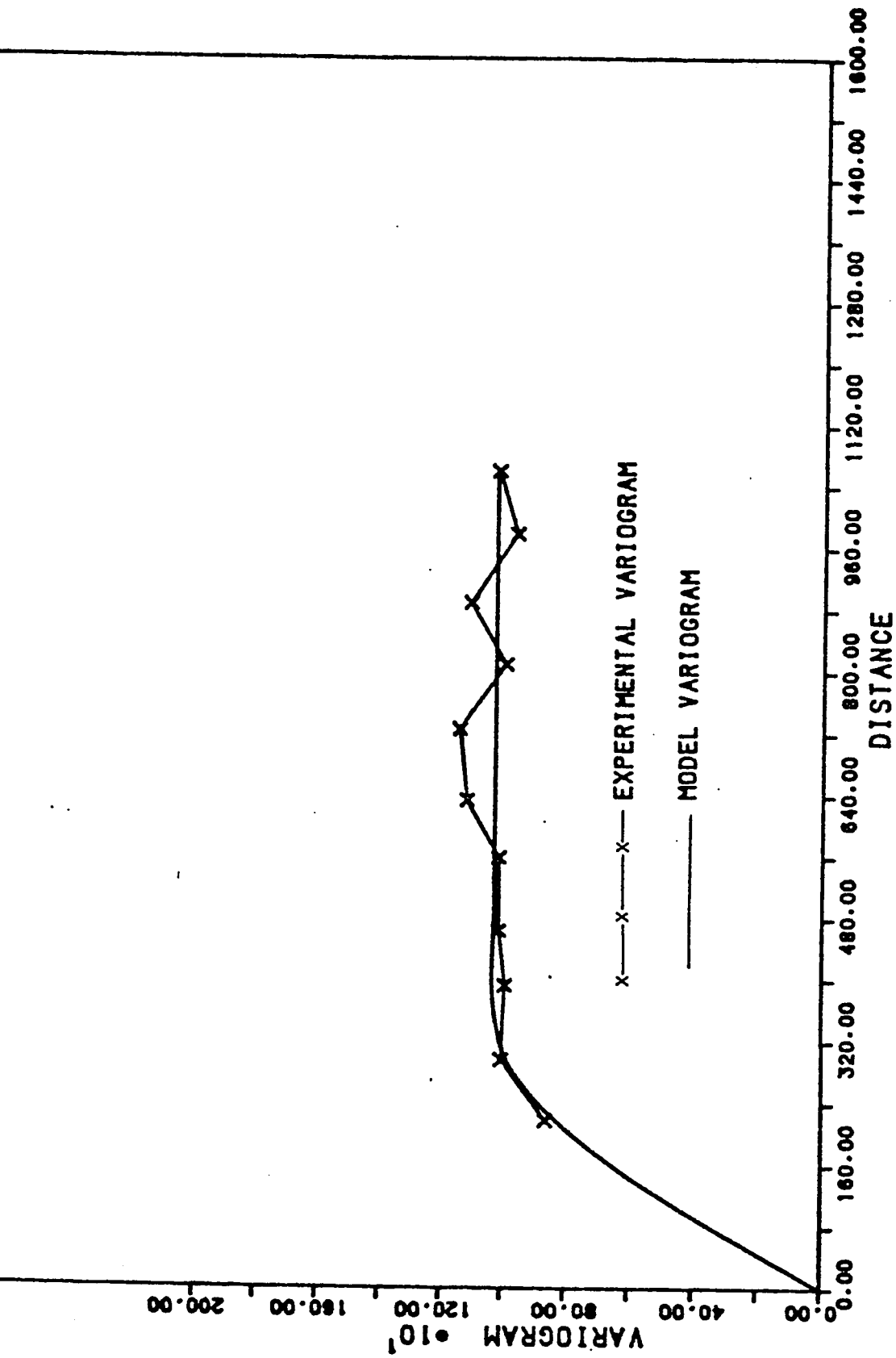


Fig. 5.8 ABU TARTUR - HORIZONTAL VARIOGRAM AND FITTED MODEL (ACCUMULATION)

5.7 SUMMARY

The computation of the variograms is the first and the most important step in a geostatistical estimation procedure. The models fitted are used in subsequent estimations including global estimation and kriging.

All the experimental variograms for Abu Tartur deposit revealed spherical behaviour characterized by a general increase with the distance until the sill value is reached. The spherical models with zero nugget variances have been fitted to all the vertical and horizontal variograms. This indicates the continuity in the spatial behaviour of the variables near the origin. The spatial variation for $P_2O_5\%$ in the vertical direction is greater than that in the horizontal one. This may be due to the horizontal layering which is common in sedimentary deposits.

Chapter 6

GLOBAL ESTIMATION

6.1 INTRODUCTION

As pointed out earlier in Chapter 5, two basic geostatistical methods are available to estimate the ore reserves. These are the global and local (kriging) estimation methods. The global estimation methods permit the computation of the total tonnage, total phosphate ($P_2O_5\%$) content and the mean grade of reserves together with the associated estimation variances. The actual method employed depends on the geological features of the deposit and the methods by which it has been explored and sampled. This implies that the detailed studies on the geology of the deposit as well as the exploration and the sampling methods are necessary before applying any estimation procedure. Therefore, the detailed reviews on the geology of Abu Tartur deposit as well as the available data have been made and presented in Chapter 2 and Chapter 4 respectively.

6.2 DESCRIPTION OF METHOD

The global estimate represents the entire orebody or large part of it. A brief description of the method for determining the global estimates of the total tonnage, total phosphate content and mean grade as well as the

corresponding estimation variances is given below before the application of the method to Abu Tartur phosphate deposit.

6.2.1 Estimation of Tonnage

The estimate for the total tonnage (T) can be expressed simply as follows:

$$T = S \cdot \bar{t} \cdot d. \quad (6.1)$$

where S is the total surface area of the deposit,

\bar{t} is the mean thickness,

and d is the density.

The relative estimation variance for tonnage can be expressed as follows:

$$\sigma_{T/T}^2 = \sigma_{S/S}^2 + \sigma_{\bar{t}/\bar{t}}^2 + \sigma_{d/d}^2 \quad (6.2)$$

where the three terms on the right-hand side are the relative estimation variances of the surface area, the mean thickness and the density respectively. If the variation in density can be assumed to be negligible, the relative estimation variance of total tonnage is reduced to:

$$\sigma_{T/T}^2 = \sigma_{S/S}^2 + \sigma_{\bar{t}/\bar{t}}^2 \quad (6.3)$$

The computations of the relative estimation variance for surface area and thickness are described in the following paragraphs.

Relative estimation variance for surface area

The estimated area of the deposit is simply the area of one grid panel (whose dimensions ℓ and h) multiplied by the total number of grids (n),

$$S = n \times \ell \times h$$

To compute the relative estimation variance of the surface area, Matheron (1968) has derived the following expression:

$$\sigma_S^2/S^2 = 1/n^2 [(1/6)N_2 + 0.0609(N_1^2/N_2)] \quad \text{with } N_2 < N_1 \quad (6.4)$$

where $2N_1$ is the total number of positive grid sides parallel to one axis of the grid and $2N_2$ is the total number of positive grid sides parallel to the other axis.

In Abu Tartur example as shown in Fig. 6.1, random stratified grid (RSG) has been fitted to the drill-hole intersections resulting in 278 square grid with 400 m x 400 m dimensions. Thus, the surface area is

$$S = 278 \times 400 \times 400 = 44.48 \times 10^6 \text{ sq. m.}$$

$$2N_1 = 50 \text{ (number of grid sides parallel to one axis of the grid)}$$

$$2N_2 = 30 \text{ (number of grid sides parallel to the other axis of the grid)}$$

Substituting the numerical values for S , N_1 and N_2 in Eqn. (6.4),

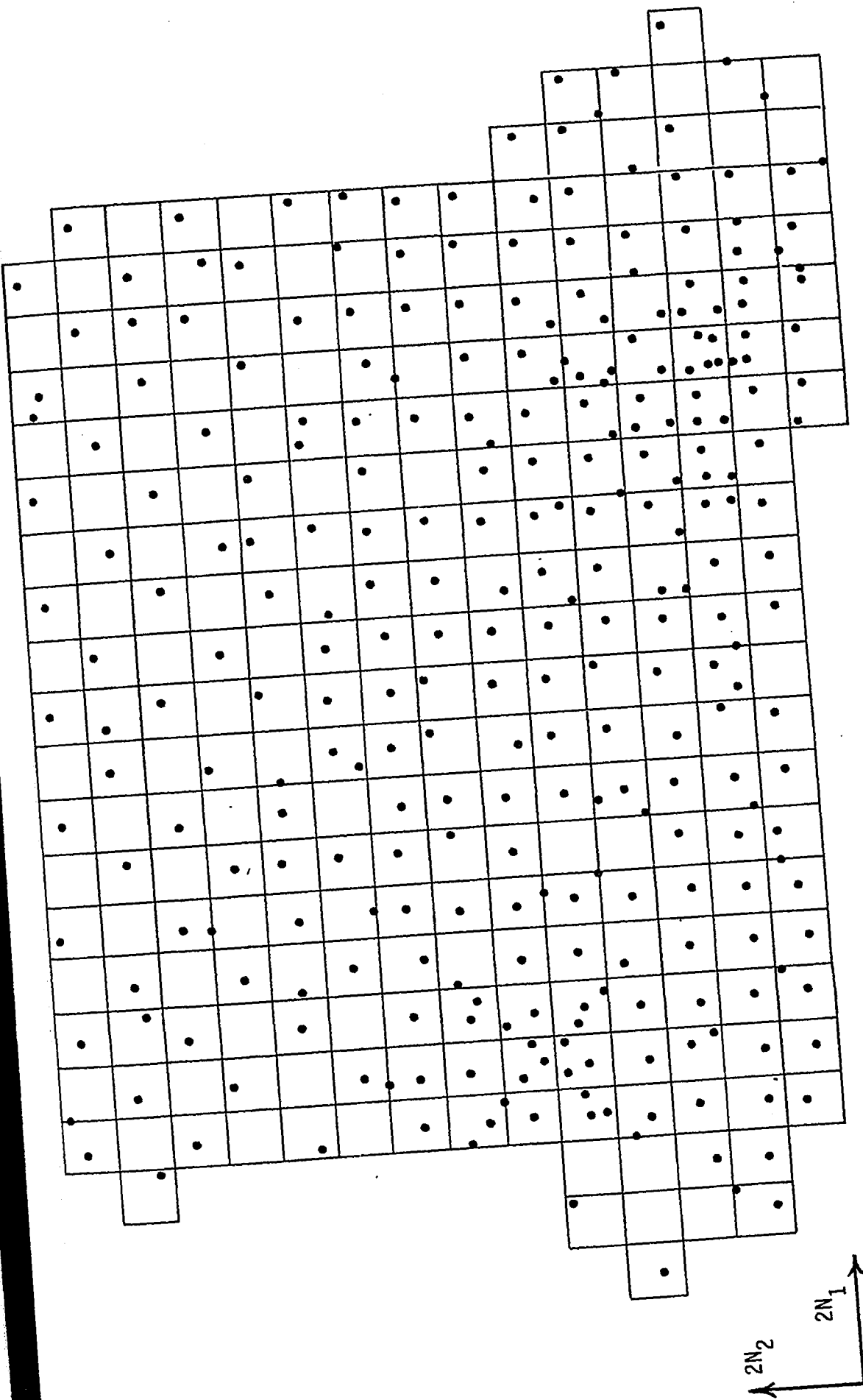


Fig. 6.1 400mx400m square RSG fitted to Abu Tartur Phosphate deposit

$$\sigma_S^2/S^2 = (1/278^2) [(15/6) + 0.0609 (25^2/15)]$$

$$\sigma_S^2/S^2 = 6.52 \times 10^{-5}$$

is obtained.

Estimation variance for mean thickness

When the spherical model is applicable, the estimation variance for the mean thickness in the case of RSG can be estimated using the following expression:

$$\sigma_t^2 = \frac{1}{n} [C_o + C.F(l/a, h/a)] \quad (6.5)$$

where C_o , C and a are the variogram model parameters for thickness and $F(l/a, h/a)$ is a factor obtained from the chart given in Fig. 6.2.

6.2.2 Estimation of Phosphate Content

The total quantity of P_2O_5 (Q) is the product of the total estimated tonnage of the deposit and the mean grade

$$\text{i.e.} \quad Q = T \times \bar{g} \quad (6.6)$$

$$\text{or} \quad Q = \bar{ac} \times S \times d$$

where \bar{g} is the mean grade and \bar{ac} the mean accumulation.

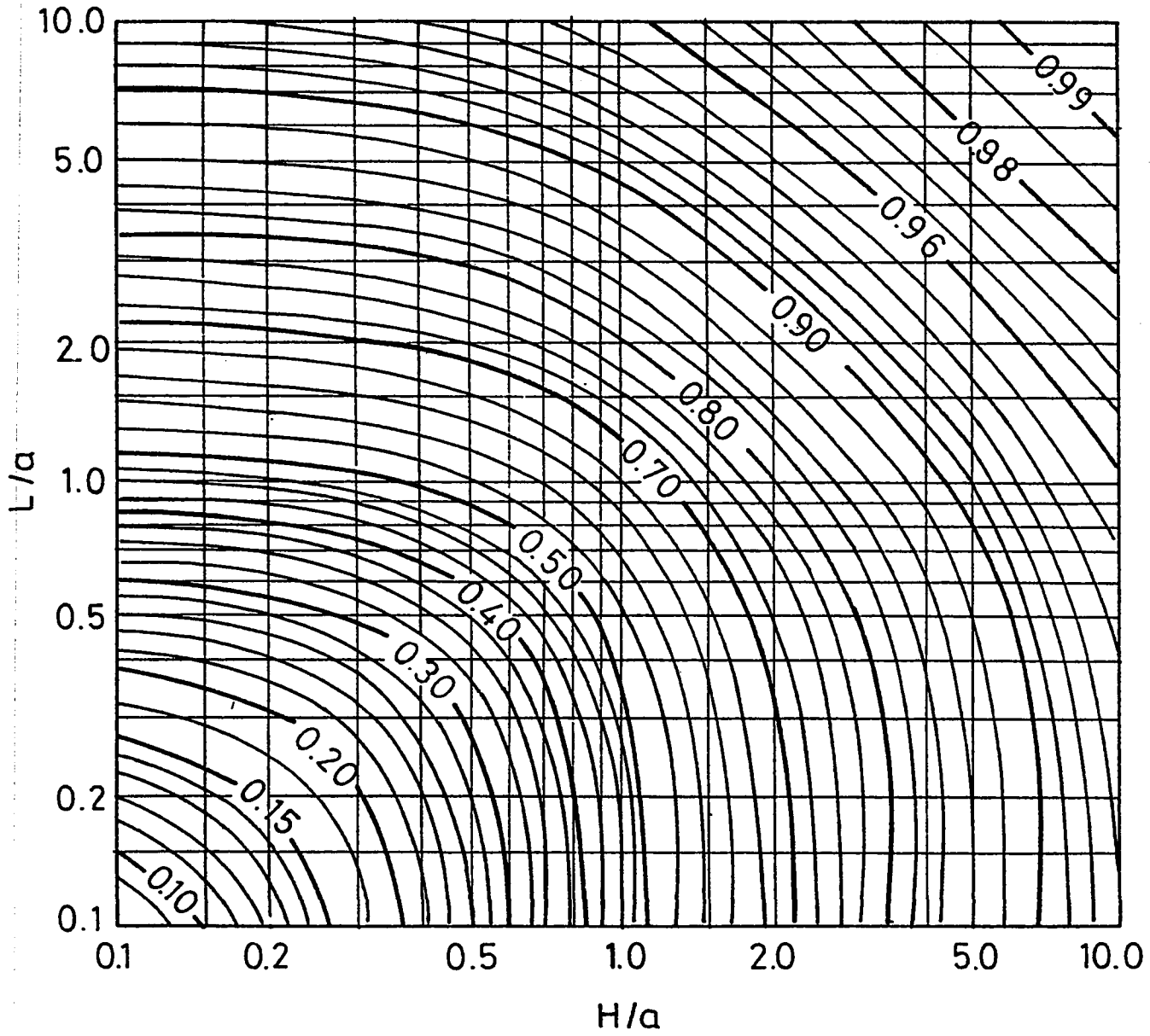


Fig.6.2 Two-dimensional F-function, $F(H/a, L/a)$ for spherical model (after Royle, 1972).

The relative estimation variance of the total P_2O_5 content is given by

$$\sigma_Q^2/Q^2 = \sigma_{ac}^2/ac + \sigma_S^2/S^2 \quad (6.7)$$

The computation of the relative estimation variance of surface area has already been shown in section 6.2.1. The estimation variance for accumulation can be estimated similar to that of mean thickness using the variogram parameters

$$\sigma_{ac}^2 = \frac{1}{n} [C_0 + C.F(l/a, h/a)] \quad (6.8)$$

where C_0 , C and a are the variogram model parameters for accumulation.

6.2.3 Estimation of Mean Grade

The mean grade is obtained simply by dividing the mean accumulation (\overline{ac}) value by the mean thickness (\overline{t})

$$\overline{g} = \overline{ac}/\overline{t} \quad (6.9)$$

The estimation variance for the mean grade is given by

$$\sigma_g^2/g^2 = \sigma_{ac}^2/\overline{ac}^2 + \sigma_t^2/\overline{t}^2 - 2\rho_{ac.t} (\sigma_{ac}/\overline{ac} \cdot \sigma_t/\overline{t}) \quad (6.10)$$

where $\rho_{ac.t}$ is the correlation coefficient between the accumulation and thickness.

6.3 APPLICATION TO ABU TARTUR PHOSPHATE DEPOSIT

The global estimation method, described in the previous paragraphs, has been applied to a part of Abu Tartur phosphate deposit. A RSG with 400 m x 400 m dimensions has been fitted to the drill-hole intersections resulting in 278 square grids shown in Fig. 6.1. As pointed out earlier to derive the global estimates, the mean thickness, the mean accumulation and the density values are also required. These values have been estimated to be 2.95 m, 76.75% m and 2.35 tons/cu. m. respectively.

To compute the estimation variances associated with the global estimates, the model variogram parameters and the correlation coefficient between thickness and accumulation are required. The values of model variogram parameters for the variables under consideration are listed in Table 6.1. The correlation coefficient between accumulation and thickness has been estimated to be 0.96.

6.3.1 Estimation of Tonnage

Substituting the numerical values in Eqn. (6.1), the estimate for the total tonnage (T) is obtained as follows:

$$T = 44.48 \times 10^6 \times 2.95 \times 2.35$$

$$T = 308.36 \text{ Mt.}$$

TABLE 6.1. Variogram Parameters.

Variables	C_0	C_1	C_2	a_1	a_2
$P_2O_5 (\%)^2$	$0.0 (\%)^2$	$3.5 (\%)^2$	$3.5 (\%)^2$	175 m	800 m
Thickness	$0.0 (m)^2$	$1.5 (m)^2$	-	375 m	-
Accumulation	$0.0 (\%m)^2$	$1020 (\% m)^2$	-	350 m	-

The relative estimation variance for the tonnage can be determined using Eqn. (6.3). The relative estimation variance for the surface area, the first term in Eqn. (6.3), was found earlier to be 6.52×10^{-5} . The second term is obtained as follows by substituting the values of model parameters and F-function in Eqn. (6.5)

$$\sigma_t^2 = (1.5/278)[F(400/375, 400/375)]$$

$$\sigma_t^2 = 0.0054[F(1.07, 1.07)]$$

$$\sigma_t^2 = 0.0037 \text{ (m)}^2$$

is obtained. Thus, the relative estimation variance for the thickness is

$$\sigma_t^2/t^2 = (0.0037)/(2.95^2)$$

$$\sigma_t^2/t^2 = 4.25 \times 10^{-4}$$

Finally, the relative estimation variance for the total tonnage is:

$$\sigma_T^2/T^2 = 6.52 \times 10^{-5} + 4.25 \times 10^{-4}$$

$$\sigma_T^2/T^2 = 4.90 \times 10^{-4}$$

$$\sigma_T/T = 0.022$$

$$\sigma_T = 6.78 \times 10^6 \quad (2\sigma_T = 13.56 \times 10^6)$$

Hence, at the 95% confidence level the reserves are approximately 308.36 ± 13.56 Mt.

Estimation of total phosphate content

The Eqn. (6.6) is used to determine the total $P_2O_5\%$ content, substituting the values of S and \overline{ac} ,

$$Q = (76.58/100) \times 44.48 \times 2.35$$

$$Q = 80.05 \text{ Mt.}$$

is found.

The relative estimation variance for the total $P_2O_5\%$ content is given by the sum of two terms: the relative estimation variance of the surface area and the relative estimation variance of the accumulation. The value of the first term has been determined already. The second term is estimated as follows:

$$\sigma_{ac}^2 = (1020/278)[F(400/350, 400/350)]$$

$$\sigma_{ac}^2 = 3.6691[F(1.14, 1.14)]$$

$$= 2.568 (\% m)^2$$

Now, the relative estimation variance for the accumulation is,

$$\sigma_{ac}^2 / \bar{ac}^2 = 2.568 / (76.58)^2 = 4.38 \times 10^{-4}$$

Hence, the relative estimation variance for the total P_2O_5 % content is,

$$\sigma_{Q/Q}^2 = 4.38 \times 10^{-4} + 6.52 \times 10^{-5}$$

$$\sigma_{Q/Q}^2 = 5.032 \times 10^{-4}$$

$$\sigma_{Q/Q} = 0.022$$

$$\sigma_{Q.} = 0.076 \times 10^6 (2\sigma_{Q.} = 0.152 \times 10^6)$$

So that the total P_2O_5 % content of the reserves is approximately 80.05 ± 0.152 Mt. at 95% confidence level.

Estimation of mean grade

The mean P_2O_5 % determined using Eqn. (6.9)

$$\bar{g} = (76.58 / 2.95) = 26\%$$

The estimation variance for the grade (σ_g^2) associated with this value is derived as follows:

$$\sigma_g^2 = 4.38 \times 10^{-4} + 4.25 \times 10^{-4} - 2(0.9629)(0.021)(0.021)$$

$$\sigma_g^2 = 1.372 \times 10^{-5}$$

$$\sigma_g = 3.704 \times 10^{-3}$$

$$\sigma_g = 0.096 \quad (2\sigma_g = 0.192)$$

Thus, at the 95% confidence level the mean P_2O_5 % estimate is approximately $26\% \pm 0.192\%$.

6.4 FINAL REMARKS

The global estimation results for Abu Tartur phosphate deposit including the estimation standard deviation, the relative estimation standard deviations and the 95% confidence limits have been listed in Table 6.2. To make the direct comparison between the reliability of the various estimates possible, the confidence limits have also been expressed in percentage terms. The values of the confidence limits are, in all cases, less than 5%. The lowest value with 0.8% belongs to the grade estimate and the highest value with 4.4% belongs to both the phosphate content and the total tonnage estimates.

TABLE 6.2. Summary of Global Estimation Results for Abu Tartur Deposit.

Variables	Estimates	Estimation standard deviation (σ_E)	Relative estimation standard deviation (σ_{E/Z^*})	95% confi- dence limits ($\pm 2\sigma_E$)	$\pm 2\sigma_E$ (%)
Surface area ($m^2 \times 10^6$)	44.48	0.358	0.008	0.718	1.6
Mean thickness (m)	2.95	0.061	0.021	0.122	4.2
Tonnage (tons $\times 10^6$)	308.36	6.780	0.022	13.560	4.4
Mean accumulation (m%)	76.58	1.602	0.021	3.204	4.1
Phosphate content (P_2O_5 %)	80.05	0.076	0.022	0.152	4.4
(tons $\times 10^6$)					
Grade (%)	26.00	0.096	0.004	0.192	0.8

Chapter 7

LOCAL ESTIMATION (KRIGING)

7.1 INTRODUCTION

Kriging, the procedure used to obtain local estimates, has been described in detail by several workers including David (1977), Journel and Huijbregts (1978), and Brooker (1979). It is the fundamental estimation method in geostatistics with widespread practical applications. In mineral evaluation, the kriging provides the minimum variance unbiased estimates referred to as the kriged estimates for blocks of specified size. The minimum variance, known as the kriging variance associated with each estimate, is used to measure the reliability of the estimate. In the following section, a brief description of the block kriging is given before its application to Abu Tartur deposit.

7.2 BLOCK KRIGING

Let x_1, x_2, \dots, x_n be grades to be used to estimate the grade of a block of ore. This estimate is given by:

$$Z_K^* = \sum_{i=1}^n \lambda_i x_i \quad (7.1)$$

where λ_i are the weighting coefficients assigned to the samples.

Two conditions must be fulfilled to make Z^* the best possible linear estimator:

(i) Z_K^* must be an unbiased:

$$\text{i.e. } E[Z - Z^*] = 0 \quad (7.2)$$

where Z is the actual value of the block. This condition implies that sum of the weights is equal to unity, i.e.

$$\sum_{i=1}^n \lambda_i = 1 \quad (7.3)$$

ii) The estimation variance: $E[(Z - Z^*)^2]$ must be minimum.

The minimization of the variance under the constraint $\sum \lambda_i = 1$ leads to the minimization of $E[(Z - Z^*)^2] + 2\mu(\sum \lambda_i - 1)$ where μ is a lagrange multiplier.

The estimation variance $E[(Z - Z^*)^2]$ can be expanded as follows:

$$\begin{aligned} E[(Z - Z^*)^2] &= E(Z^2) - 2E(ZZ^*) + E(Z^*{}^2) \\ &= E(Z^2) - 2E(Z \sum \lambda_i x_i) + E(\sum \lambda_i \lambda_j x_i x_j) \\ &= \sigma_Z^2 - 2 \sum \lambda_i \sigma_{Zx_i} + \sum \lambda_i \lambda_j \sigma_{x_i x_j} \end{aligned} \quad (7.4)$$

Now,

$$\frac{\partial}{\partial \Sigma \lambda_i} [\sigma_Z^2 - 2 \Sigma \lambda_i \sigma_{Zx_i} + \Sigma \lambda_i \lambda_j \sigma_{x_i x_j} + 2\mu(\Sigma \lambda_i - 1)] = 0$$

gives the following system known as the kriging system:

$$\left. \begin{aligned} \Sigma \lambda_j \sigma_{x_i x_j} + \mu &= \sigma_{Zx_i} & i = 1, 2, \dots, n \\ \Sigma \lambda_i &= 1 \end{aligned} \right\} \quad \text{I}$$

multiplying both sides of the first expression in system I by $\Sigma \lambda_i$, and

substituting $\Sigma \lambda_i \lambda_j \sigma_{x_i x_j} = \sigma_{Zx_i}^2 = -\mu$ in Eqn. (7.4) gives the kriging variance, σ_k^2

$$\sigma_k^2 = \sigma_Z^2 - \Sigma \lambda_j \sigma_{Zx_i} - \mu \quad (7.5)$$

The kriging system can also be expressed in terms of the variogram function. Substituting $\gamma(\infty) - \gamma(h)$ for $\sigma(h)$ produces,

$$\left. \begin{aligned} \Sigma \lambda_j \gamma_{x_i x_j} - \mu &= \gamma_{Zx_i} & i = 1, 2, \dots, n \\ \Sigma \lambda_i &= 1 \end{aligned} \right\} \quad \text{II}$$

and the corresponding kriging variance is given as follows:

$$\sigma_k^2 = -\gamma + \sum \lambda_i \gamma_i - \mu \quad (7.6)$$

The kriging system, which is a system of $n+1$ equations with $n+1$ unknowns can be written in matrix form as follows:

$$[\Sigma][A] = [D]$$

$$[\Sigma] = \begin{bmatrix} \gamma_{11} & \gamma_{12} & \cdots & \gamma_{1n} & 1 \\ \gamma_{21} & \gamma_{22} & \cdots & \gamma_{2n} & 1 \\ \cdot & \cdot & & \cdot & \cdot \\ \cdot & \cdot & & \cdot & \cdot \\ \gamma_{n1} & \gamma_{n2} & & \gamma_{nn} & 1 \\ 1 & 1 & & 1 & 0 \end{bmatrix}$$

$$[A] = \begin{bmatrix} \lambda_1 \\ \lambda_2 \\ \cdot \\ \cdot \\ \lambda_n \\ \mu \end{bmatrix} \quad \text{and} \quad [D] = \begin{bmatrix} \lambda_{Zx_1} \\ \lambda_{Zx_2} \\ \cdot \\ \cdot \\ \lambda_{Zx_n} \\ 1 \end{bmatrix}$$

7.3 BLOCK KRIGING FOR ABUT TARTUR DEPOSIT

To determine the kriged estimates of P_2O_5 % for Abu Tartur phosphate deposit, the deposit was divided into horizontal slices (as in the variogram calculations) having 1 m thickness. Using KRIGE3 program of GEOSTAT package (1984) the two-dimensional kriging of the blocks with 400 m x 400 m x 1 m dimensions, lying in each slice were carried out. Considering the variation in the spatial behavior of P_2O_5 % in the horizontal and vertical directions, an ellipsoid of influence was specified for blocks. The X, Y and Z dimensions of the ellipsoid were chosen to be 500 m x 500 m and 1 m respectively. To kriging a particular block only the samples which fell within the ellipsoid centered at the block were used.

The output generated by the kriging program includes the following information:

- a. X direction index of the block.
- b. Y direction index of the block.
- c. Z direction index of the block.
- d. Number of samples used to Kriging the block.
- e. Kriged estimate for P_2O_5 %.
- f. Relative Kriging standard deviation.

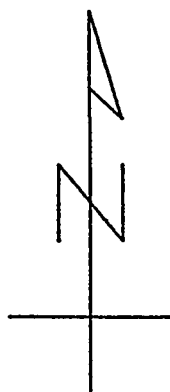
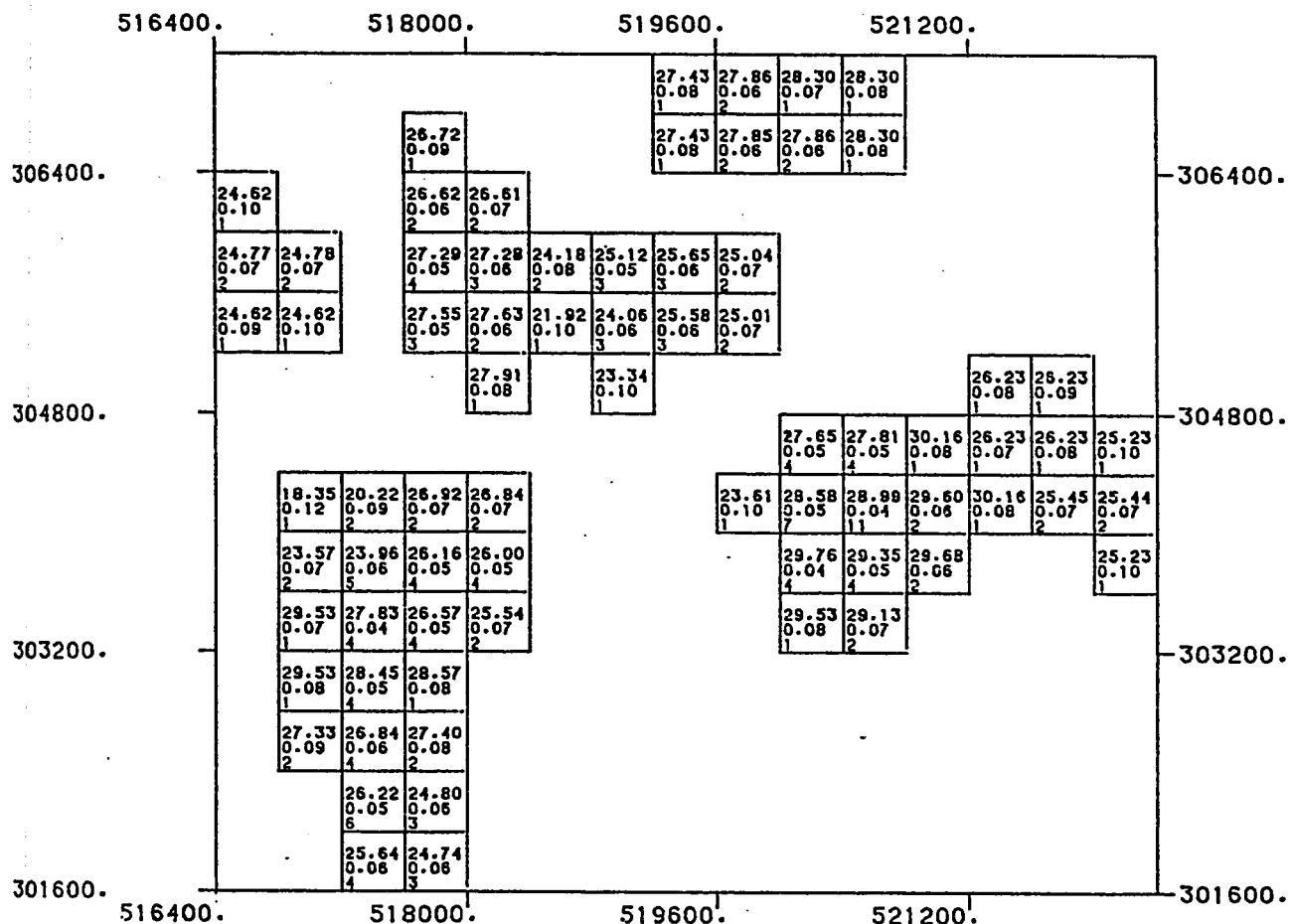
The kriging output was used as the input data for another computer program (BLKPLT) for plotting the estimated blocks on the horizontal levels. The plots for P_2O_5 % estimates on these levels are illustrated in Appendix D. 114 pages of plots with each page representing one level has been included in

Appendix D. The levels without kriged blocks and those contained less than 5 blocks were not included. Within the spaces representing blocks in the plots, the values of kriged estimates, the relative kriging standard deviation and the number of samples have been printed respectively from top to bottom.

The kriging variance is a measure of the reliability of the corresponding kriged estimate. A large kriging variance relative to the estimate implies a poor estimate, whereas low kriging variance a good estimate. Assuming the normal distribution of kriging variances, at the 95% confidence level, the confidence limits for the kriged estimate will be $Z^* \pm 2\sigma_k$, where σ_k is the kriging standard deviation, and Z^* is the kriged estimate.

The following example from the level 113 (see Fig. 7.1) shows how the confidence limits to the estimated block grades can be computed. The block with the central coordinates, of $X = 521000$ and $Y = 304200$ has the kriged estimate (Z^*) equal to 29.6% and the relative kriging standard deviation (σ_k/Z^*) equal to 0.06. Therefore, the value of σ_k is equal to 1.776 (%) and $2\sigma_k = 3.552$ (%). At 95% confidence level, the confidence limits for the estimated grade of this particular block will be 29.6 ± 3.55 . The confidence limits for most of the blocks are relatively narrow implying the reliability of estimates.

The kriging standard deviations depend on the structural model (variogram model) and on the relative geometries of the samples used in estimation and the block to be estimated. The results indicate that for Abu Tartur deposit most of the blocks have similar values of the relative kriging standard deviations. This is, of course, due to the regular nature of samples



ABU TARTUR PHOSPHATE DEPOSIT
Fig.7.1 RESULTS OF BLOCK KRIGING

(Z = 384.5)

LEVEL NUMBER : 113

800.0 0.0 800.0 1600.0



SCALE OF MAP : 1:100,000

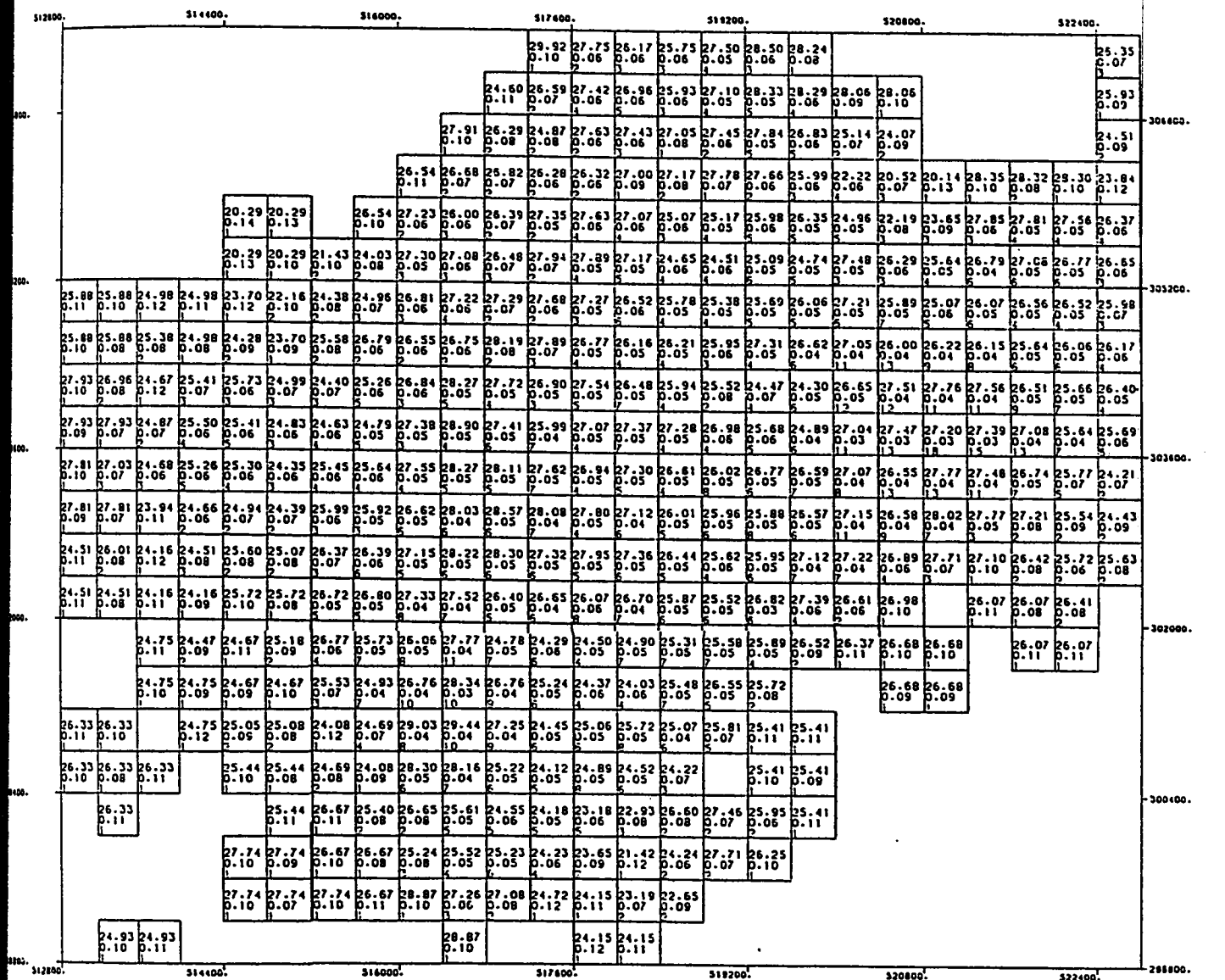
DATA PROCESSED AT: U P M - D P C , DHAHRAN
SOFTWARE BY : GEOSTAT SYSTEMS, MONTREAL

with similar geometric arrangements. Towards the edges, however the number of samples used to krig blocks are reduced resulting in somewhat higher relative kriging standard deviations. The values of relative kriging standard deviations for the most internal blocks are in the order of 0.09 or less and for the edge blocks in the order of 0.13.

The block kriging has also been performed using average P_2O_5 values leading to the kriged estimates over the average thickness of the drill-holes. The kriging output (which included the coordinates of the blocks, the kriged estimates and the corresponding relative kriging standard deviation) was later processed by the ISOPOLY and BLKPLT programs to produce contour maps and block plots map respectively. The block plot illustrated in Fig. 7.2 shows the kriged estimate, relative kriging standard deviation and number of samples respectively in each block from top to bottom.

The comparison of the contour map of the kriged block estimates illustrated in Fig. 7.3 and the isograde map for the average P_2O_5 % illustrated in Fig. 4.3 indicates that the general pattern appears to be similar. There are, however, some differences in the range of P_2O_5 % values. As expected, the isograde map for the sample values shows greater fluctuations than the isograde map for the kriged block estimates.

The contour maps of both the relative kriging standard deviation values multiplied by 100 and the kriging standard deviations are illustrated in Figs. 7.4 and 7.5 respectively. The relative kriging standard deviation map shows a very low fluctuation with values mostly ranging between 6 and 12. This pattern is an indication of the similarities of the relative kriging standard deviations for most block.



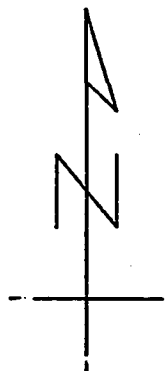
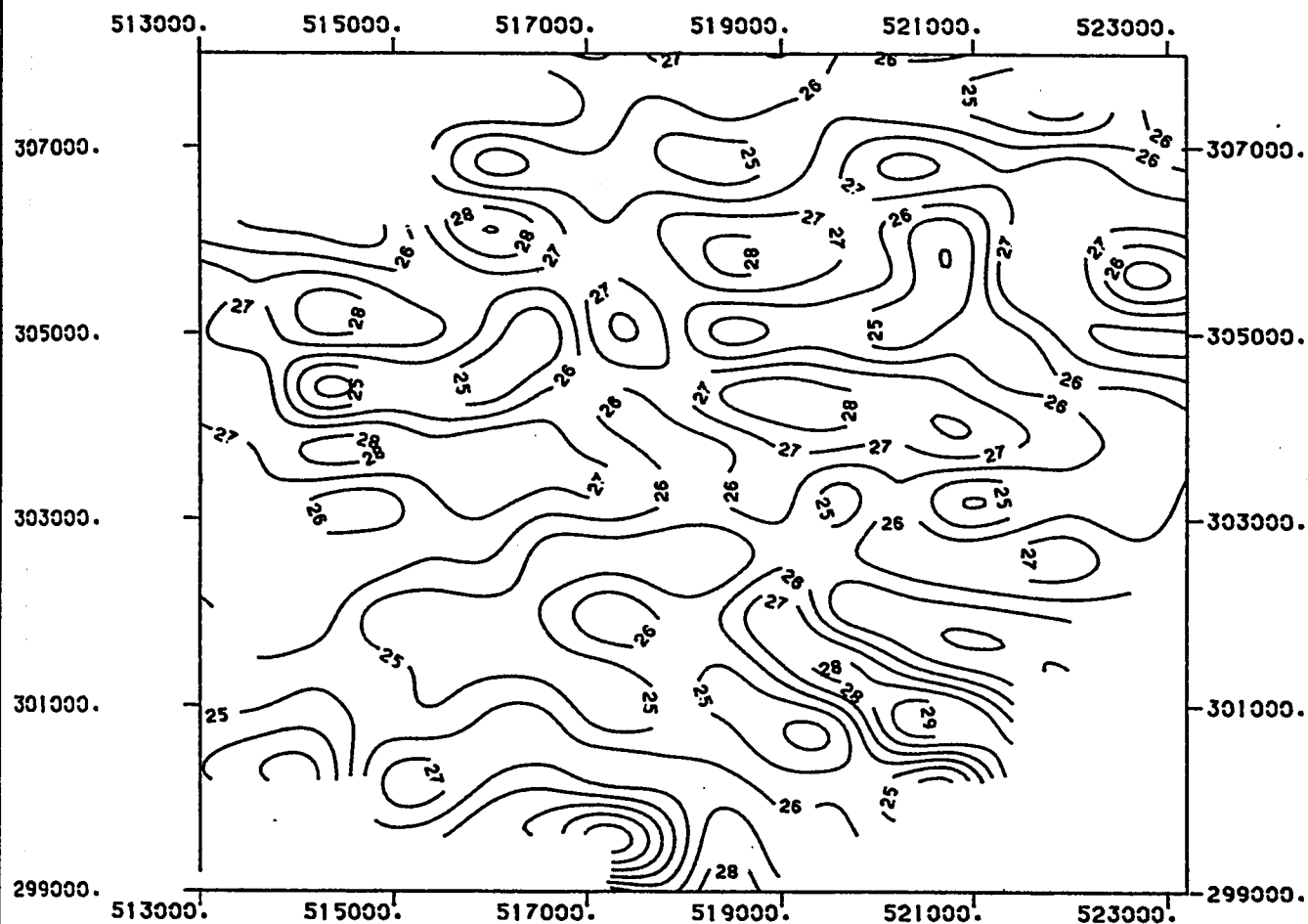
•ABU TARTUR PHOSPHATE DEPOSIT•
FIG: 7.2 RESULTS OF BLOCK
KRIGING PLOTTED ON HORIZONTAL PLANE

LEVEL NUMBER : 1

800.0 0.0 800.0 1600.0


SCALE OF MAP

DATA PROCESSED AT U P H - D P C , DHAKRAH
SOFTWARE BY : GEOSTAT SYSTEMS, MONTREAL

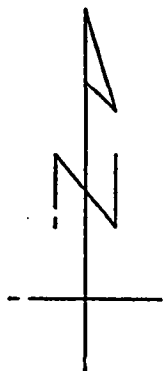
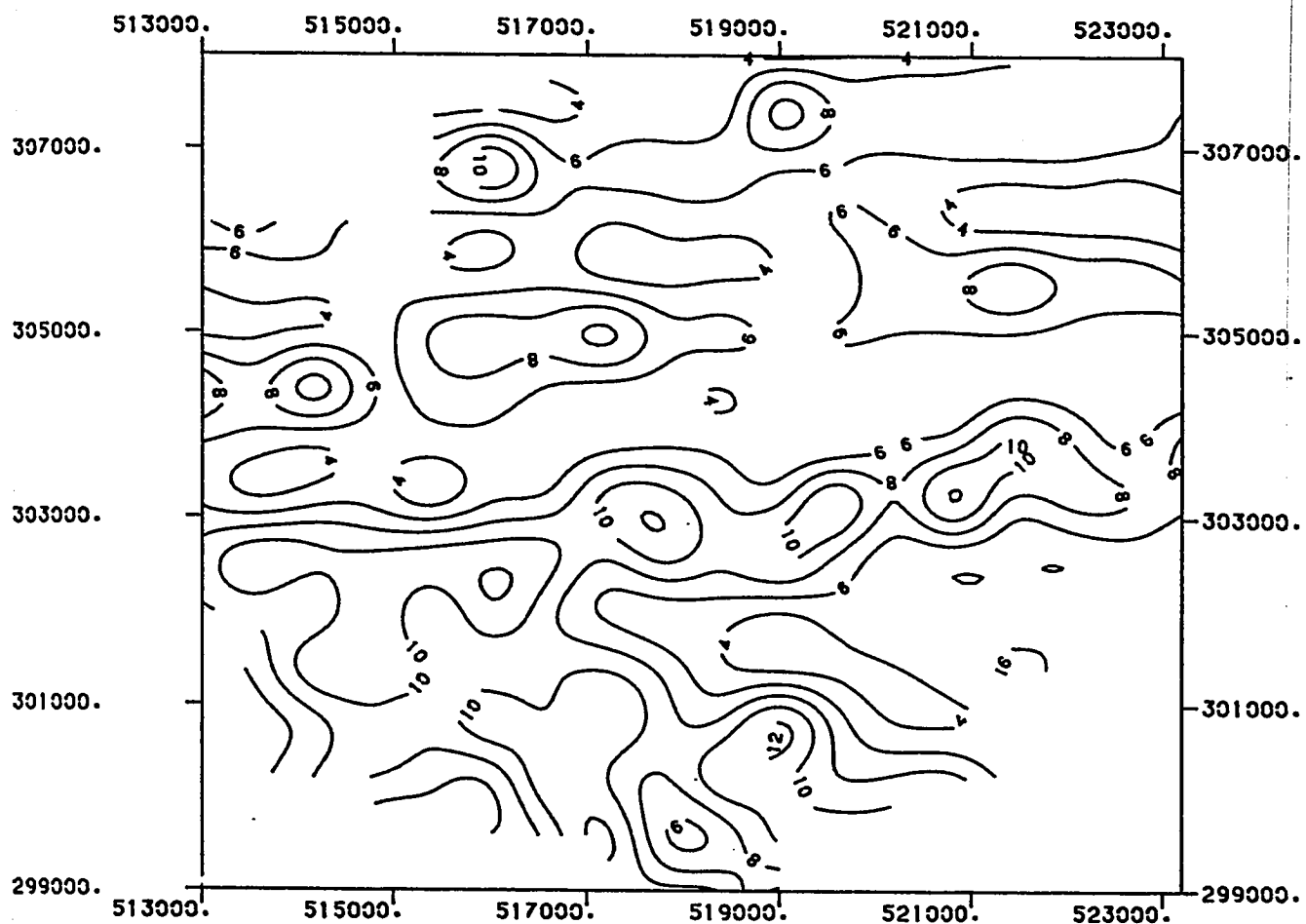


*** ABU TARTUR PHOSPHATE DEPOSIT ***

FIG. 7. 3 ISOGRADE MAP BASED ON
KRIGED BLOCK ESTIMATES

1200.0 0.0 1200.0 2400.0

 SCALE OF MAP

DATA PROCESSED FOR: A. A. ABDELLATIF, MS. UPM.
 SOFTWARE BY : GEOSTAT SYSTEMS, MONTREAL



*** ABU TARTUR PHOSPHATE DEPOSIT ***

FIG. 7.4. MAP OF RELATIVE KRIGING

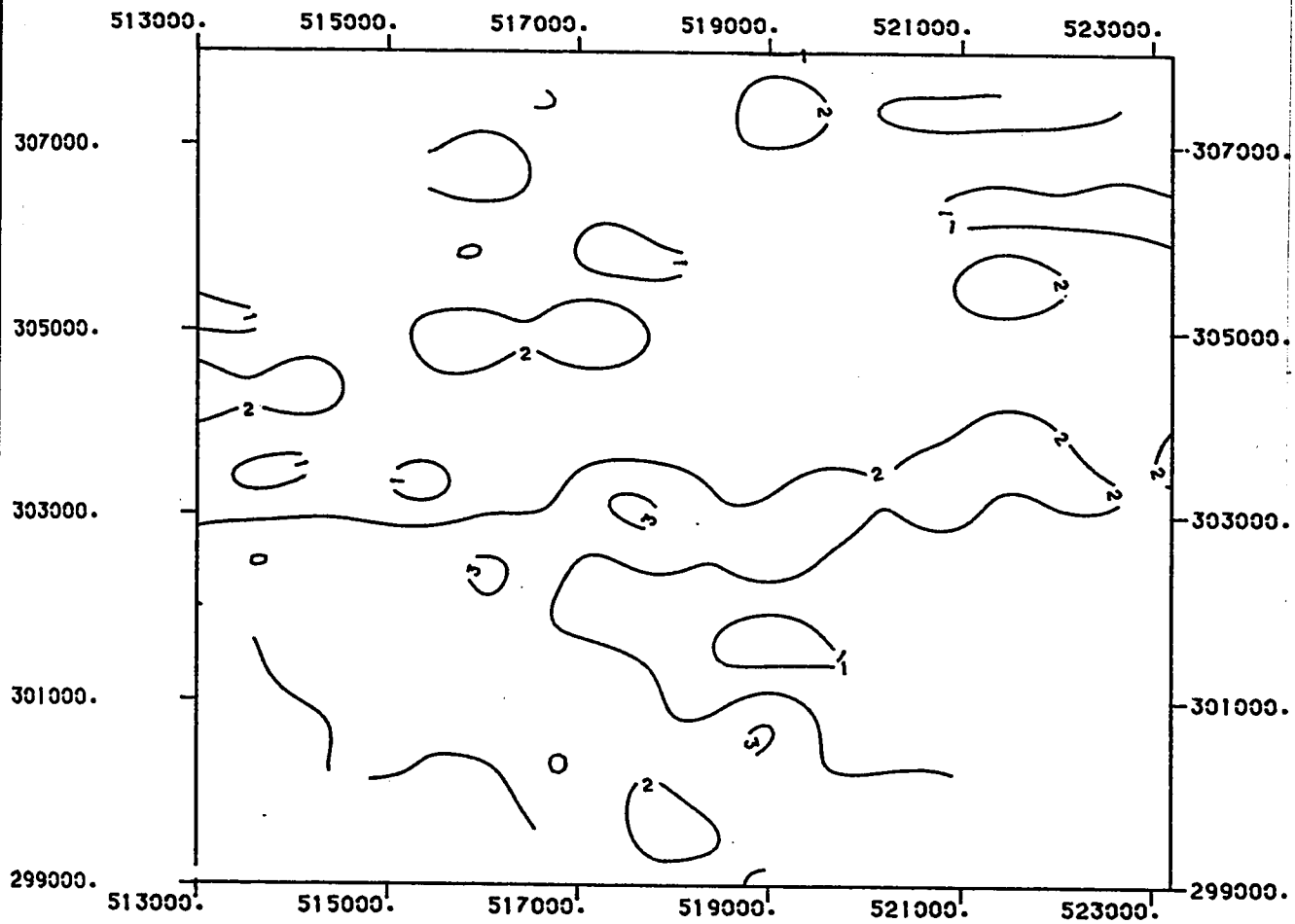
STANDARD DEVIATION = 100

1200.0 0.0 1200.0 2400.0



SCALE OF MAP

DATA PROCESSED FOR: A. A. ASDELLATIF, MS. UPM.
SOFTWARE BY : GEOSTAT SYSTEMS, MONTREAL



*** ABU TARTUR PHOSPHATE DEPOSIT ***

FIG. 7.5 • MAP OF KRIGING STANDARD DEV.

1200.0 0.0 1200.0 2400.0



SCALE OF MAP

DATA PROCESSED FOR: A. A. ABDELLATIF, MS, UPM.
SOFTWARE BY : GEOSTAT SYSTEMS, MONTREAL

7.4 GRADE-TONNAGE RELATIONSHIP

7.4.1 General

As pointed earlier, the main objective of this study is to estimate reserves of Abu Tartur phosphate deposits. However, this objective cannot be accomplished fully unless the relationship between the grade (P_2O_5 %) and tonnage is also determined. Such relationship should be based on the distribution of selective mining units the size of which depends on economical and technical considerations that vary with time and the nature of the deposit. The distribution of the sample values according to the volume-variance relationship will differ from the distribution of the selective mining units. Therefore, using the sampling distribution to predict grade-tonnage relationship will be incorrect.

To derive grade-tonnage relationship based on any distribution, the mean, variance and the type of distribution must be known. The mean of the distribution of the selective units will be the same as that of the kriged block values. The variance is estimated from the variance of the kriged block estimates and the dispersion variance of the values of selection units within the block. It follows that, the reliability of the grade-tonnage relationship will depend on the quality of the block estimates.

7.4.2 Results for Abu Tartur Deposit

The grade-tonnage relationship for Abu Tartur deposit based on the kriged block estimates was constructed using program REPORT. This is a FORTRAN program (GEOSTAT computer package, 1984) designed to produce grade-tonnage reports using the file of kriged block values as input. Assuming the lognormal distribution for the values of selection units, the variance of the distribution is estimated by combining the kriging variance and the dispersion variance. The dispersion variance, $\sigma^2(v/v)$, is defined as the variance of the distribution of values of selection unit (v) within the estimated block (V). This value can be derived from the charts given in the geostatistical literature (Matheron 1971, David 1977) or estimated using the program KRIVAR. In the case of Abu Tartur, considering the dimensions of selection unit and kriged blocks to be 25 m x 25 m x 1 m and 400 m x 400 m x 1 m respectively, the value for the dispersion variance was derived using program KRIVAR.

The output of the program REPORT (i.e. grade-tonnage relationship) is presented in Table 7.1. The relationship between the mean grade ($P_2O_5\%$) and the tonnage (Mt) is also presented in a graphical form in Fig. 7.6. There is an inverse relationship between the phosphate grade and the tonnage. The tonnage of phosphate corresponding to a given grade of $P_2O_5\%$ can directly be read off from the curve. For example, there are 1410 Mt of phosphate reserves corresponding the phosphate grade of 26.4%, and 904 Mt of reserves corresponding to 28%.

TABLE 7.1. Grade-Tonnage Relationship.

Grade interval P 205		Mean Grade P 205	Tonnage $\times 10^6$	Mean Grade above lower limit	Tonnage $\times 10^6$
0.000	18.000	17.150	4.5	26.399	1410.7
18.000	19.000	18.553	6.1	26.428	1406.3
19.000	20.000	19.547	11.0	26.462	1400.2
20.000	21.000	20.548	19.5	26.517	1389.2
21.000	22.000	21.549	34.9	26.602	1369.7
22.000	23.000	22.546	61.6	26.734	1334.7
23.000	24.000	23.538	101.6	26.937	1273.2
24.000	25.000	24.527	150.6	27.232	1171.6
25.000	26.000	25.516	196.3	27.631	1021.0
26.000	27.000	26.504	222.0	28.134	824.7
27.000	28.000	27.490	214.0	28.734	602.8
28.000	29.000	28.474	172.7	29.419	388.7
29.000	30.000	29.457	114.6	30.175	216.1
30.000	31.000	30.439	61.8	30.987	101.4
31.000	32.000	31.422	26.9	31.842	39.6
32.000	99.999	32.729	12.7	32.729	12.7

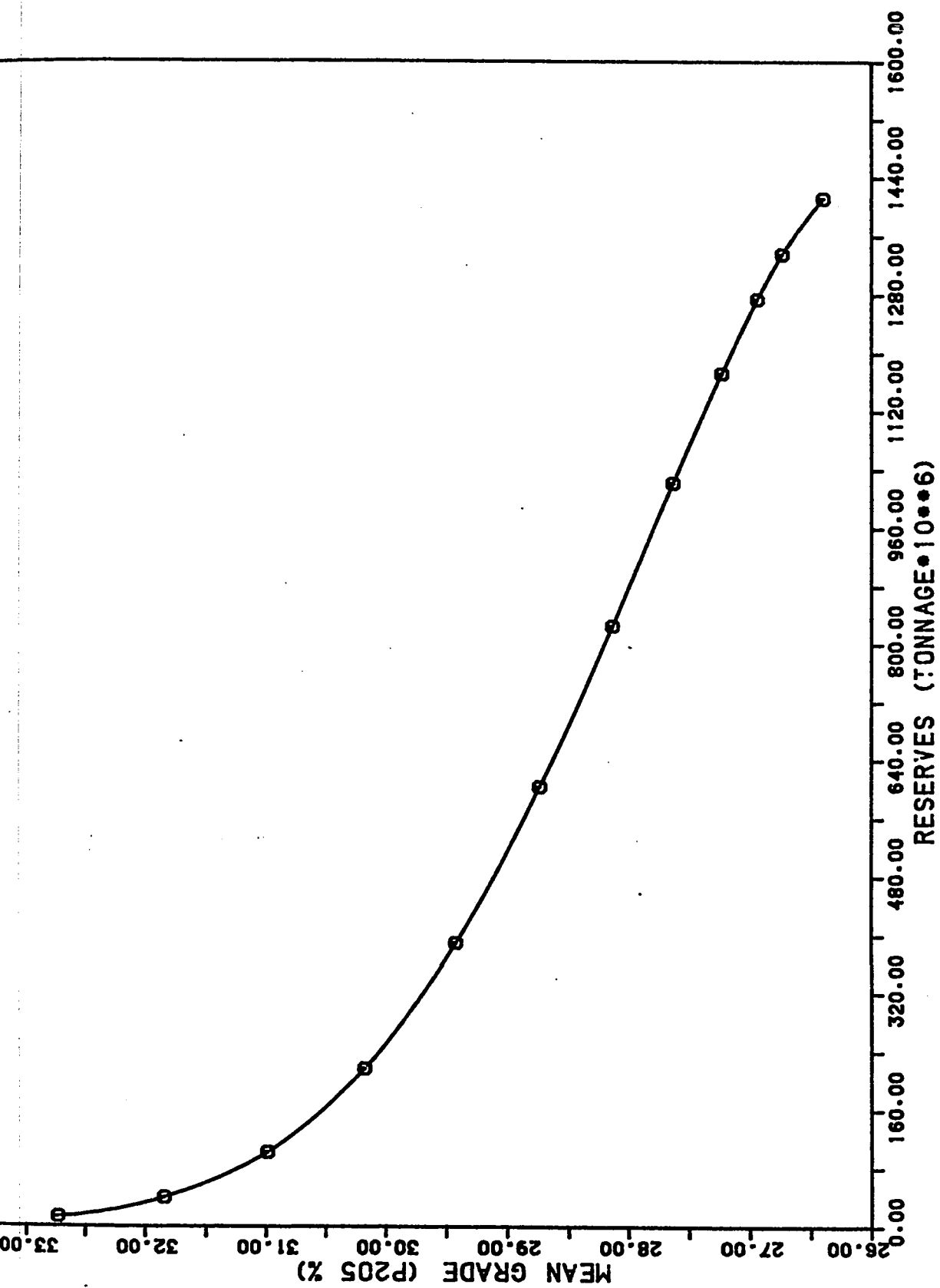


Fig.7.6 GRADE-TONNAGE RELATIONSHIP (ABU TARTUR PHOSPHATE DEPOSIT)

Finally, it should be added that the grade-tonnage relationship is valuable tool in planning. Based on the available kriged estimates, such relationships can be derived for other selective units as required. However, as more data becomes available, the kriged estimates and the grade-tonnage relationship should regularly updated.

7.5 COMBINING KRIGED ESTIMATES

The global estimates for the deposit can also be derived by combining the kriged block estimates. Since all the blocks are identical in size, the computations are greatly simplified. The total phosphate volume is obtained by multiplying the surface area of one block with the total number of blocks and the block thickness, i.e.

$$V = n.S.t.$$

where n is the total number of blocks,

S is the surface area of one block,

t is the block thickness.

In the case of Abu Tartur deposit, 3752 blocks each having 400 m x 400 m surface area and 1 m thickness were estimated. Therefore the total volume

$$\begin{aligned} V &= 3752 \times 400 \times 400 \times 1 \\ &= 600.32 \times 10^6 \text{ cu.m.} \end{aligned}$$

The corresponding tonnage is estimated by simply multiplying the volume with the density which is approximately 2.35 tons per cu.m. in this case.

$$\begin{aligned} \text{i.e. } T &= 600.32 \times 10^6 \times 2.35 \\ T &= 1410.75 \text{ Mt.} \end{aligned}$$

To obtain the estimation variance associated with these estimates, a procedure similar to the one described in Chapter 6 can be used. In this case, however, a regular grid has to be fitted to each slice having kriged blocks and the relative estimation variance for the surface area estimated. Finally, the relative estimation variances for the individual slices (σ_{Si}^2/S_i^2) are combined to give the global relative estimation variance for the surface area as follows:

$$\sigma_S^2/S^2 = \Sigma \sigma_{Si}^2 \cdot S_i^2 / (\Sigma S_i)^2 \quad (7.7)$$

σ_t^2/t_t^2 will be zero, as all the slice thicknesses are known exactly, and the remaining calculations proceed as explained in Chapter 6.

The estimation variance for the grade can be computed using the variogram parameters for grade. A compound spherical model has been fitted to the grade variogram with the following parameters:

$$C_0 = 0.0(\%)^2, \quad C_1 = 2.4(\%)^2, \quad C_2 = 2.1(\%)^2$$

$$a_1 = 80 \text{ m and } a_2 = 700 \text{ m.}$$

The estimation variance for the grade is given by

$$\sigma_g^2 = 1/n(C_0 + C_1 F_1 + C_2 F_2) \quad (7.8)$$

where $F_1 = F(l/a_1, h/a_1)$ and $F_2 = F(l/a_2, h/a_2)$ are factors obtained from the chart given in Fig. 6.2 and n is the total number of blocks. Substituting the numerical values in Eqn. (7.8)

$$\begin{aligned}
\sigma_g^2 &= (1/3752)[2.4(400/80, 400/80) + 2.1(400/700, 400/700)] \\
&= (1/3752)[2.4(5, 5) + 2.1(0.571, 0.571)] \\
&= (1/3752)[2.4(0.981) + 2.1(0.421)] \\
\sigma_g^2 &= 8.63139 \times 10^{-4} \\
\sigma_g &\approx 0.03(2\sigma_g = 0.06\%).,
\end{aligned}$$

is obtained.

The mean grade for the phosphate deposit is estimated as the mean grade of the kriged block estimates ($g^* = 26.4\%$). Thus at 95% confidence level, the confidence limits for the grade is $26.4\% \pm 0.06\%$.

Chapter 8

GENERAL SUMMARY AND CONCLUSIONS

The Abu Tartur Phosphate deposits (Western Desert, Egypt) were laid down in the coastal part of an inter-platform, marine trough which covered most of northern Africa and western Asia. This marine trough extended from Mauritania in the west to the western Iraqi Desert in the east. In such a vast trough, the optimum depositional environments for phosphate accumulation were attained at different periods between the Late Cretaceous and the Middle Eocene times. In Abu Tartur area, as well as throughout most of Egypt, such optimum conditions for the phosphate deposition were obtained during the Late-Campanian time and hence phosphate deposits were laid down in a more or less-continuous belt extending from the Western Desert Oases into the Nile Valley and from there to the Red Sea coast and the Sinai peninsula into Palestine, Jordan and Syria. Paleocene-Middle Eocene phosphate deposits are also recorded in north-western Saudi Arabia and in Western Iraq.

Phosphates in Abu Tartur area are found in two main horizons within the Late Campanian Sibaiya Formation. Both the P_2O_5 grade and the thickness of the main phosphate bed (i.e. the lower horizon) in 347 drill-holes drilled on a regular grid of 400 m x 400 m dimensions formed the basic data set for the geostatistical estimation of phosphate reserves.

The main conclusions drawn from this study can be summarized as follows:

- a. The preliminary statistical analysis of the available data, provided means, variances and standard deviations for grade ($P_2O_5\%$), thickness (m) and accumulation (%m) within the whole deposit. The average value for P_2O_5 grade has been estimated to be 26.58% and the average values for the thickness and the accumulation have been estimated to be 2.95 (m) and 76.58 (%m) respectively.
- b. The thickness of the phosphate horizon ranges from about 100 cm to about 500 cm. with very small and gradual changes in most part of the plateau. The grade varies in a fairly uniform manner between 18% and 28%.
- c. The histogram for the grade ($P_2O_5\%$) is characterized by a slight negative skew and the histograms for both the thickness and the accumulation by slight positive skews. However, they can all be approximated by normal distributions. The percentage cumulative frequency distribution plots on the normal-probability papers can be represented by straight lines further demonstrating the validity of this approximation.
- d. The results of variogram analysis indicate that spherical models could appropriately be fitted to all experimental variograms. However, the models fitted to both thickness and accumulation

are simple spherical whereas the model fitted to $P_2O_5\%$ variogram is compound spherical. All of these models have revealed excellent continuity near the origin as expected from a sedimentary deposit.

- e. The global estimates for the average grade, the total tonnage and the total phosphate content in the central part of the deposit have been computed. The estimate for the average grade is $26\% \pm 0.19\% P_2O_5$ and the estimates for the total tonnage and the total phosphate content are 308.36 ± 13.56 Mt, and 80.05 ± 0.15 Mt respectively.
- f. The local estimation based on $P_2O_5\%$ of 1m-composite samples has been carried out using the geostatistical procedure known as the kriging. 3752 blocks having $400\text{ m} \times 400\text{ m} \times 1\text{ m}$ dimensions were kriged and the results for each block were plotted on the horizontal planes. The relative kriging standard deviations associated with the estimates for most of the blocks are less than 0.09 indicating the reliability of the kriged estimates.
- g. Kriging was also performed on the average grade values along the drill-holes. 401 blocks were kriged and the results were plotted on a horizontal plane. The contour maps have been prepared for the kriged estimate, the relative kriging standard

deviation $\times 100$ and the standard deviation. Using these maps, the confidence limits assigned to the grade value at any given point can be computed. These maps can also be of considerable value in production planning.

- h. Based on the kriged block estimates, the grade-tonnage curve was constructed. The tonnage of phosphate corresponding to a given cut off grade can be read off this curve. The curve indicates that the total tonnage of the phosphate corresponding to 26.4% P_2O_5 is 1410.75 Mt.
- i. Finally, the kriged blocks were combined to estimate the total tonnage. This method provided a tonnage estimate which compares well with the one derived from the grade tonnage relationship.

REFERENCES

- Alfaro, M.A., and F. Miguez (1976), "Optimal interpolation using transitive methods", *Advanced Geostatistics in the Mining Industry*, Reidel, Holland, pp. 91-99.
- Ashour, M.M. (1978), "Microstratigraphical analysis of the Late-Cretaceous, Early Paleogene Succession in Egypt typified by the Dakhla Nile Valley Succession", Ph.D. thesis, Assiut University, Egypt.
- Ashour, M.M. (1983), "Lithofacies of Late-Cretaceous-Early Paleogene Succession in Egypt", *Proceedings of the First Jordanian Geological Conference*, Hitteen Printing Press-Amman-Jordan, pp. 10-71.
- Awad, G.H., and Ghobrial, M.G., (1966), *Zonal Stratigraphy of Kharga Oasis*. Geol. Survey Egypt, Paper No. 34, 77 p.
- Baxter, C.H. and D. Parks (1957), "Examination and valuation of mineral property", Fourth edition, by R.D. Parks, Addison Wesley, 507 p.
- Beadnell, H.J.L., (1901), *Dakhla Oasis. Its Topography and Geology*. Survey of Egypt, Survey Egypt, 107 p.
- Blais, R.A. and P.A. Carlier (1968), "Application of geostatistics in ore evaluation. In ore reserve estimation and grade control", *Can. Int. Min-Metall., Spec. vol. 9*, pp. 4-68.
- Brooker, P.I. (1979), "Kriging", *Engineering and Mining Journal*, Sept. 1979, pp. 148-153.
- Bubeniceek, L. and A. Haas (1969), "Method of calculation of the iron ore reserves in the Lorraine deposit". In *a Decade of Digital Computing in the Mineral Industry*, edit., A. Weiss, AIME, New York, pp. 179-210.

- Clark, I. (1979), "The semivariogram", Engineering and Mining Journal, July and August 1979, pp. 90-97.
- David, M. (1970), "Geostatistical ore estimation—a step-by-step case study", 9th International Symposium on Applications of Computers and Mathematics in the Mineral Industry, Can. Inst. Min. Metall., Spec. vol. 12, pp. 185-191.
- David, M. (1976), "The practice of kriging", Advanced Geostatistics in the Mining Industry, Reidel, Holland, pp. 91-99.
- David, M. (1977), "Geostatistical Ore Reserves Estimations", Elsevier, Amsterdam, 364p.
- Dowed, P. and M. David (1976), "Planning from estimates: sensitivity of mine production schedules to estimation methods", Advanced Geostatistics in the Mining Industry, Dordrecht, Holland, Reidel, pp. 163-183.
- El-Kammer, A.M., (1974). Comparative mineralogical and geochemical study on the Egyptian Phosphorites from Nile Valley, Quseir area and Kharga Oasis, Ph.D. thesis, Cairo University.
- El-Naggar, Z.R. (1963), Geology and Stratigraphic Paleontology of the Esna-Idfu Region, Nile Valley, Egypt, U.A.R.: Unpub. Ph.D. thesis, Univ. of Wales, U.K.
- El-Naggar, Z.R. (1966a), "Stratigraphy and planktonic forminifera of the Upper Cretaceous.
- El-Naggar, Z.R. (1966b), "Stratigraphy and Planktonic Forminifera of the Upper Cretaceous-Lower Tertiary Succession in the Esna-Idfu Region, Nile Valley", Egypt, the British Museum (Natural History), London, 291p.

- El-Naggar, Z.R. (1970), "On a proposed lithostratigraphic subdivision for the Late-Cretaceous, Early Paleogene Succession in the Nile Valley, Egypt, Seventh, Arab Petroleum Conferences, printed at Al-Rissala Press, Kuwait, 50 p.
- El-Naggar, Z.R., and M.M. Ashour (1983), "Microstratigraphical of the Late Cretaceous, Early Paleogene Succession in Egypt, by the Dakhla, Nile Valley and Red Sea coast section", in: Proceedings of the First Jordanian Geological Conference, Hitteen Printing Press-Amman, Jordan, pp. 112-180.
- El-Mabrouk, F.A., (1975). Comparative geochemistry and pilot plant extraction of some Egyptian phosphates. Ph.D. thesis, Ain Shams University.
- El-Nassan, B.A., and A.I. Afonin, (1970). Report on geology, Mineralogy and petrography of phosphorites in southern part of Abu Tartur area (Western Desert), Geol. Surv. Egypt.
- El-Tahlawi, A., A.S. Wassef, B. El-Nassan, N.I. Yudin, D.V. Kylvor, D.V. Ylov, P.N. Gurov, A.I. Afonin (1973). On the results of geological exploration of Abu Tartur Phosphate Deposit with Calculation of Reserves according to Category C_1 .
- El-Tahlawi, A., S.Z. Gabra, A.A. Morozu, A.I. Sashin, V.B. Defu, and P.A. Khilstov (1977): Report on the results of explorational works at the Abu Tartur phosphate deposit during 1976, Egyptian Geological Survey and Mining Authority, 78p.

- Geostat Package, (1984), "Geostatistical ore reserve estimation", Version 3-0, Geostat Systems International Inc., Montreal, Canada.
- Ghobrial, M.G. and B. Issawi (1961). The geology of Dakhla area, Geol. Survey Egypt, 53p.
- Guarasio, M., and A. Turchi (1977), "Exploration data management and evaluation technique for uranium mining projects", 14th Symposium on Computer Application in the Mineral Industries, American Inst. Min. Metal. and Petro Eng., New York, pp. 351-367.
- Hazen, S.W. (1961), "Statistical analysis of sample data for estimating ore", U.S. Department of the Interior, Bureau of Mines R.I. 5835.
- Hazen, S.W. (1967), "Assigning an area of influence for an assay obtained in mine sampling", U.S. Department of the Interior, Bureau of Mines R.I. 6955.
- Hazen, S.W. (1968), "Ore reserve calculations", CIM Special Volume 8, pp. 11-32.
- Hermína, M.H., M.G. Ghobrial and B. Issawi (1961), "The geology of the Dakhla area", General Organization for Government Printing Offices, Cairo, 33p.
- Hermína, M.H. (1967), "Geology of the north-western approaches of Kharga", Geol. Survey Egypt, paper No. 44, 88p.
- Hermína, M.H. (1973), "Preliminary evaluation of Machrabi-Liffiya rites", Abu Tartur area, Western Desert, Egypt. Annals of the Geol. Survey Egypt, vol. III, pp. 39-74.

- Hermina, M.H. (1974), "The phosphate deposits of Egypt", The Third Arab Conference for Mineral Resources, Jeddah, pp. 110-152.
- Huijbregts, C., and G. Matheron (1971), "Universal kriging", (An optimal method for estimating and contouring in trend surface analysis. In decision making in the Mineral Industry, Can. Inst. Min. Metall., pp. 159-169.
- Huijbregts, C. (1976), "Selection and grade-tonnage relationships", Advanced Geostatistics, in the Mining Industry, Dordrecht, Holland, Reidel, pp. 113-135.
- Journal, A.G. (1976), "Ore grade distributions and conditional simulations-two geostatistical approaches", NATO Advanced Study Institute, Advanced Geostatistics in the Mining Industry, Dordrecht, Holland, Reidel, pp. 195-202.
- Journal, A.G., C. Huijbregts (1978), "Mining Geostatistics", Academic Press, London, 600p.
- Journal, A.G. (1979), "Geostatistical simulation methods for exploration and mine planning", Engineering and Mining Journal, Dec. 1979, pp. 86-91.
- Kamel, O.A., M.E. Hilmy and R.K. Bekir (1977). Mineralogy of Abu Tartur Phosphorites, J. Geol., 21, No. 2, pp. 133-157, Egypt.
- Kim, Y.C. and E.Y. Baafi (1984), "Combining local kriging variances for short-term mine planning". NATO ASI Series, Geostatistics for Natural Resources Characterization, Part I, D. Reidel, Boston, pp. 107-125.

- Knudsen, H.P., Y.C. Kim and E. Muller (1978), "Comparative study of the geostatistical ore reserve estimation method over the conventional methods", Society of Mining Engineers, pp. 54-58.
- Krige, D.G., and J.M. Rendu (1975), "The fitting of contour surfaces to hanging and footwall data for an irregular ore body", 13th Symposium on Computer Applications in the Mineral Industries, Clausthal-Zellerfeld, West Germany.
- Krige, D.G. (1976), "A review of development of geostatistics in South Africa", Advanced Geostatistics in the Mining Industry, Dordrecht, Holland, Reidel, pp. 279-293.
- Marechal, A. (1976), "Selecting mineable blocks, Experimental results observed on a simulated orebody", Advanced Geostatistics in the Mining Industry, Dordrecht, Holland, Reidel, pp. 137-161.
- Matheron, G. (1963), "Principles of geostatistics", Economic Geology Publishing Corporation, pp. 224-244.
- Matheron, G., (1968), Osnovy Prikladnot Geostatistiki, Mir Editions, Moscow, 408p.
- Matheron, G., (1971), The theory of regionalized variables and its applications. Les cahiers du CMM, Fasc. no. 5, ENSMP, Paris, 211p.
- Omre, H. (1984), "The variogram and its estimations", NATO ASI Series, Geostatistics for Natural Resources Characterization, Part I, D-Reidel, Boston, pp. 107-125.
- Parker, H. (1977), "Geostatistical determination of the size and grade of orebodies by computer method", National Council for U.S. China, Trade Tech. Exchange, 62p.

- Parker, H. (1979), "The volume variance relationship: a useful tool for mine planning", *Engineering and Mining Journal*, Oct. 1979, pp. 106-123.
- Patterson, J.A. (1959), "Estimating ore reserves following logical steps", *Eng. and Mining Jour.* 160, 11, 112, 115p.
- Peters, W.C. (1978), "Exploration and Mining Geology", John Wiley & Sons, New York, 696p.
- Popoff, C. (1966), "Computing reserves of mineral deposits: principles and conventional methods", Bureau of Mines, Washington, D.C., 113p.
- Rendu, J.M. (1978), "An introduction to geostatistical methods of mineral evaluation", *South African Inst.* 84p.
- Rendu, J.M. (1980), "Kriging for ore valuation and mine planning a case study", *Engineering and Mining Journal*, Jan. 1980, pp. 114-120.
- Rendu, J.M. (1984), "Geostatistical modelling and geological controls", *The Proceeding of 18th APCOM Symposium*, pp. 467-476.
- Royle, A.G. and E. Hosgit (1974), "Local estimation of sand and gravel reserves by geostatistical methods", *Trans. Instu. Min. Metall.*, A53-A62.
- Royle, A.G. (1977), "Global estimates of ore reserves", *Trans. Instn. Min. Metall.*, vol. 86, pp. A9-A17.
- Royle, A.G. (1979), "Why geostatistics?", *Engineering and Mining Journal*, May 1979, 16p.
- Royle, A.G. (1980), "Estimating global ore reserves in a single deposit", *Minerals Sci. Engg.* vol. 12, no. 1, pp. 37-50.

- Rutledge, R.W. (1976), "The potential of geostatistics in the development of mining", *Advanced Geostatistics in the Mining Industry*, Dordrecht, Holland, Reidel, pp. 295-311.
- Sahin, A. (1977), "Spatial distribution in the Bonthe rutile deposits of Sierralleone", Ph.D. thesis, University of Leeds.
- Sahin, A. (1984), "Geostatistical prediction of grain-size fluctuations in feed to Reichert cones, Trans. of Institution of Min. and Metall., Section C (C1-C5).
- Said, R. (1960), "The Geology of Egypt", Elsevier Publishing Company, Amsterdam, New York, 377p.
- Sandefur, R.L. and D.C. Grant, "Geostatistics applied to roll front uranium, a case study in Wyoming", *Engineering and Mining Journal*, F.
- Sinclair, A.J. and J. Deraisme (1974), "Geostatistical study of the Eagle Copper Vein", Northern British Columbia, *Can. Inst. Min. Metall. Bull.* 67, pp. 131-142.
- Sofremines and Alusuisse (1977), "Overall project appraisal report geology and geostatistics", France and Switzerland, 179p.
- Tobia, S.K. and A.A. Fekry (1964), Geochemistry of some Egyptian phosphate deposits. *Jour. Geol., U.A.R.*, 8, pp. 11-19.
- Zaghloul, Z.N and B. Mabrouk (1964). On uranium in Dakhla and Mahamid Phosphate Deposits. *Jour. Geol., U.A.R.*, 8, pp. 79-86.
- Zittel, K.A. Von, et al., (1883), *Beitrage Zur Geologie und Paleontologie der Libyschen Wuste und der angrenzenden Gebiete Von Aegypten: Paleontographica Stuttgart V. 30, 3rd. Ser., pts I, II: p. 147 + 238, PLS-1-36.*

APPENDIX A

An excerpt from master file

1--N1-5	521300.00	310492.00	549.00	0.00	-90.0
3--N1-5	120.60	121.20	26.40	0.60	
3--N1-5	121.20	121.65	31.12	0.45	
3--N1-5	121.65	122.10	29.23	0.45	
3--N1-5	122.10	122.50	29.87	0.40	
1--N111	516196.00	310325.00	568.00	0.00	-90.0
3--N111	208.50	208.95	19.74	0.45	
3--N111	208.95	209.45	00.00	0.50	
3--N111	209.45	209.60	23.00	0.15	
3--N111	209.60	211.65	00.00	2.05	
3--N111	211.65	212.35	24.49	0.70	
1--N1-3	522900.00	310285.00	540.20	0.00	-90.0
3--N1-3	102.30	102.65	24.07	0.35	
3--N1-3	102.65	102.90	16.29	0.25	
3--N1-3	102.90	103.15	22.09	0.25	
3--N1-3	103.15	104.05	27.66	0.90	
3--N1-3	104.05	104.70	27.50	0.65	
1--N1-9	517820.00	310232.00	563.20	0.00	-90.0
3--N1-9	177.95	178.35	27.00	0.40	
3--N1-9	178.35	179.15	23.42	0.80	
3--N1-9	179.15	180.00	21.41	0.85	
3--N1-9	180.00	180.65	28.23	0.65	
3--N1-9	180.65	182.10	28.89	1.45	
1--N1-1	524400.00	310225.00	541.40	0.00	-90.0
3--N1-1	98.60	98.90	29.57	0.30	
3--N1-1	98.90	99.35	24.87	0.45	
3--N1-1	99.35	100.20	27.16	0.85	
3--N1-1	100.20	100.80	26.17	0.60	
3--N1-1	100.80	100.90	12.94	0.10	
3--N1-1	100.90	101.60	26.33	0.70	
1--TN33	525735.00	309895.00	420.90	0.00	-90.0
3--TN33	0.00	1.40	18.05	1.40	
3--TN33	1.40	2.40	19.69	1.00	
1--D-10	521225.50	309607.50	540.80	0.00	-90.0

APPENDIX B

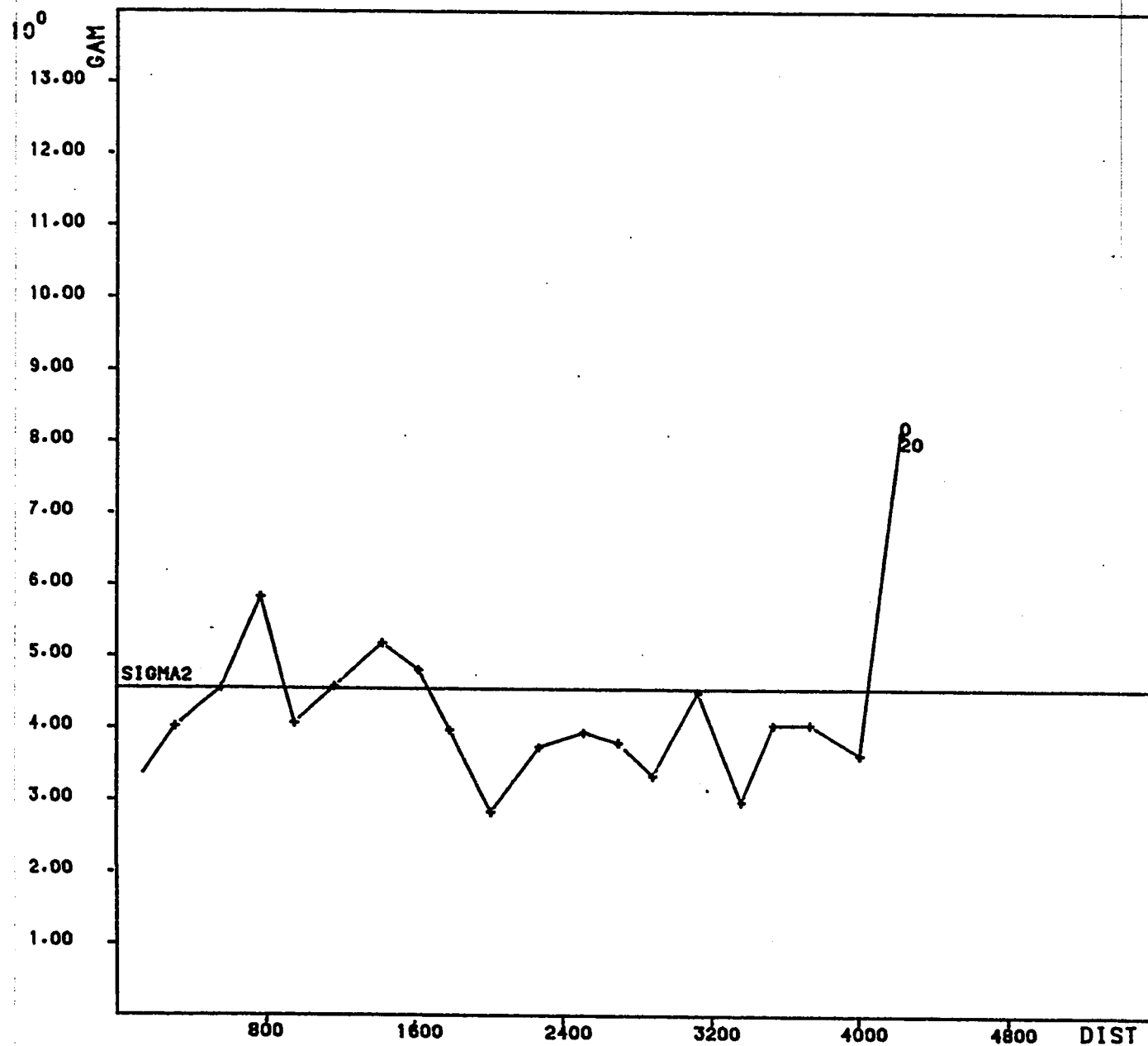
An excerpt from 1-m composite file

D.H.NO.	X	Y	Z	P205
-N1-5	521300.00	310492.00	428.50	26.400
-N1-5	521300.00	310492.00	427.50	29.514
-N1-5	521300.00	310492.00	426.50	29.742
-N111	516196.00	310325.00	359.50	17.766
-N111	516196.00	310325.00	358.50	3.450
-N111	516196.00	310325.00	357.50	0.000
-N111	516196.00	310325.00	356.50	8.572
-N111	516196.00	310325.00	355.50	24.490
-N1-3	522900.00	310285.00	437.70	21.009
-N1-3	522900.00	310285.00	436.70	26.825
-N1-3	522900.00	310285.00	435.70	27.511
-N1-9	517820.00	310232.00	385.70	27.000
-N1-9	517820.00	310232.00	384.70	24.673
-N1-9	517820.00	310232.00	383.70	21.711
-N1-9	517820.00	310232.00	382.70	28.461
-N1-9	517820.00	310232.00	381.70	28.890
-N1-9	517820.00	310232.00	380.70	28.890
-N1-1	524400.00	310225.00	442.90	28.395
-N1-1	524400.00	310225.00	441.90	26.358
-N1-1	524400.00	310225.00	440.90	25.061
-N1-1	524400.00	310225.00	439.90	26.330
-TN33	525735.00	309895.00	420.40	18.050
-TN33	525735.00	309895.00	419.40	19.034
-TN33	525735.00	309895.00	418.40	19.690
-D-10	521225.50	309607.50	427.30	25.970
-D-10	521225.50	309607.50	426.30	25.970
-D-10	521225.50	309607.50	425.30	25.970
-NG-9	517570.00	308803.00	363.50	16.620
-NG-3	522760.00	308745.00	437.30	22.450
-NG-3	522760.00	308745.00	436.30	24.654
-NG-3	522760.00	308745.00	435.30	26.553

APPENDIX C**Directional Variograms**

- C1. Abu Tartur-program vario3- horizontal variogram (P205% 1m-composite)
- C2. Abu Tartur-program vario3- horizontal variogram (P205% 1m-composite)
- C3. Abu Tartur-program vario3- horizontal variogram (P205% 1m-composite)
- C4. Abu Tartur-program vario3- horizontal variogram (P205% 1m-composite)
- C5. Abu Tartur-program vario3- horizontal variogram (P205%)
- C6. Abu Tartur-program vario3- horizontal variogram (P205%)
- C7. Abu Tartur-program vario3- horizontal variogram (P205%)
- C8. Abu Tartur-program vario3- horizontal variogram (P205%)
- C9. Abu Tartur-program vario3- horizontal variogram (thickness)
- C10. Abu Tartur-program vario3- horizontal variogram (thickness)
- C11. Abu Tartur-program vario3- horizontal variogram (thickness)
- C12. Abu Tartur-program vario3- horizontal variogram (thickness)
- C13. Abu Tartur-program vario3- horizontal variogram (accumulation)
- C14. Abu Tartur-program vario3- horizontal variogram (accumulation)
- C15. Abu Tartur-program vario3- horizontal variogram (accumulation)
- C16. Abu Tartur-program vario3- horizontal variogram (accumulation)

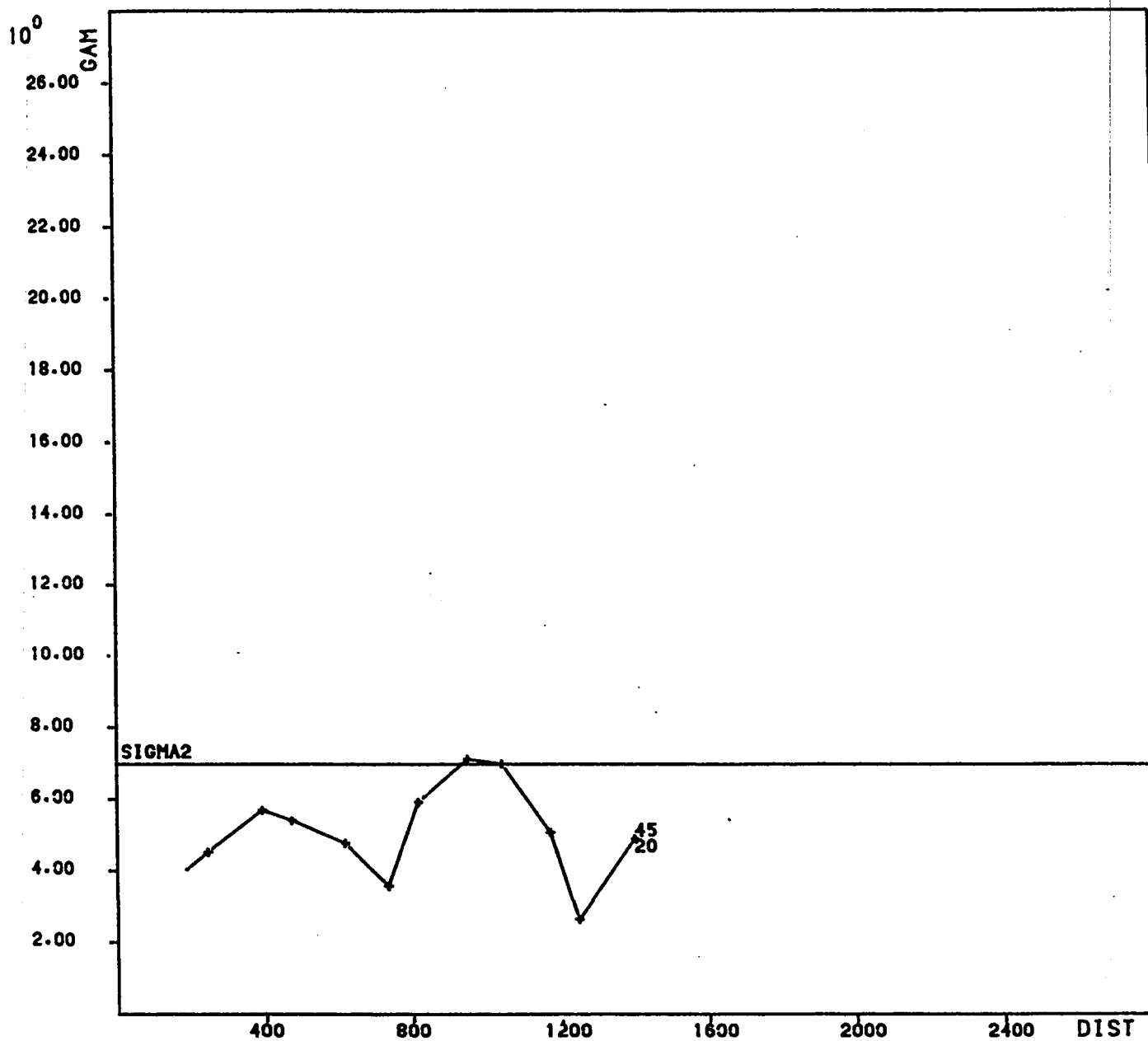
(C1)



VARIABLE P205
ABU TARTUR PORGRAM VR103 - HORIZONTAL VARIOGRAM (1M.COMPOSITES)

ABSOLUTE VARIOGRAM

(C2)



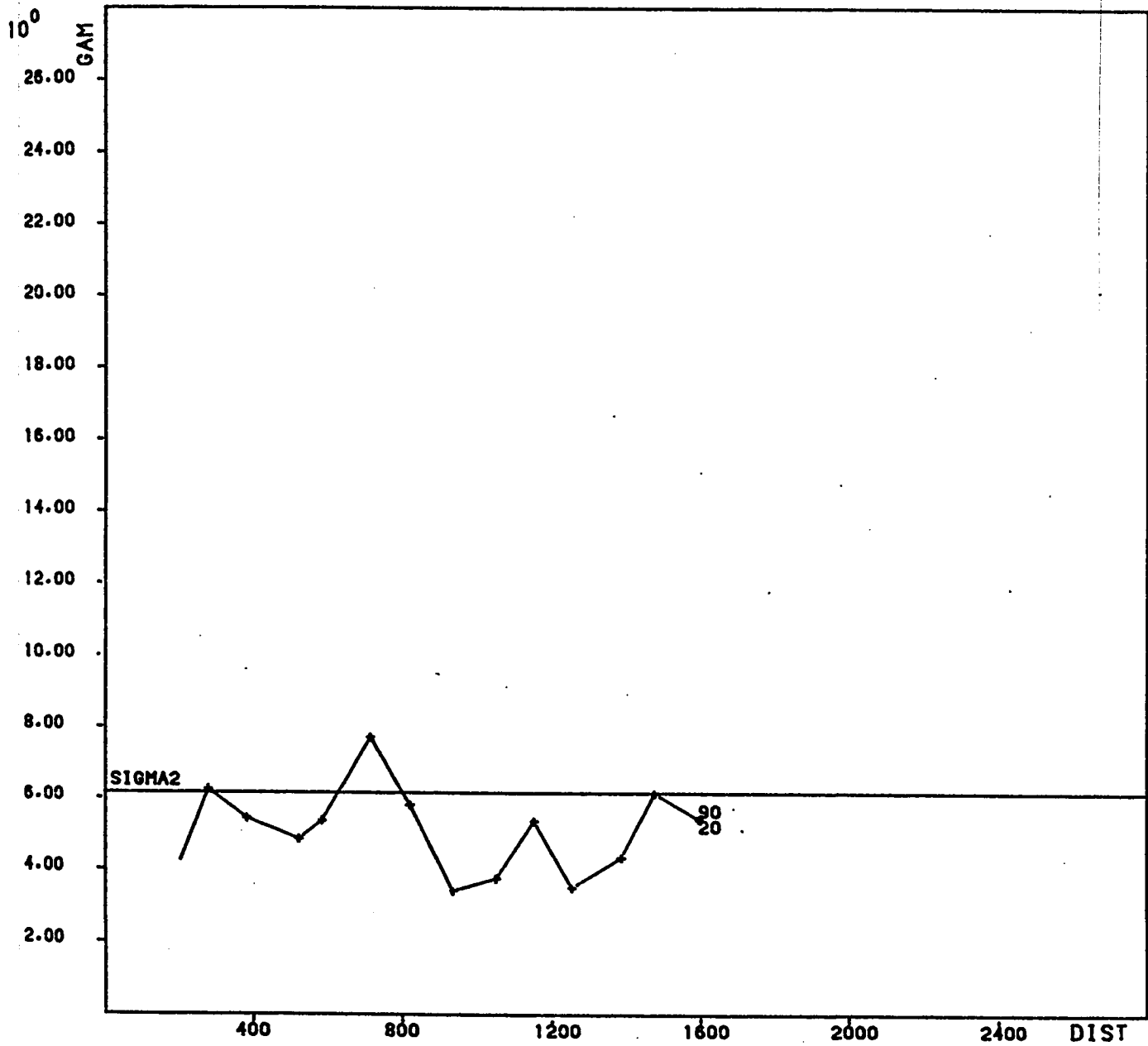
VARIABLE P205

ABSOLUTE

VARIOGRAM

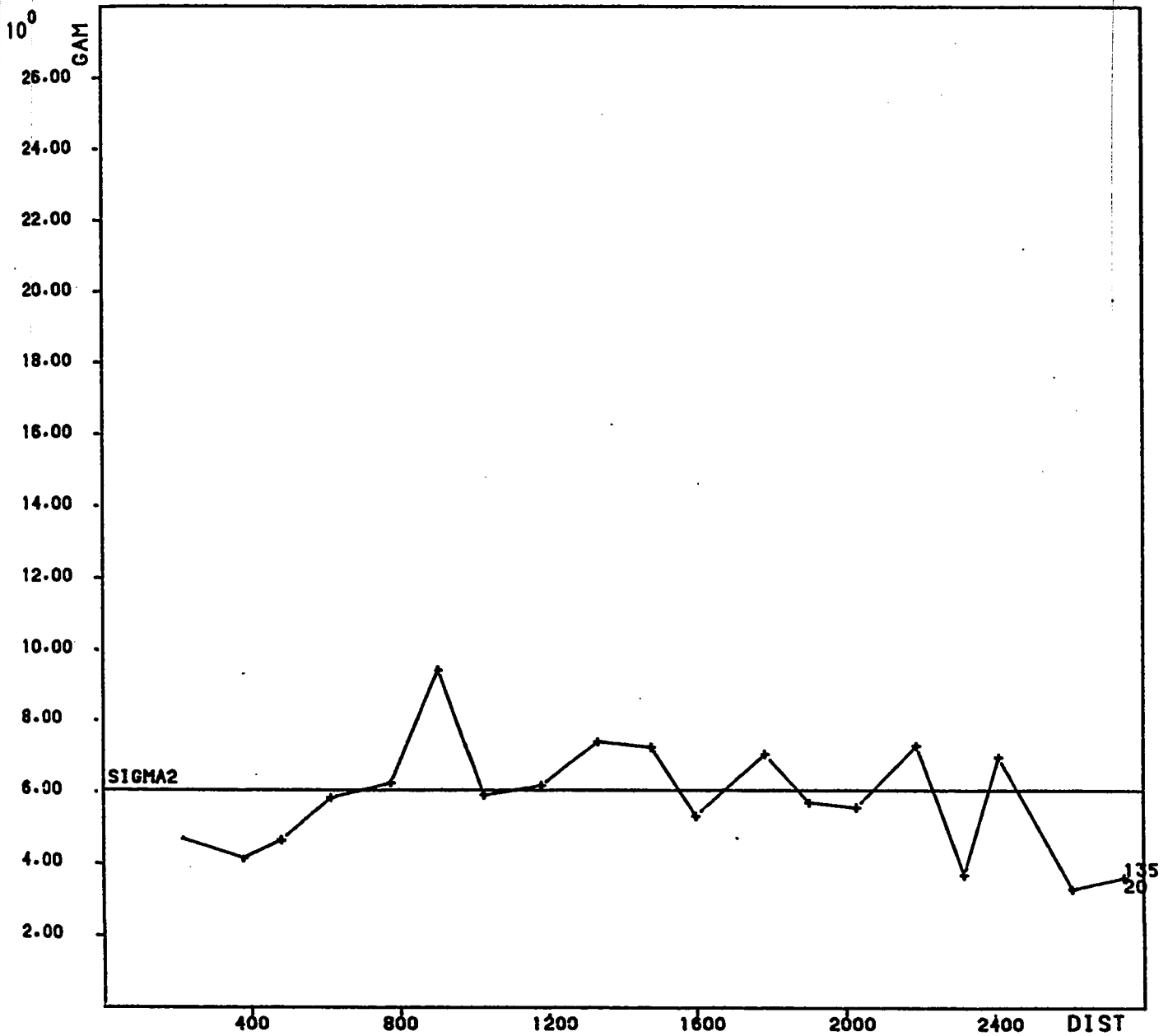
ABU TARTUR PORGRAM VR103 - HORIZONTAL VARIOGRAM (1M.COMPOSITES)

(C3)



VARIABLE P205 ABSOLUTE VARIOGRAM
ABU TARTUR PORGRAM VRIO3 - HORIZONTAL VARIOGRAM (1M.COMPOSITES)

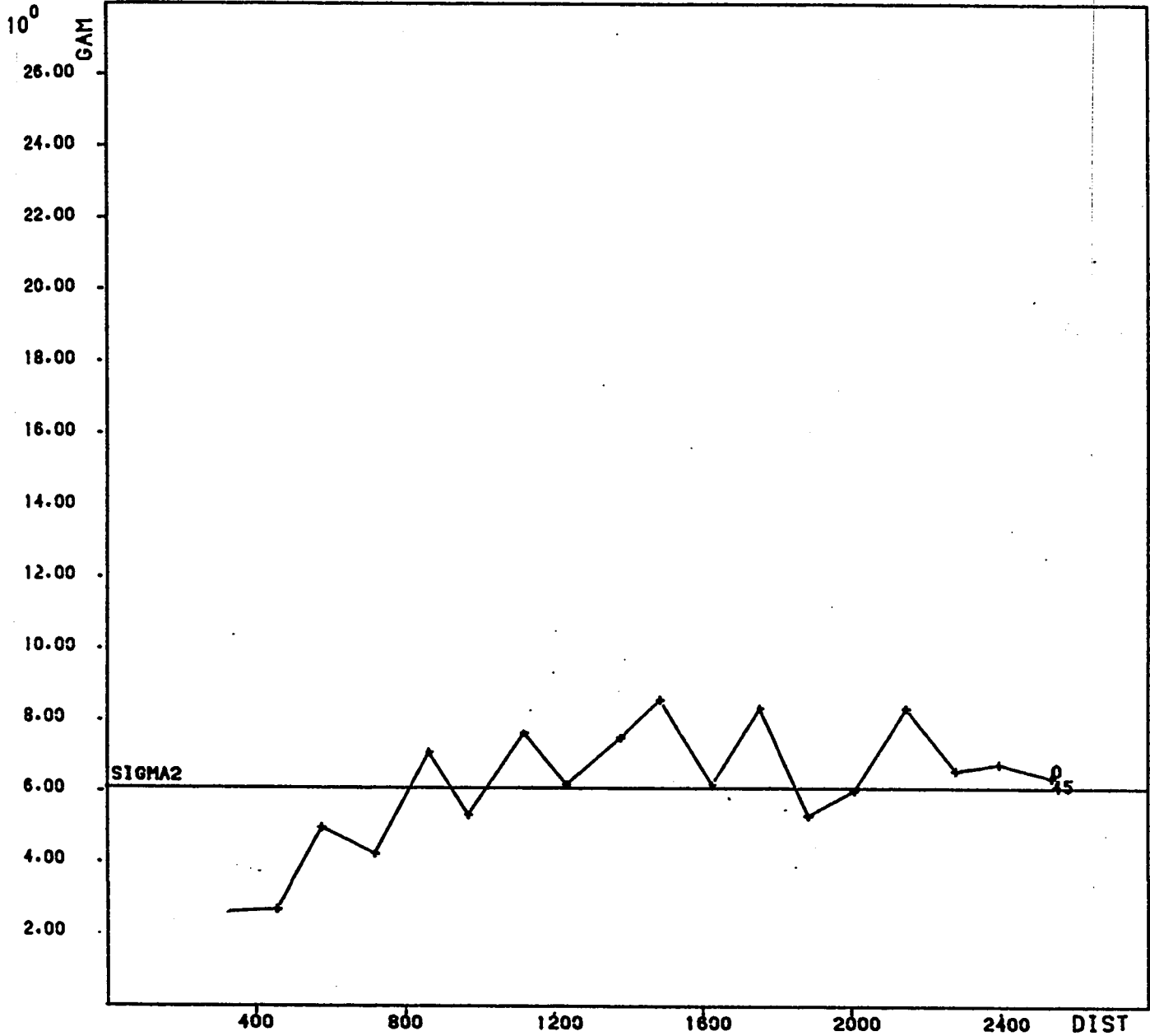
(C4)



VARIABLE P205
ABU TARTUR PORGRAM VR103 - HORIZONTAL VARIOGRAM (1M.COMPOSITES)

ABSOLUTE VARIOGRAM

(C5)



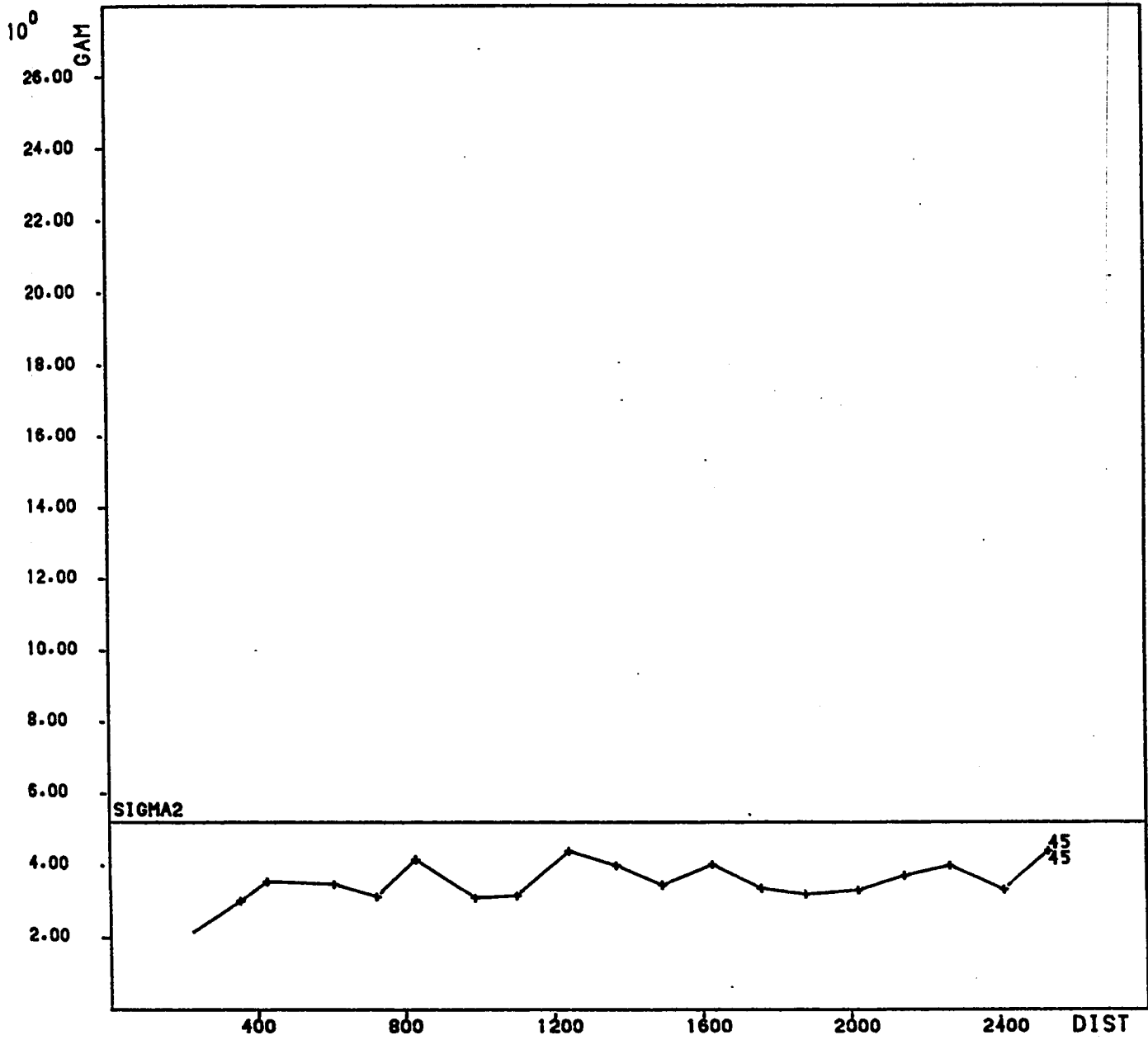
VARIABLE P205

ABSOLUTE

VARIOGRAM

ABU TARTUR PROGRAM VARIO3-HORIZONTAL VARIOGRAM

(C6)



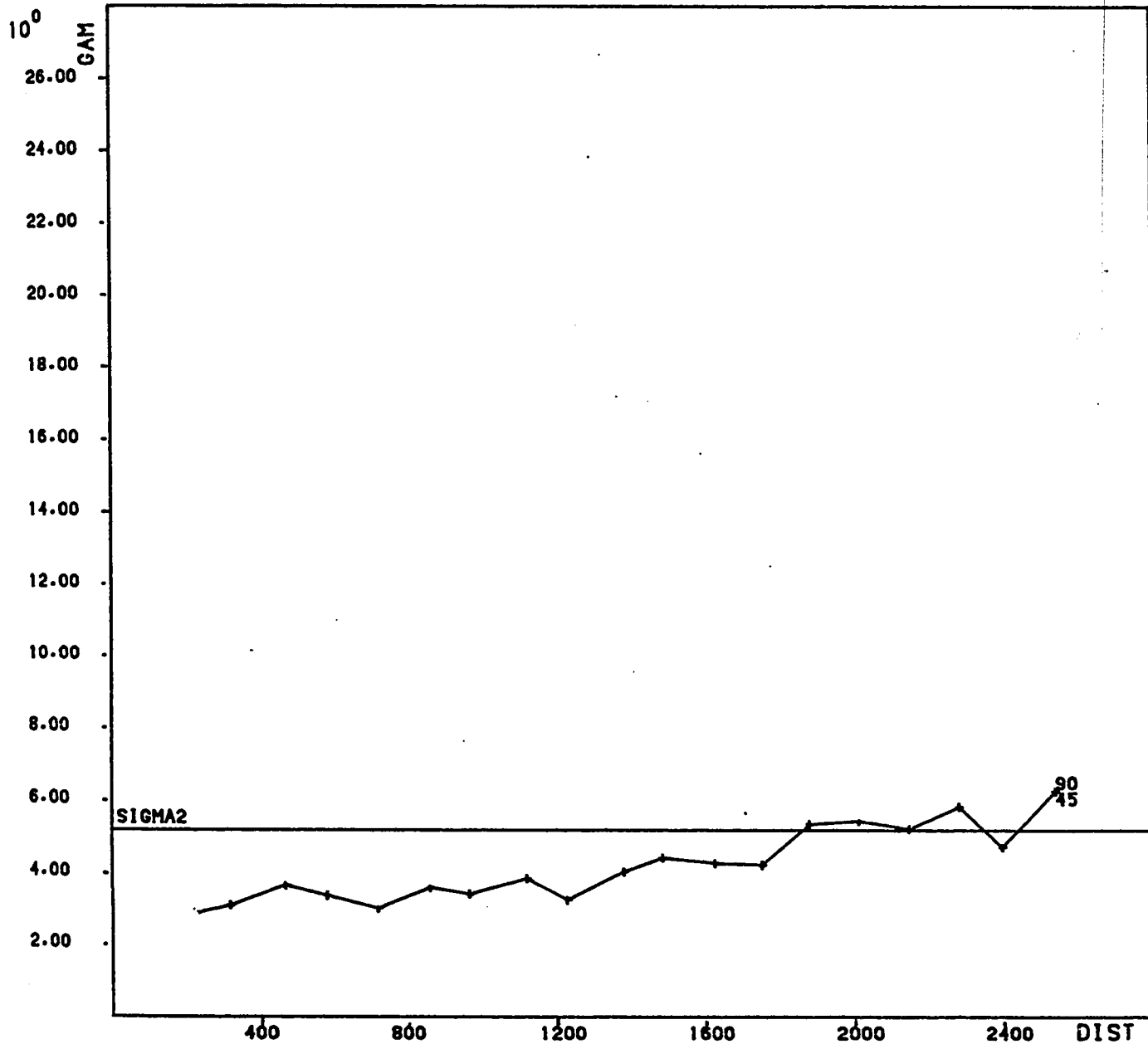
VARIABLE P205

ABSOLUTE

VARIOGRAM

ABU TARTUR PROGRAM VARIO3-HORIZONTAL VARIOGRAM

(C7)



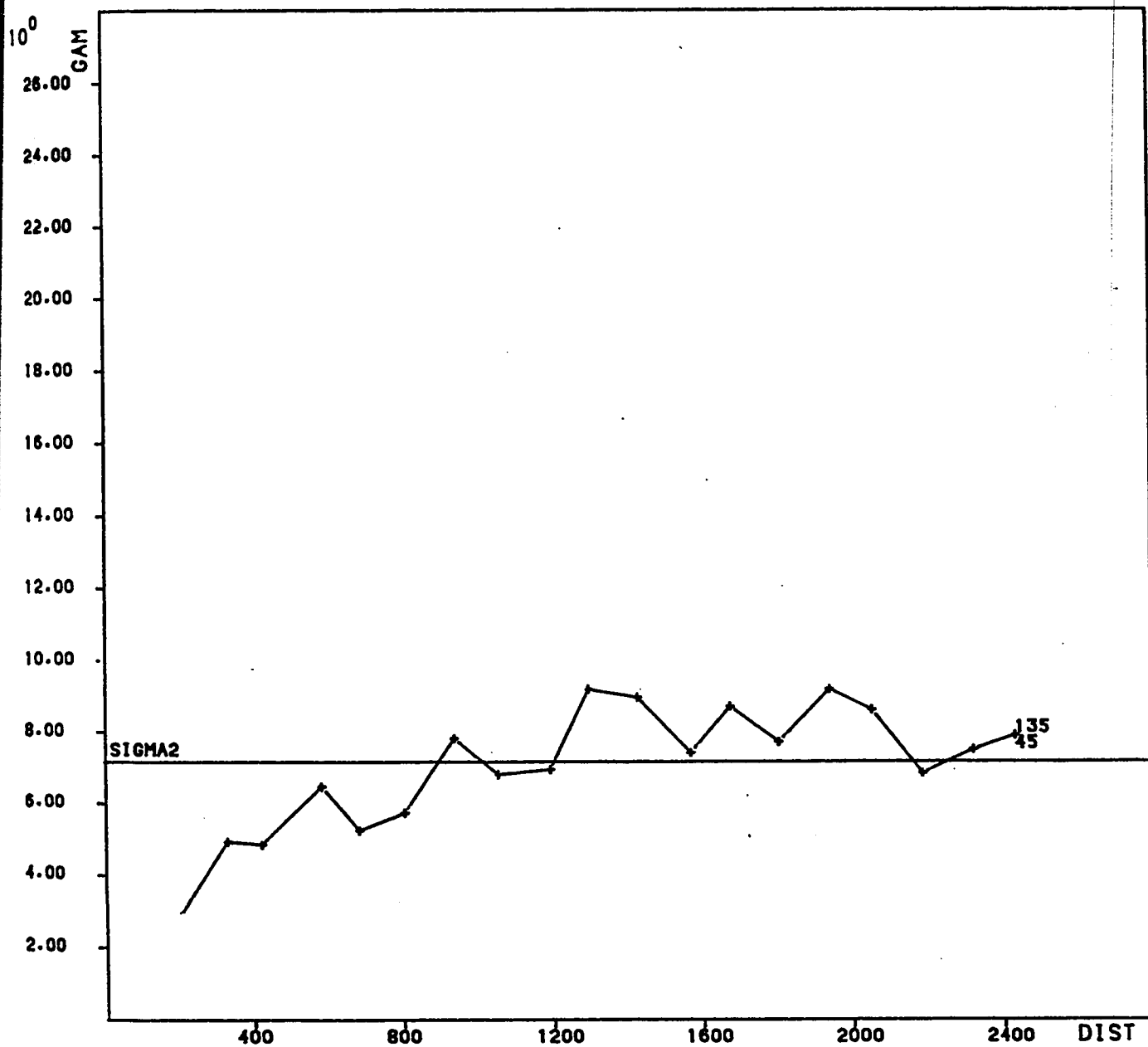
VARIABLE P205

ABSOLUTE

VARIOGRAM

ABU TARTUR PROGRAM VARIO3-HORIZONTAL VARIOGRAM

(C8)



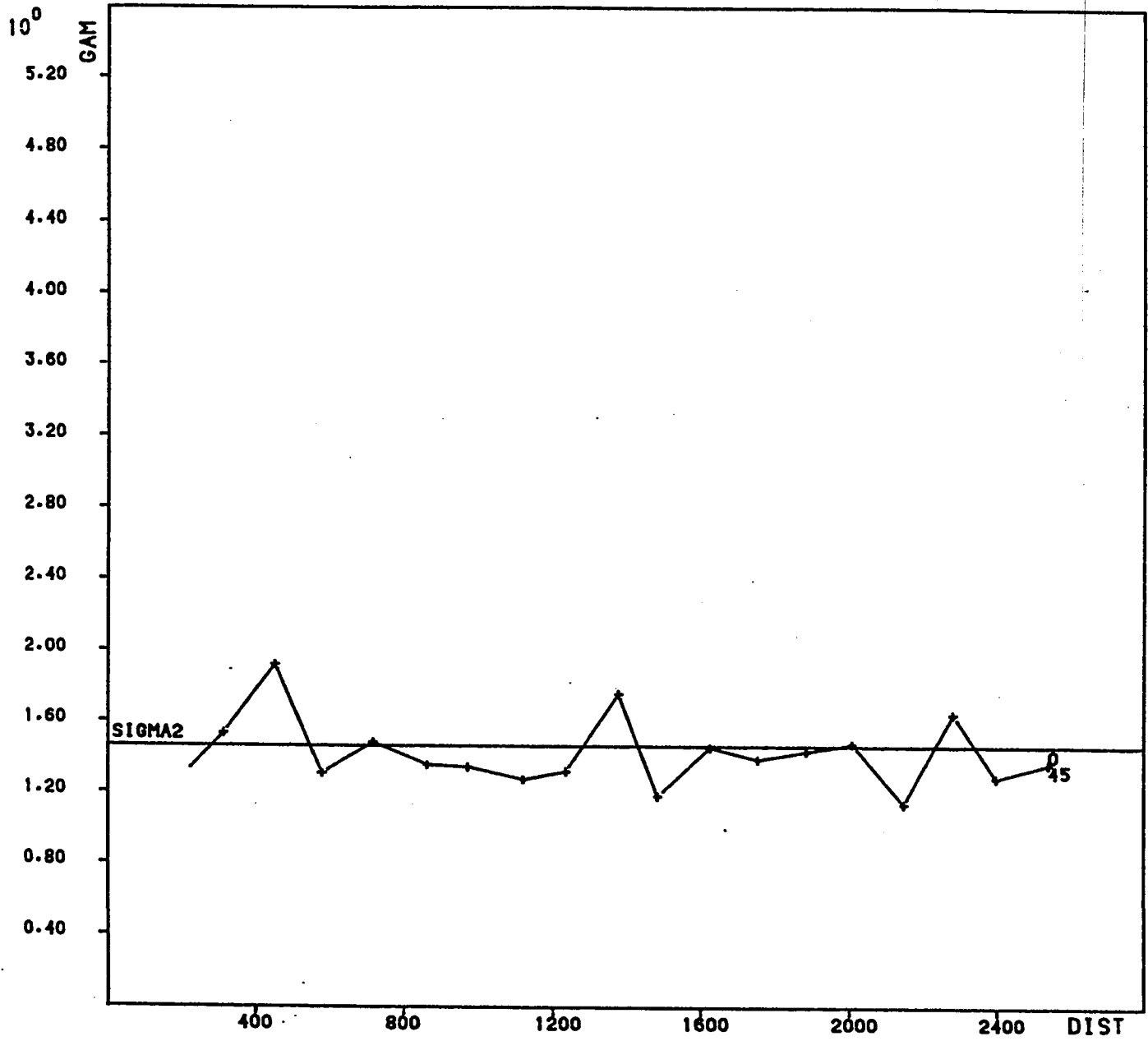
VARIABLE P205

ABSOLUTE

VARIOGRAM

ABU TARTUR PROGRAM VARIO3-HORIZONTAL VARIOGRAM

(C9)

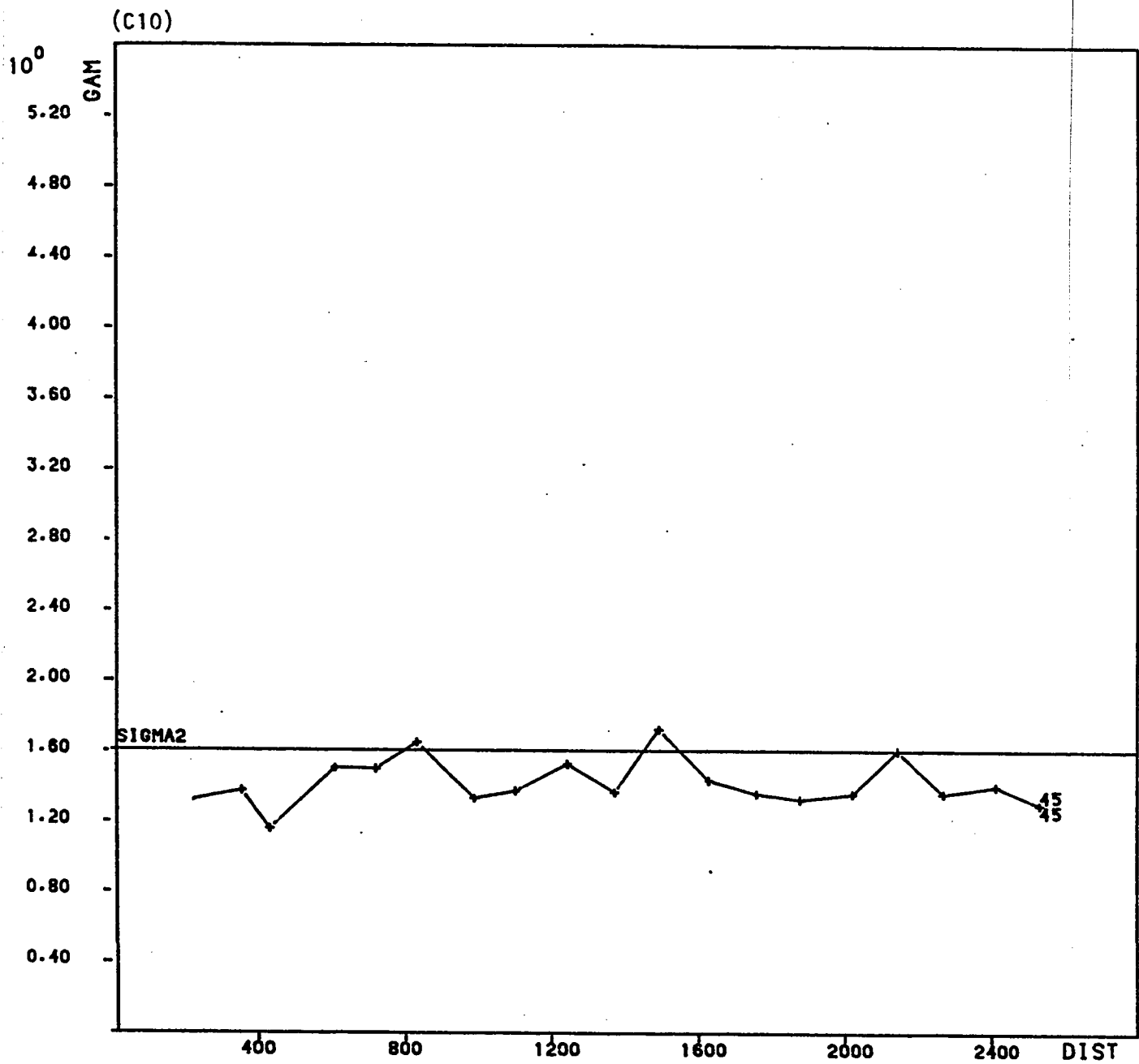


VARIABLE H

ABSOLUTE

VARIOGRAM

ABU TARTUR PROGRAM VARIO3-HORIZONTAL VARIOGRAM

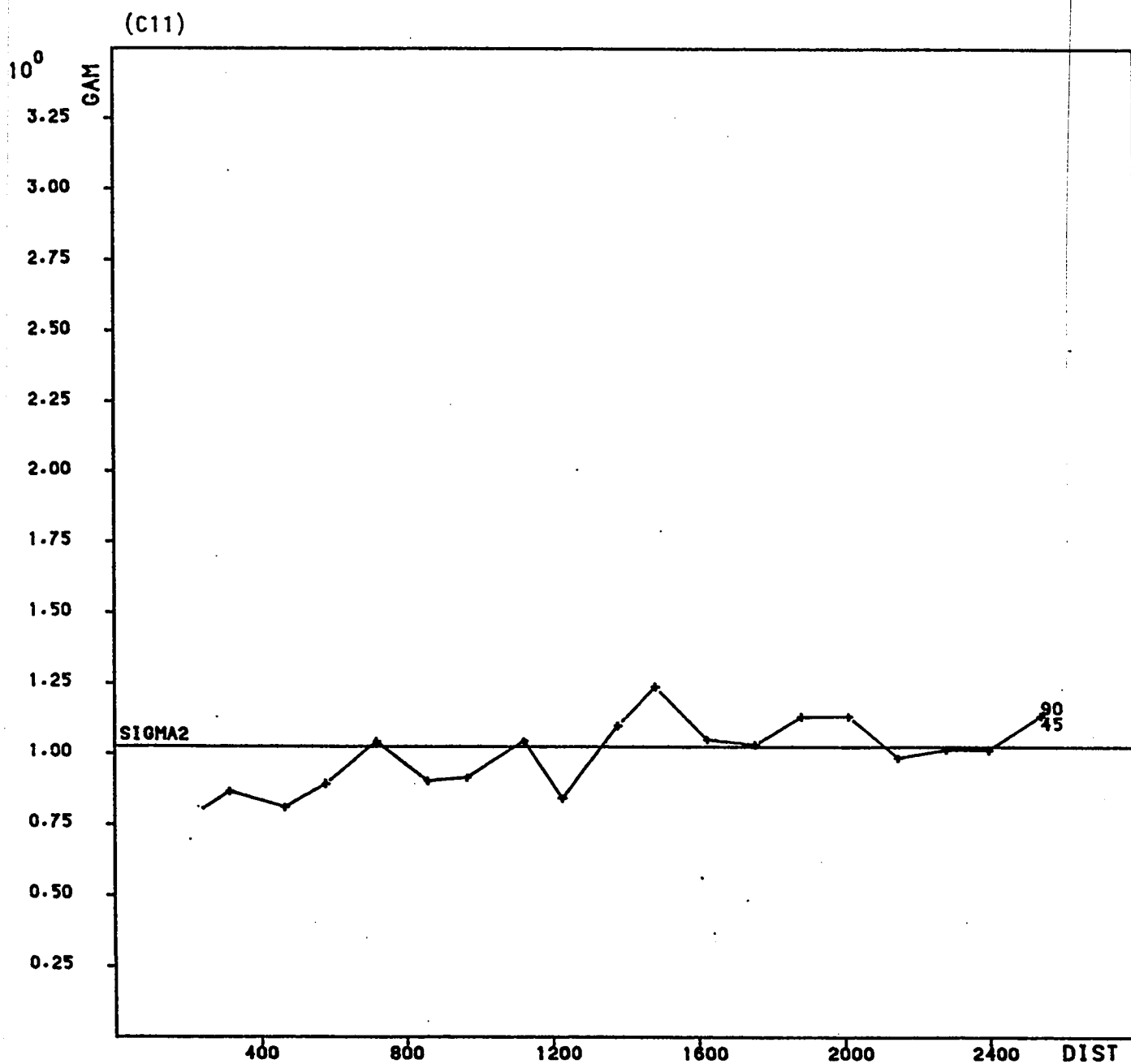


VARIABLE H

ABSOLUTE

VARIOGRAM

ABU TARTUR PROGRAM VARIO3-HORIZONTAL VARIOGRAM



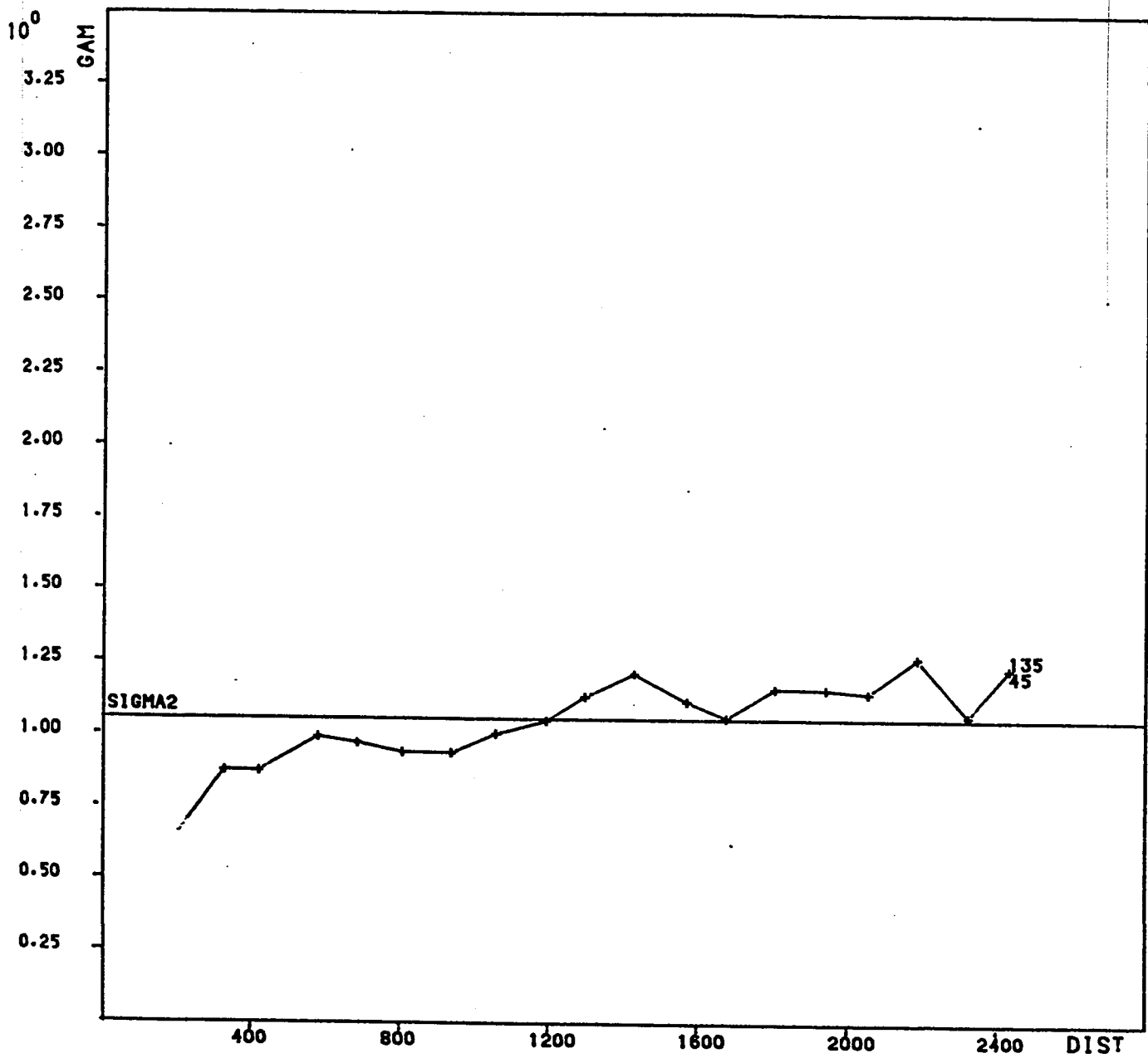
VARIABLE H

ABSOLUTE

VARIogram

ABU TARTUR PROGRAM VARIO3-HORIZONTAL VARIogram

(C12)



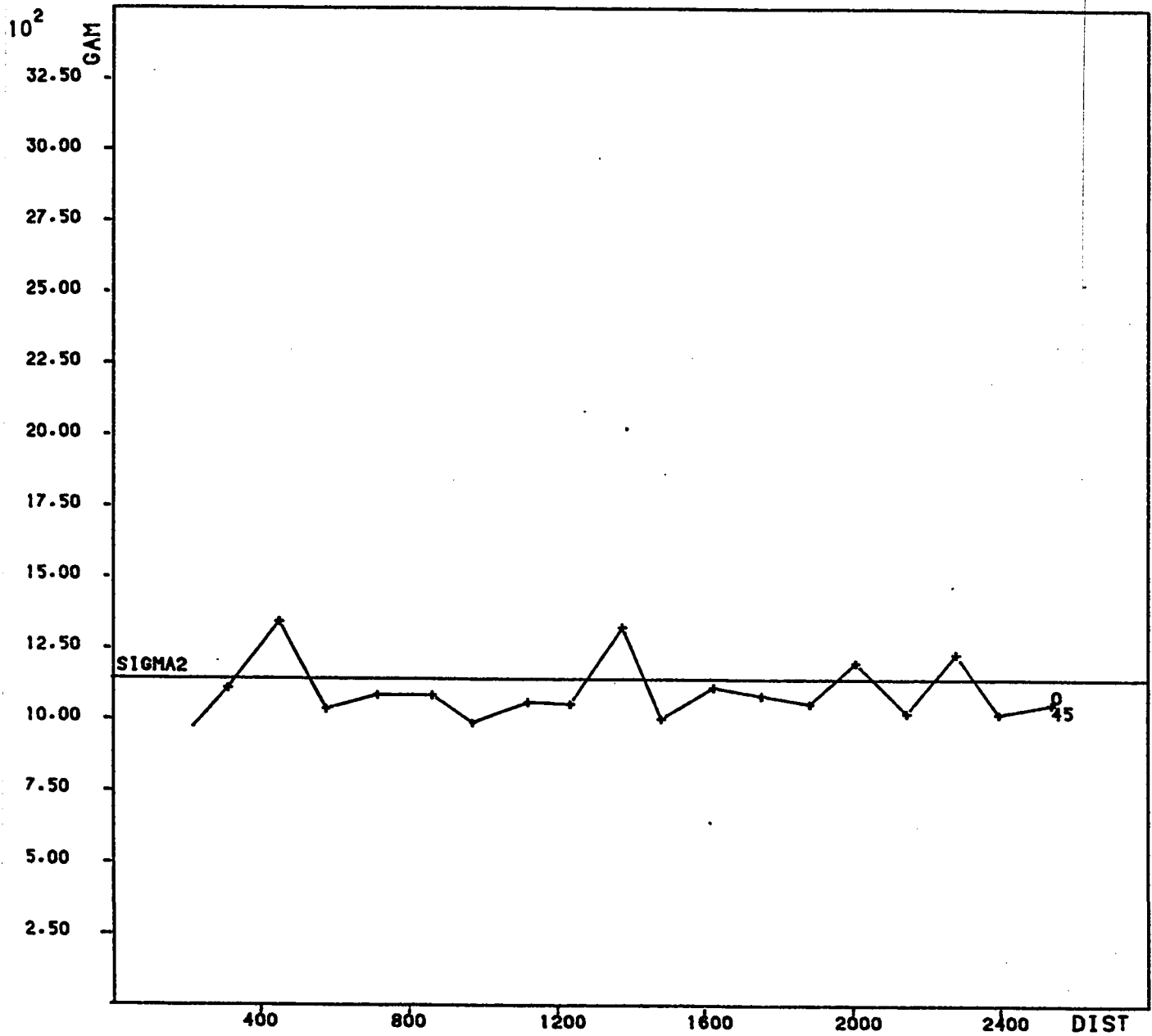
VARIABLE H

ABSOLUTE

VARIOGRAM

ABU TARTUR PROGRAM VARIO3-HORIZONTAL VARIOGRAM

(C13)



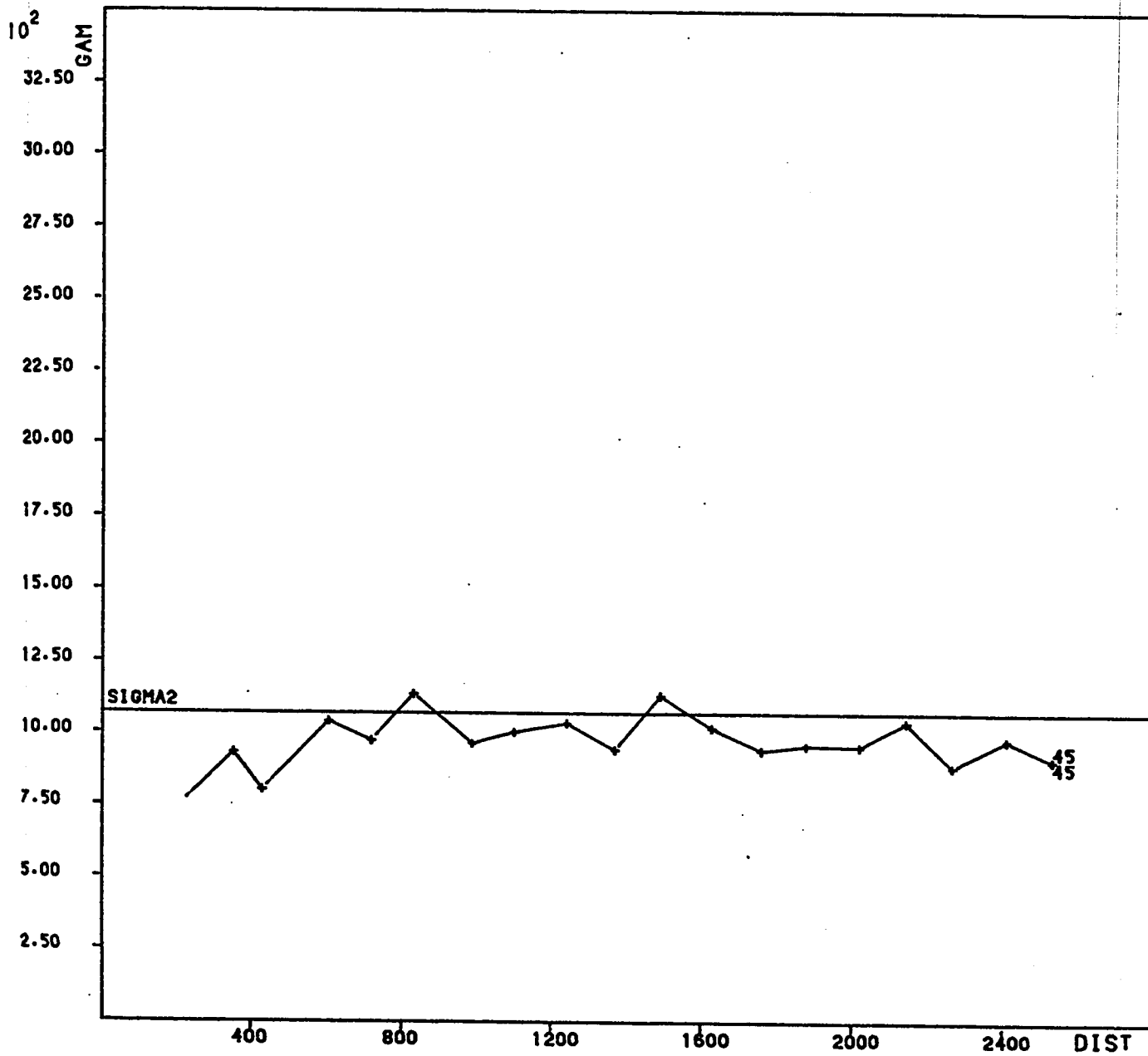
VARIABLE ACCU

ABSOLUTE

VARIogram

ABU TARTUR PROGRAM VARIO3-HORIZONTAL VARIogram

(C14)



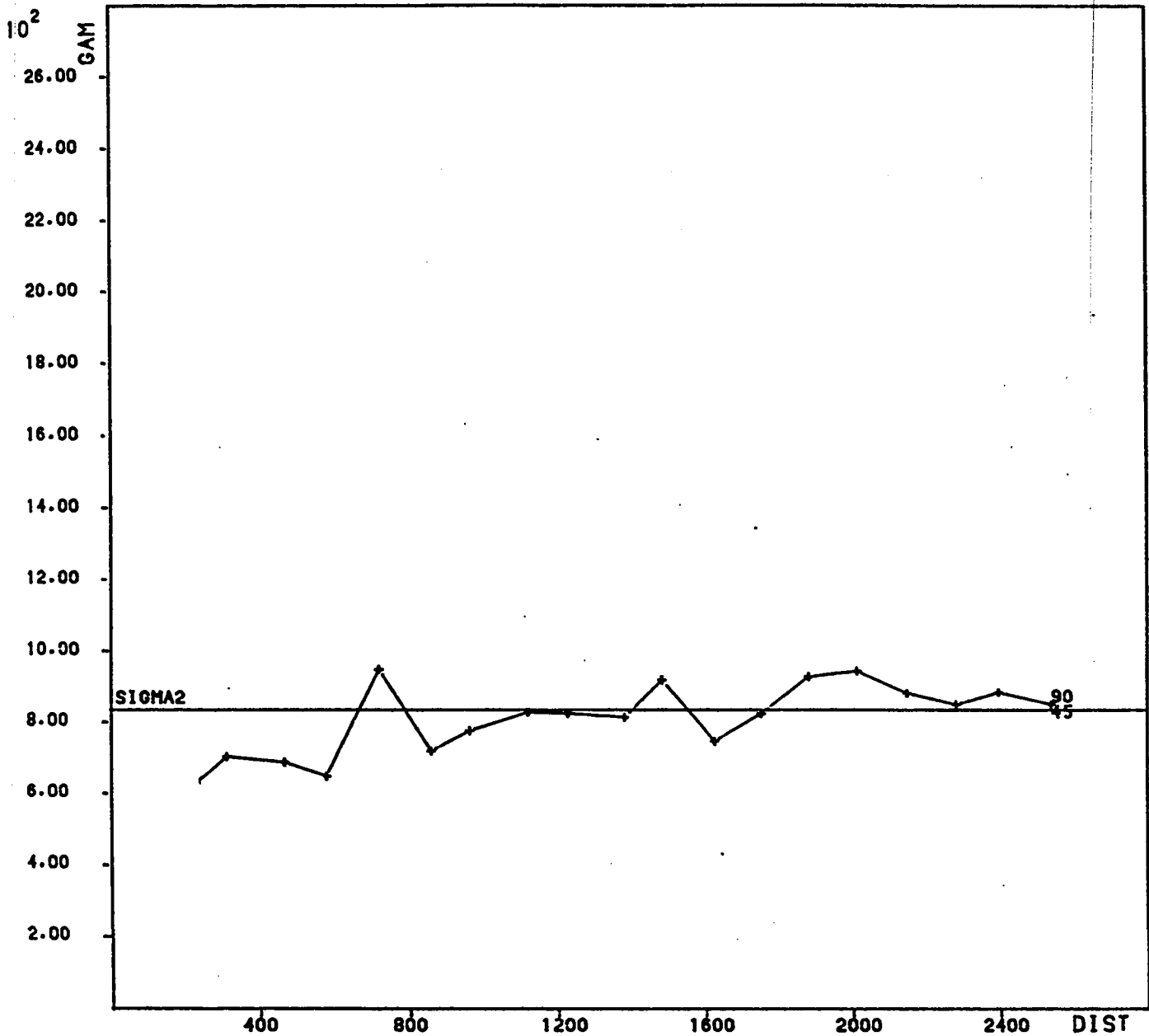
VARIABLE ACCU

ABSOLUTE

VARIOGRAM

ABU TARTUR PROGRAM VARIO3-HORIZONTAL VARIOGRAM

(C15)



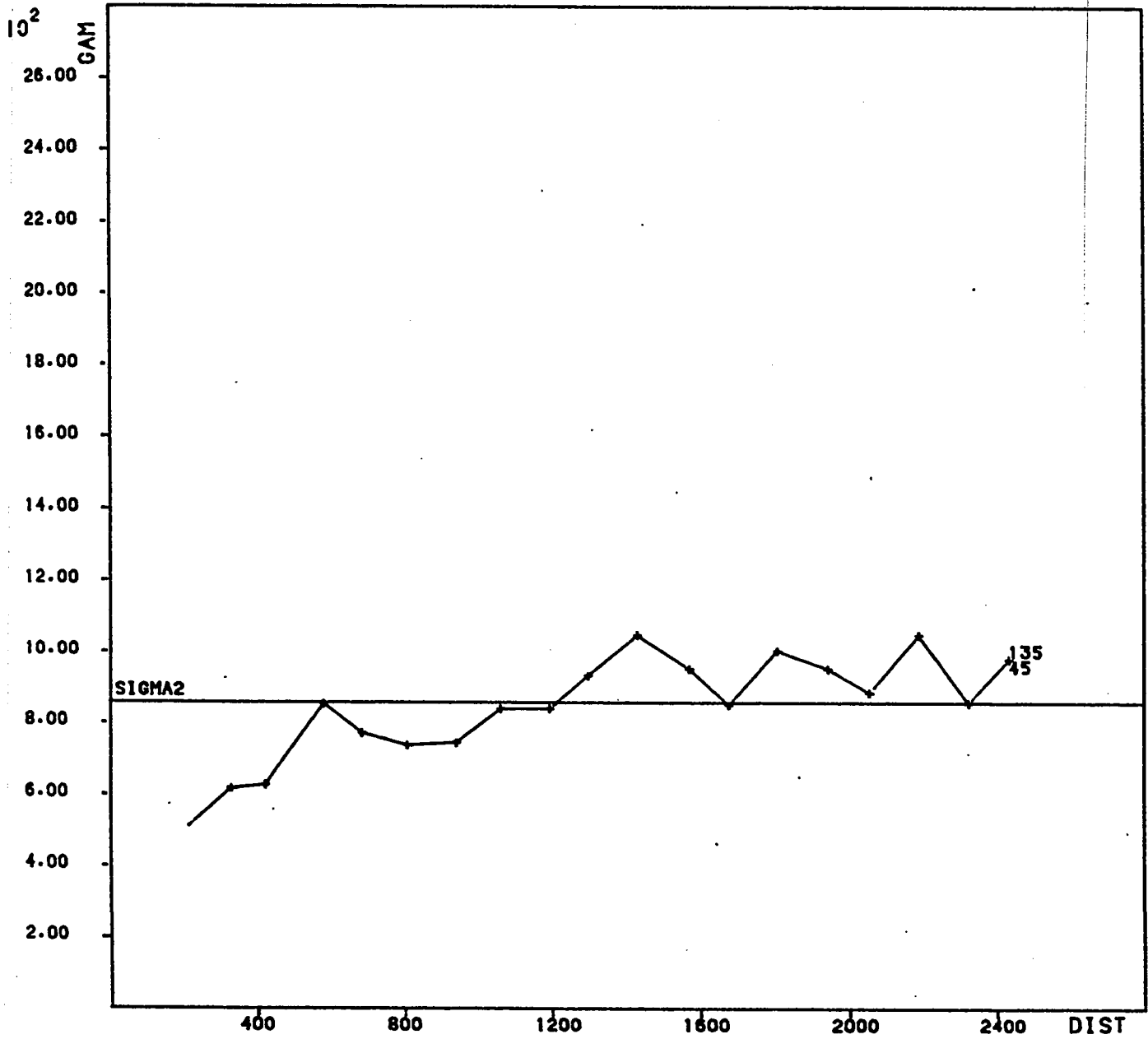
VARIABLE ACCU

ABSOLUTE

VARIGRAM

ABU TARTUR PROGRAM VARIO3-HORIZONTAL VARIGRAM

(C16)



VARIABLE ACCU

ABSOLUTE

VARIogram

ABU TARTUR PROGRAM VARIO3-HORIZONTAL VARIOGRAM

APPENDIX D

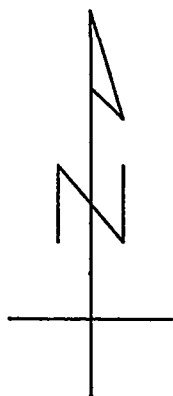
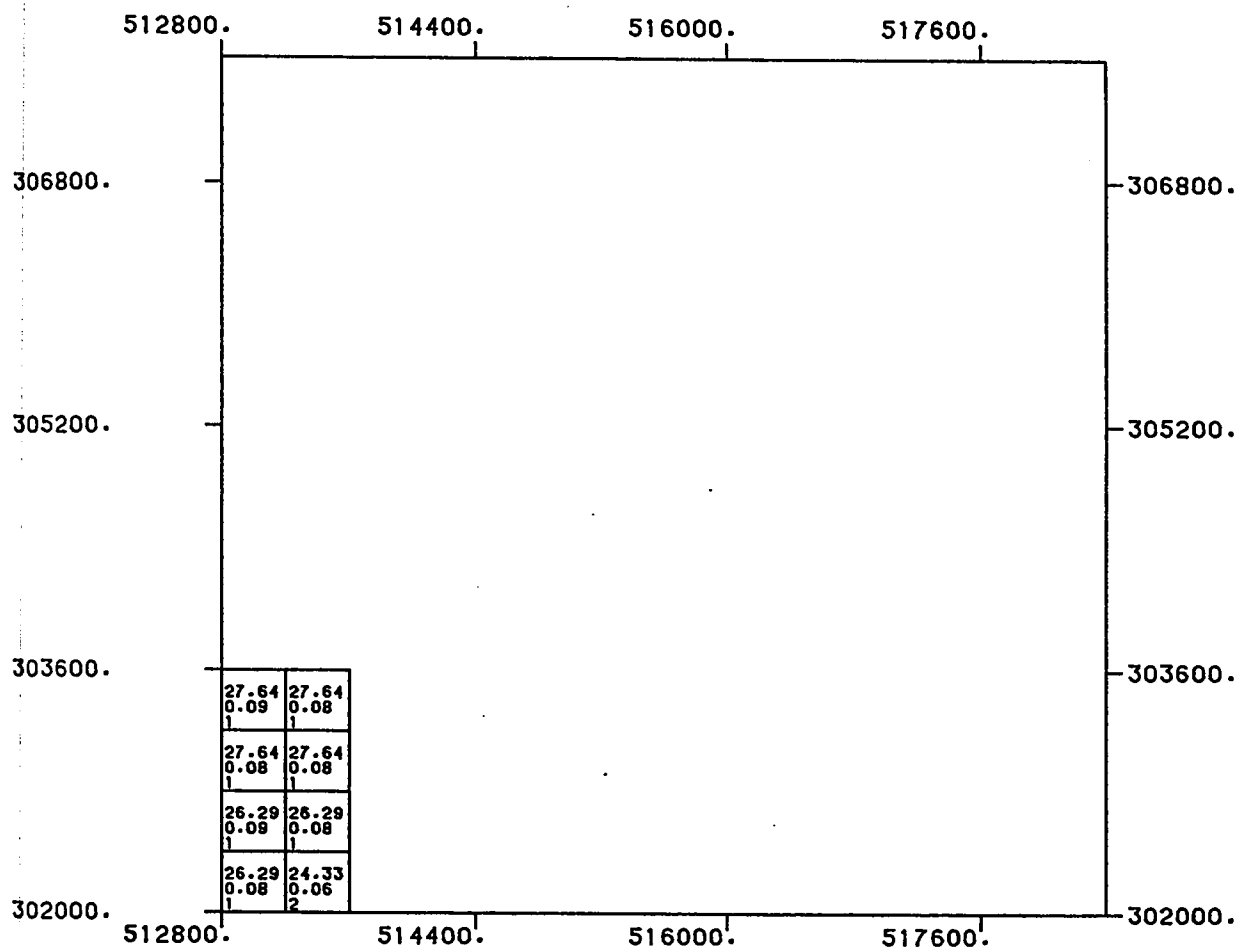
Results of kriging plotted on
horizontal planes (P205%)

D1.	Results of block kriging for level 3
D2.	Results of block kriging for level 4
D3.	Results of block kriging for level 5
D4.	Results of block kriging for level 6
D5.	Results of block kriging for level 7
D6.	Results of block kriging for level 16
D7.	Results of block kriging for level 17
D8.	Results of block kriging for level 18
D9.	Results of block kriging for level 19
D10.	Results of block kriging for level 20
D11.	Results of block kriging for level 21
D12.	Results of block kriging for level 22
D13.	Results of block kriging for level 23
D14.	Results of block kriging for level 24
D15.	Results of block kriging for level 25
D16.	Results of block kriging for level 26
D17.	Results of block kriging for level 35
D18.	Results of block kriging for level 36
D19.	Results of block kriging for level 37
D20.	Results of block kriging for level 38
D21.	Results of block kriging for level 45
D22.	Results of block kriging for level 46
D23.	Results of block kriging for level 47
D24.	Results of block kriging for level 48
D25.	Results of block kriging for level 49
D26.	Results of block kriging for level 50
D27.	Results of block kriging for level 53
D28.	Results of block kriging for level 55
D29.	Results of block kriging for level 56
D30.	Results of block kriging for level 62
D31.	Results of block kriging for level 63
D32.	Results of block kriging for level 64
D33.	Results of block kriging for level 69
D34.	Results of block kriging for level 70
D35.	Results of block kriging for level 71

D36. Results of block kriging for level 72
D37. Results of block kriging for level 73
D38. Results of block kriging for level 74
D39. Results of block kriging for level 75
D40. Results of block kriging for level 76
D41. Results of block kriging for level 77
D42. Results of block kriging for level 78
D43. Results of block kriging for level 79
D44. Results of block kriging for level 80
D45. Results of block kriging for level 81
D46. Results of block kriging for level 82
D47. Results of block kriging for level 83
D48. Results of block kriging for level 84
D49. Results of block kriging for level 85
D50. Results of block kriging for level 86
D51. Results of block kriging for level 87
D52. Results of block kriging for level 88
D53. Results of block kriging for level 89
D54. Results of block kriging for level 90
D55. Results of block kriging for level 91
D56. Results of block kriging for level 92
D57. Results of block kriging for level 93
D58. Results of block kriging for level 94
D59. Results of block kriging for level 95
D60. Results of block kriging for level 96
D61. Results of block kriging for level 97
D62. Results of block kriging for level 98
D63. Results of block kriging for level 99
D64. Results of block kriging for level 100
D65. Results of block kriging for level 101
D66. Results of block kriging for level 102
D67. Results of block kriging for level 103
D68. Results of block kriging for level 104
D69. Results of block kriging for level 105
D70. Results of block kriging for level 106
D71. Results of block kriging for level 107
D72. Results of block kriging for level 108
D73. Results of block kriging for level 109
D74. Results of block kriging for level 110
D75. Results of block kriging for level 111
D76. Results of block kriging for level 112
D77. Results of block kriging for level 113
D78. Results of block kriging for level 114
D79. Results of block kriging for level 115
D80. Results of block kriging for level 116
D81. Results of block kriging for level 117

D82. Results of block kriging for level 118
D83. Results of block kriging for level 119
D84. Results of block kriging for level 120
D85. Results of block kriging for level 121
D86. Results of block kriging for level 122
D87. Results of block kriging for level 123
D88. Results of block kriging for level 124
D89. Results of block kriging for level 125
D90. Results of block kriging for level 126
D91. Results of block kriging for level 127
D92. Results of block kriging for level 128
D93. Results of block kriging for level 129
D94. Results of block kriging for level 130
D95. Results of block kriging for level 131
D96. Results of block kriging for level 132
D97. Results of block kriging for level 133
D98. Results of block kriging for level 134
D99. Results of block kriging for level 135
D100. Results of block kriging for level 136
D101. Results of block kriging for level 137
D102. Results of block kriging for level 138
D103. Results of block kriging for level 139
D104. Results of block kriging for level 140
D105. Results of block kriging for level 141
D106. Results of block kriging for level 142
D107. Results of block kriging for level 143
D108. Results of block kriging for level 144
D109. Results of block kriging for level 147
D110. Results of block kriging for level 148
D111. Results of block kriging for level 149
D112. Results of block kriging for level 150
D113. Results of block kriging for level 151
D114. Results of block kriging for level 155

(D1)



ABU TARTUR PHOSPHATE DEPOSIT
RESULTS OF BLOCK KRIGING

(Z = 274.5)

LEVEL NUMBER : 3

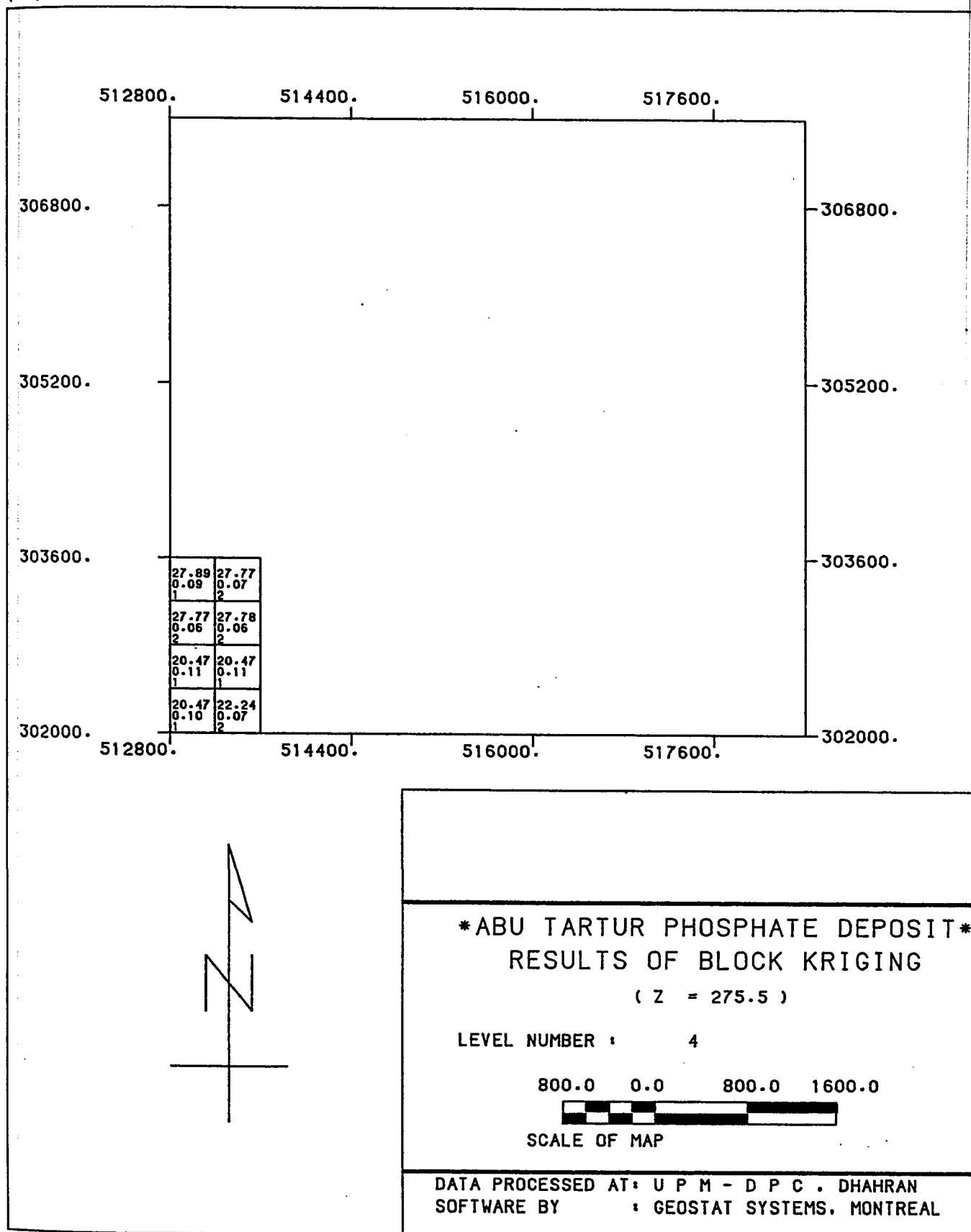
800.0 0.0 800.0 1600.0



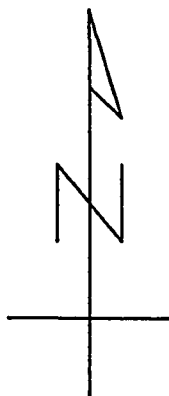
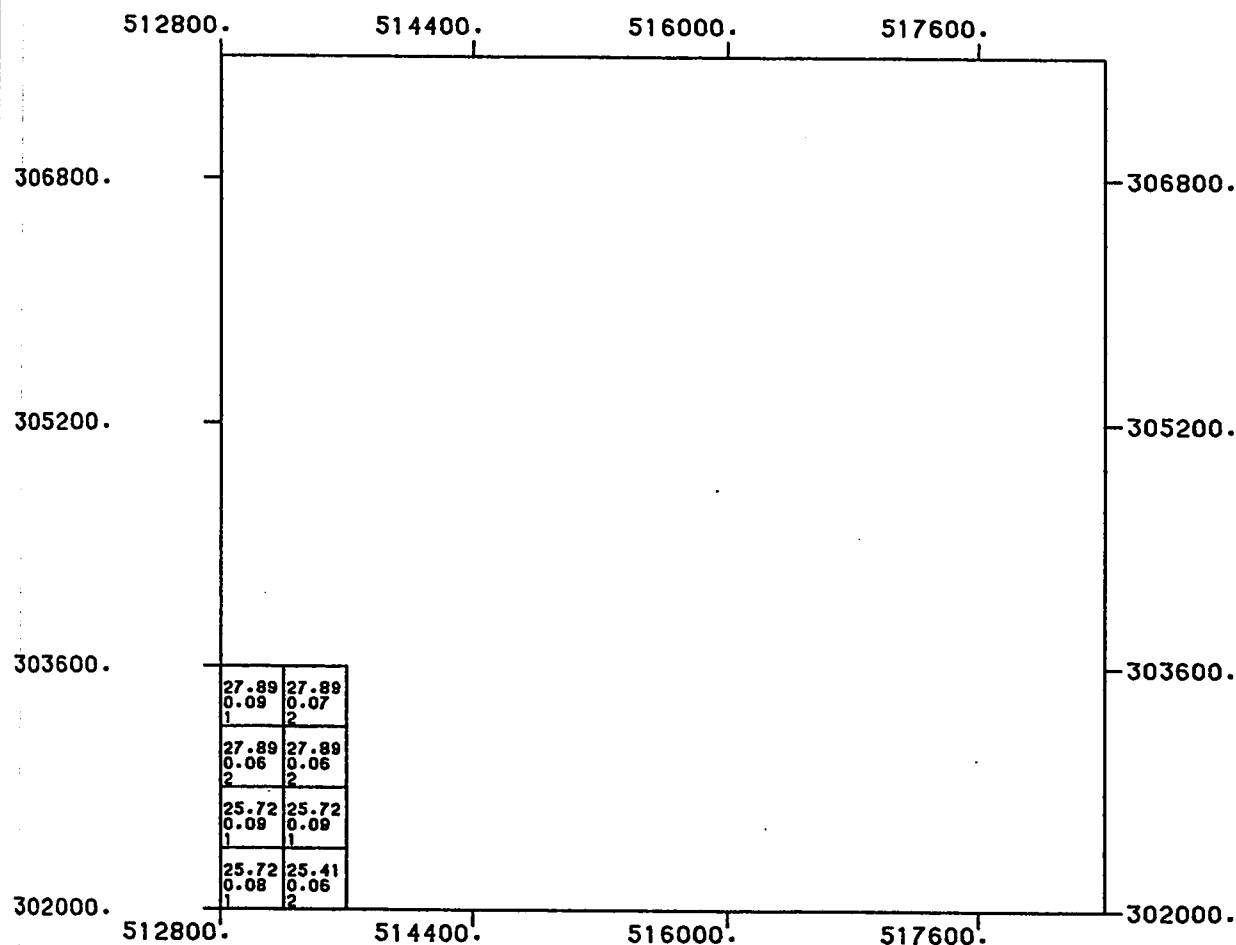
SCALE OF MAP

DATA PROCESSED AT: U P M - D P C , DHAHRAN
 SOFTWARE BY : GEOSTAT SYSTEMS, MONTREAL

(D2)



(D3)



ABU TARTUR PHOSPHATE DEPOSIT
RESULTS OF BLOCK KRIGING

(Z = 276.5)

LEVEL NUMBER : 5

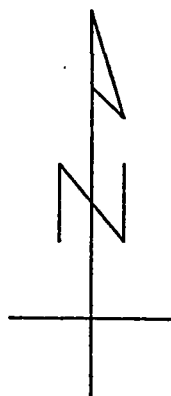
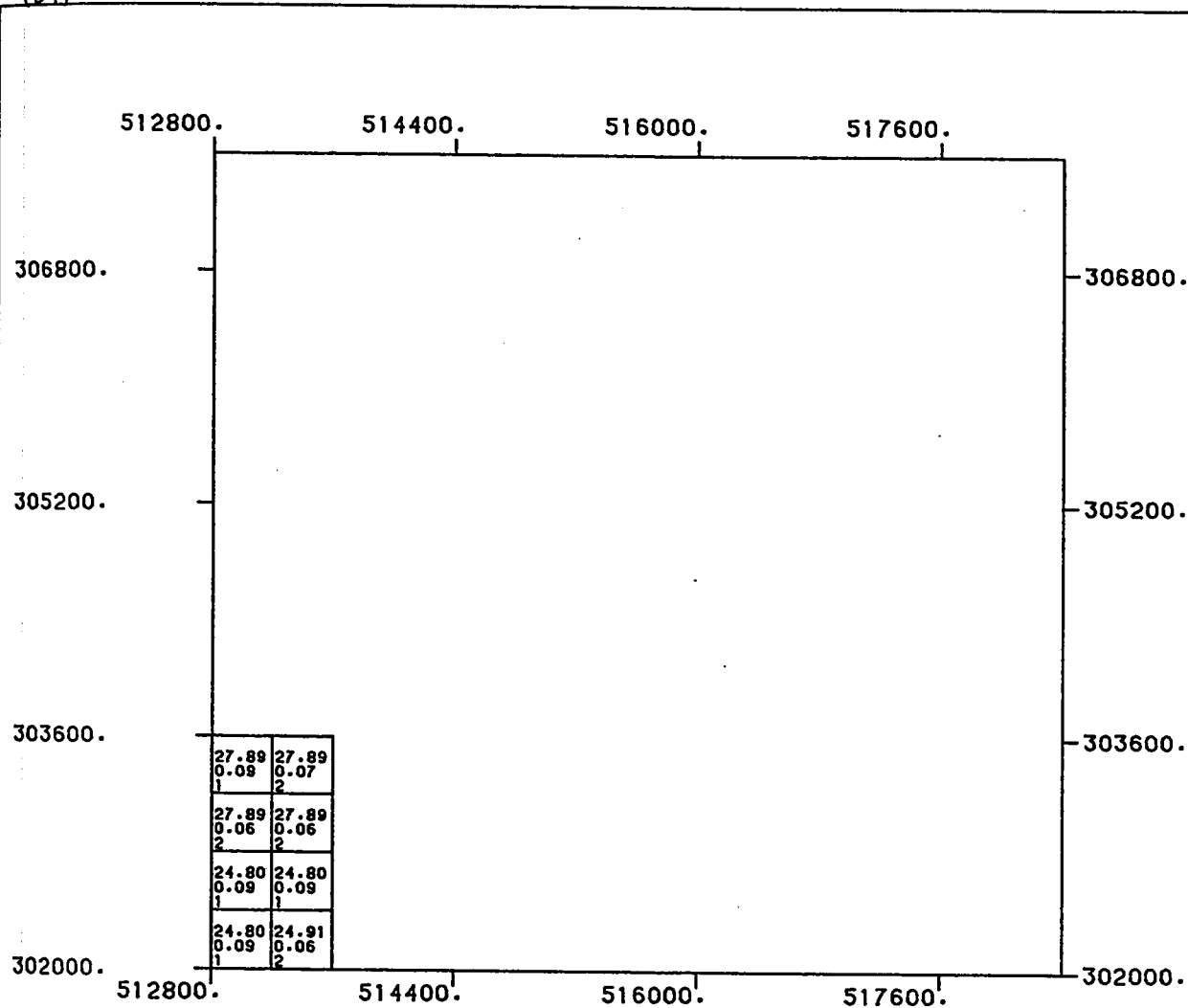
800.0 0.0 800.0 1600.0



SCALE OF MAP

DATA PROCESSED AT: U P M - D P C , DHAHRAN
SOFTWARE BY : GEOSTAT SYSTEMS, MONTREAL

(D4)



ABU TARTUR PHOSPHATE DEPOSIT
RESULTS OF BLOCK KRIGING

(Z = 277.5)

LEVEL NUMBER : 6

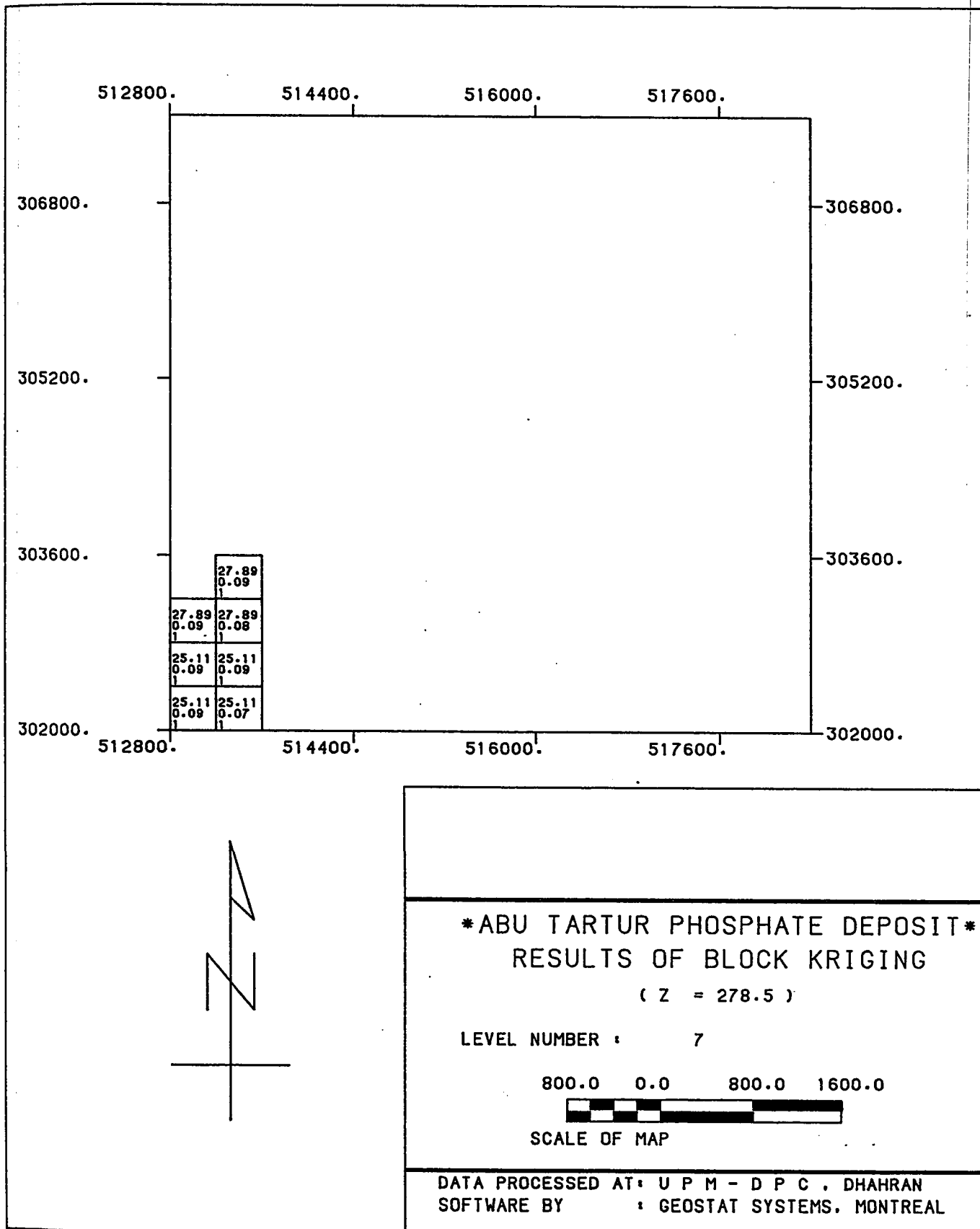
800.0 0.0 800.0 1600.0



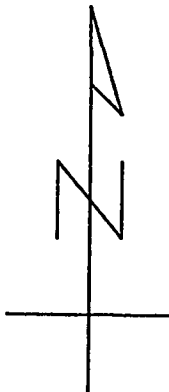
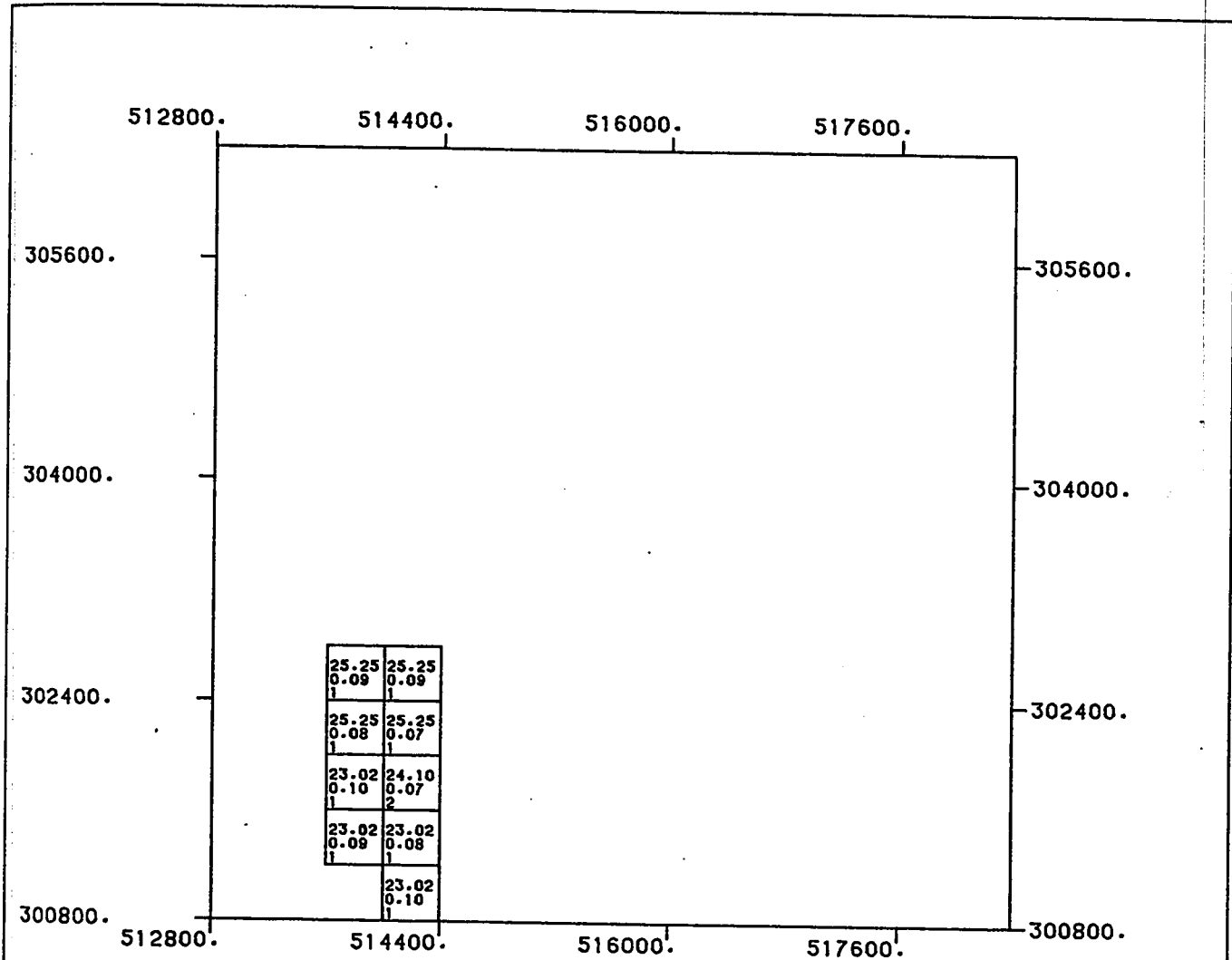
SCALE OF MAP

DATA PROCESSED AT: U P M - D P C , DHAHRAN
SOFTWARE BY : GEOSTAT SYSTEMS, MONTREAL

(D5)



(D6)



ABU TARTUR PHOSPHATE DEPOSIT
RESULTS OF BLOCK KRIGING

(Z = 287.5)

LEVEL NUMBER : 16

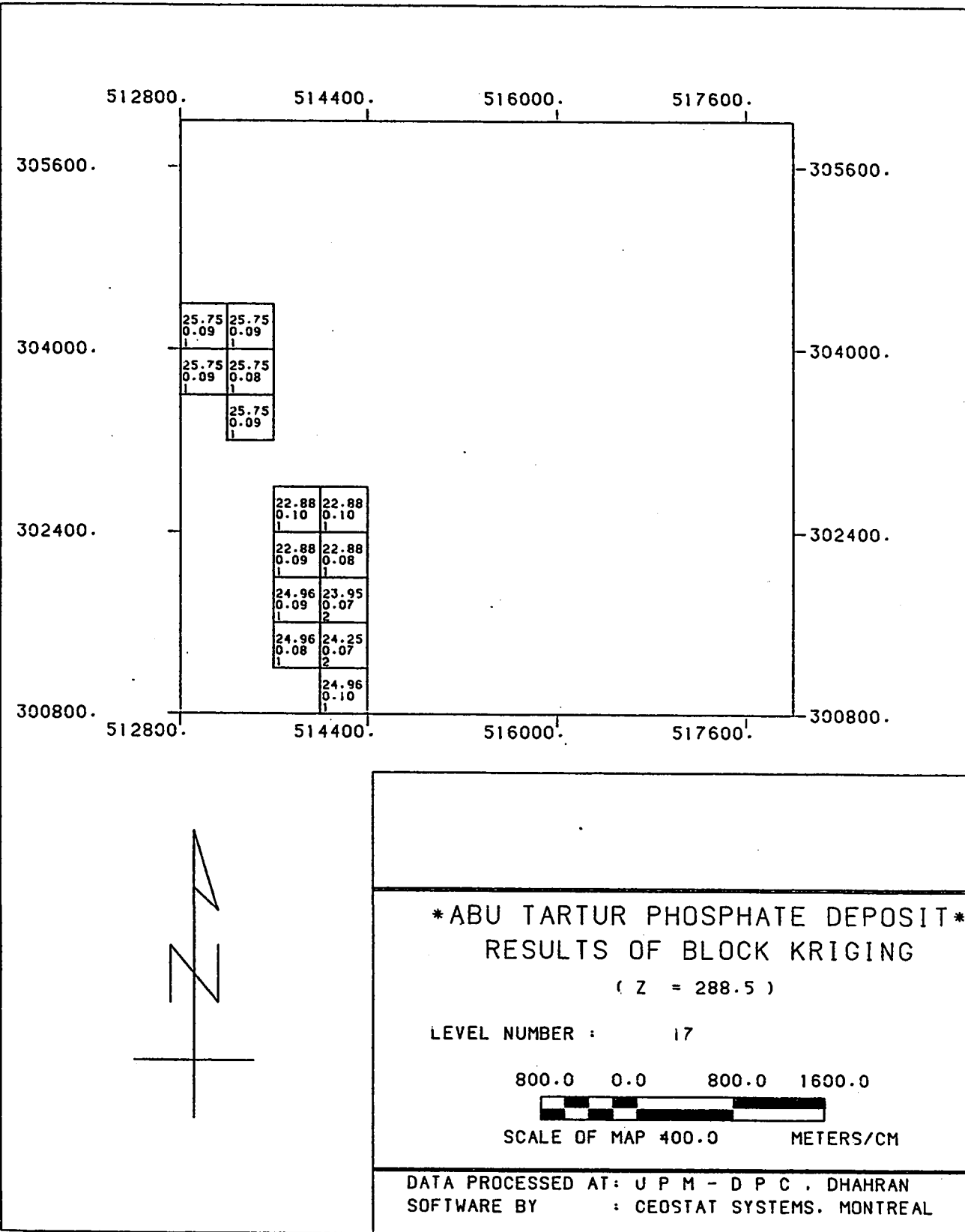
800.0 0.0 800.0 1600.0



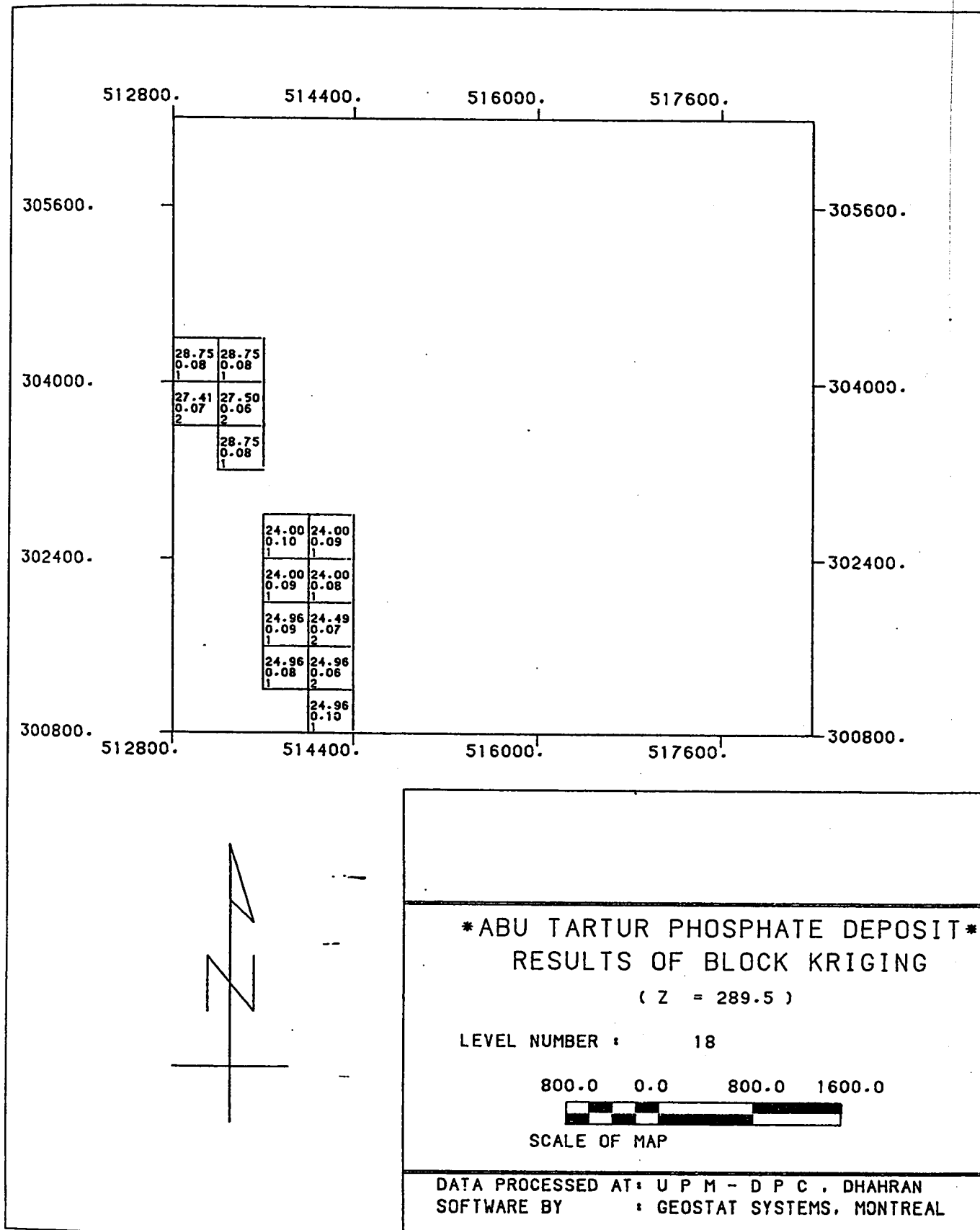
SCALE OF MAP

DATA PROCESSED AT: U P M - D P C , DHAHRAN
SOFTWARE BY : GEOSTAT SYSTEMS, MONTREAL

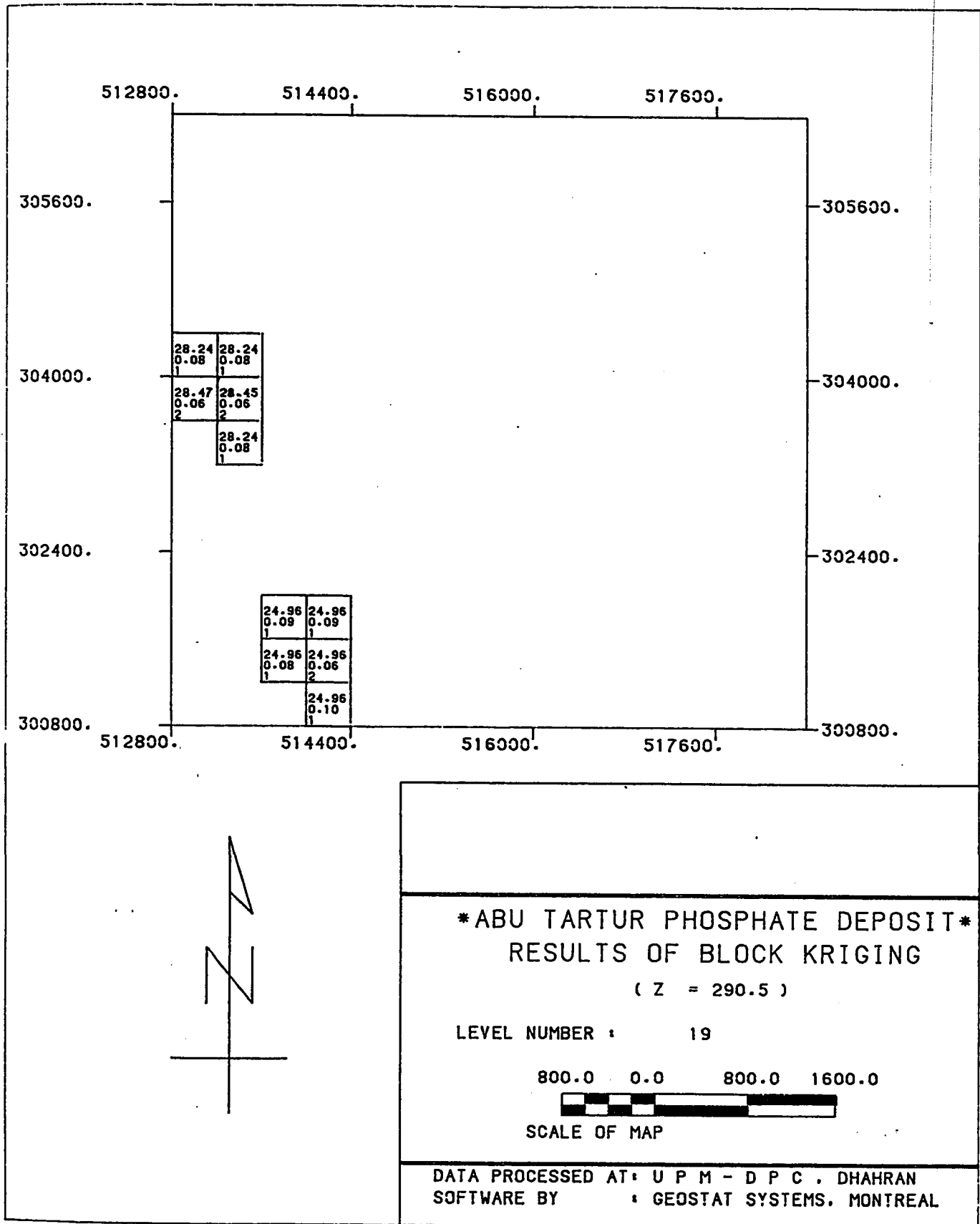
(D7)



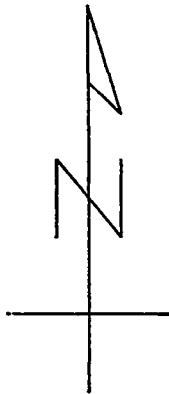
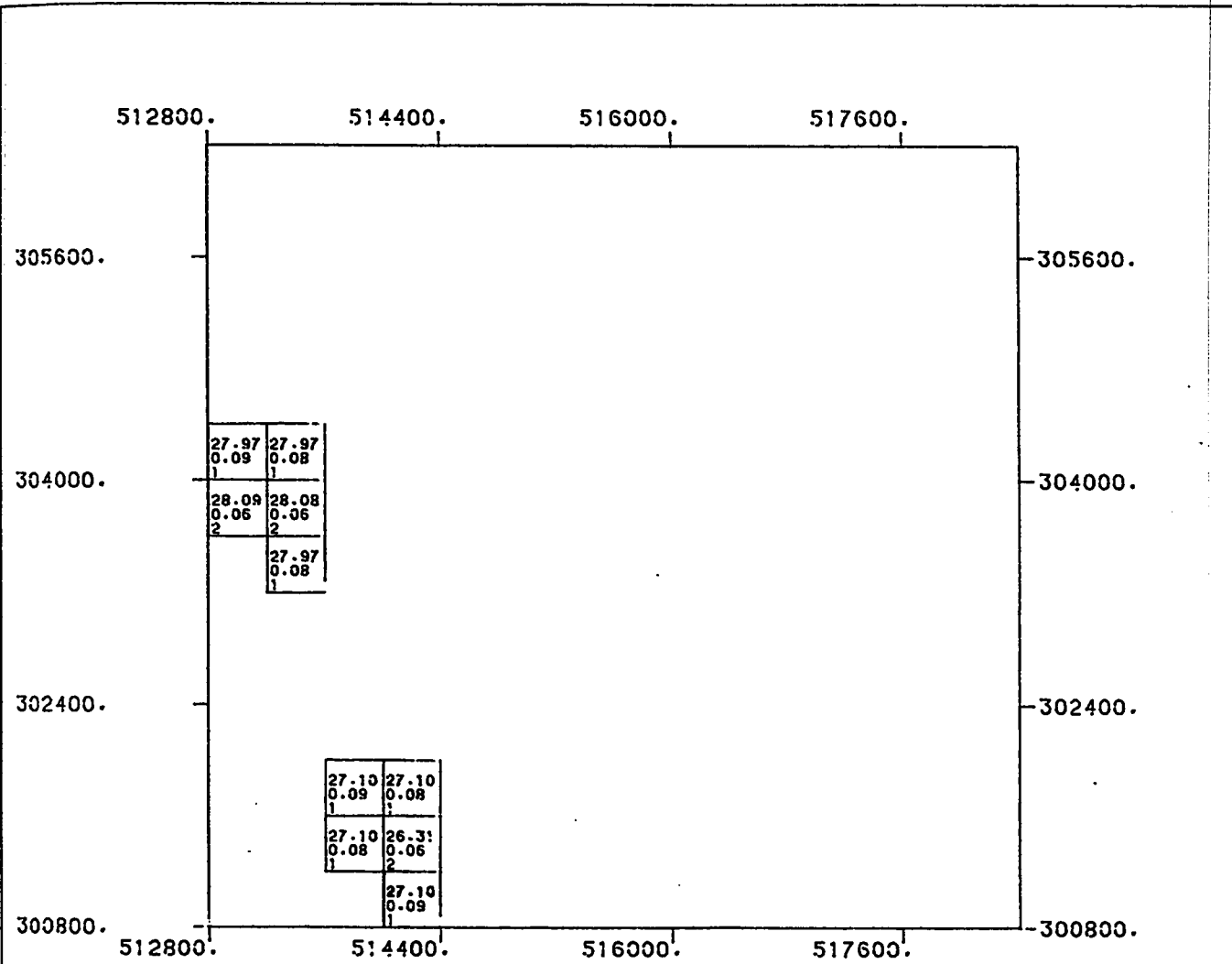
(D8)



(D9)



(D10)



ABU TARTUR PHOSPHATE DEPOSIT

RESULTS OF BLOCK KRIGING

(Z = 291.5)

LEVEL NUMBER : 20

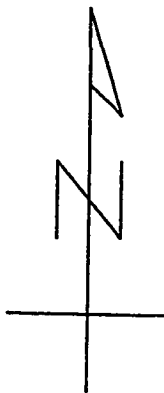
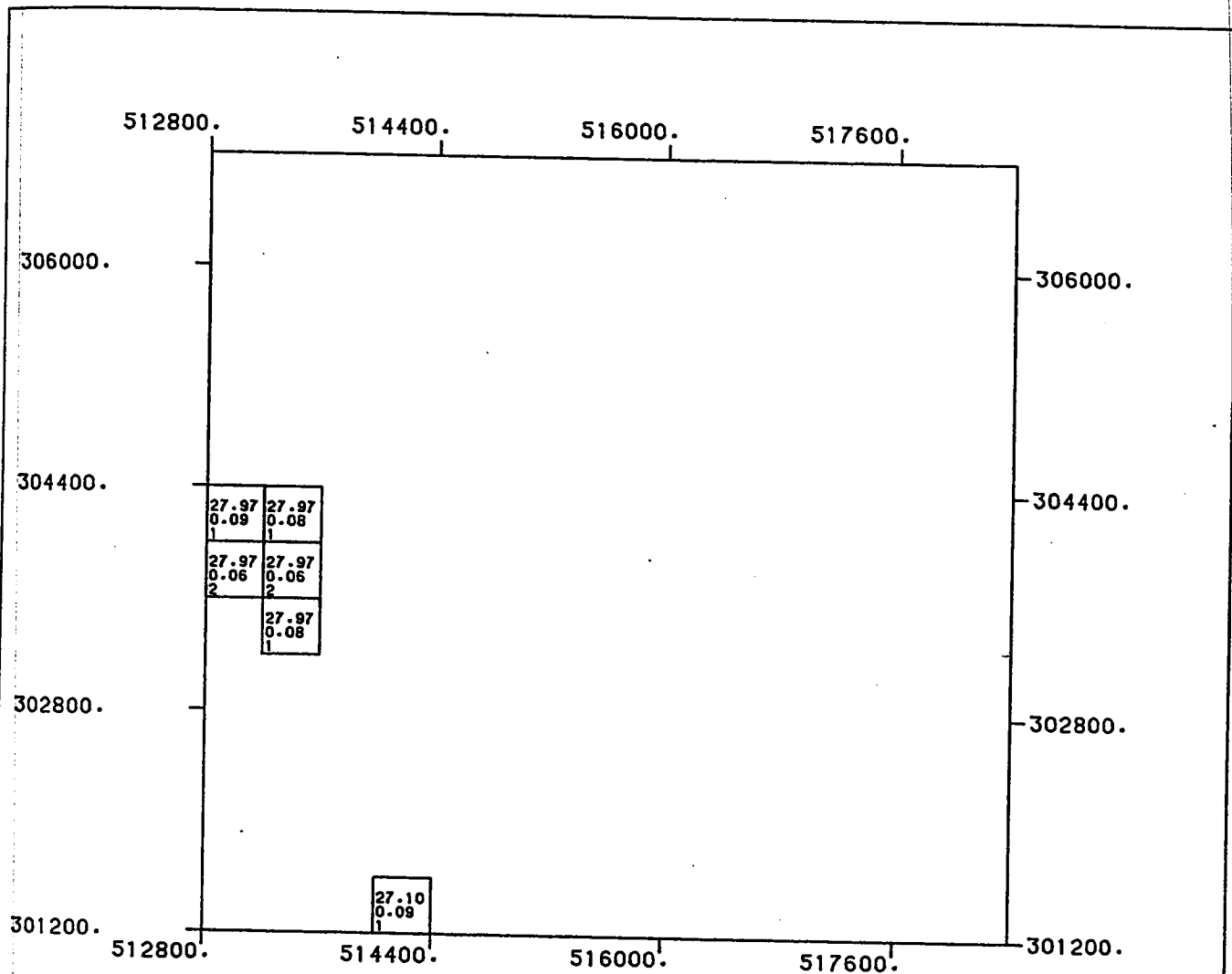
800.0 0.0 800.0 1600.0



SCALE OF MAP

DATA PROCESSED AT: U P M - D P C , DHAHRAN
SOFTWARE BY : GEOSTAT SYSTEMS, MONTREAL

(D11)



ABU TARTUR PHOSPHATE DEPOSIT
RESULTS OF BLOCK KRIGING

(Z = 292.5)

LEVEL NUMBER : 21

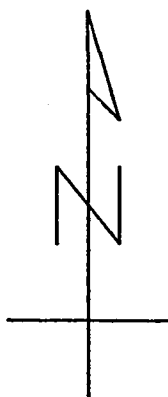
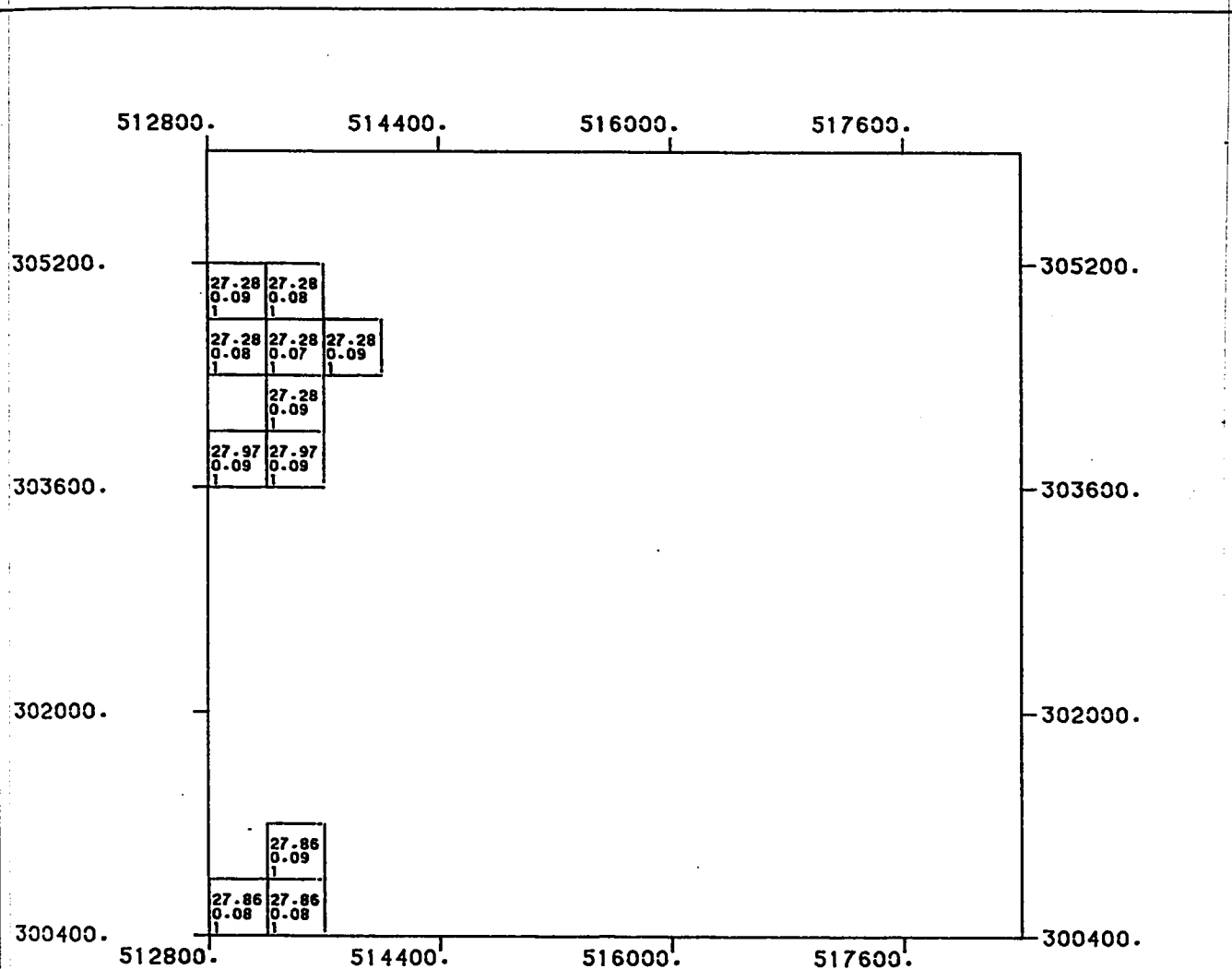
800.0 0.0 800.0 1600.0



SCALE OF MAP

DATA PROCESSED AT: U P M - D P C . DHAHRAN
 SOFTWARE BY : GEOSTAT SYSTEMS, MONTREAL

(D12)



ABU TARTUR PHOSPHATE DEPOSIT
RESULTS OF BLOCK KRIGING

(Z = 293.5)

LEVEL NUMBER : 22

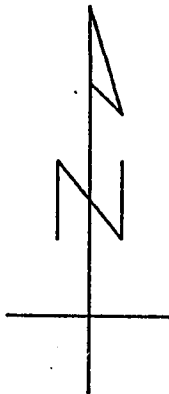
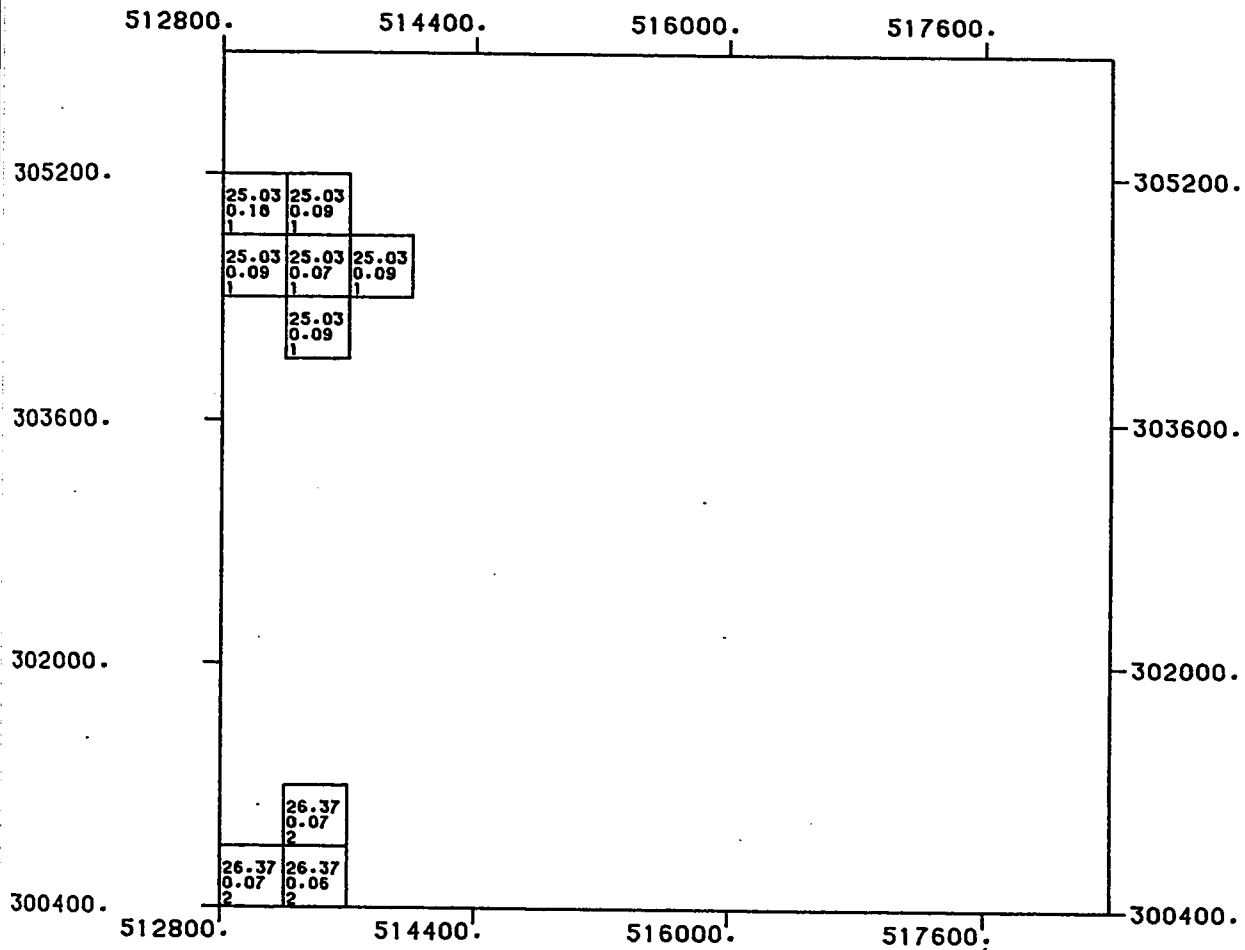
800.0 0.0 800.0 1600.0



SCALE OF MAP

DATA PROCESSED AT: U P M - D P C , DHAHRAN
 SOFTWARE BY : GEOSTAT SYSTEMS, MONTREAL

(D13)



ABU TARTUR PHOSPHATE DEPOSIT
RESULTS OF BLOCK KRIGING

(Z = 294.5)

LEVEL NUMBER : 23

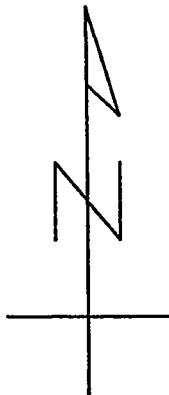
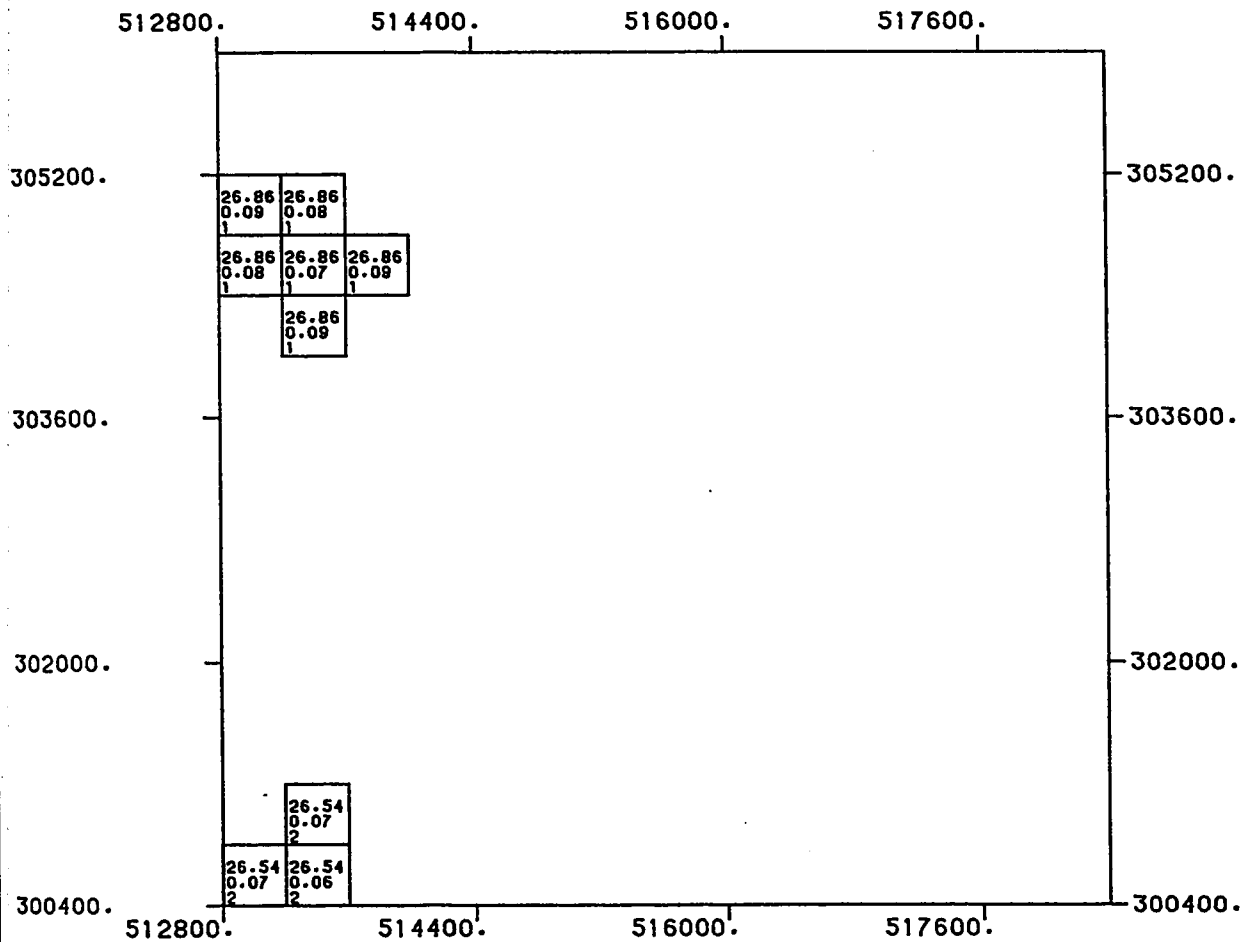
800.0 0.0 800.0 1600.0



SCALE OF MAP

DATA PROCESSED AT: U P M - D P C , DHAHRAN
 SOFTWARE BY : GEOSTAT SYSTEMS, MONTREAL

(D14)



ABU TARTUR PHOSPHATE DEPOSIT
RESULTS OF BLOCK KRIGING

(Z = 295.5)

LEVEL NUMBER : 24

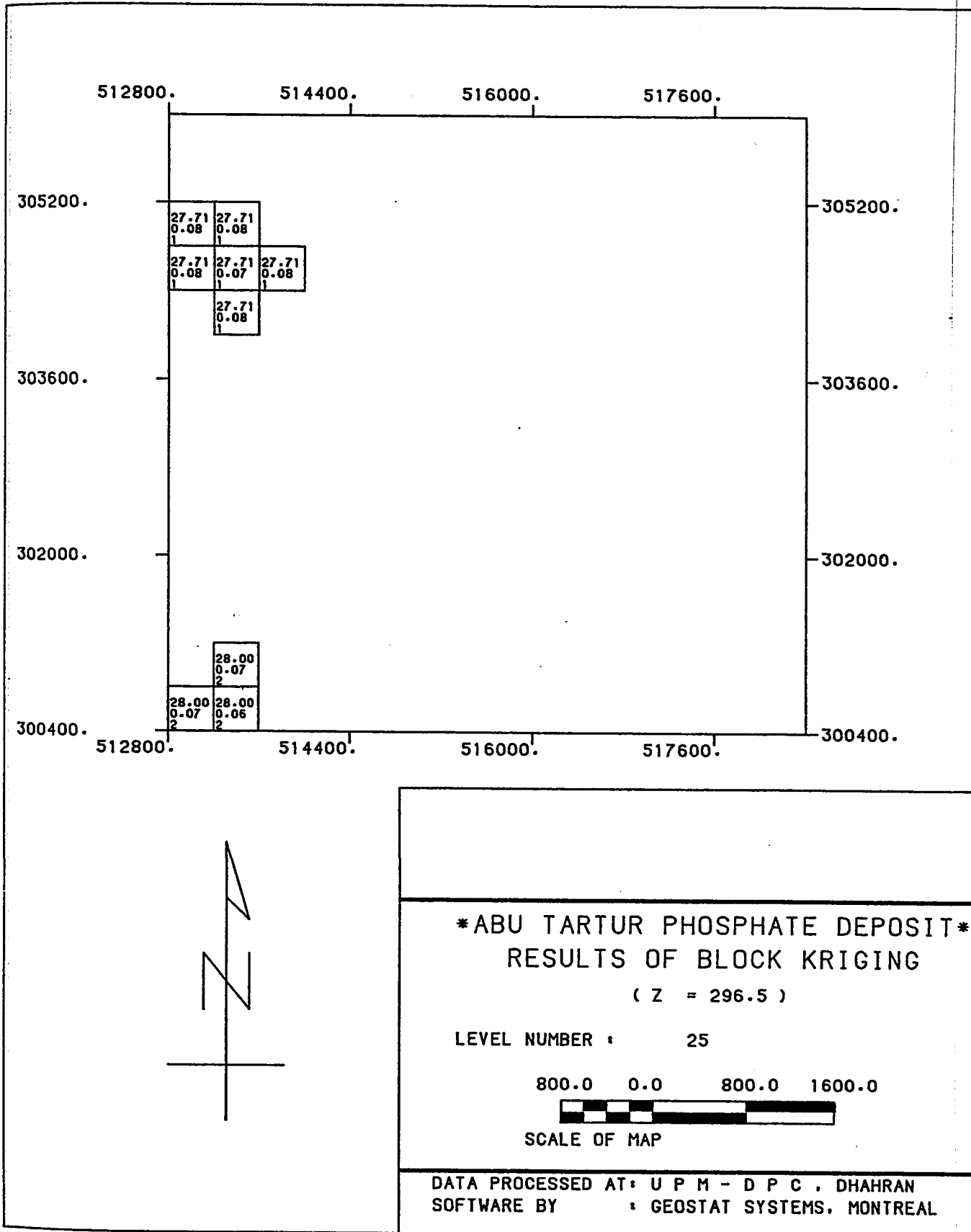
800.0 0.0 800.0 1600.0



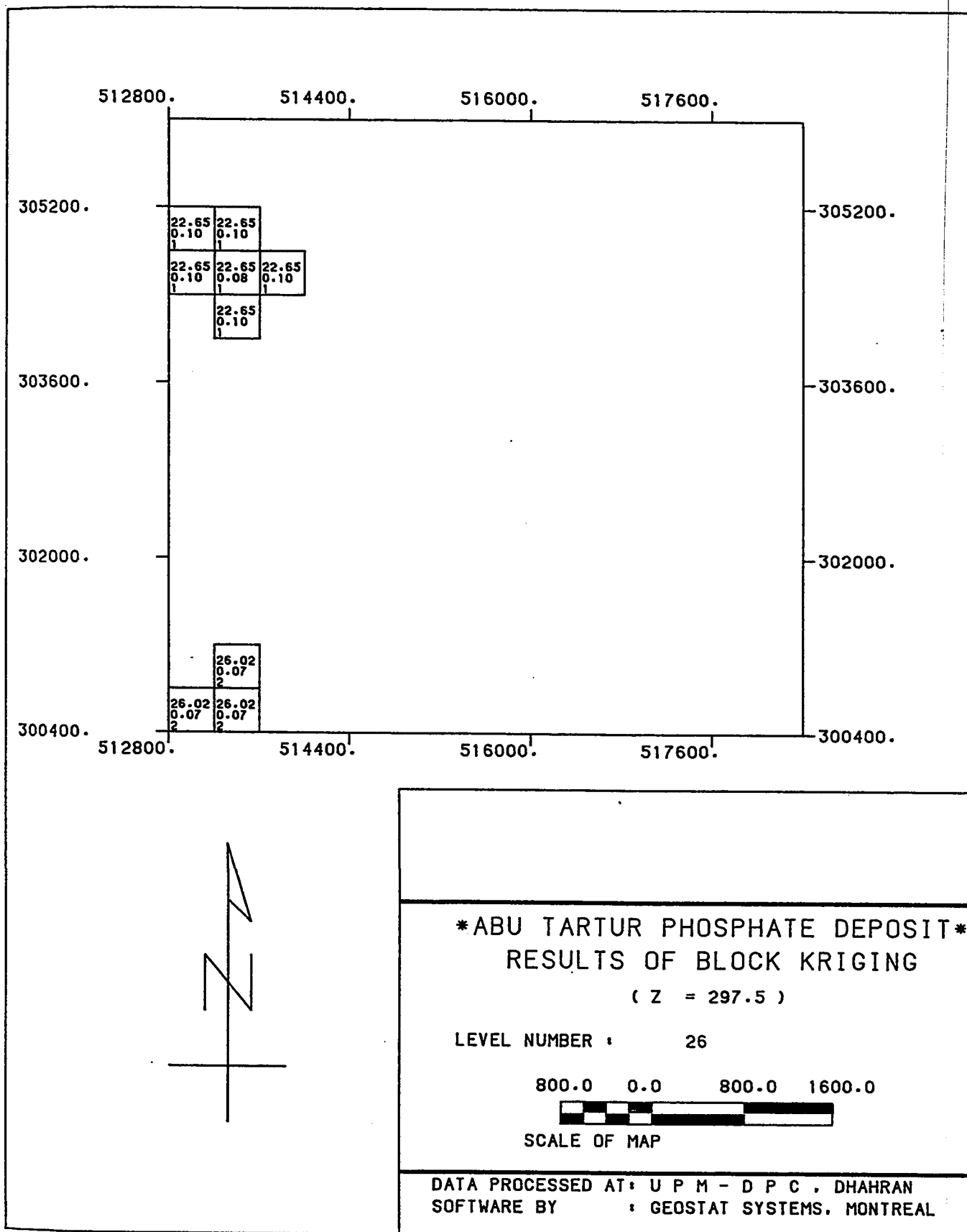
SCALE OF MAP

DATA PROCESSED AT: U P M - D P C , DHAHRAN
SOFTWARE BY : GEOSTAT SYSTEMS, MONTREAL

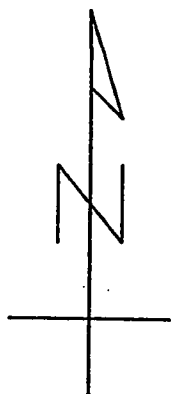
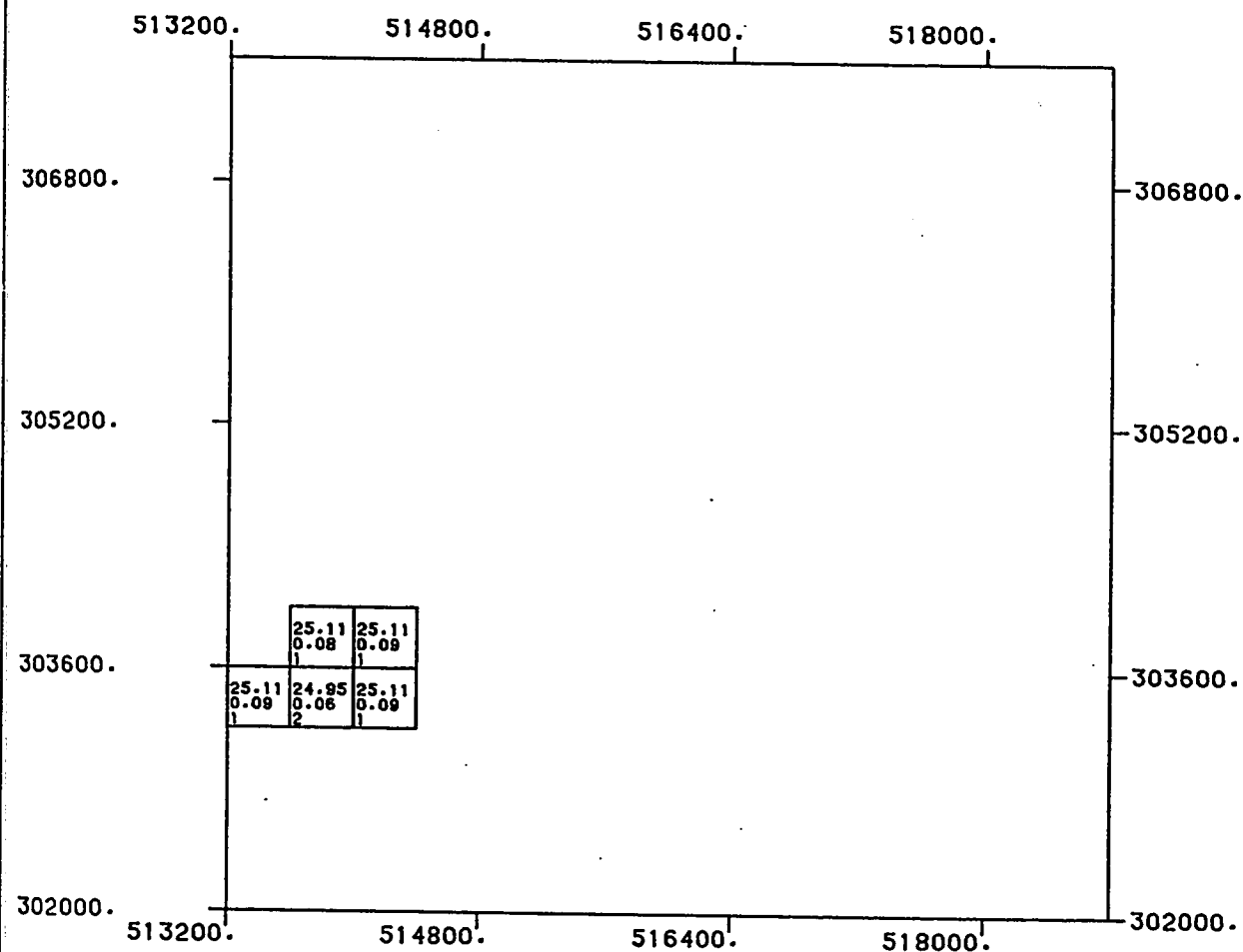
(D15)



(D16)



(D17)



ABU TARTUR PHOSPHATE DEPOSIT
RESULTS OF BLOCK KRIGING

(Z = 306.5)

LEVEL NUMBER : 35

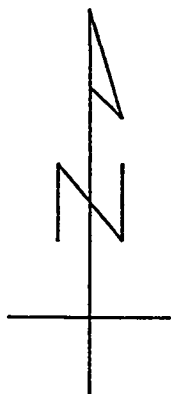
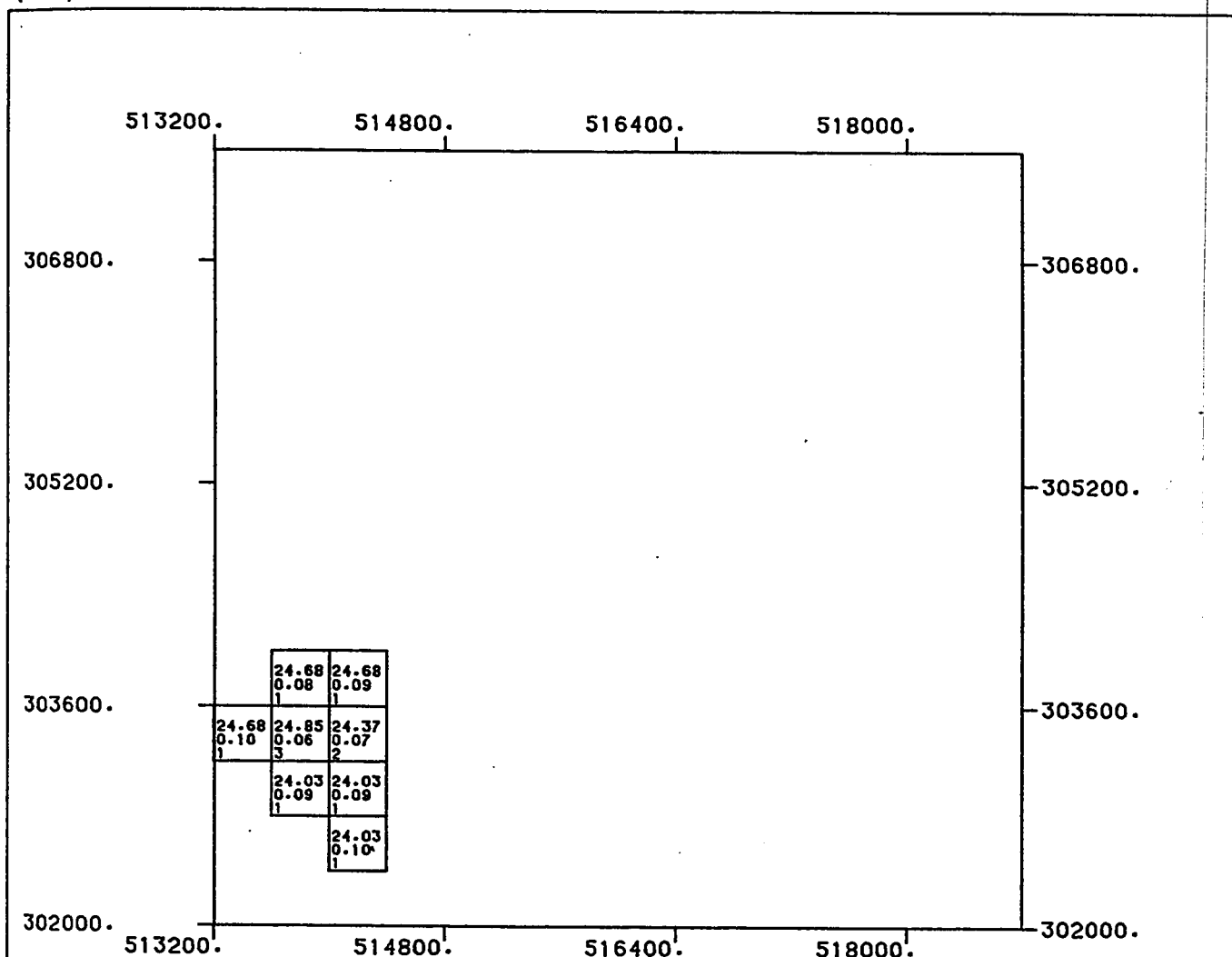
800.0 0.0 800.0 1600.0



SCALE OF MAP

DATA PROCESSED AT: U P M - D P C , DHAHRAN
 SOFTWARE BY : GEOSTAT SYSTEMS, MONTREAL

(D18)



ABU TARTUR PHOSPHATE DEPOSIT
RESULTS OF BLOCK KRIGING

(Z = 307.5)

LEVEL NUMBER : 36

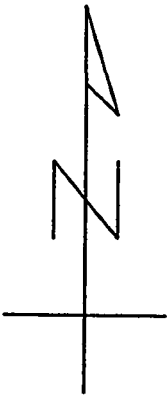
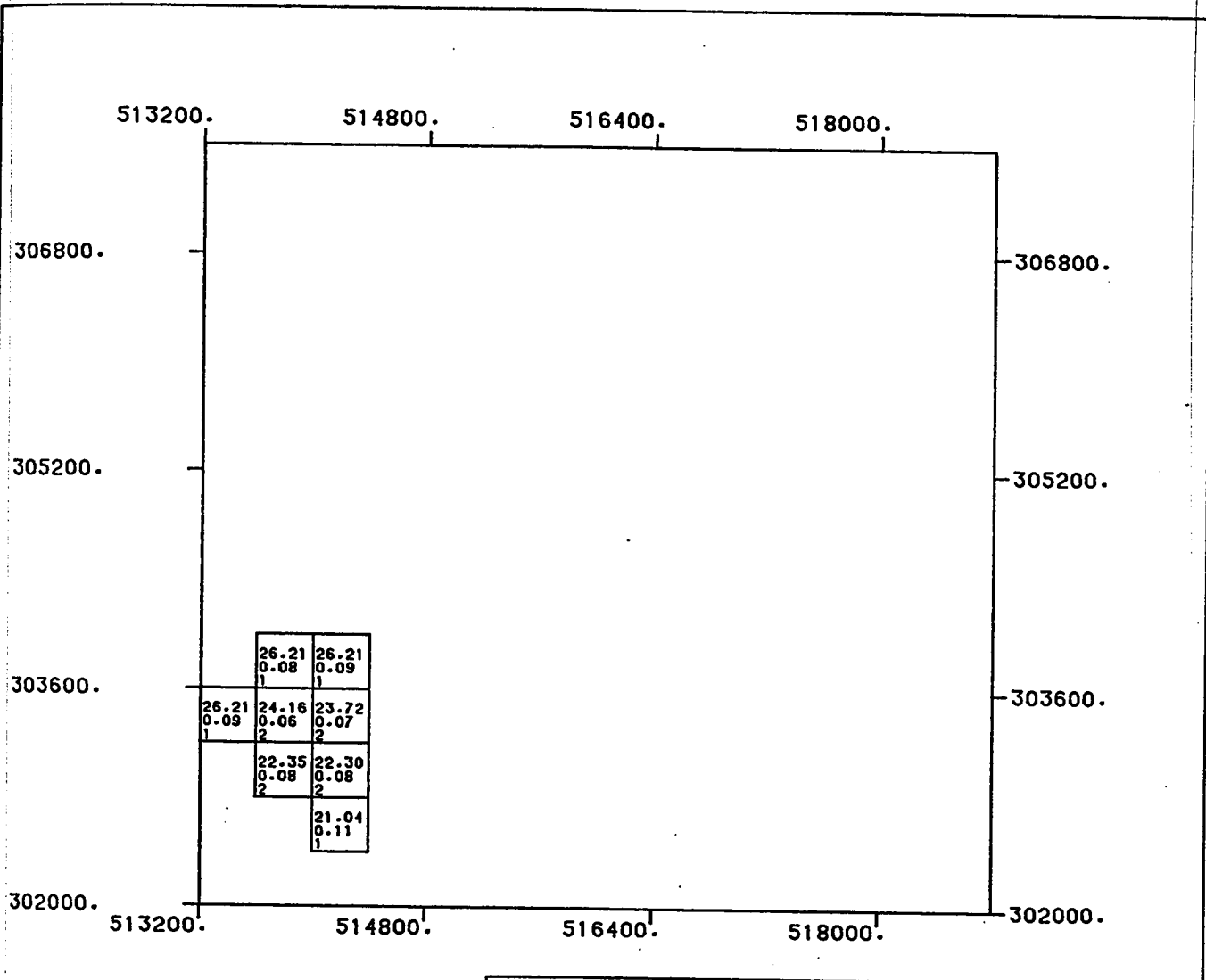
800.0 0.0 800.0 1600.0



SCALE OF MAP

DATA PROCESSED AT: U P M - D P C , DHAHRAN
 SOFTWARE BY : GEOSTAT SYSTEMS, MONTREAL

(D19)



ABU TARTUR PHOSPHATE DEPOSIT
RESULTS OF BLOCK KRIGING

(Z = 308.5)

LEVEL NUMBER : 37

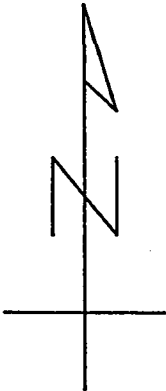
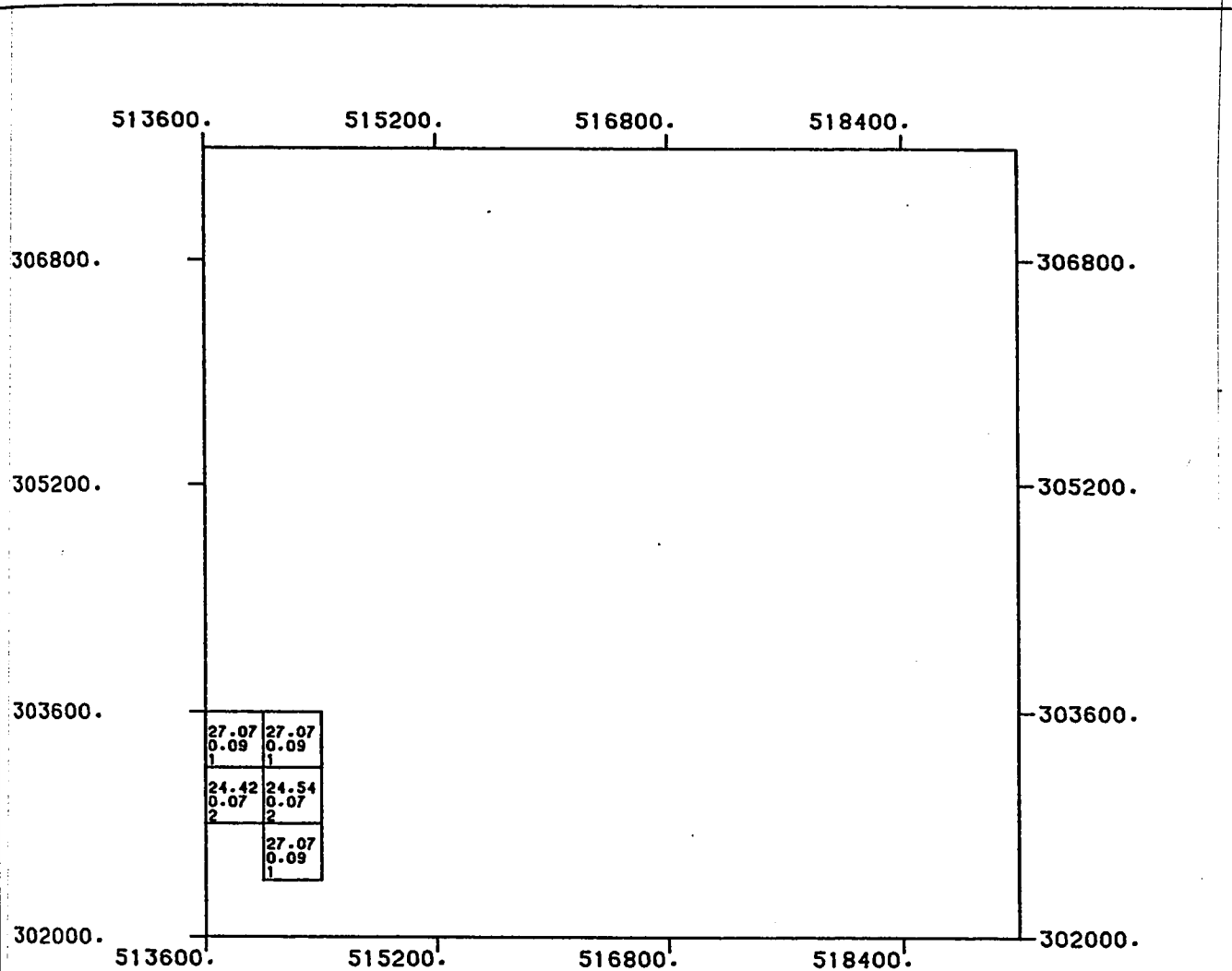
800.0 0.0 800.0 1600.0



SCALE OF MAP

DATA PROCESSED AT: U P M - D P C , DHAHRAN
 SOFTWARE BY : GEOSTAT SYSTEMS, MONTREAL

(D20)



ABU TARTUR PHOSPHATE DEPOSIT
RESULTS OF BLOCK KRIGING

(Z = 309.5)

LEVEL NUMBER : 38

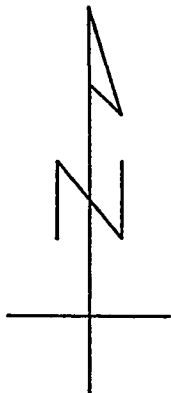
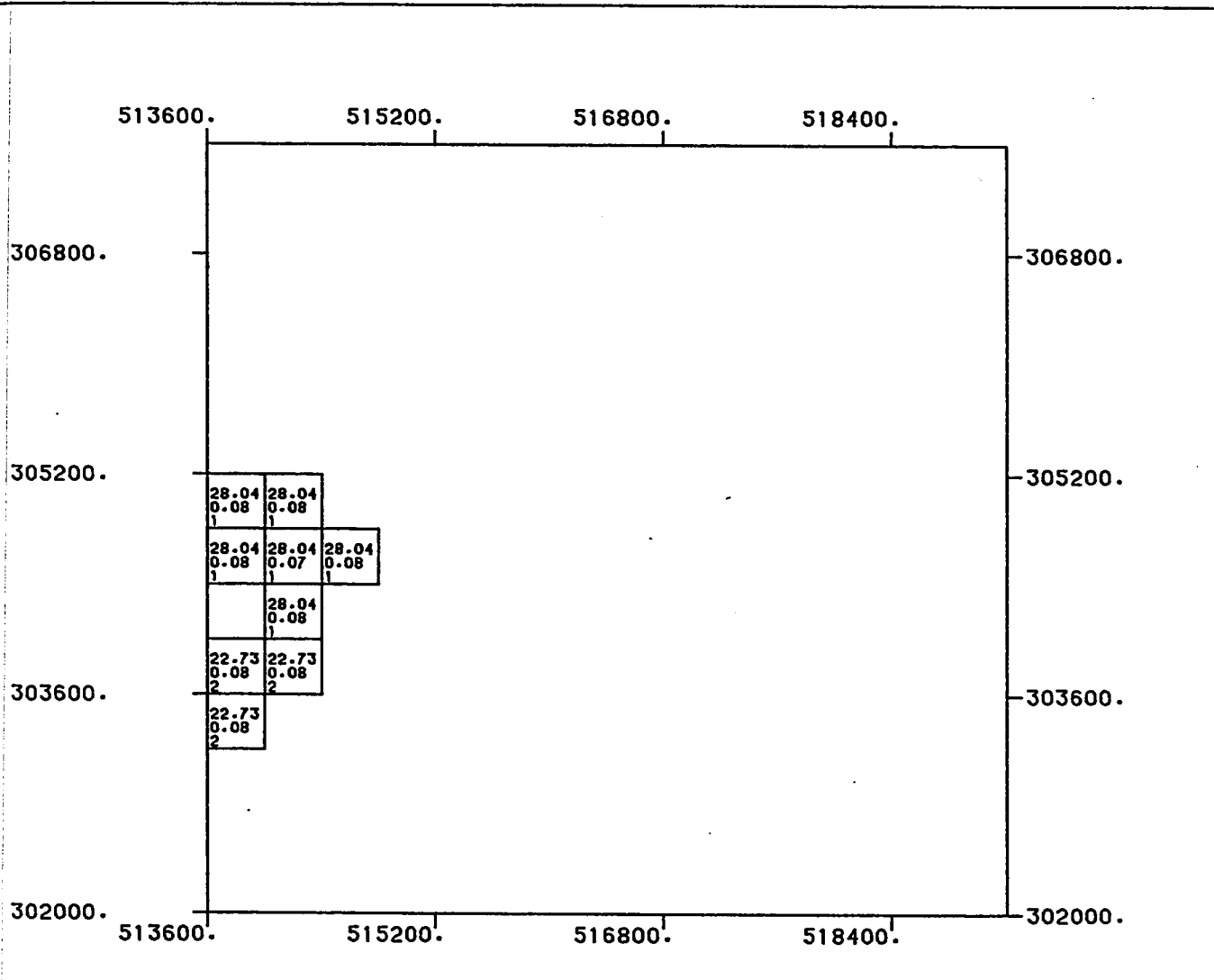
800.0 0.0 800.0 1600.0



SCALE OF MAP

DATA PROCESSED AT: U P M - D P C , DHAHRAN
 SOFTWARE BY : GEOSTAT SYSTEMS, MONTREAL

(D21)



ABU TARTUR PHOSPHATE DEPOSIT
RESULTS OF BLOCK KRIGING

(Z = 316.5)

LEVEL NUMBER : 45

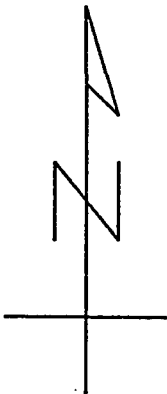
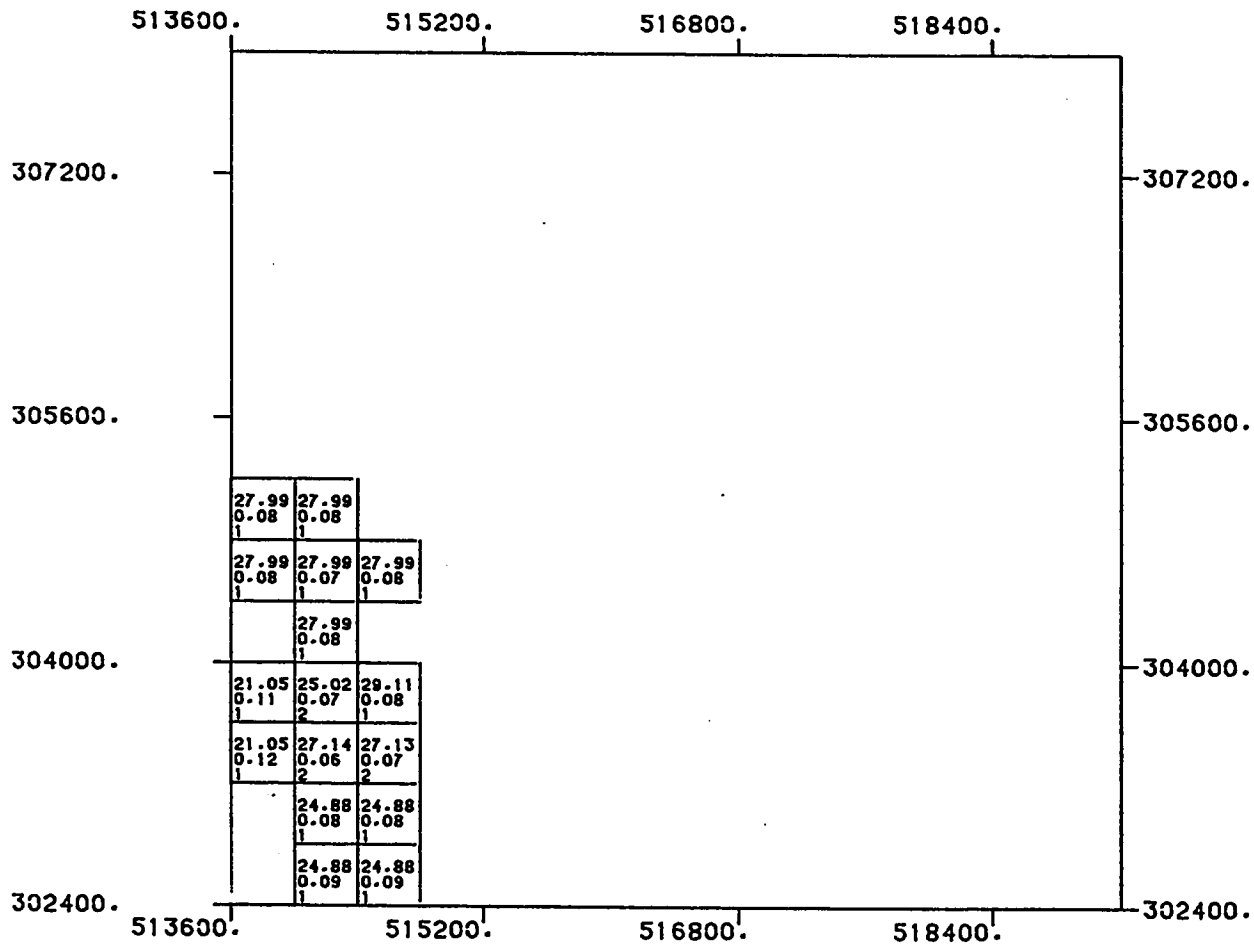
800.0 0.0 800.0 1600.0



SCALE OF MAP

DATA PROCESSED AT: U P M - D P C , DHAHRAN
 SOFTWARE BY : GEOSTAT SYSTEMS, MONTREAL

(D22)



ABU TARTUR PHOSPHATE DEPOSIT
RESULTS OF BLOCK KRIGING

(Z = 317.5)

LEVEL NUMBER : 46

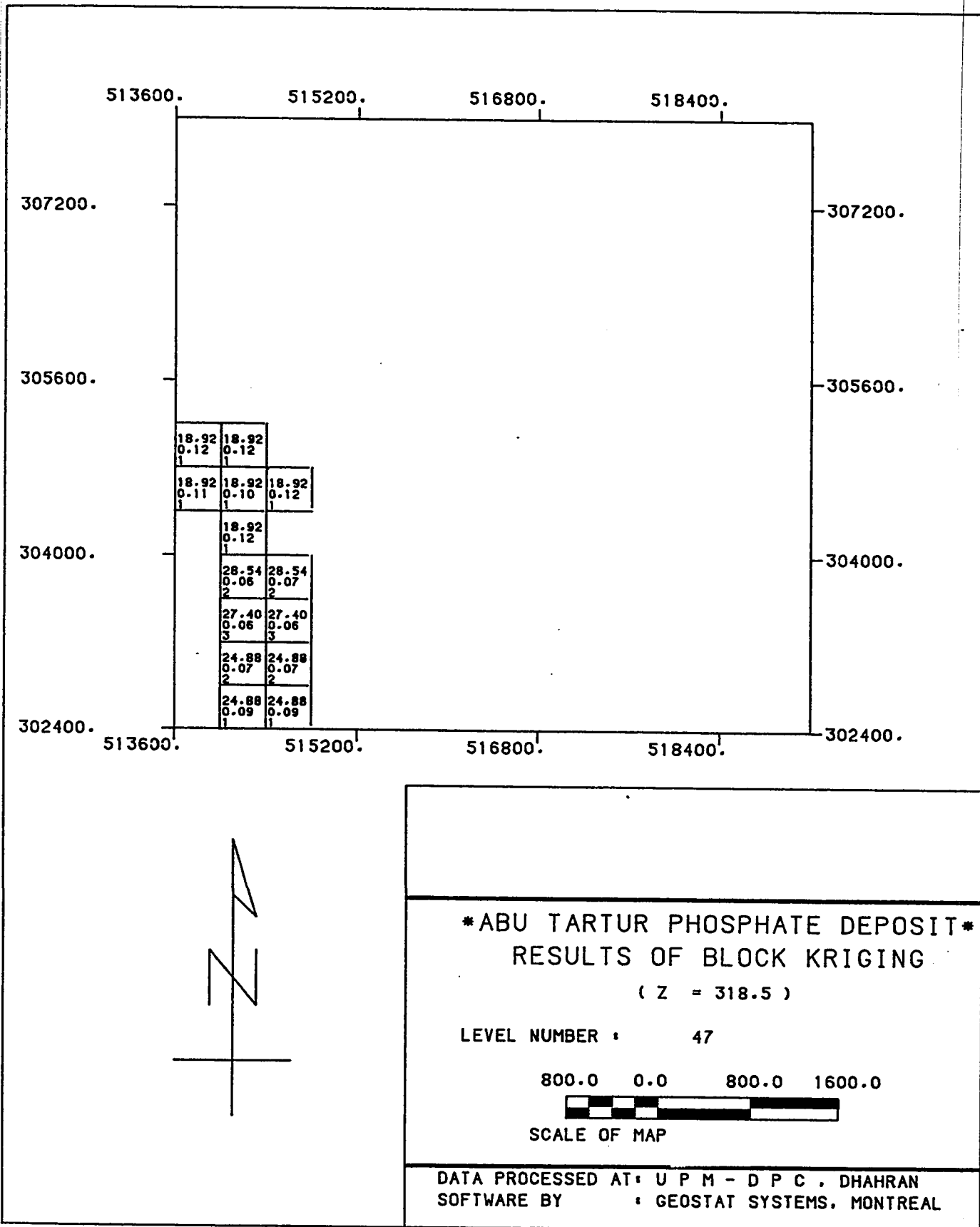
800.0 0.0 800.0 1600.0



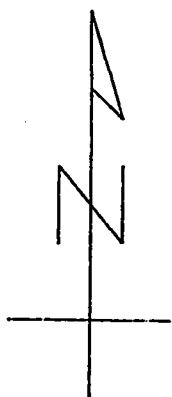
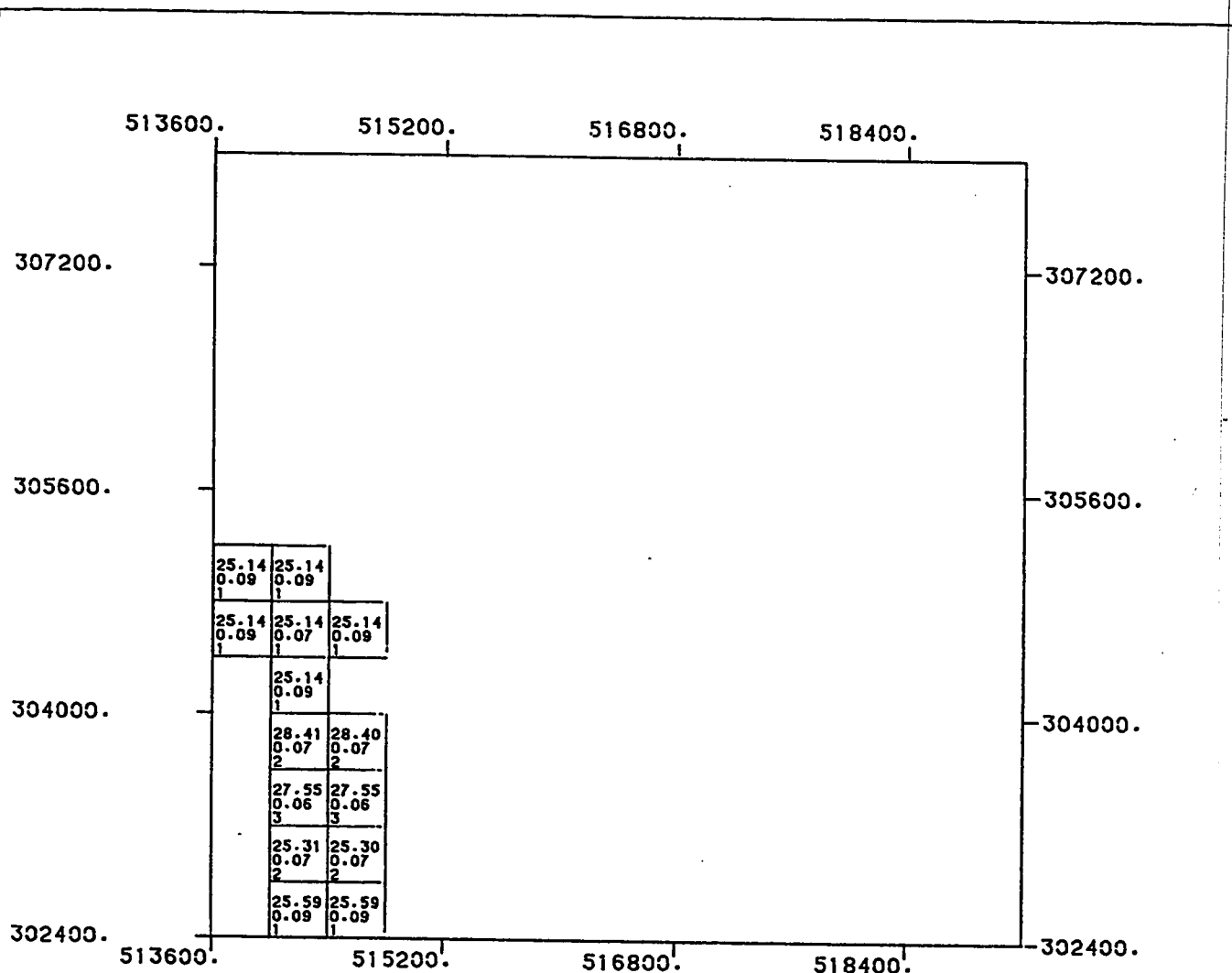
SCALE OF MAP

DATA PROCESSED AT: U P M - D P C , DHAHRAN
SOFTWARE BY : GEOSTAT SYSTEMS, MONTREAL

(D23)



(D24)



ABU TARTUR PHOSPHATE DEPOSIT

RESULTS OF BLOCK KRIGING

(Z = 319.5)

LEVEL NUMBER : 48

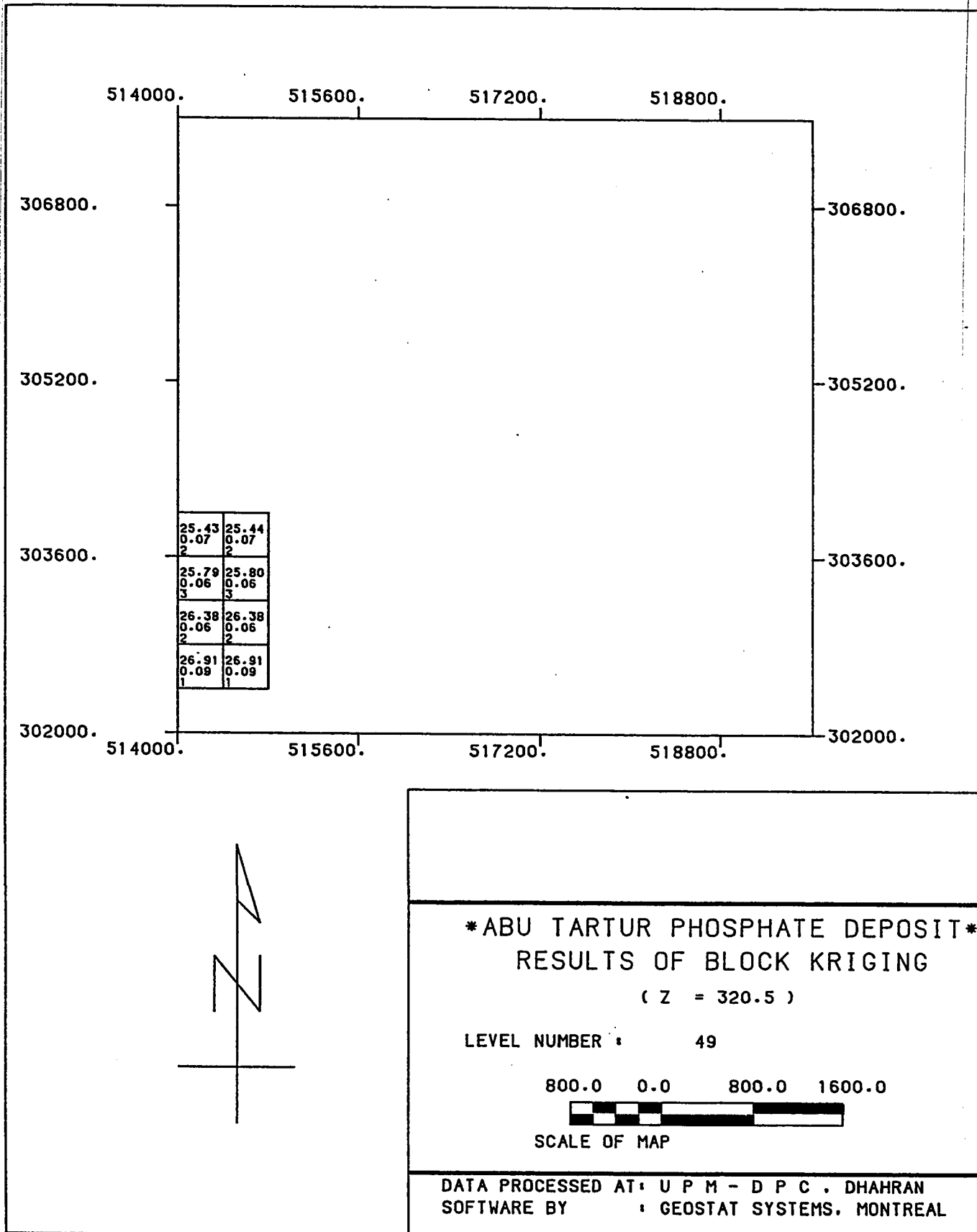
800.0 0.0 800.0 1600.0



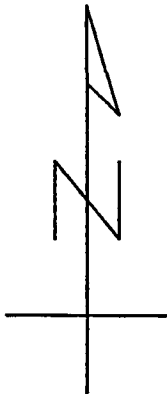
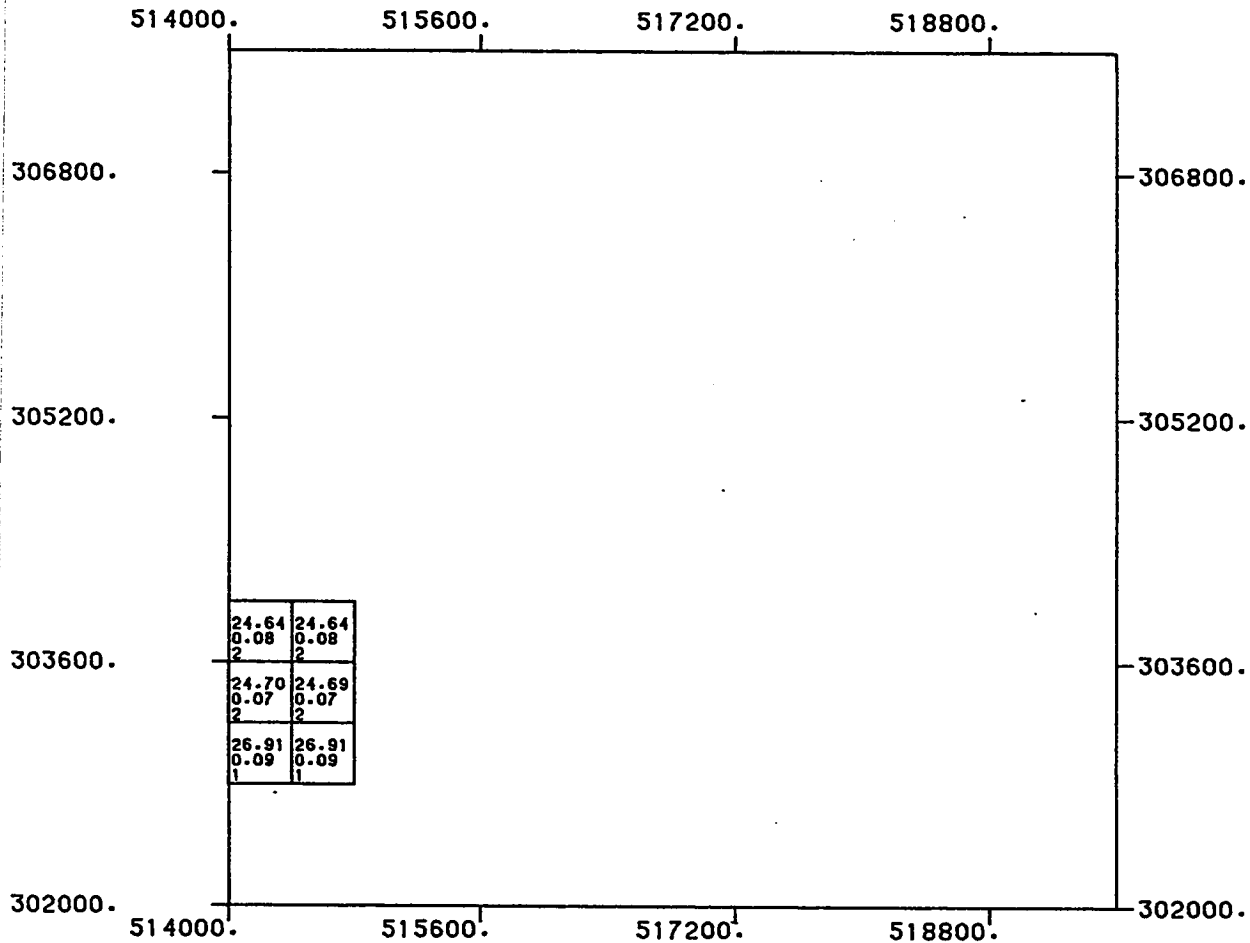
SCALE OF MAP

DATA PROCESSED AT: U P M - D P C , DHAHRAN
SOFTWARE BY : GEOSTAT SYSTEMS, MONTREAL

(D25)



(D26)



ABU TARTUR PHOSPHATE DEPOSIT
RESULTS OF BLOCK KRIGING

(Z = 321.5)

LEVEL NUMBER : 50

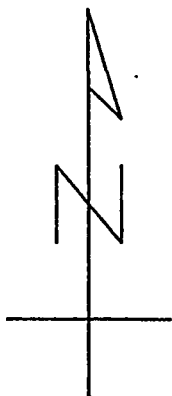
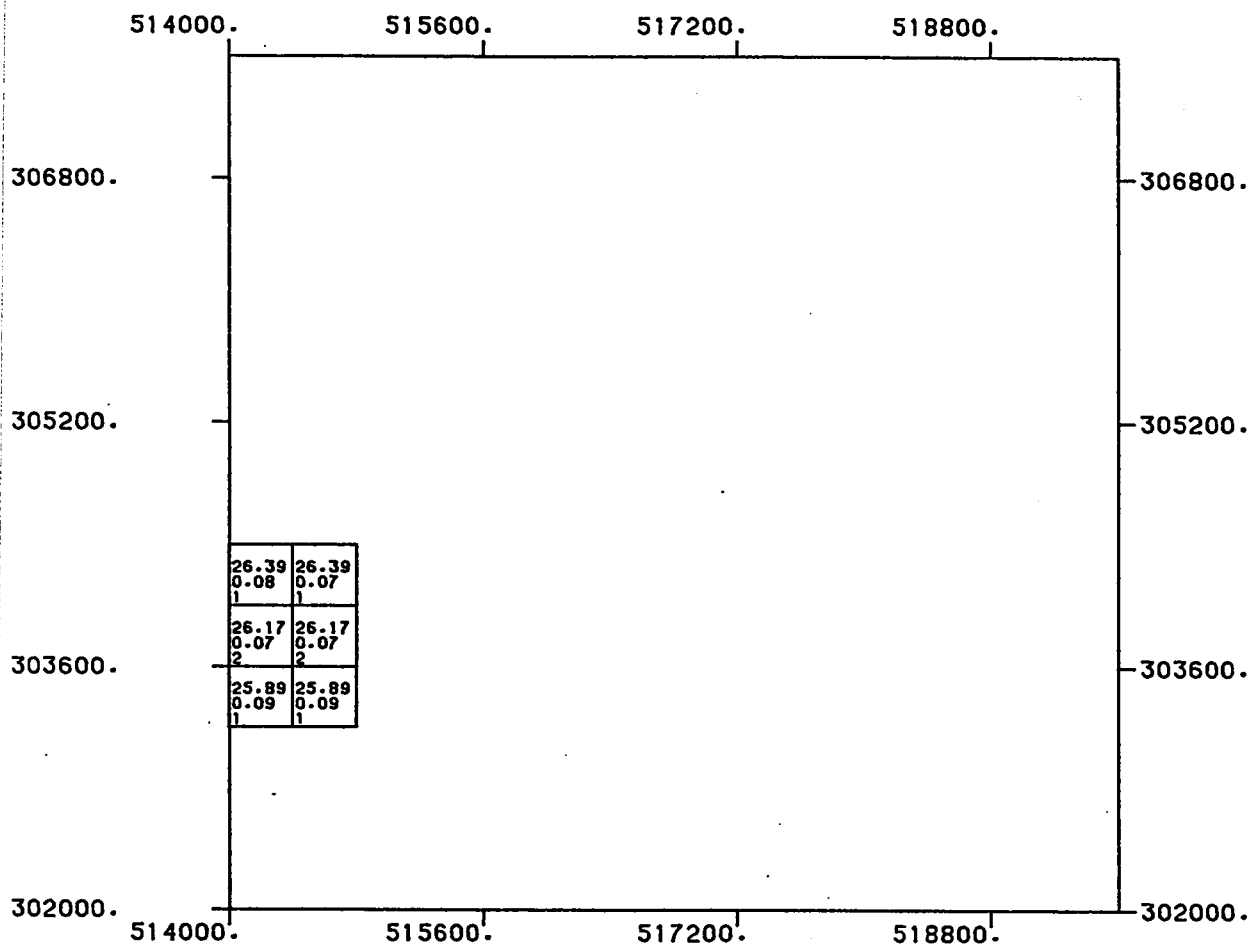
800.0 0.0 800.0 1600.0



SCALE OF MAP

DATA PROCESSED AT: U P M - D P C . DHAHRAN
 SOFTWARE BY : GEOSTAT SYSTEMS. MONTREAL

(D27)



ABU TARTUR PHOSPHATE DEPOSIT
RESULTS OF BLOCK KRIGING

(Z = 324.5)

LEVEL NUMBER : 53

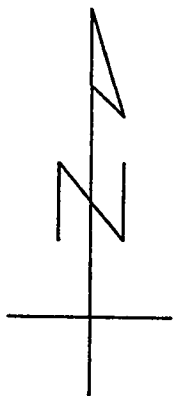
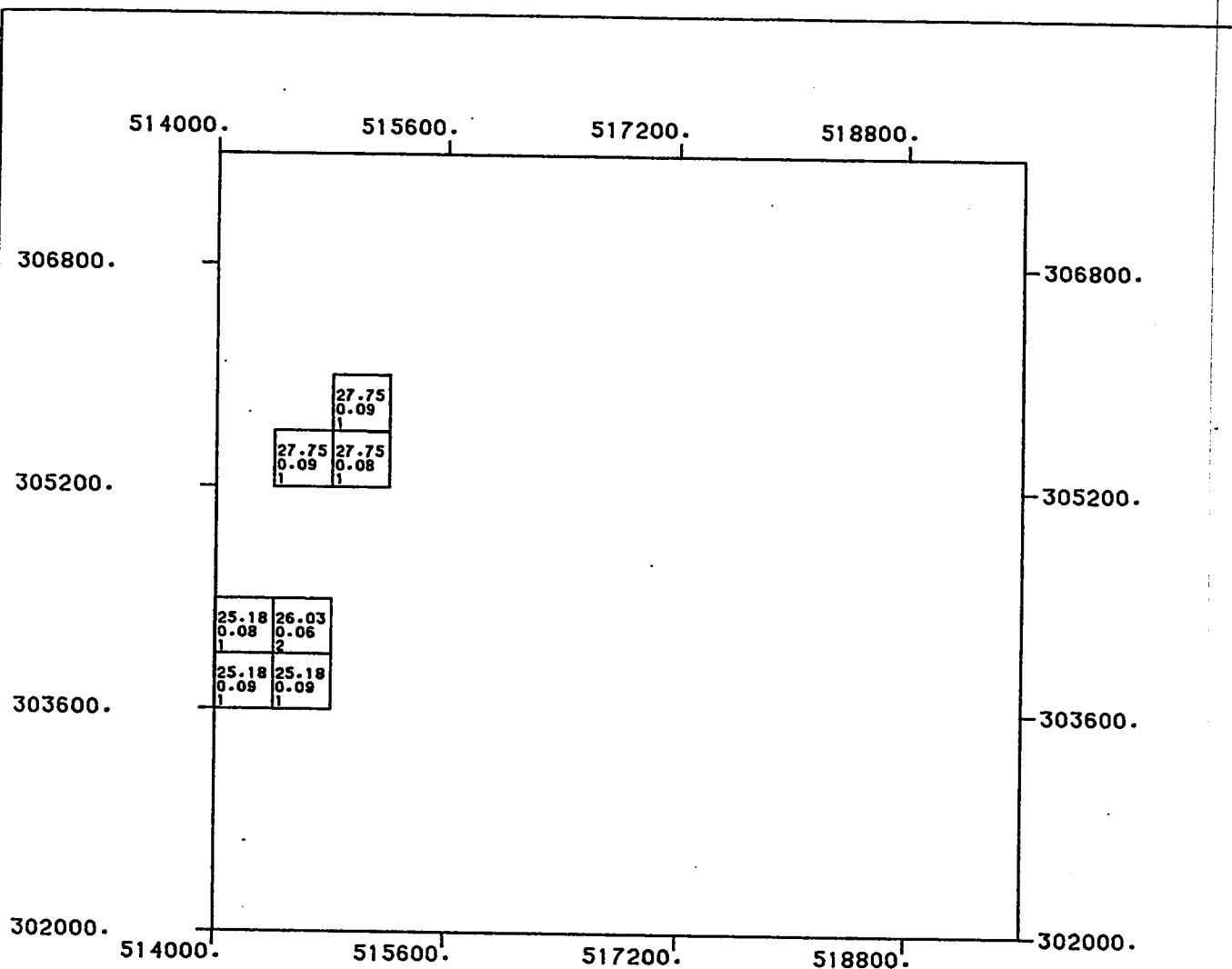
800.0 0.0 800.0 1600.0



SCALE OF MAP

DATA PROCESSED AT: U P M - D P C . DHAHRAN
 SOFTWARE BY : GEOSTAT SYSTEMS, MONTREAL

(D28)



ABU TARTUR PHOSPHATE DEPOSIT
RESULTS OF BLOCK KRIGING

(Z = 326.5)

LEVEL NUMBER : 55

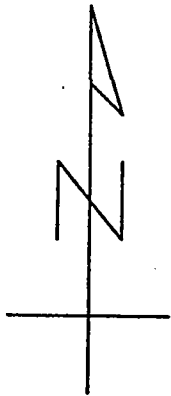
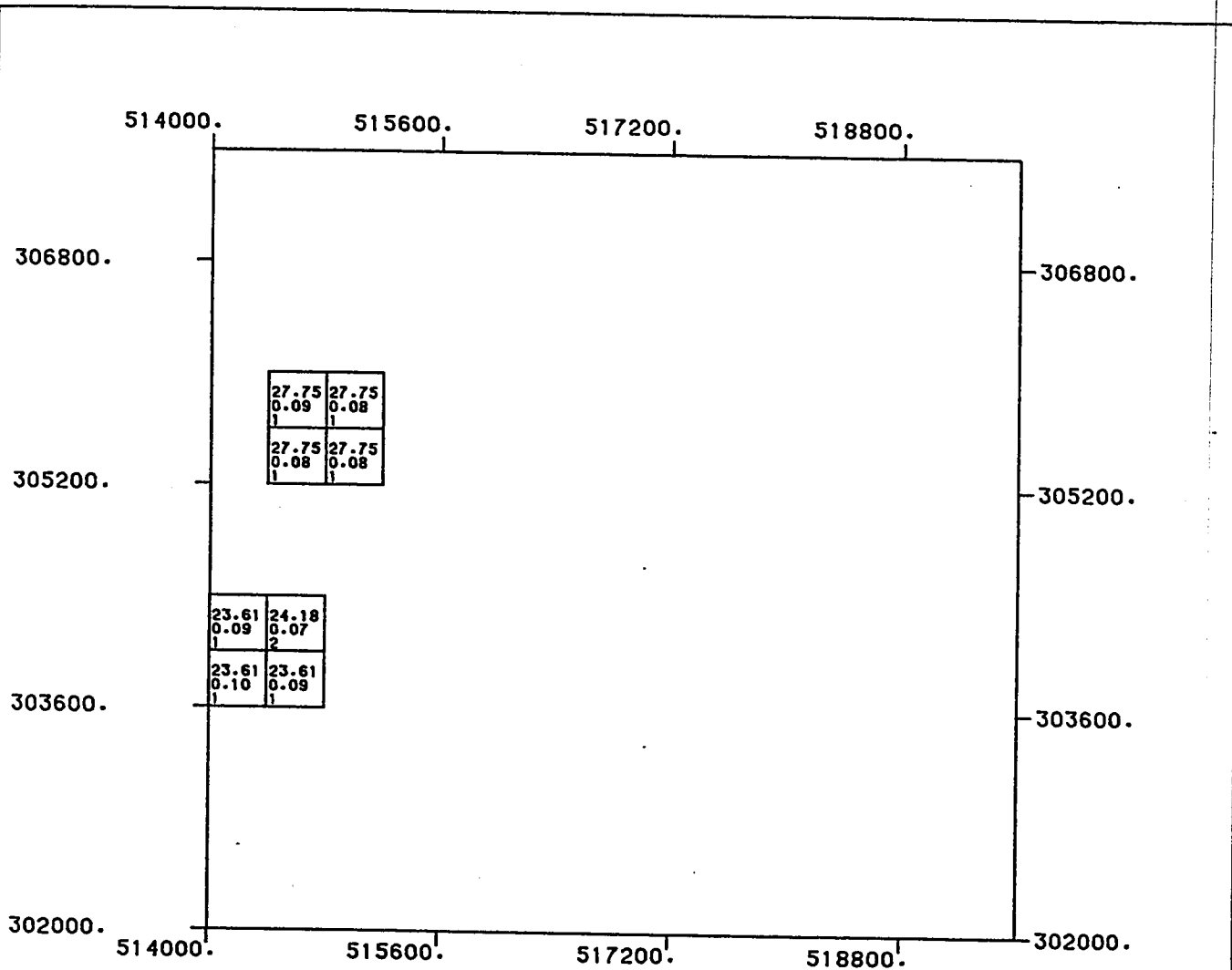
800.0 0.0 800.0 1600.0



SCALE OF MAP

DATA PROCESSED AT: U P M - D P C , DHAHRAN
SOFTWARE BY : GEOSTAT SYSTEMS, MONTREAL

(D29)



ABU TARTUR PHOSPHATE DEPOSIT
RESULTS OF BLOCK KRIGING

(Z = 327.5)

LEVEL NUMBER : 56

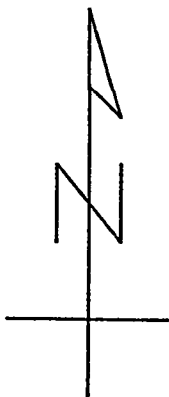
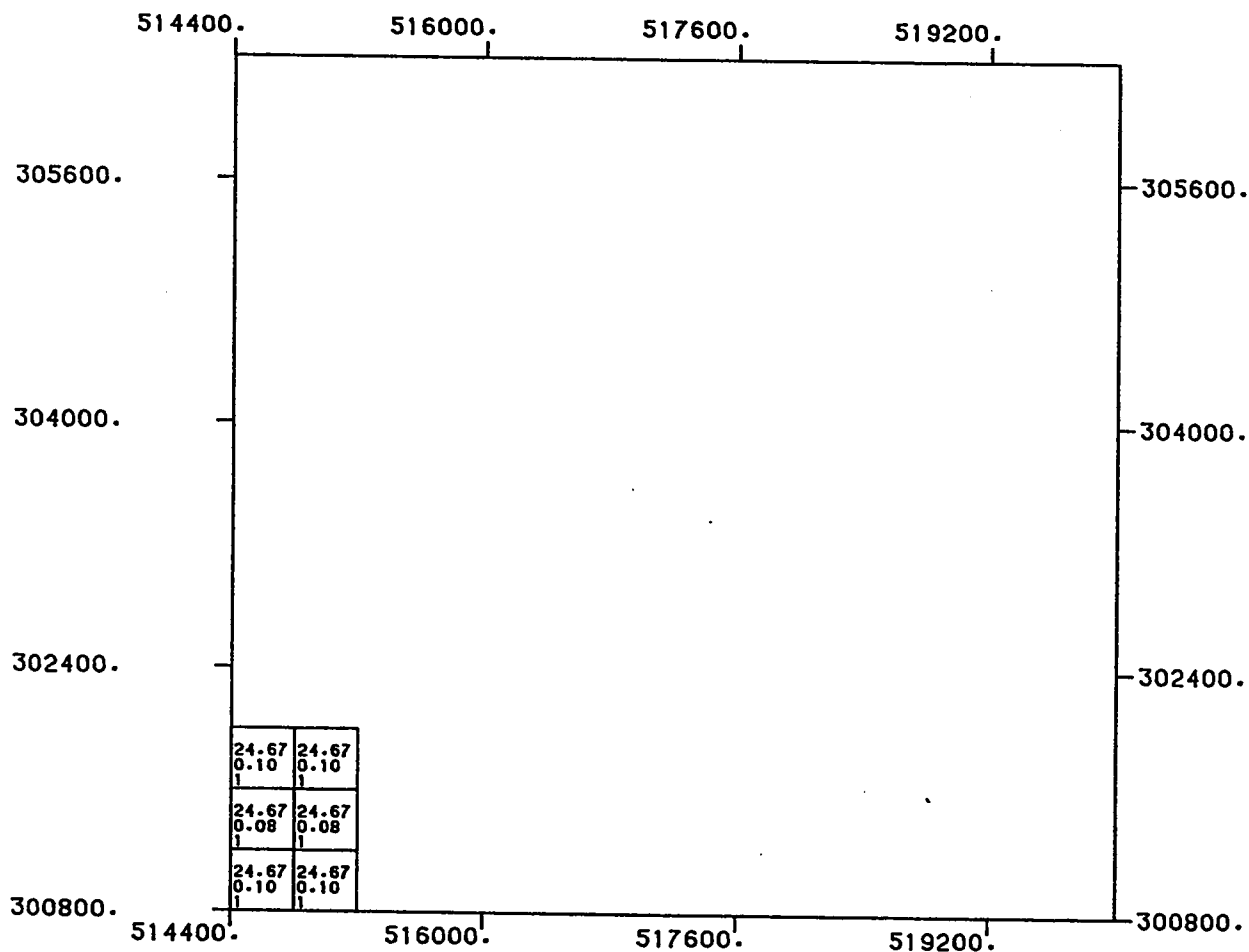
800.0 0.0 800.0 1600.0



SCALE OF MAP

DATA PROCESSED AT: U P M - D P C , DHAHRAN
 SOFTWARE BY : GEOSTAT SYSTEMS, MONTREAL

(D30)



ABU TARTUR PHOSPHATE DEPOSIT
RESULTS OF BLOCK KRIGING

(Z = 333.5)

LEVEL NUMBER : 62

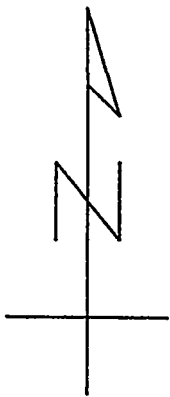
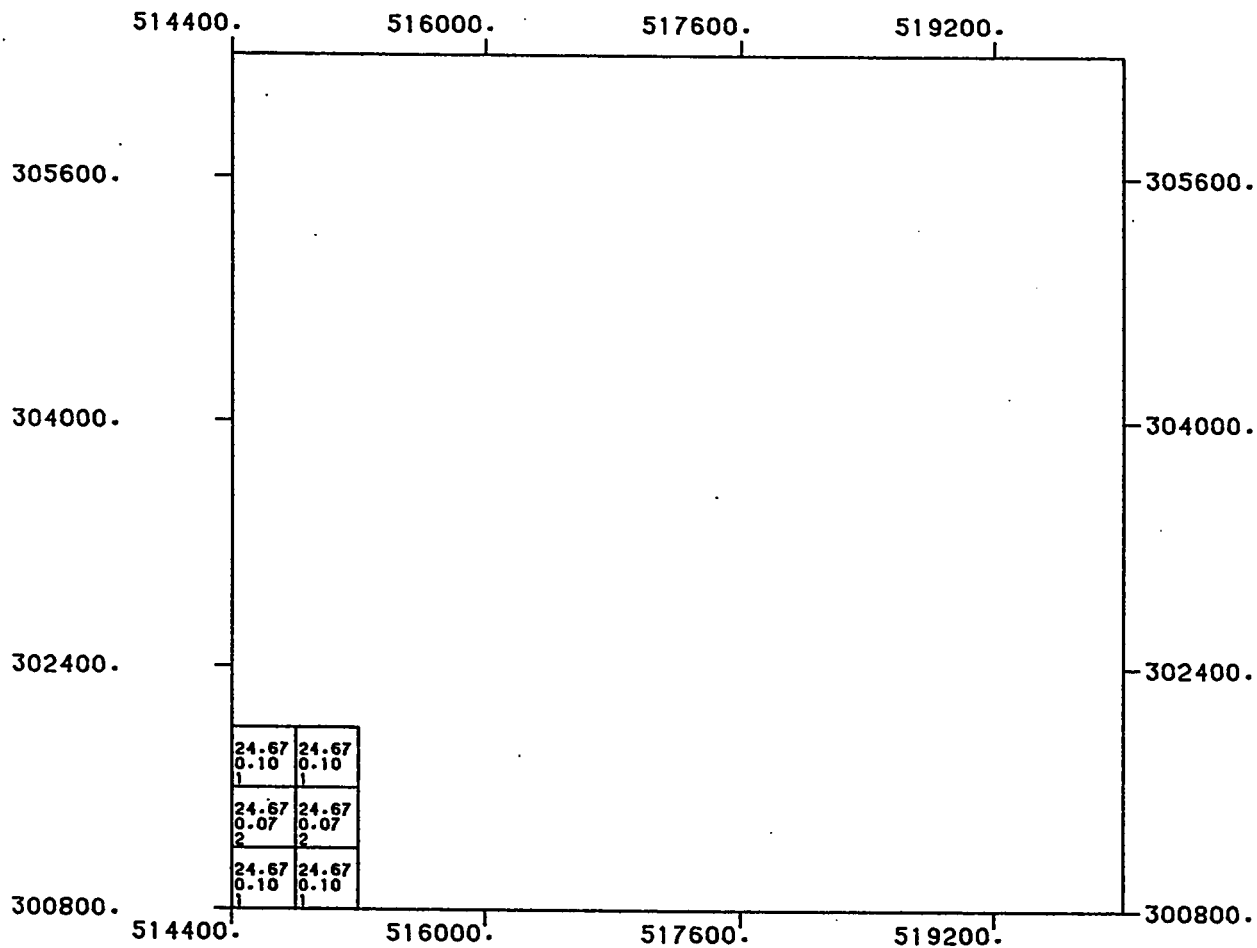
800.0 0.0 800.0 1600.0



SCALE OF MAP

DATA PROCESSED AT: U P M - D P C , DHAHRAN
 SOFTWARE BY : GEOSTAT SYSTEMS, MONTREAL

(D31)



ABU TARTUR PHOSPHATE DEPOSIT
RESULTS OF BLOCK KRIGING

(Z = 334.5)

LEVEL NUMBER : 63

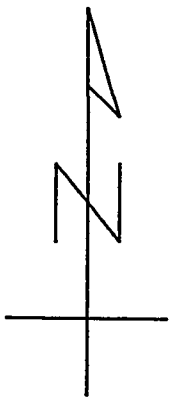
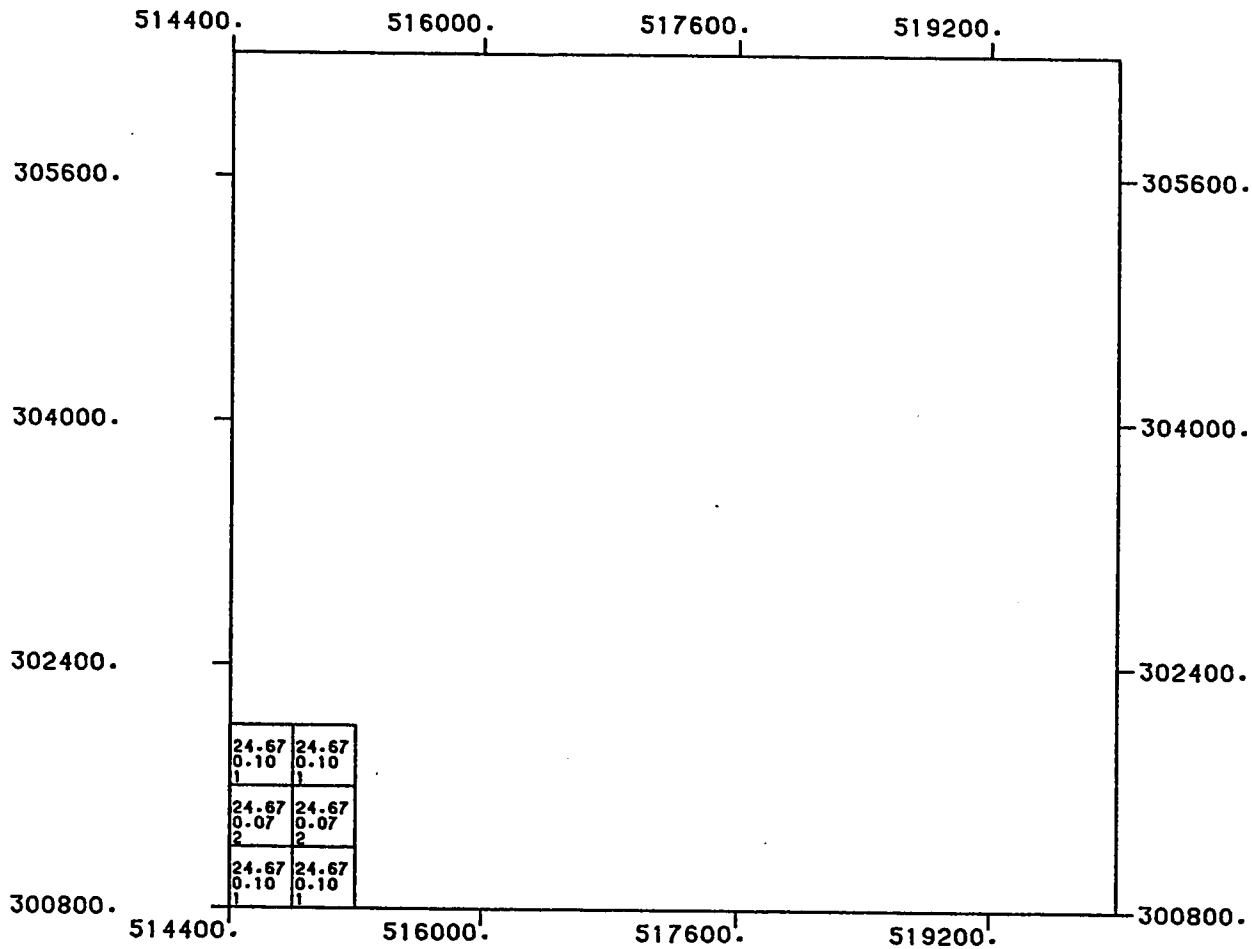
800.0 0.0 800.0 1600.0



SCALE OF MAP

DATA PROCESSED AT: U P M - D P C , DHAHRAN
 SOFTWARE BY : GEOSTAT SYSTEMS, MONTREAL

(D32)



ABU TARTUR PHOSPHATE DEPOSIT
RESULTS OF BLOCK KRIGING

(Z = 335.5)

LEVEL NUMBER : 64

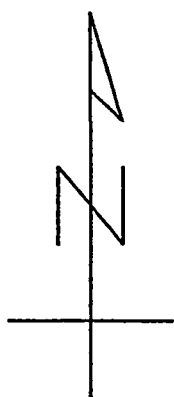
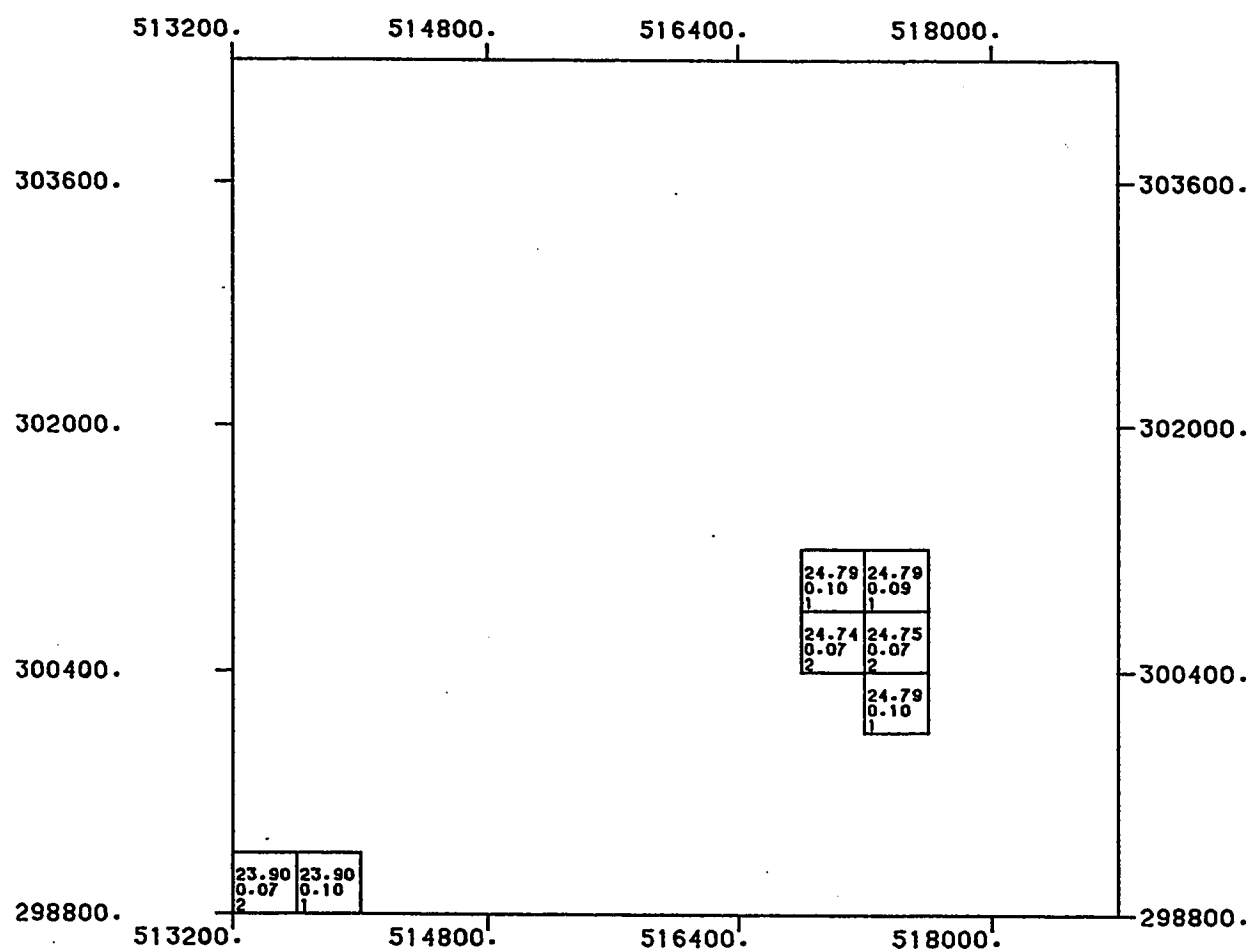
800.0 0.0 800.0 1600.0



SCALE OF MAP

DATA PROCESSED AT: U P M - D P C , DHAHRAN
SOFTWARE BY : GEOSTAT SYSTEMS, MONTREAL

(D33)



ABU TARTUR PHOSPHATE DEPOSIT
RESULTS OF BLOCK KRIGING

(Z = 340.5)

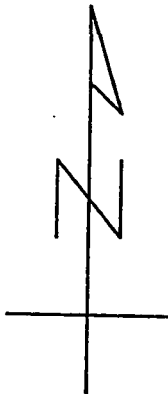
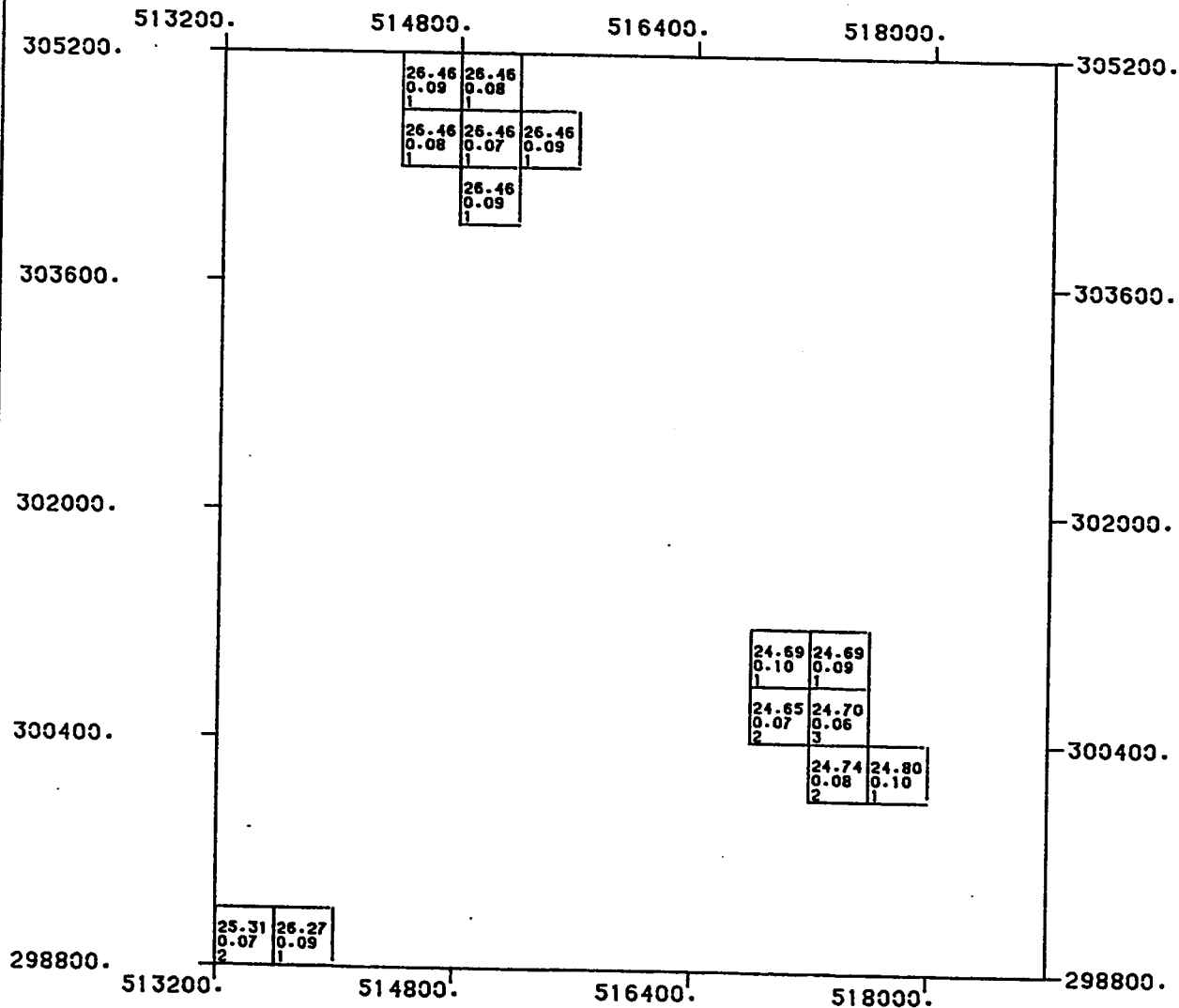
LEVEL NUMBER : 69

800.0 0.0 800.0 1600.0



SCALE OF MAP

DATA PROCESSED AT: U P M - D P C , DHAHRAN
 SOFTWARE BY : GEOSTAT SYSTEMS, MONTREAL



ABU TARTUR PHOSPHATE DEPOSIT
RESULTS OF BLOCK KRIGING

(Z = 341.5)

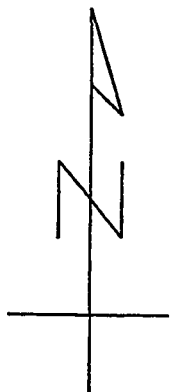
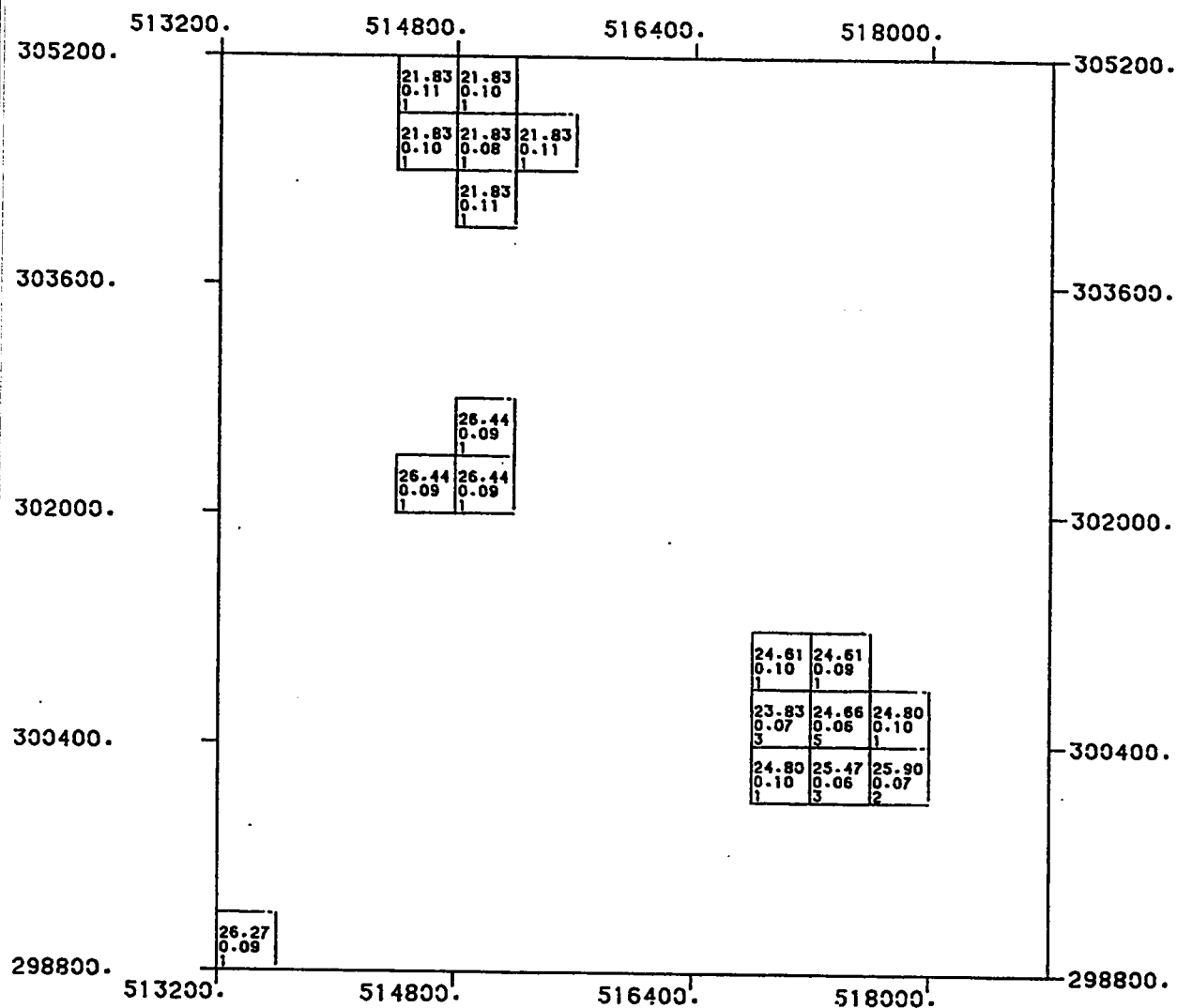
LEVEL NUMBER : 70

800.0 0.0 800.0 1600.0



SCALE OF MAP

DATA PROCESSED AT: U P M - D P C , DHAHRAN
 SOFTWARE BY : GEOSTAT SYSTEMS, MONTREAL



ABU TARTUR PHOSPHATE DEPOSIT
RESULTS OF BLOCK KRIGING

(Z = 342.5)

LEVEL NUMBER : 71

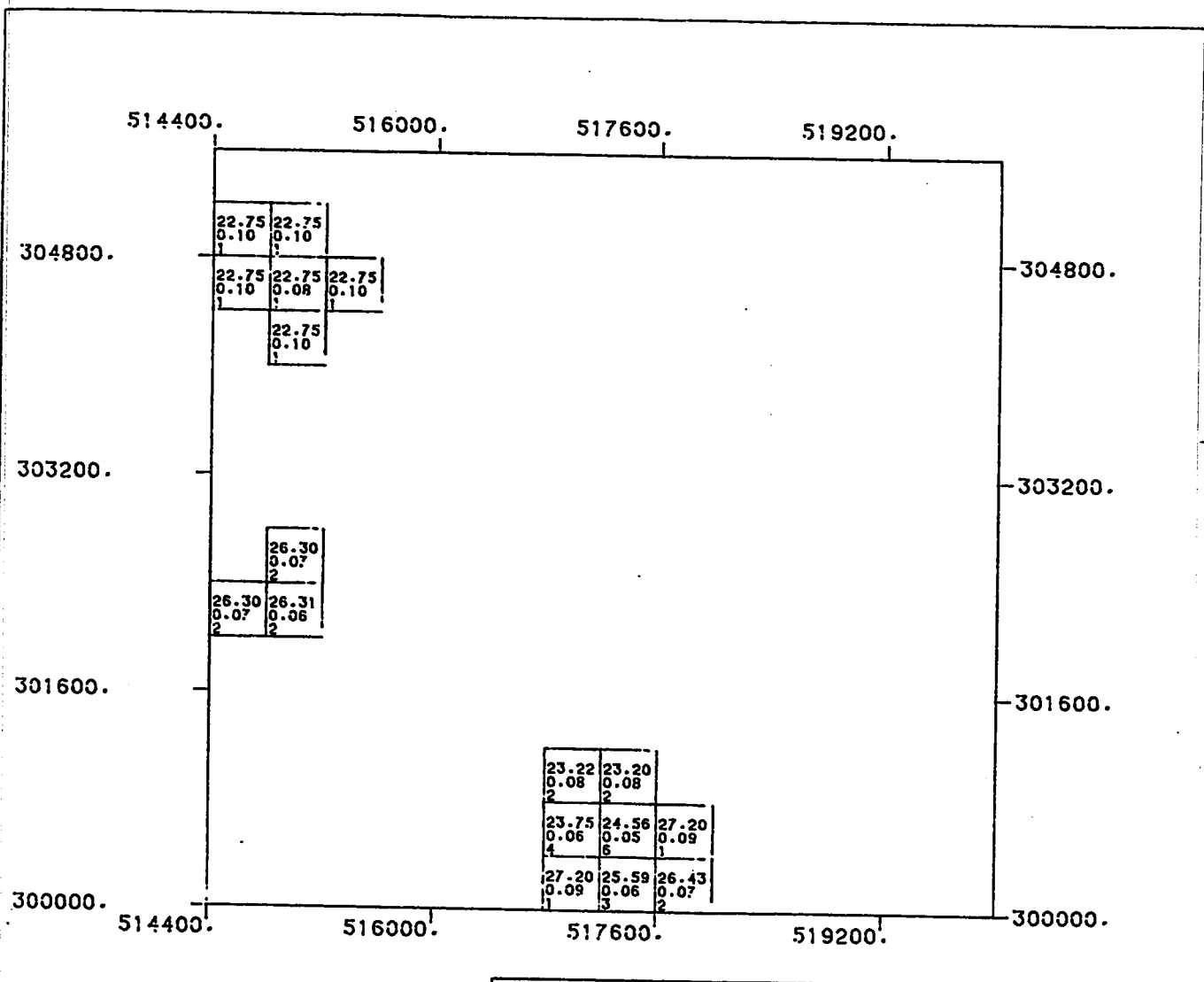
800.0 0.0 800.0 1600.0



SCALE OF MAP

DATA PROCESSED AT: U P M - D P C , DHAHRAN
 SOFTWARE BY : GEOSTAT SYSTEMS, MONTREAL

(D36)



ABU TARTUR PHOSPHATE DEPOSIT
RESULTS OF BLOCK KRIGING

(Z = 343.5)

LEVEL NUMBER : 72

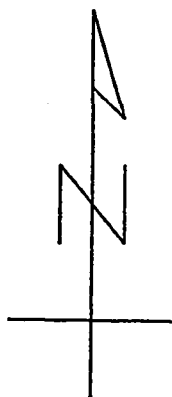
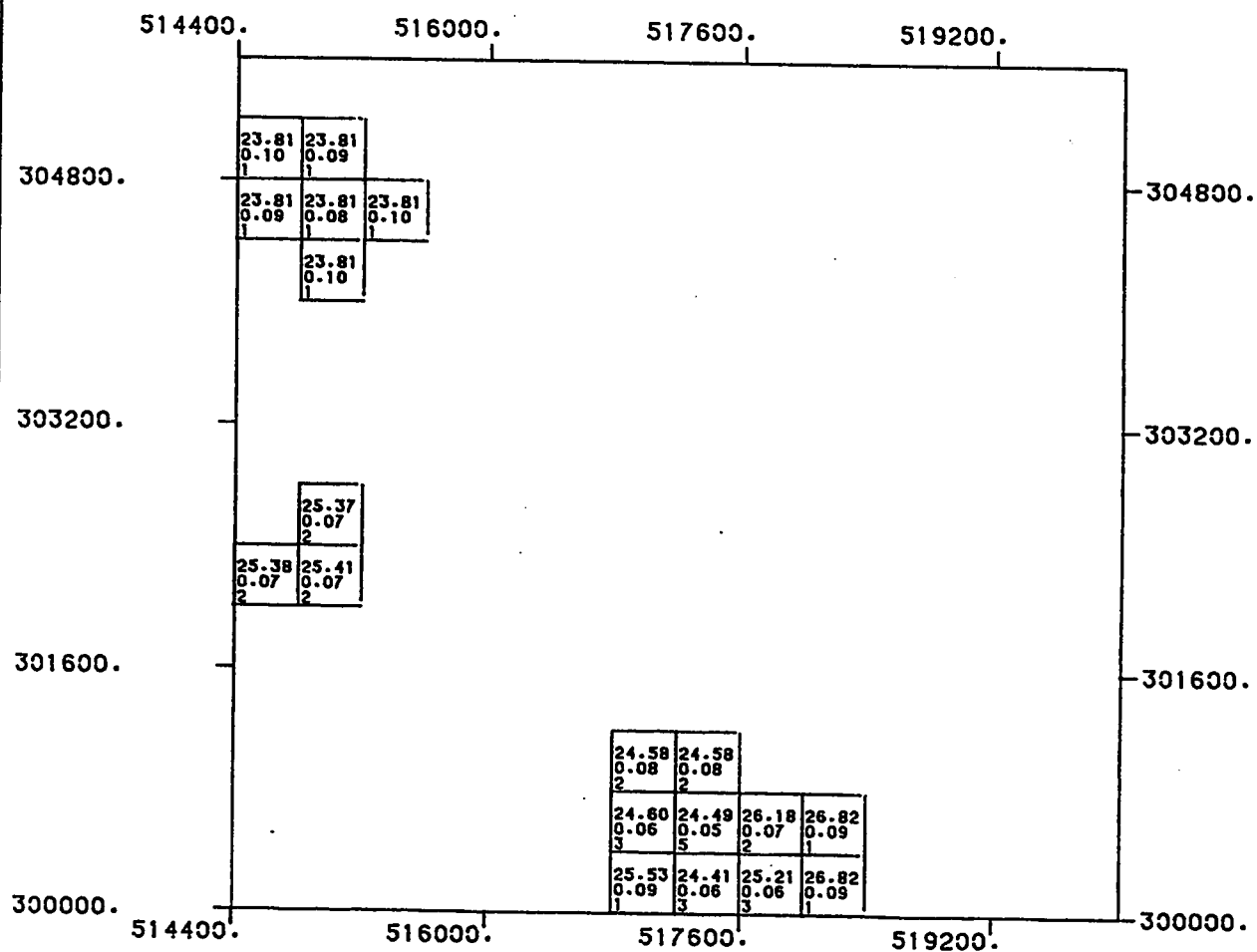
800.0 0.0 800.0 1600.0



SCALE OF MAP

DATA PROCESSED AT: U P M - D P C , DHAHRAN
SOFTWARE BY : GEOSTAT SYSTEMS, MONTREAL

(D37)



ABU TARTUR PHOSPHATE DEPOSIT
RESULTS OF BLOCK KRIGING

(Z = 344.5)

LEVEL NUMBER : 73

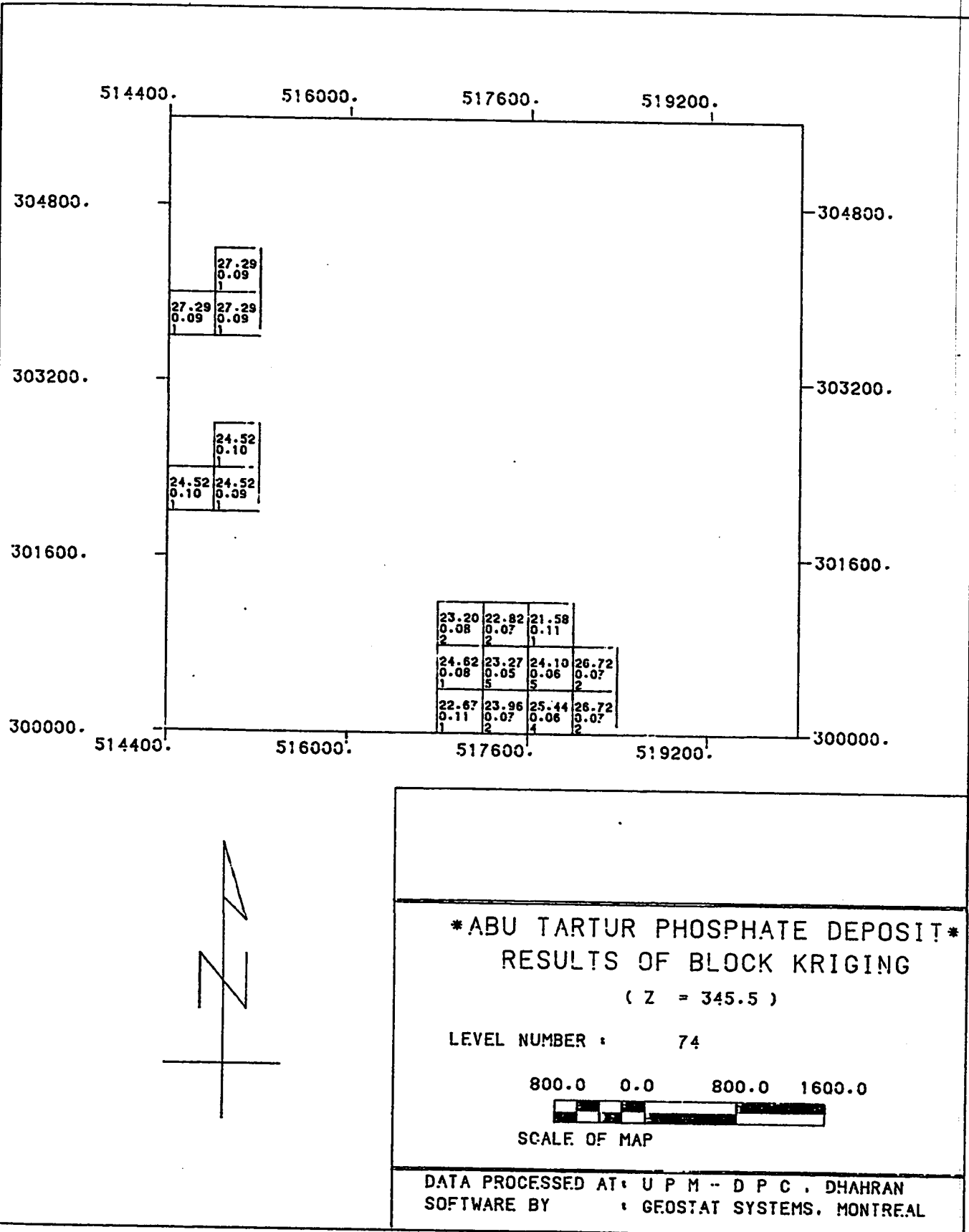
800.0 0.0 800.0 1600.0



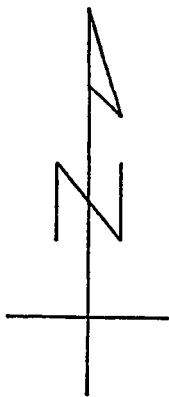
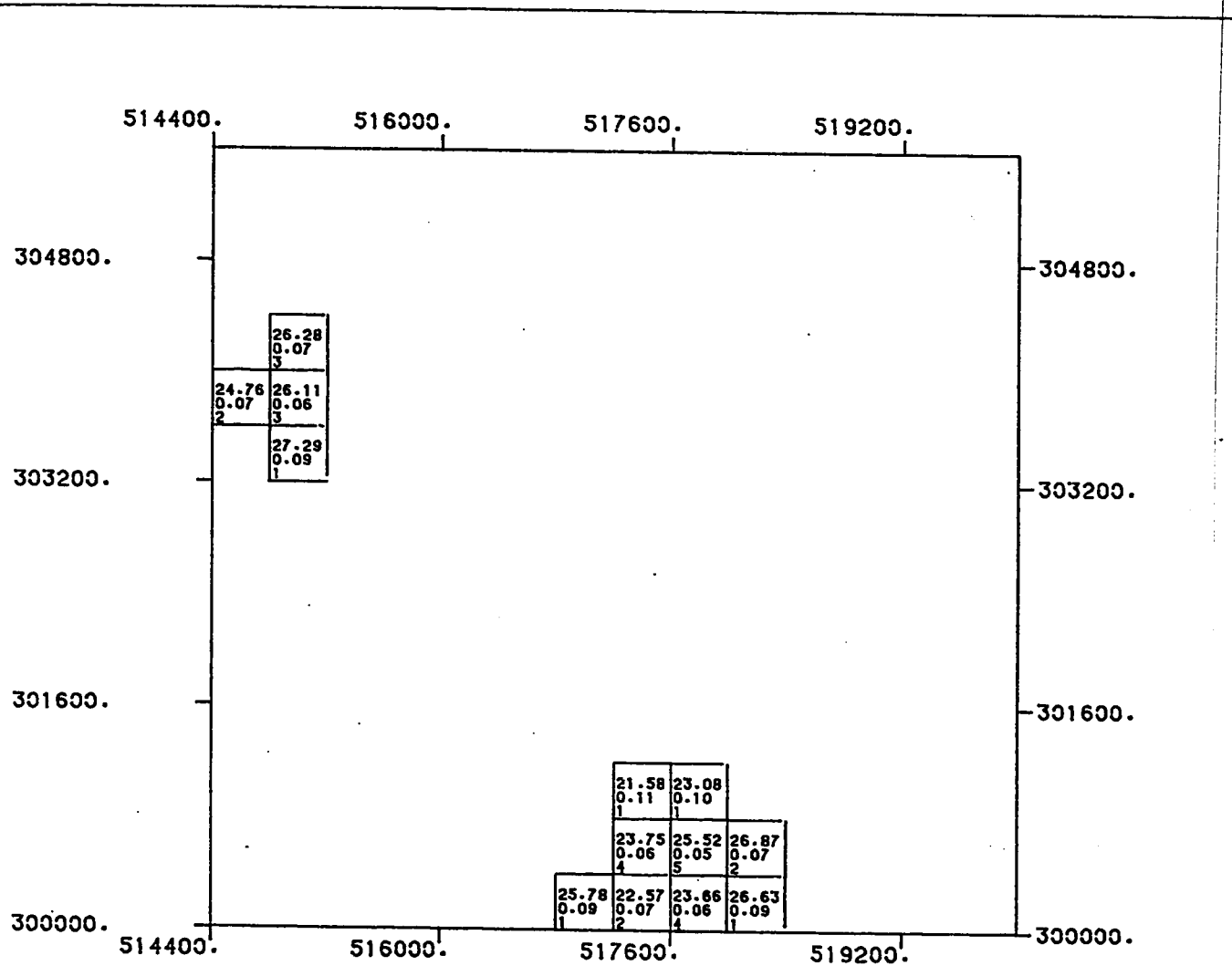
SCALE OF MAP

DATA PROCESSED AT: U P M - D P C . DHAHRAN
SOFTWARE BY : GEOSTAT SYSTEMS. MONTREAL

(D38)



(D39)



ABU TARTUR PHOSPHATE DEPOSIT
RESULTS OF BLOCK KRIGING

(Z = 346.5)

LEVEL NUMBER : 75

800.0 0.0 800.0 1600.0

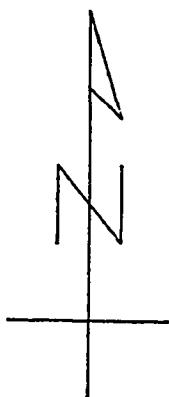
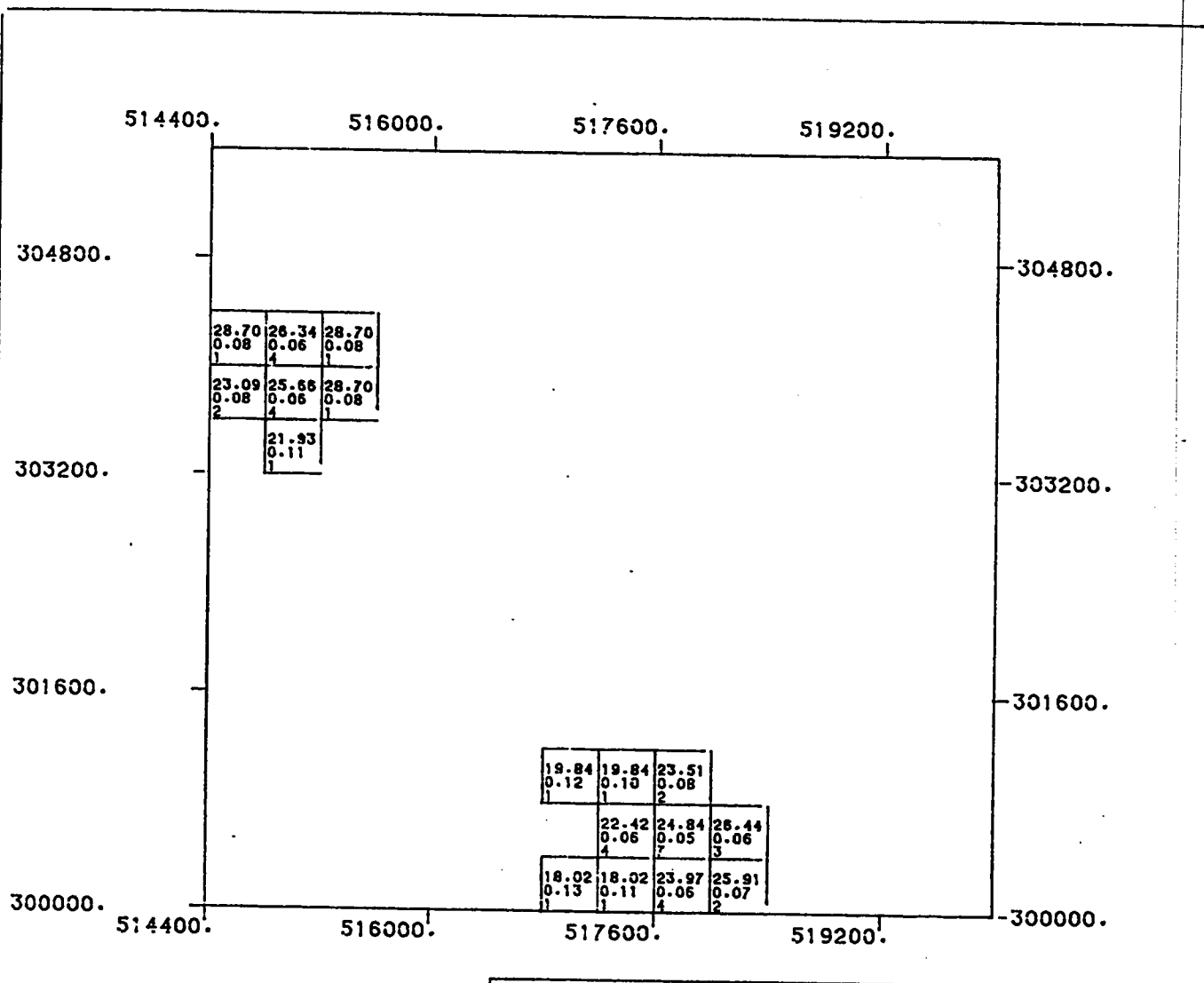


SCALE OF MAP

DATA PROCESSED AT: U P M - D P C , DHAHRAN
SOFTWARE BY : GEOSTAT SYSTEMS, MONTREAL

(D40)

173



ABU TARTUR PHOSPHATE DEPOSIT
RESULTS OF BLOCK KRIGING
(Z = 347.5)

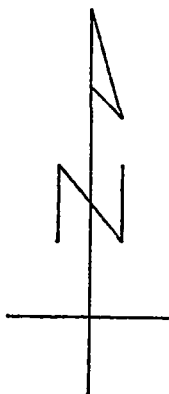
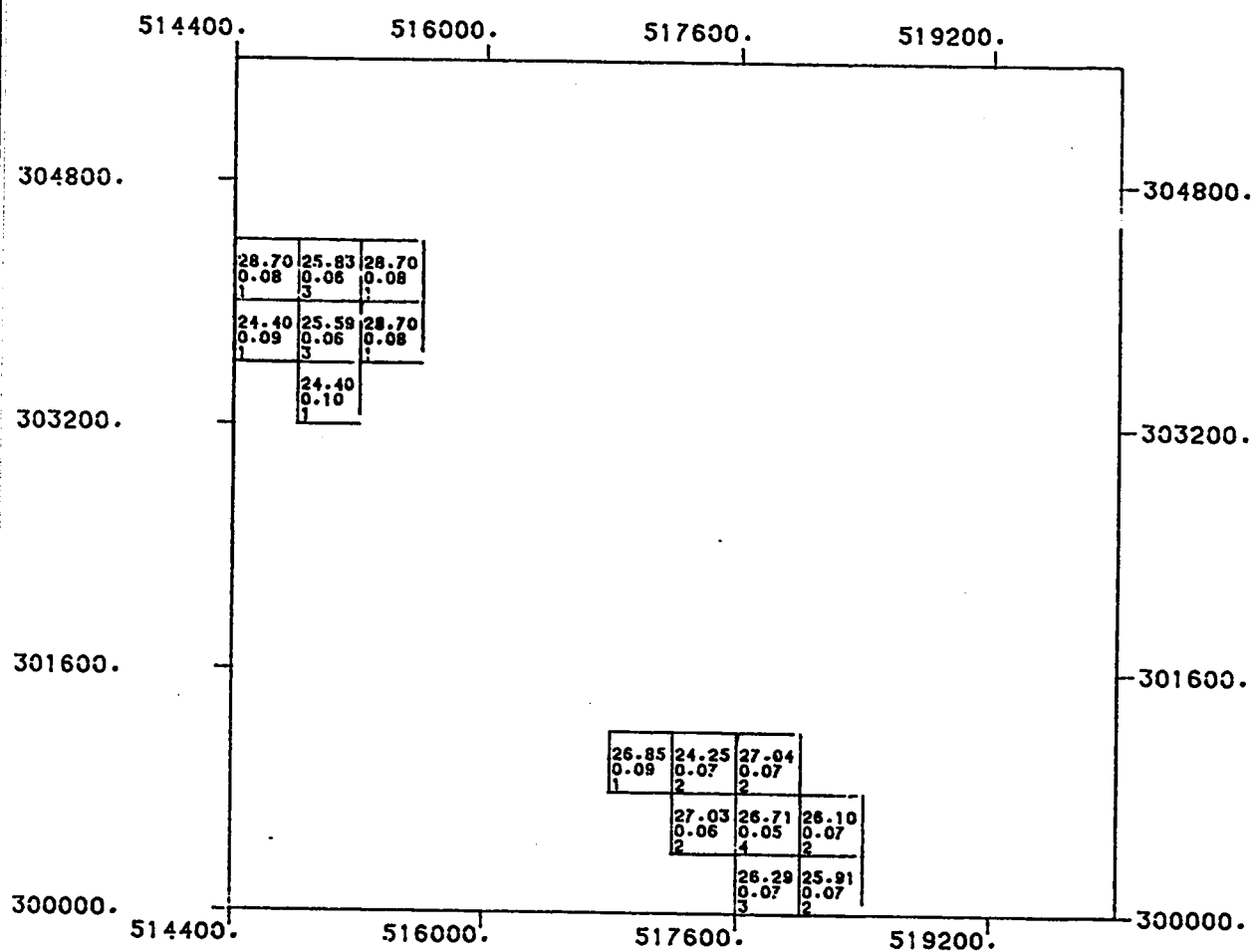
LEVEL NUMBER : 76

800.0 0.0 800.0 1600.0



SCALE OF MAP

DATA PROCESSED AT: U P M - D P C , DHAHRAN
SOFTWARE BY : GEOSTAT SYSTEMS, MONTREAL



ABU TARTUR PHOSPHATE DEPOSIT
RESULTS OF BLOCK KRIGING

(Z = 348.5)

LEVEL NUMBER : 77

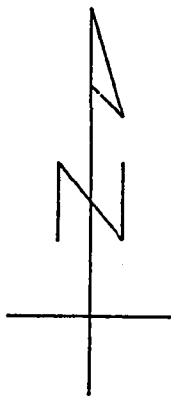
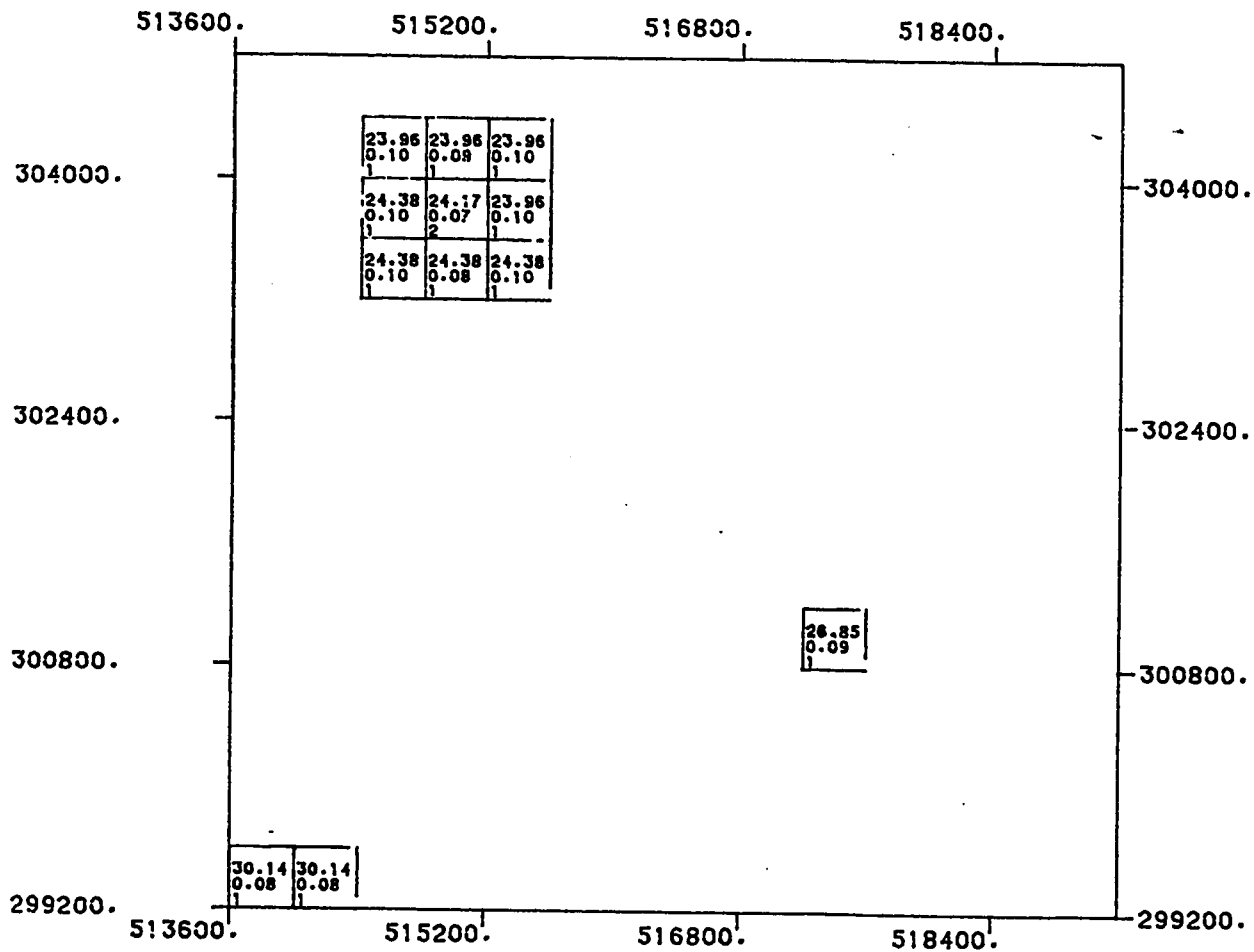
800.0 0.0 800.0 1600.0



SCALE OF MAP

DATA PROCESSED AT: U P M - D P C , DHAHRAN
 SOFTWARE BY : GEOSTAT SYSTEMS, MONTREAL

(D42)



ABU TARTUR PHOSPHATE DEPOSIT
RESULTS OF BLOCK KRIGING

(Z = 349.5)

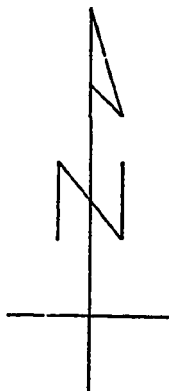
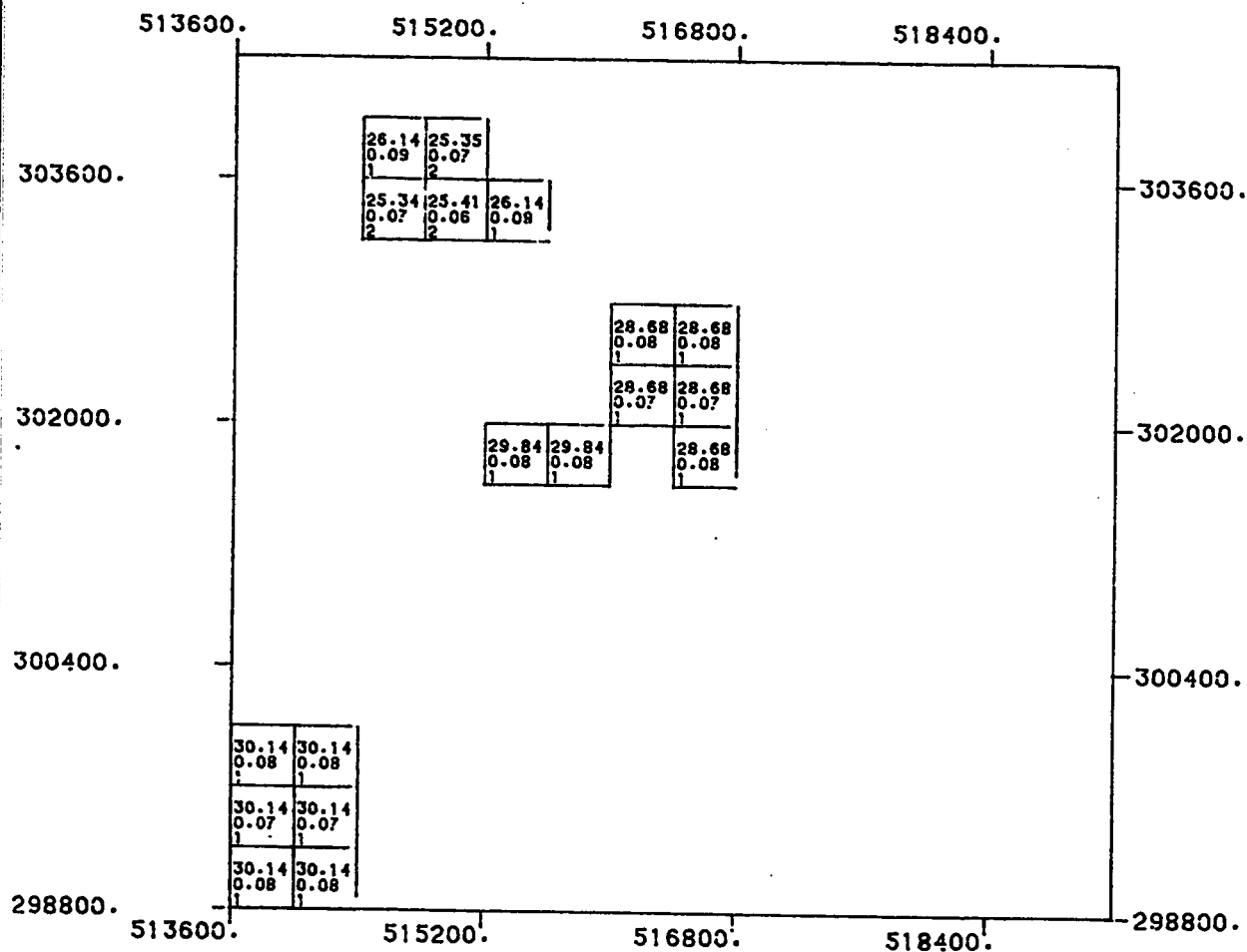
LEVEL NUMBER : 78

800.0 0.0 800.0 1600.0



SCALE OF MAP

DATA PROCESSED AT: U P M - D P C , DHAHRAN
 SOFTWARE BY : GEOSTAT SYSTEMS, MONTREAL



(Z = 350.5)

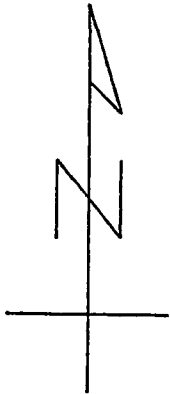
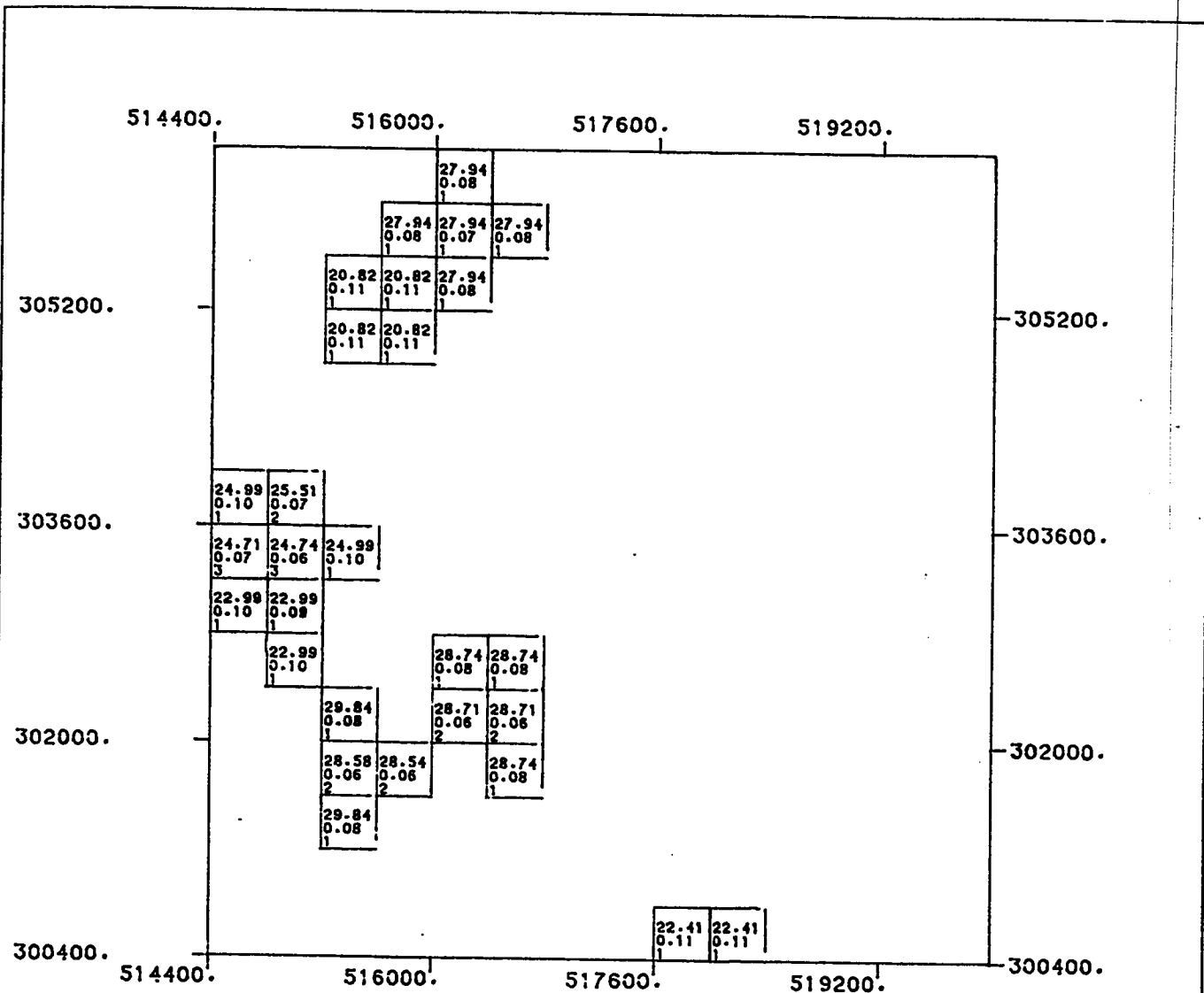
LEVEL NUMBER : 79

800.0 0.0 800.0 1600.0

SCALE OF MAP

DATA PROCESSED AT: U P M - D P C , DHAHRAN
SOFTWARE BY : GEOSTAT SYSTEMS, MONTREAL

(D44)



ABU TARTUR PHOSPHATE DEPOSIT
RESULTS OF BLOCK KRIGING

(Z = 351.5)

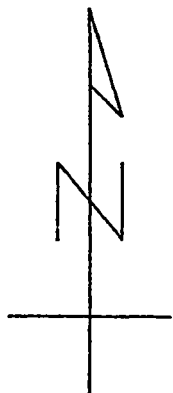
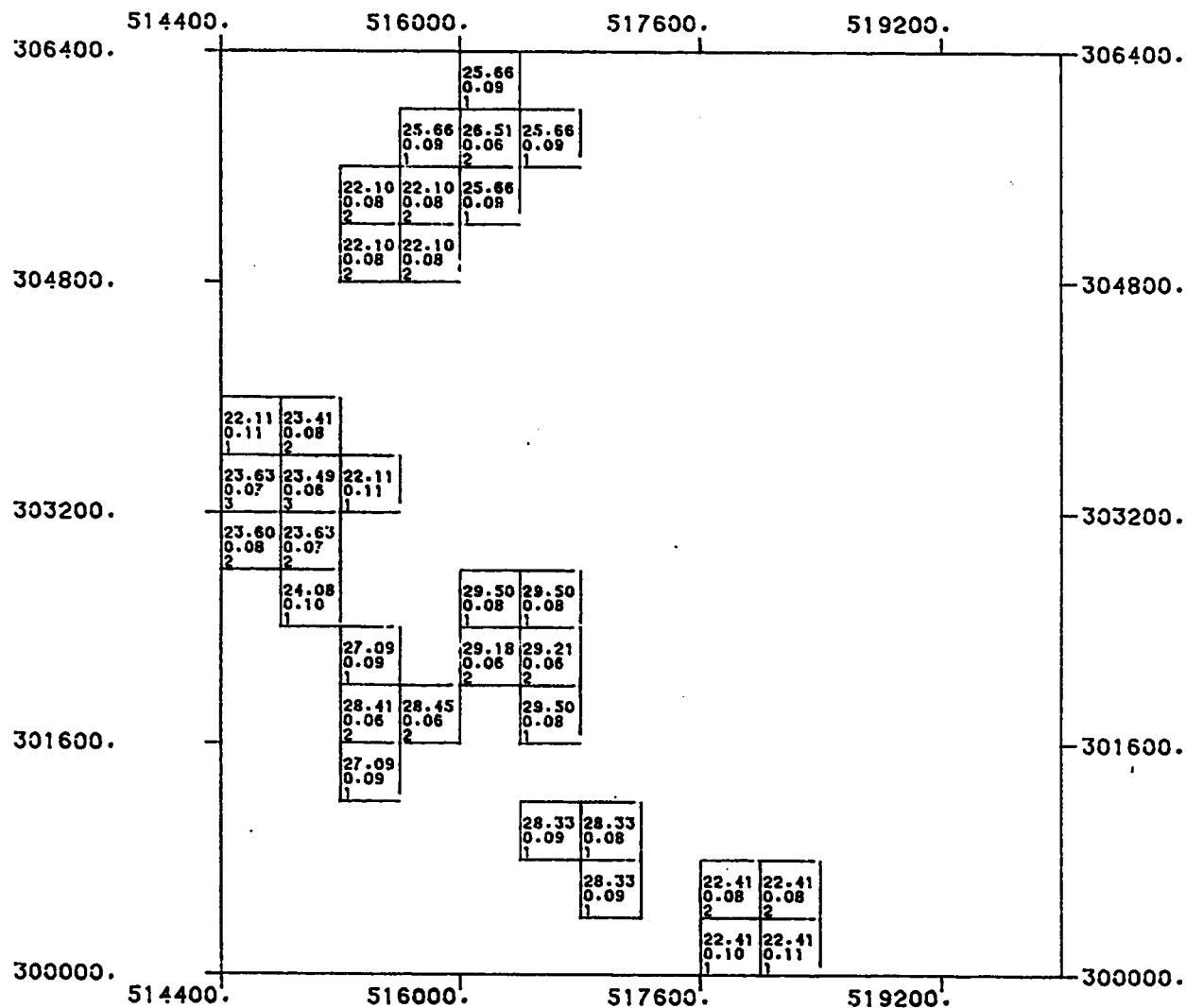
LEVEL NUMBER : 80

800.0 0.0 800.0 1600.0



SCALE OF MAP

DATA PROCESSED AT: U P M - D P C . DHAHRAN
 SOFTWARE BY : GEOSTAT SYSTEMS. MONTREAL



ABU TARTUR PHOSPHATE DEPOSIT
RESULTS OF BLOCK KRIGING

(Z = 352.5)

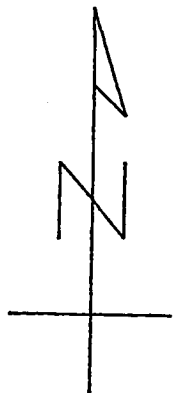
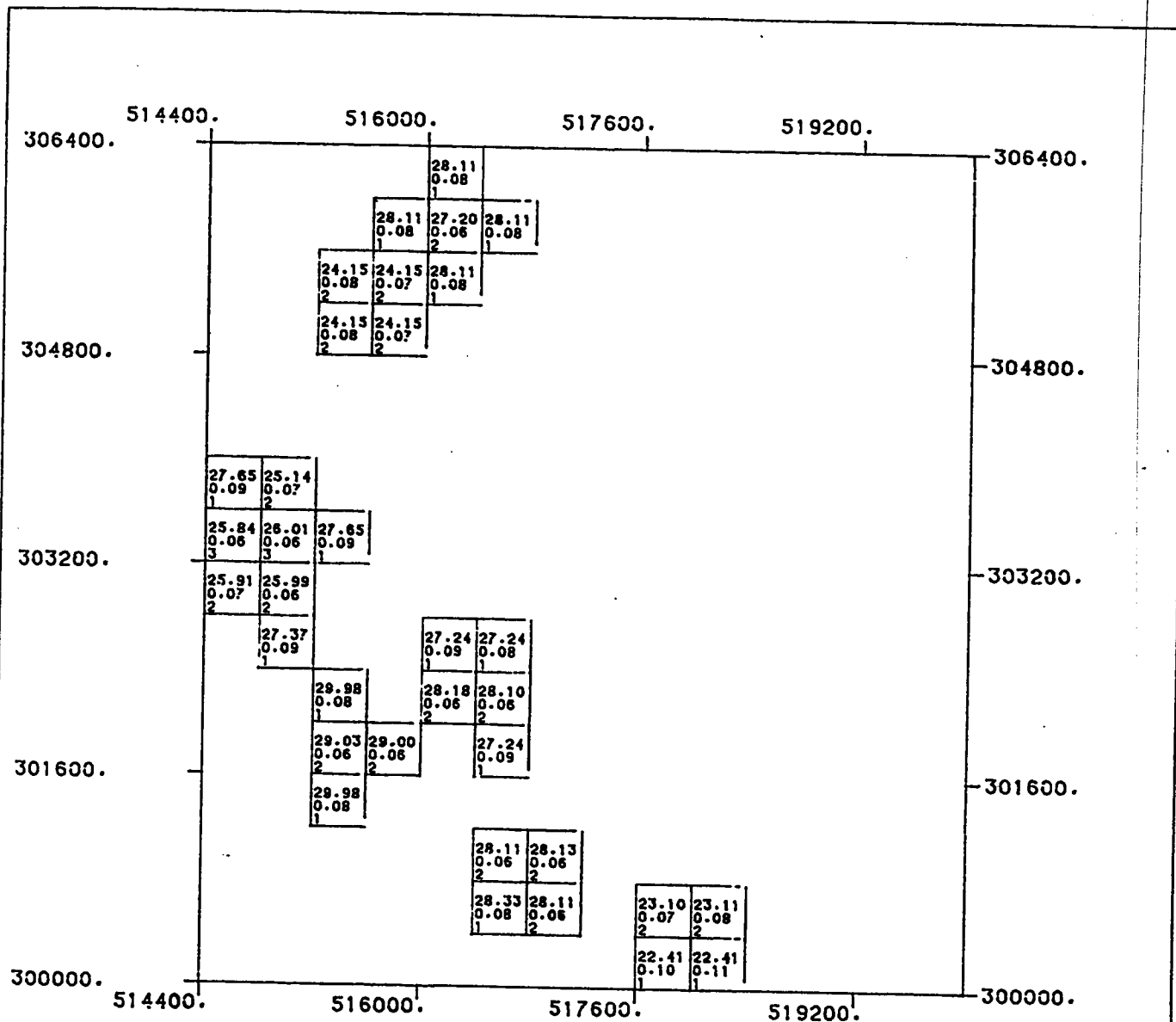
LEVEL NUMBER : 81

800.0 0.0 800.0 1600.0



SCALE OF MAP

DATA PROCESSED AT: U P M - D P C , DHAHRAN
SOFTWARE BY : GEOSTAT SYSTEMS, MONTREAL



ABU TARTUR PHOSPHATE DEPOSIT
RESULTS OF BLOCK KRIGING

(Z = 353.5)

LEVEL NUMBER : 82

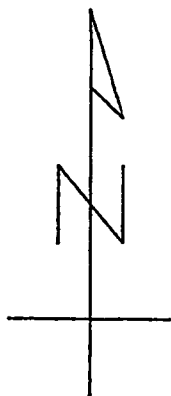
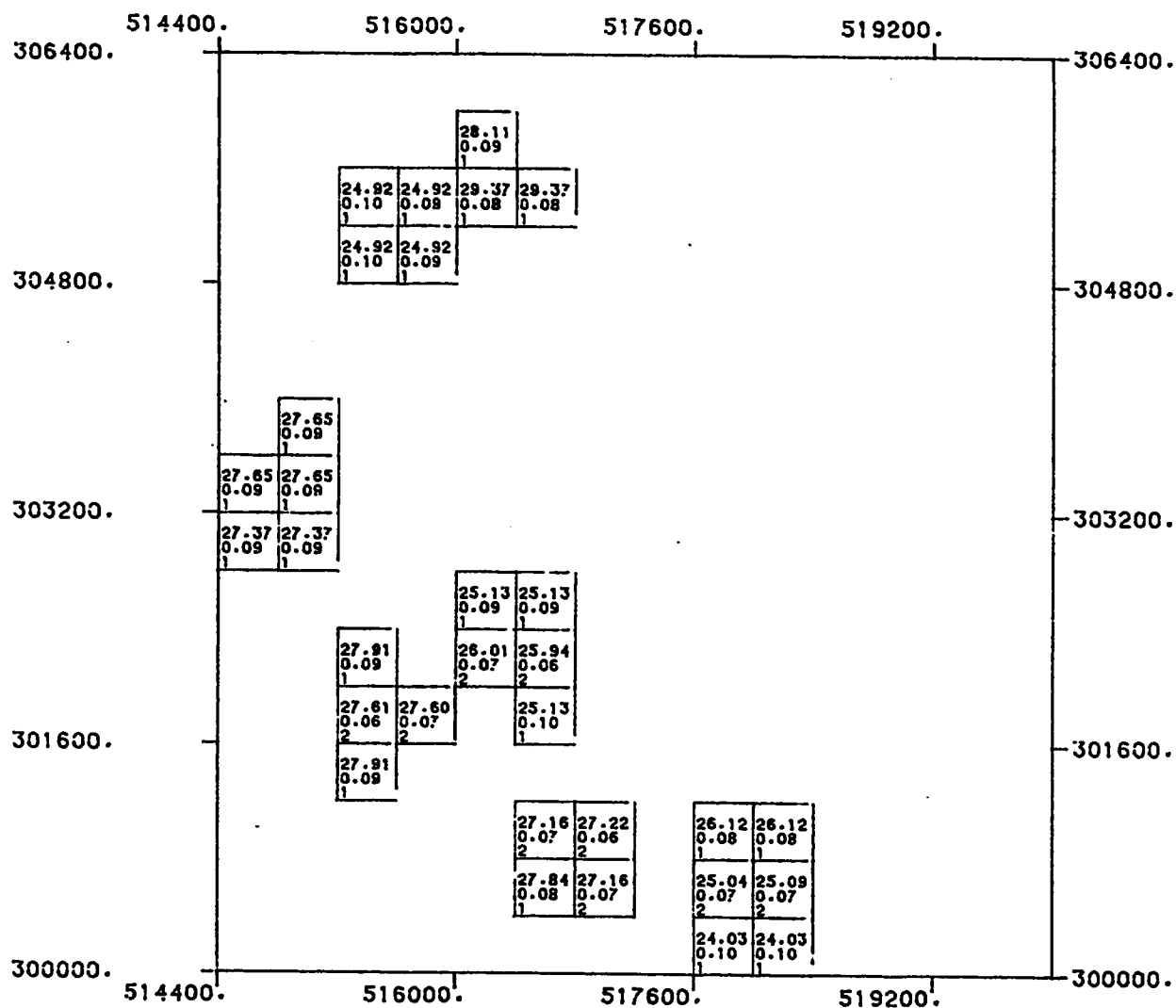
800.0 0.0 800.0 1600.0



SCALE OF MAP

DATA PROCESSED AT: U P M - D P C , DHAHRAN
SOFTWARE BY : GEOSTAT SYSTEMS, MONTREAL

(D47)



ABU TARTUR PHOSPHATE DEPOSIT
RESULTS OF BLOCK KRIGING

(Z = 354.5)

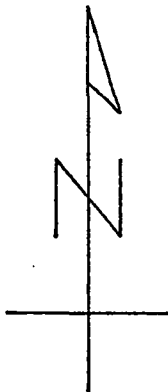
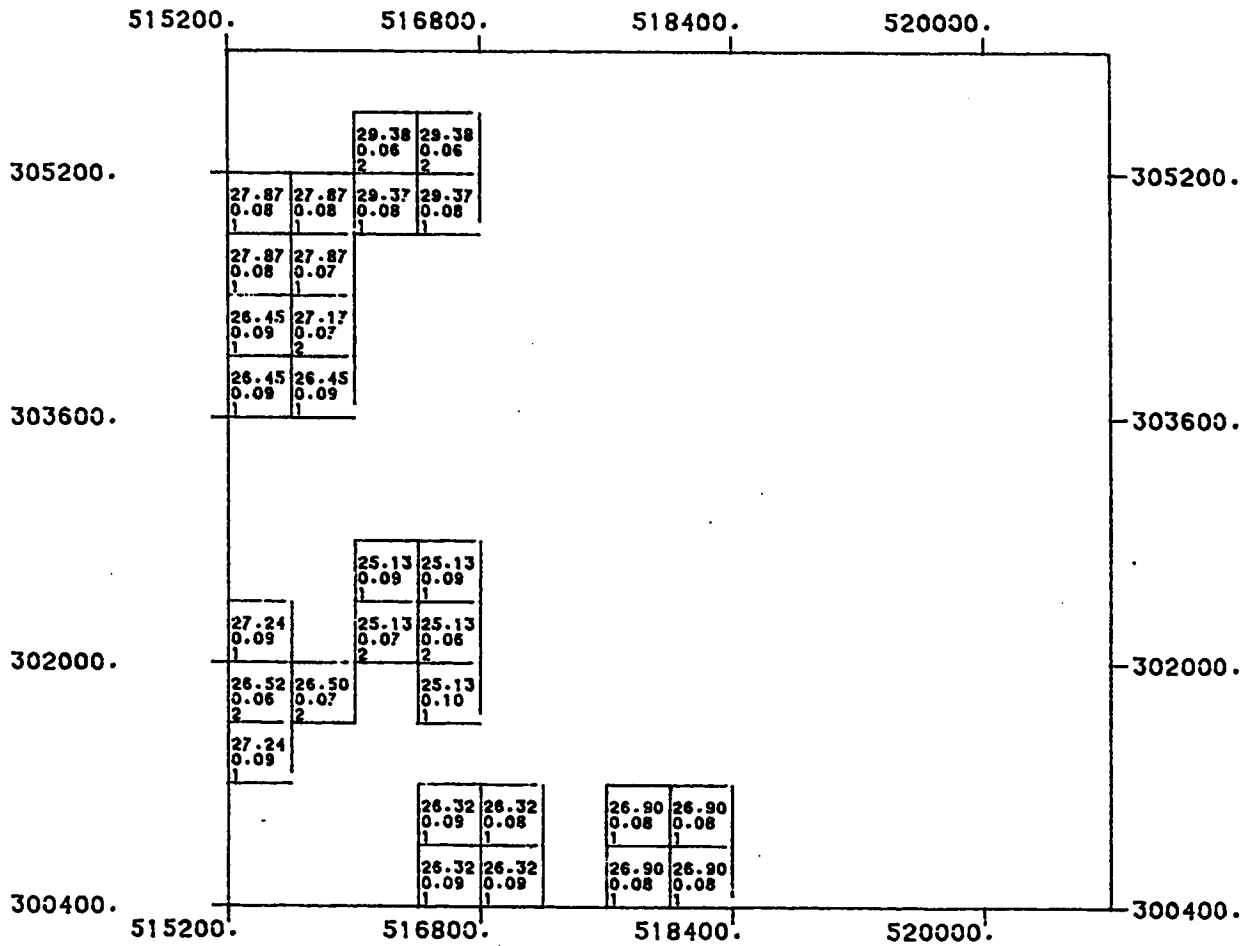
LEVEL NUMBER : 83

800.0 0.0 800.0 1600.0



SCALE OF MAP

DATA PROCESSED AT: U P M - D P C , DHAHRAN
SOFTWARE BY : GEOSTAT SYSTEMS, MONTREAL



ABU TARTUR PHOSPHATE DEPOSIT
RESULTS OF BLOCK KRIGING
(Z = 355.5)

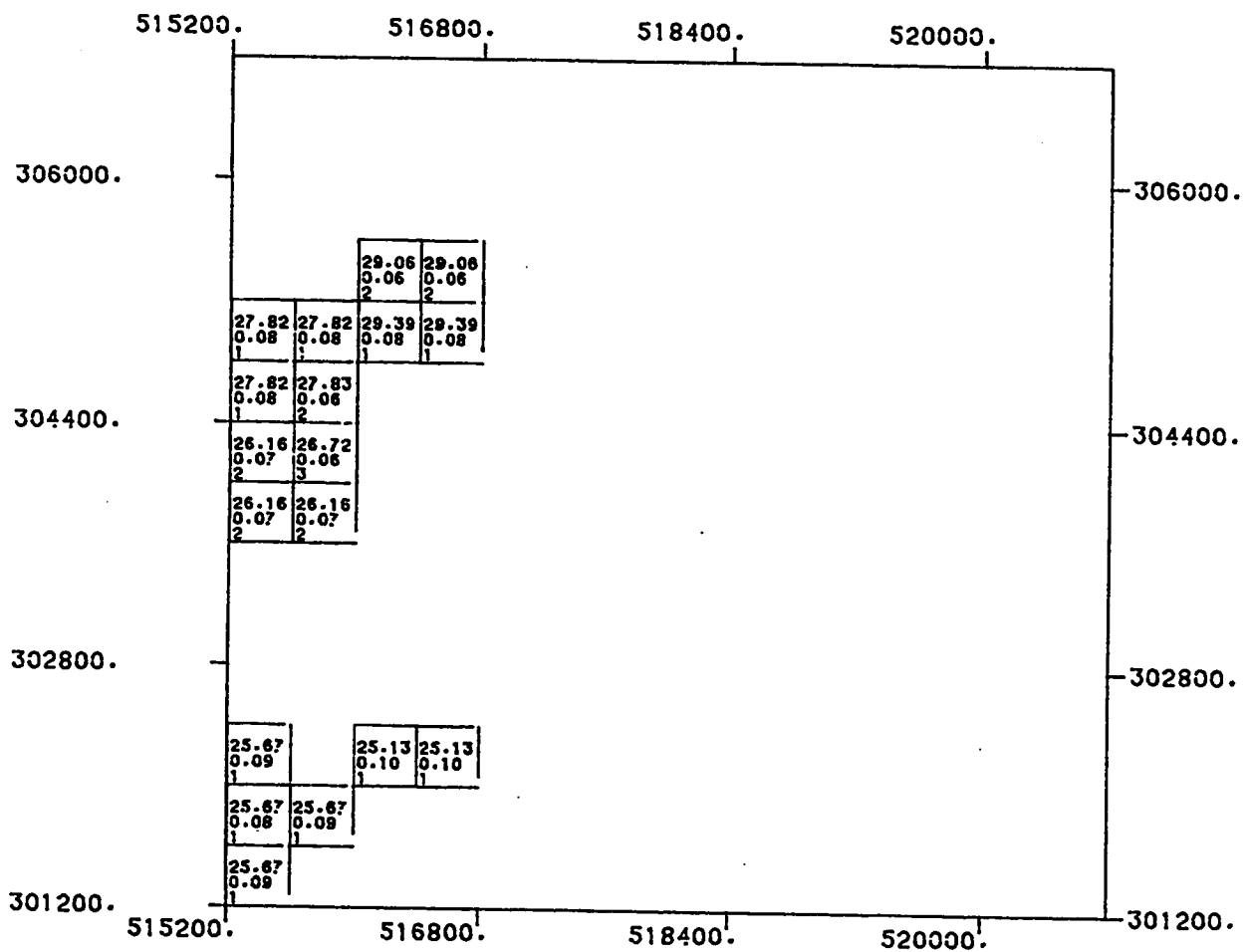
LEVEL NUMBER : 84

800.0 0.0 800.0 1600.0



SCALE OF MAP

DATA PROCESSED AT: U P M - D P C . DHAHRAN
SOFTWARE BY : GEOSTAT SYSTEMS. MONTREAL



ABU TARTUR PHOSPHATE DEPOSIT
RESULTS OF BLOCK KRIGING

(Z = 356.5)

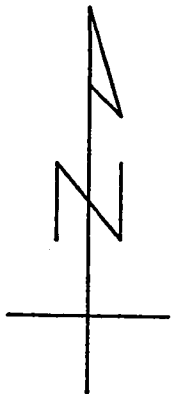
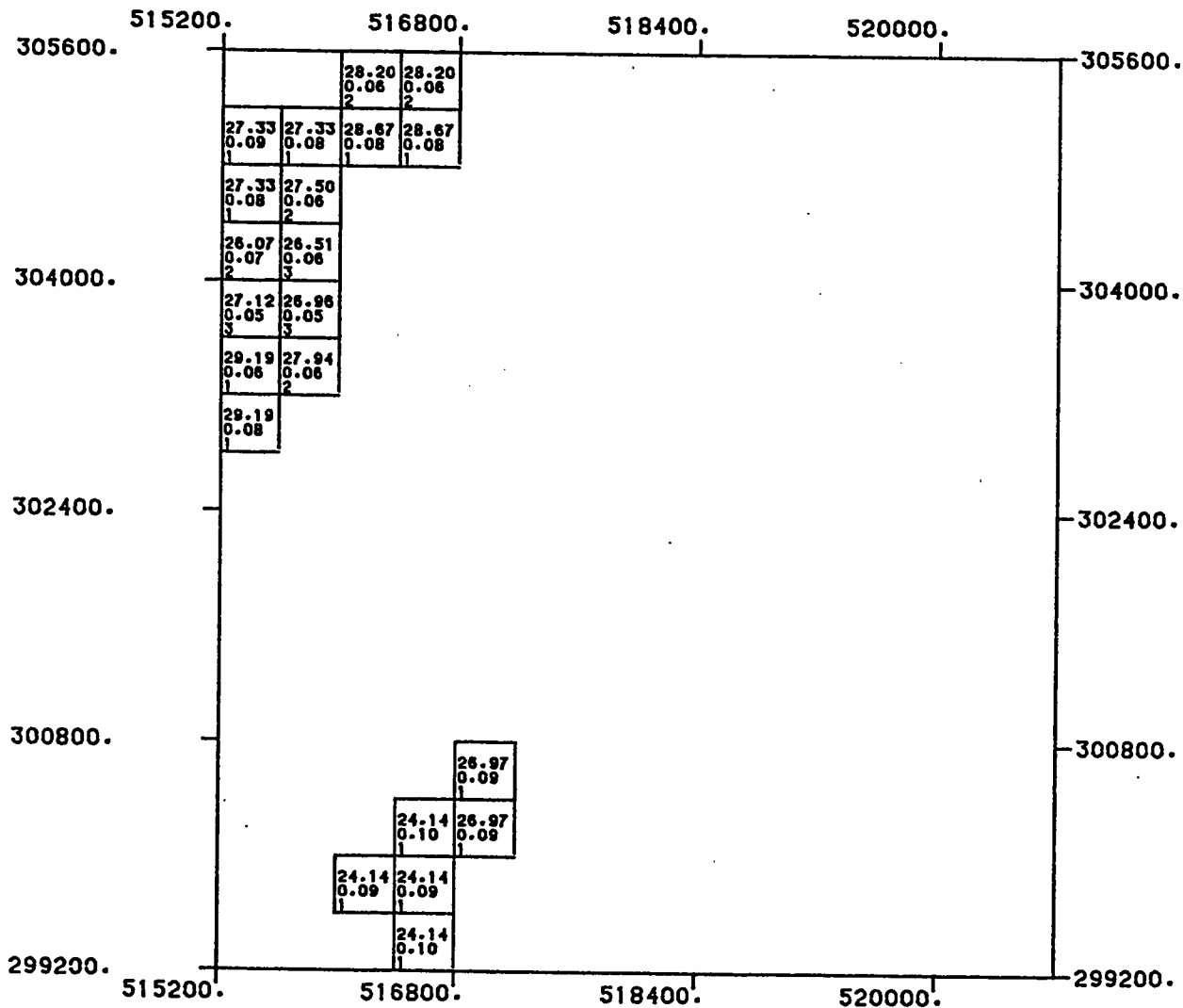
LEVEL NUMBER : 85

800.0	0.0	800.0	1600.0
-------	-----	-------	--------

SCALE OF MAP

DATA PROCESSED AT: U P M - D P C , DHAHRAN
SOFTWARE BY : GEOSTAT SYSTEMS. MONTREAL

(D50)



ABU TARTUR PHOSPHATE DEPOSIT
RESULTS OF BLOCK KRIGING

($Z = 357.5$)

LEVEL NUMBER : 86

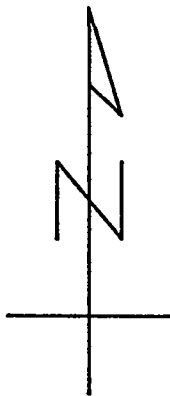
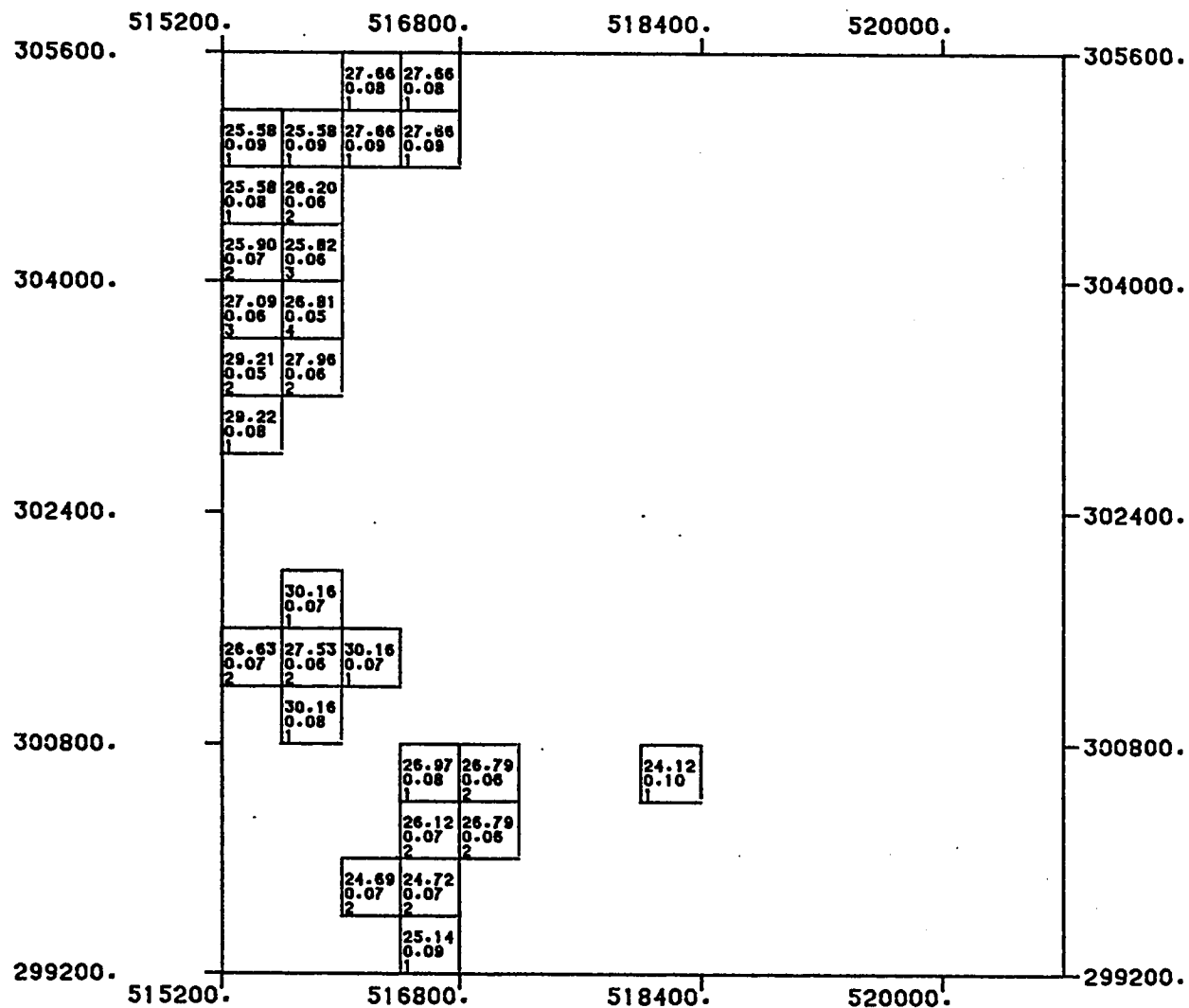
800.0 0.0 800.0 1600.0



SCALE OF MAP

DATA PROCESSED AT: U P M - D P C , DHAHRAN
 SOFTWARE BY : GEOSTAT SYSTEMS, MONTREAL

(D51)



ABU TARTUR PHOSPHATE DEPOSIT
RESULTS OF BLOCK KRIGING

(Z = 358.5)

LEVEL NUMBER : 87

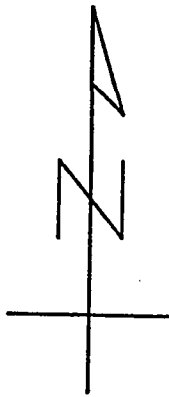
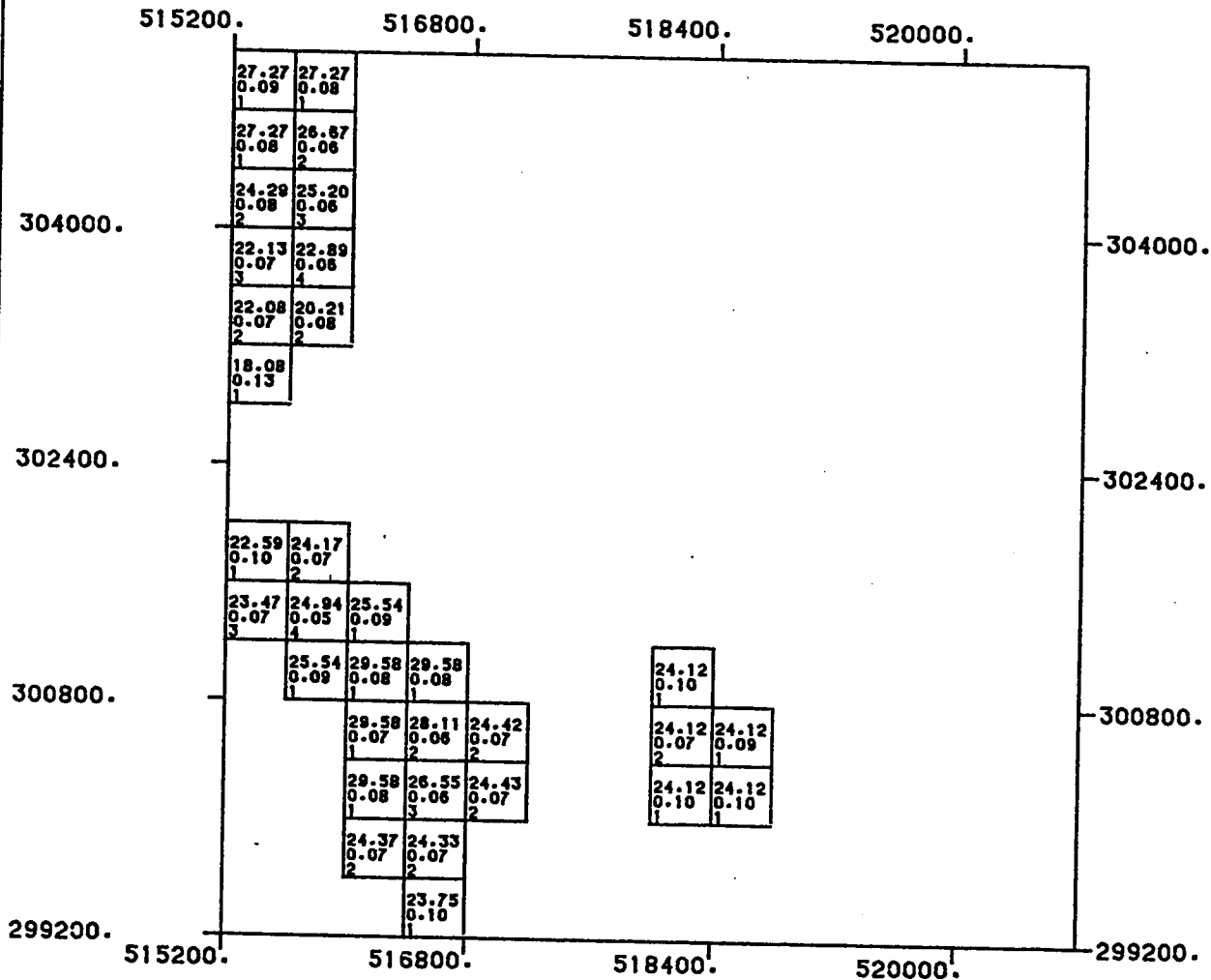
800.0 0.0 800.0 1600.0



SCALE OF MAP

DATA PROCESSED AT: U P M - D P C , DHAHRAN
SOFTWARE BY : GEOSTAT SYSTEMS, MONTREAL

(D52)



ABU TARTUR PHOSPHATE DEPOSIT
RESULTS OF BLOCK KRIGING

(Z = 359.5)

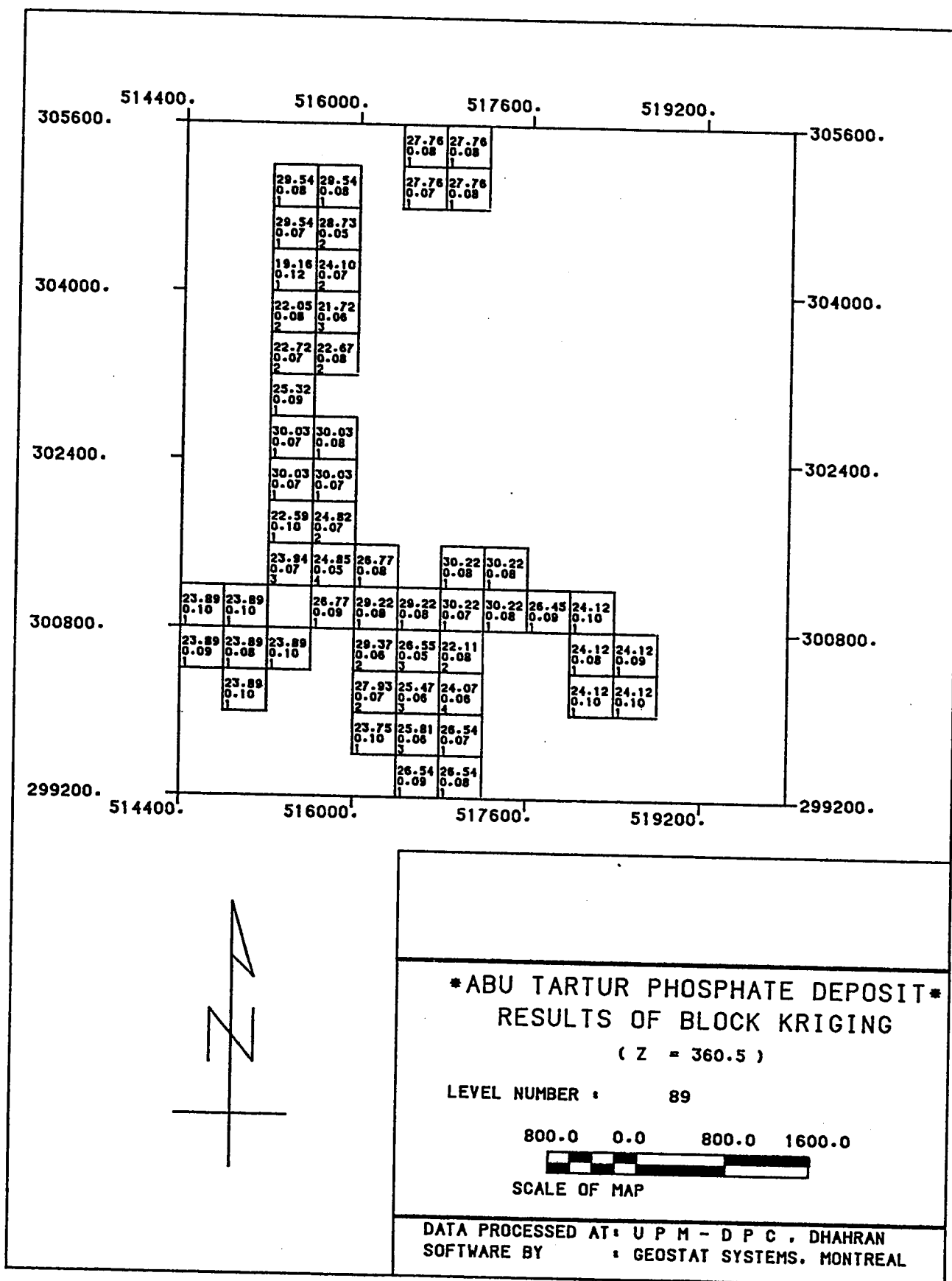
LEVEL NUMBER : 88

800.0 0.0 800.0 1600.0

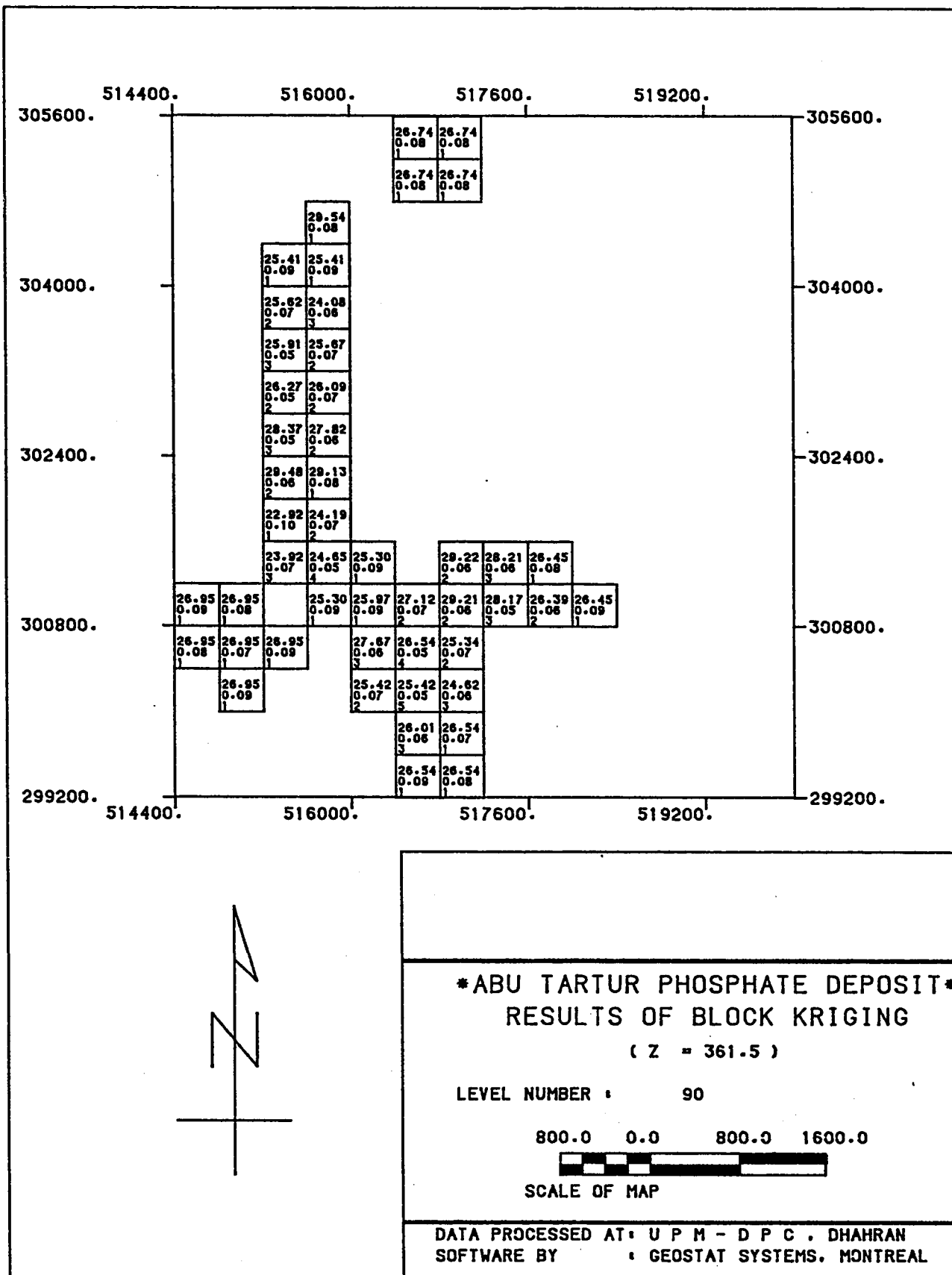


SCALE OF MAP

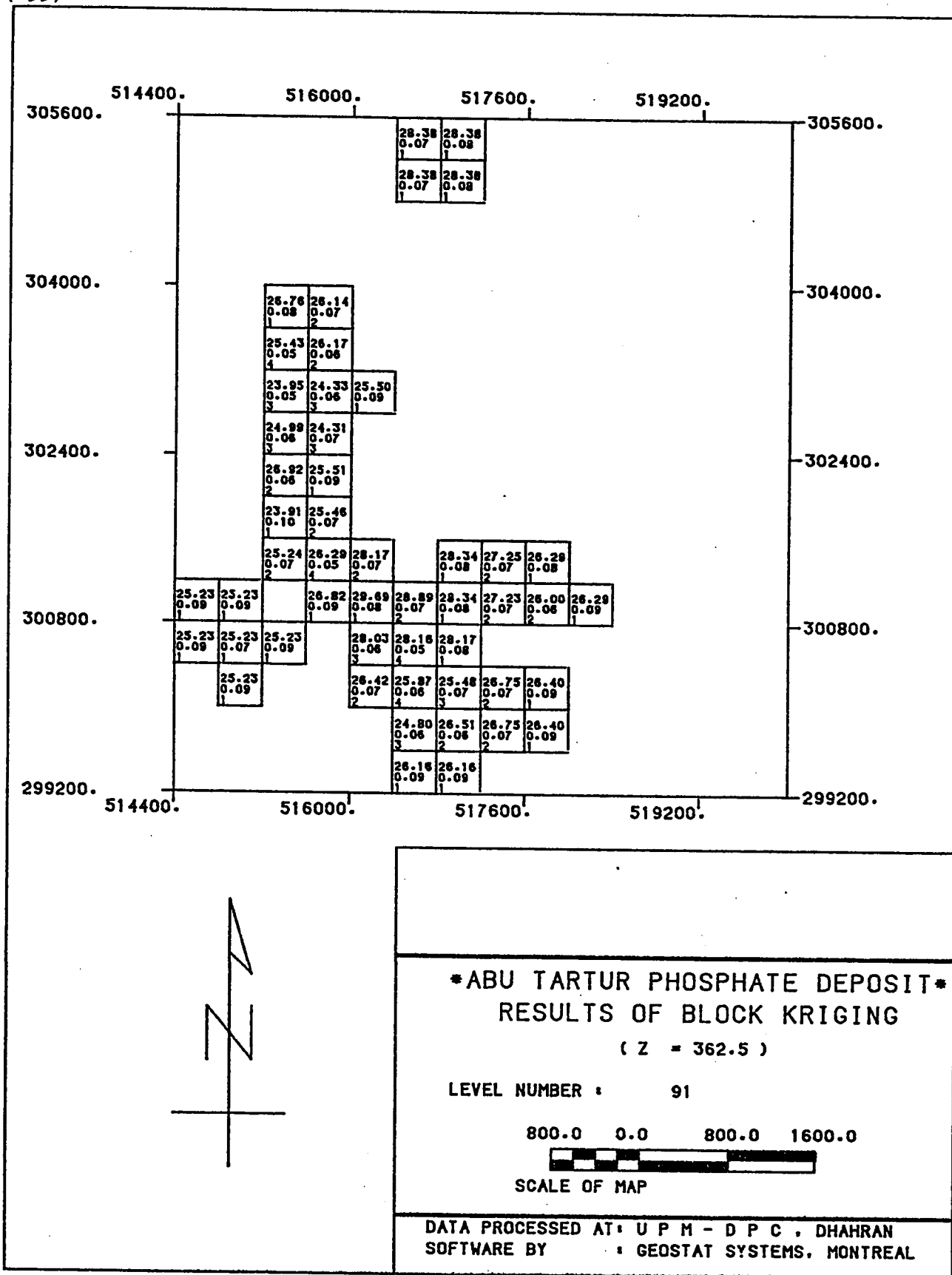
DATA PROCESSED AT: U P M - D P C , DHAHRAN
SOFTWARE BY : GEOSTAT SYSTEMS, MONTREAL

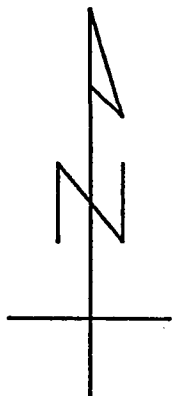
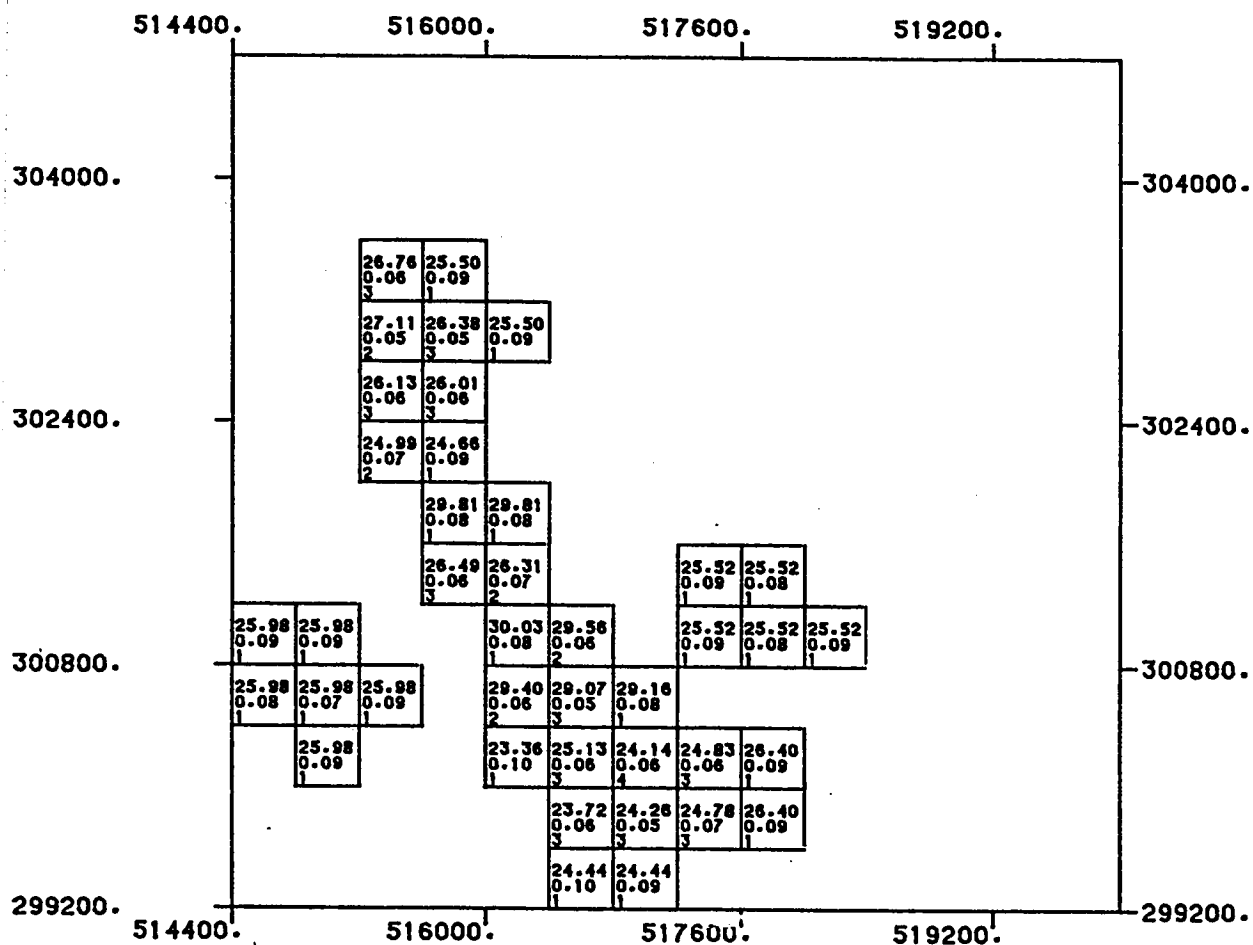


(D54)



(D55)





(Z = 363.5)

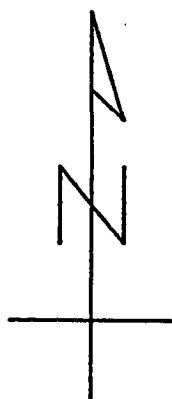
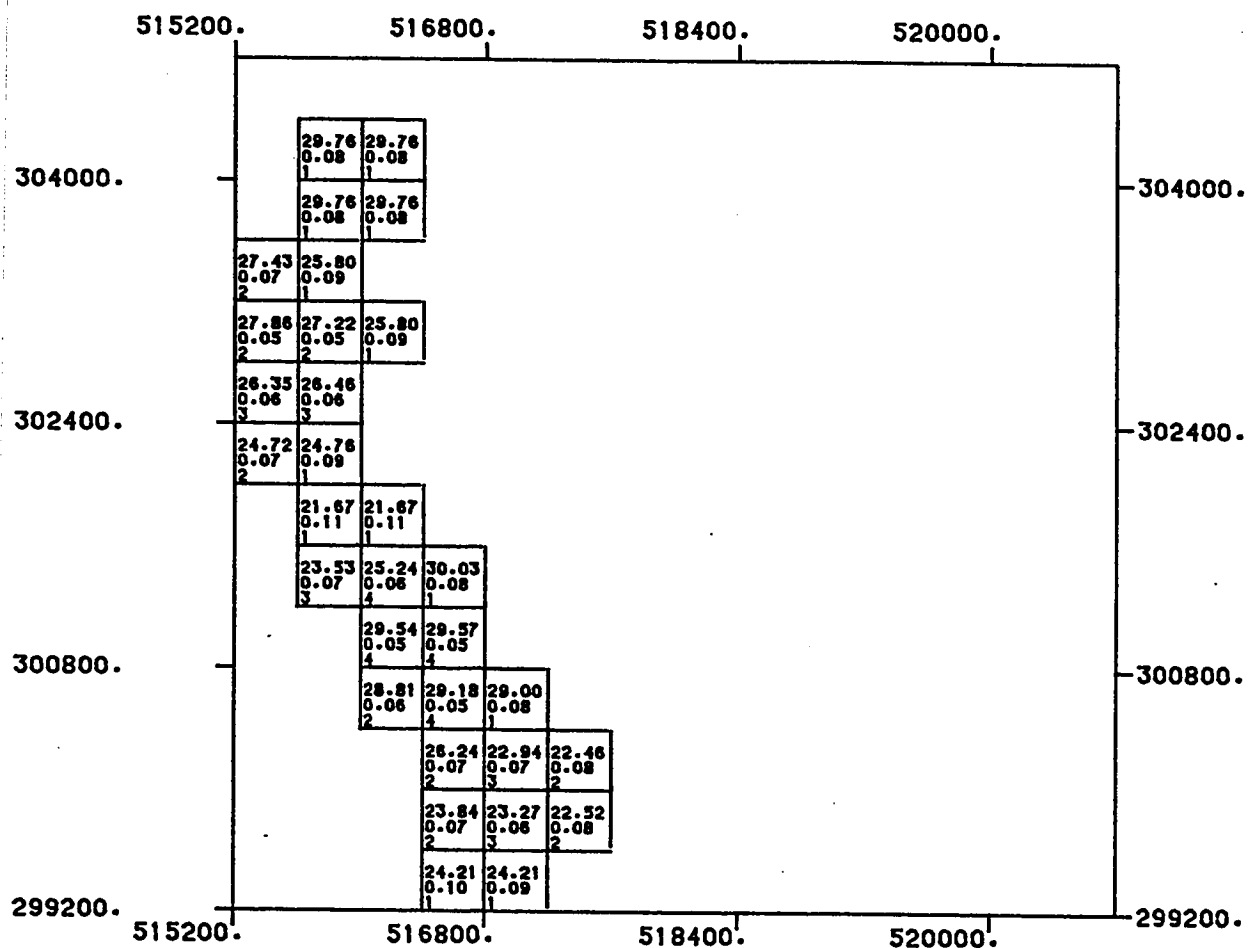
LEVEL NUMBER : 92

800.0 0.0 800.0 1600.0

SCALE OF MAP

DATA PROCESSED AT: U P M - D P C , DHAHRAN
SOFTWARE BY : GEOSTAT SYSTEMS, MONTREAL

(D57)



ABU TARTUR PHOSPHATE DEPOSIT
RESULTS OF BLOCK KRIGING

(Z = 364.5)

LEVEL NUMBER : 93

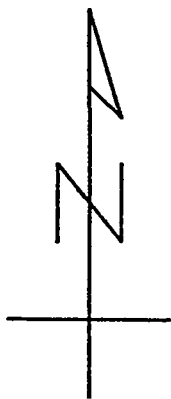
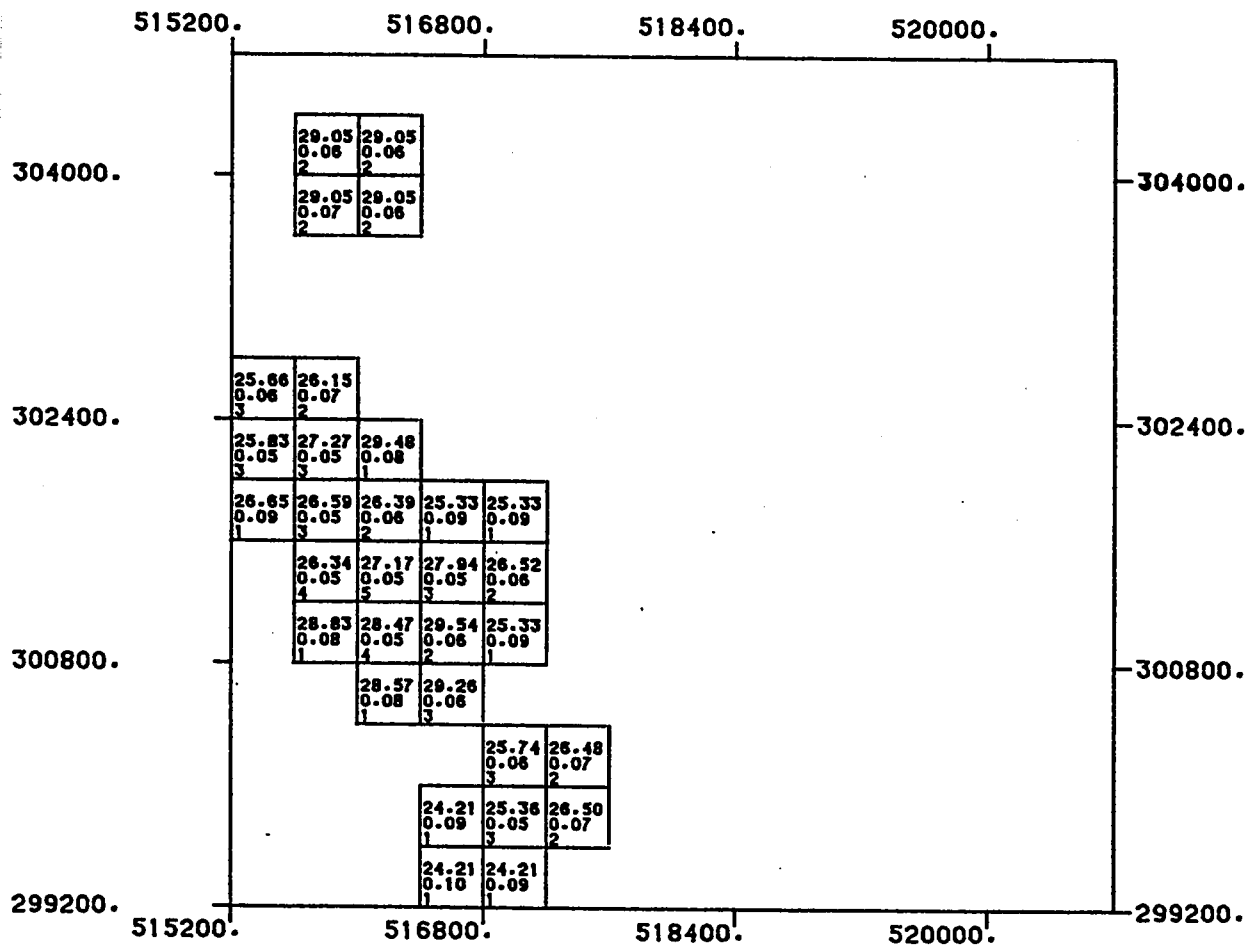
800.0 0.0 800.0 1600.0



SCALE OF MAP

DATA PROCESSED AT: U P M - D P C , DHAHRAN
 SOFTWARE BY : GEOSTAT SYSTEMS, MONTREAL

(D58)



ABU TARTUR PHOSPHATE DEPOSIT
RESULTS OF BLOCK KRIGING

(Z = 365.5)

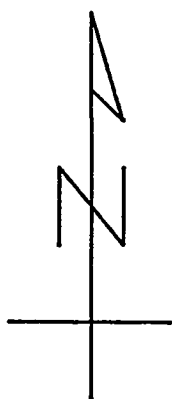
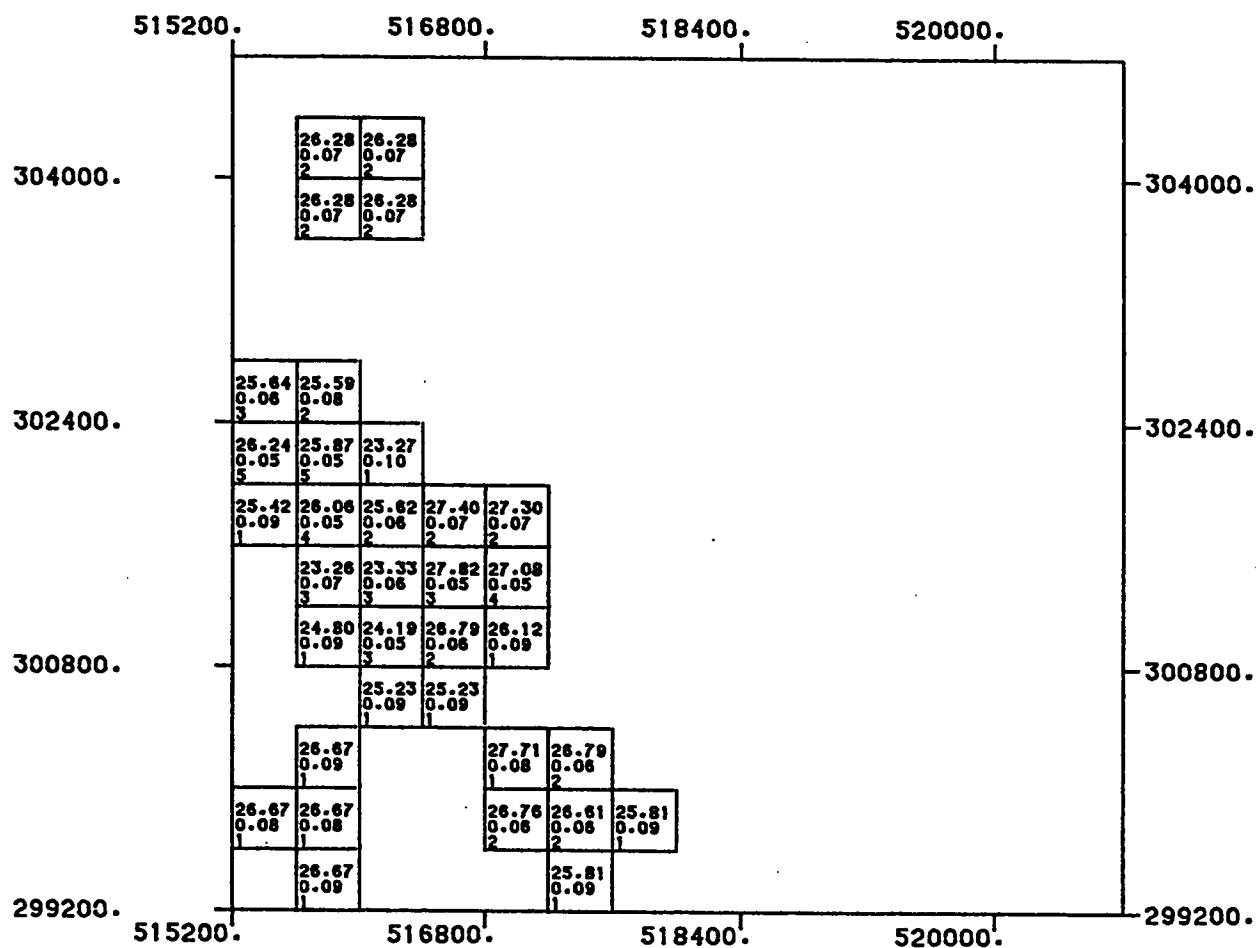
LEVEL NUMBER : 94

800.0 0.0 800.0 1600.0



SCALE OF MAP

DATA PROCESSED AT: U P M - D P C , DHAHRAN
 SOFTWARE BY : GEOSTAT SYSTEMS, MONTREAL



ABU TARTUR PHOSPHATE DEPOSIT
RESULTS OF BLOCK KRIGING

(Z = 366.5)

LEVEL NUMBER : 95

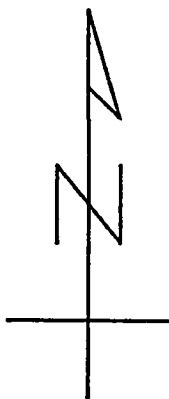
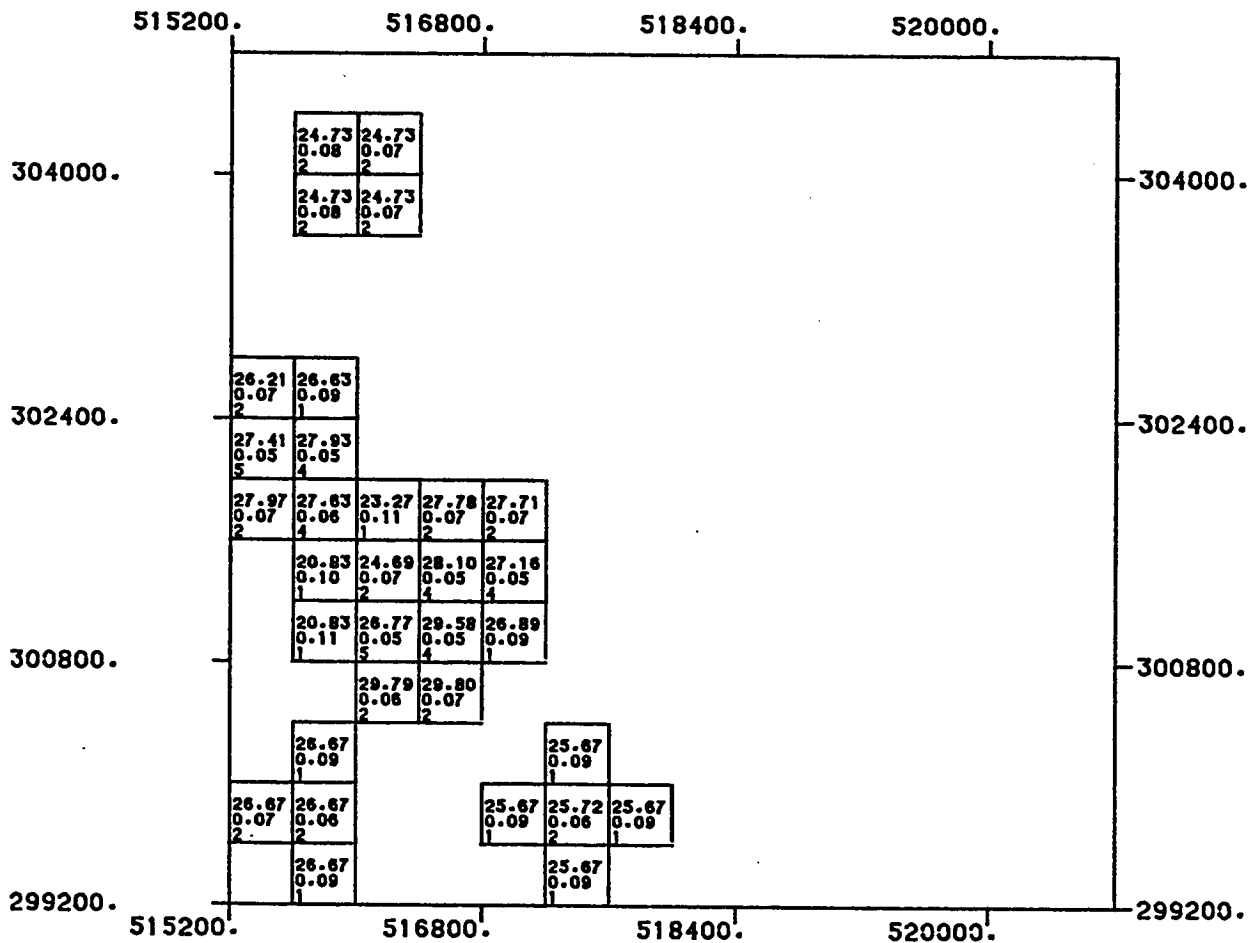
800.0 0.0 800.0 1600.0



SCALE OF MAP

DATA PROCESSED AT: U P M - D P C , DHAHRAN
SOFTWARE BY : GEOSTAT SYSTEMS, MONTREAL

(D60)



ABU TARTUR PHOSPHATE DEPOSIT
RESULTS OF BLOCK KRIGING

(Z = 367.5)

LEVEL NUMBER : 96

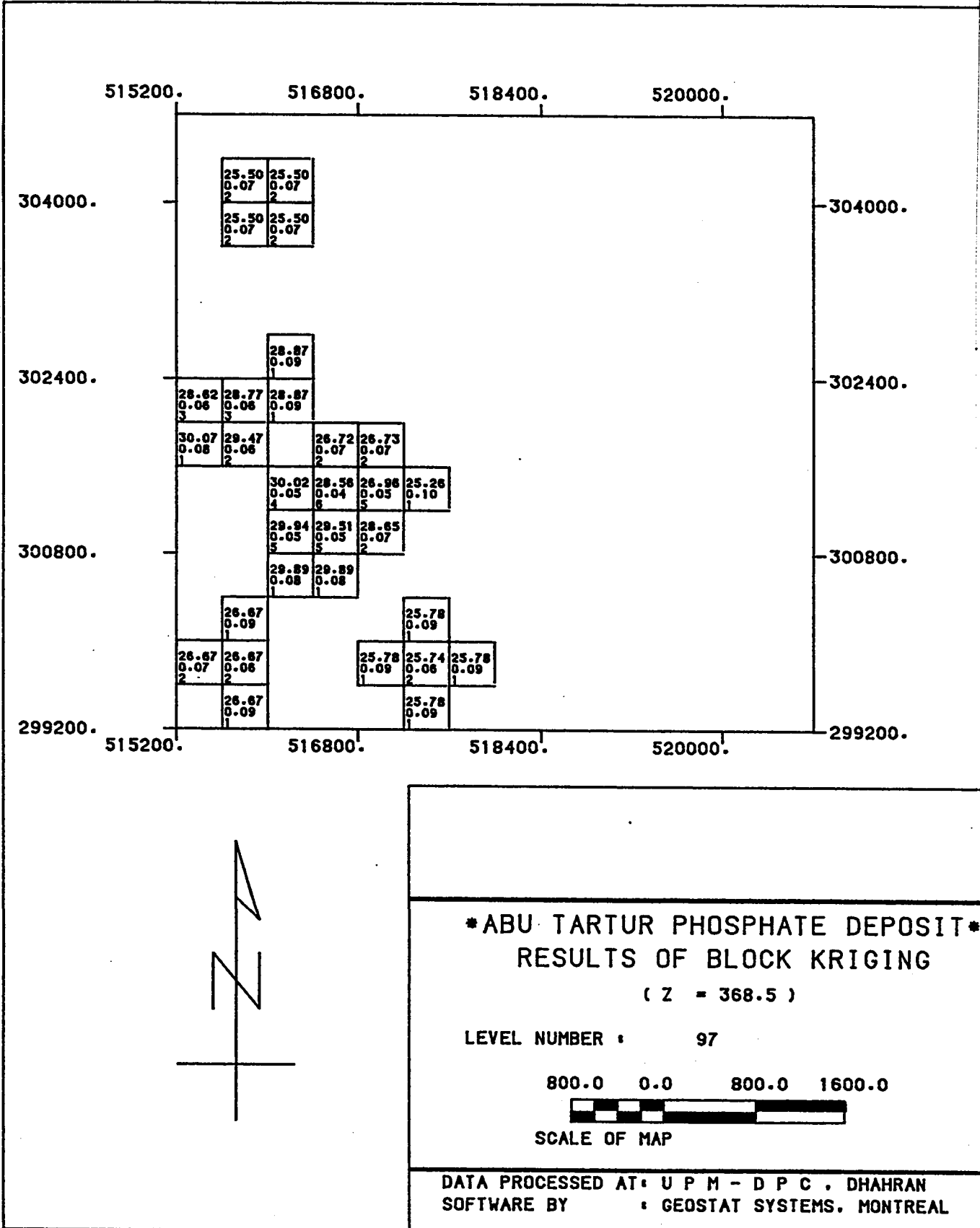
800.0 0.0 800.0 1600.0



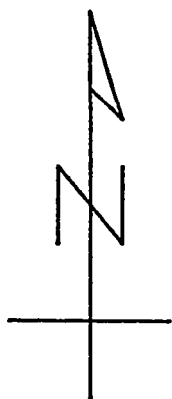
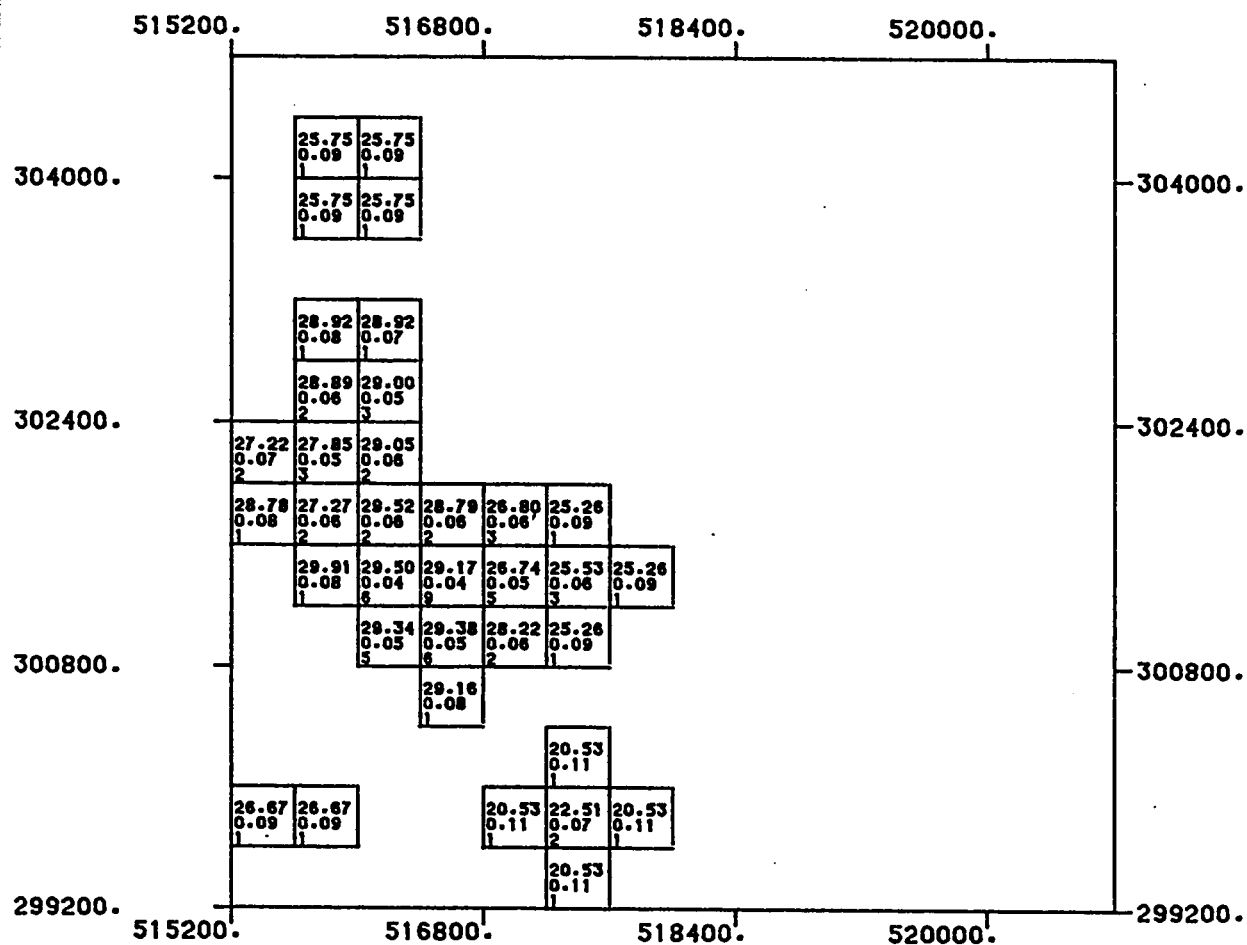
SCALE OF MAP

DATA PROCESSED AT: U P M - D P C , DHAHRAN
 SOFTWARE BY : GEOSTAT SYSTEMS, MONTREAL

(D61)



(D62)



ABU TARTUR PHOSPHATE DEPOSIT
RESULTS OF BLOCK KRIGING

(Z = 369.5)

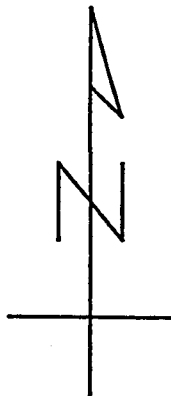
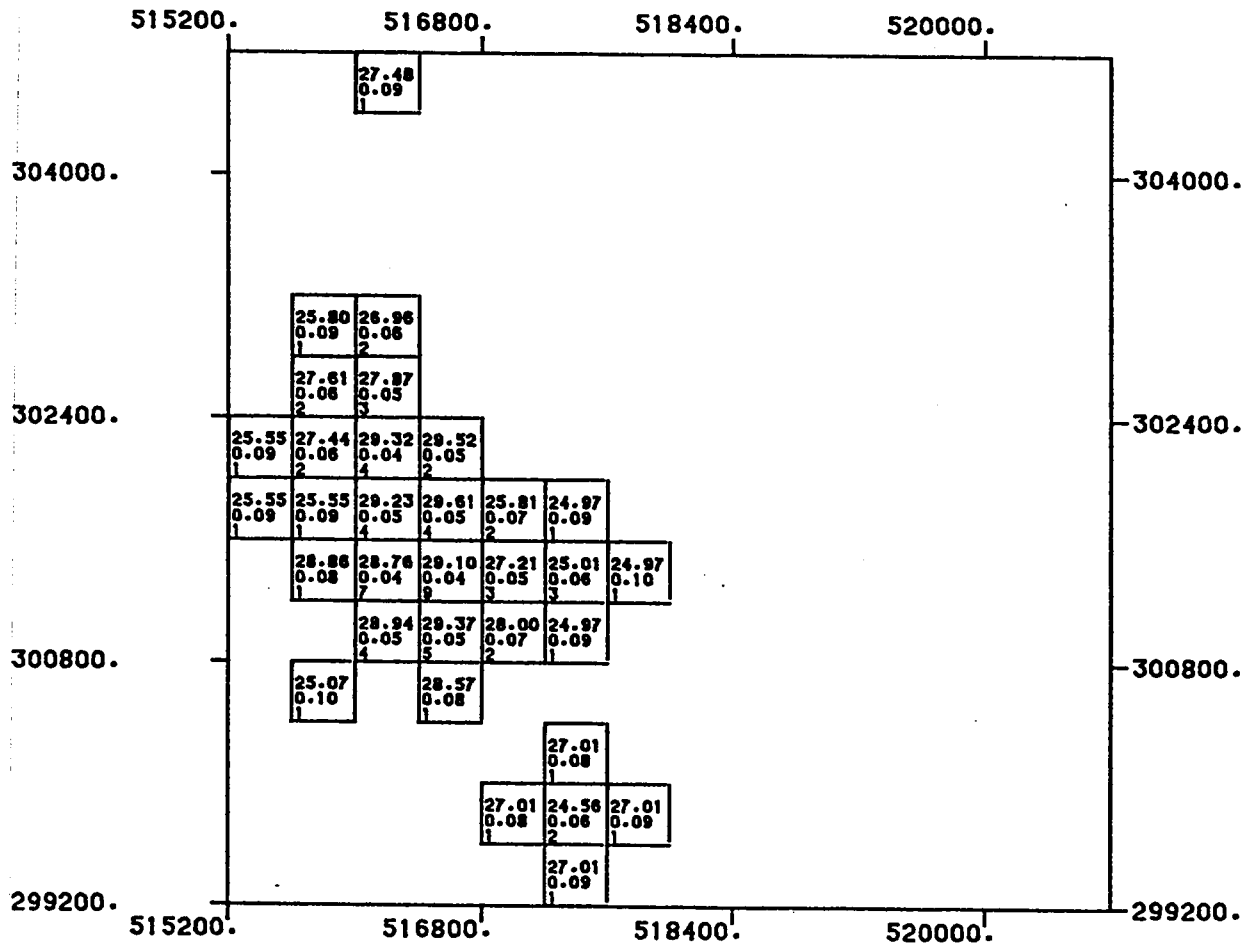
LEVEL NUMBER : 98

800.0 0.0 800.0 1600.0



SCALE OF MAP

DATA PROCESSED AT: U P M - D P C , DHAHRAN
 SOFTWARE BY : GEOSTAT SYSTEMS, MONTREAL



ABU TARTUR PHOSPHATE DEPOSIT
RESULTS OF BLOCK KRIGING

(Z = 370.5)

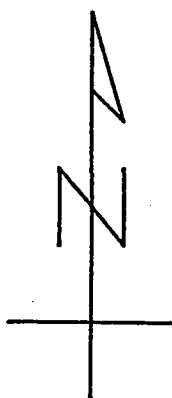
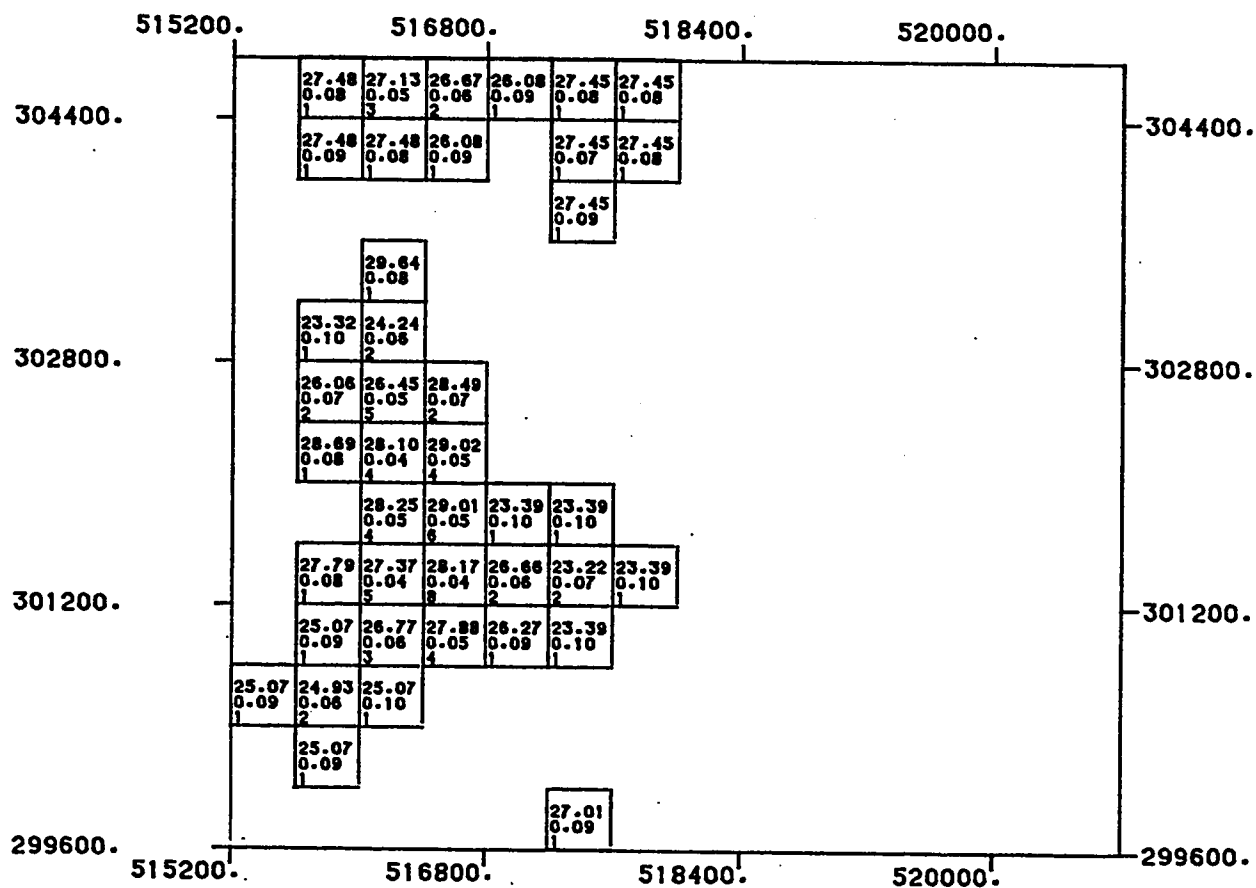
LEVEL NUMBER : 99

800.0 0.0 800.0 1600.0



SCALE OF MAP

DATA PROCESSED AT: U P M - D P C , DHAHRAN
SOFTWARE BY : GEOSTAT SYSTEMS, MONTREAL



ABU TARTUR PHOSPHATE DEPOSIT
RESULTS OF BLOCK KRIGING
(Z = 371.5)

LEVEL NUMBER : 100

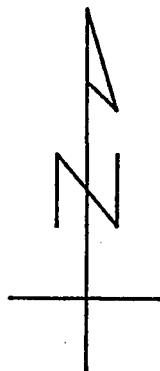
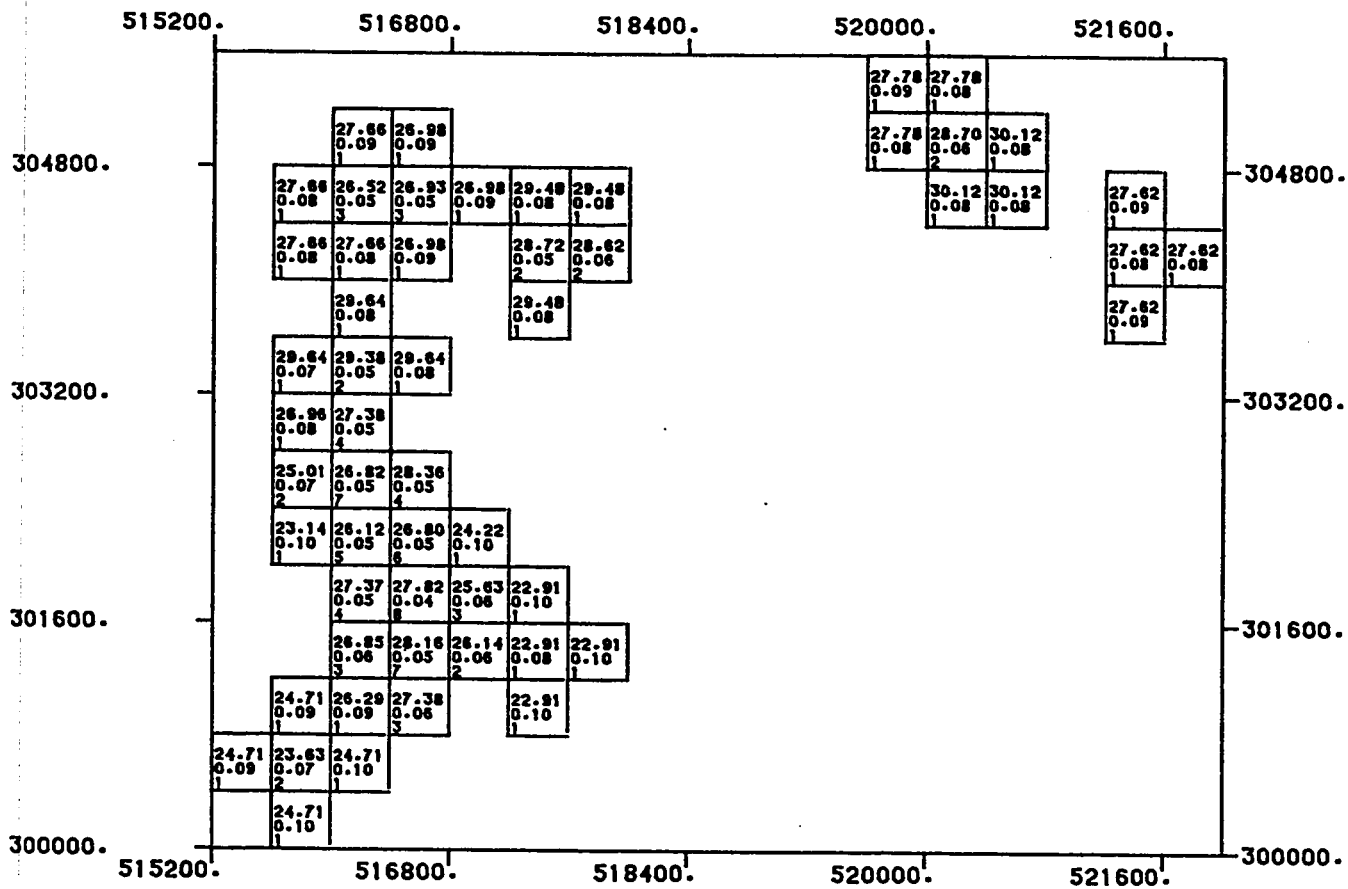
800.0 0.0 800.0 1600.0



SCALE OF MAP

DATA PROCESSED AT: U P M - D P C , DHAHRAN
SOFTWARE BY : GEOSTAT SYSTEMS, MONTREAL

(D65)



ABU TARTUR PHOSPHATE DEPOSIT
RESULTS OF BLOCK KRIGING

(Z = 372.5)

LEVEL NUMBER : 101

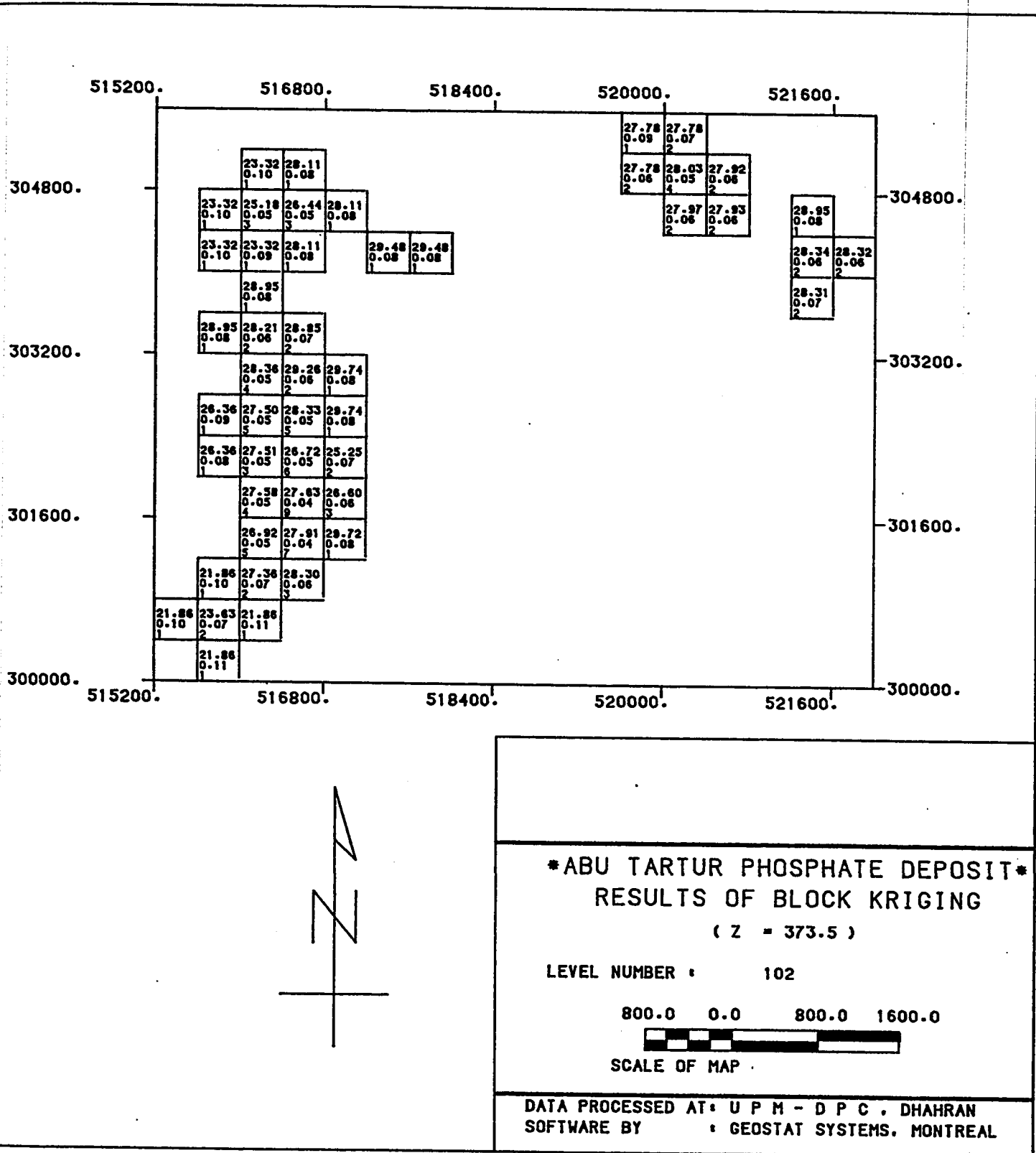
800.0 0.0 800.0 1600.0

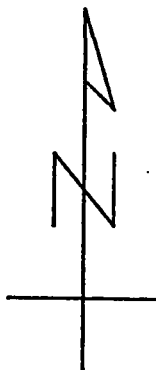
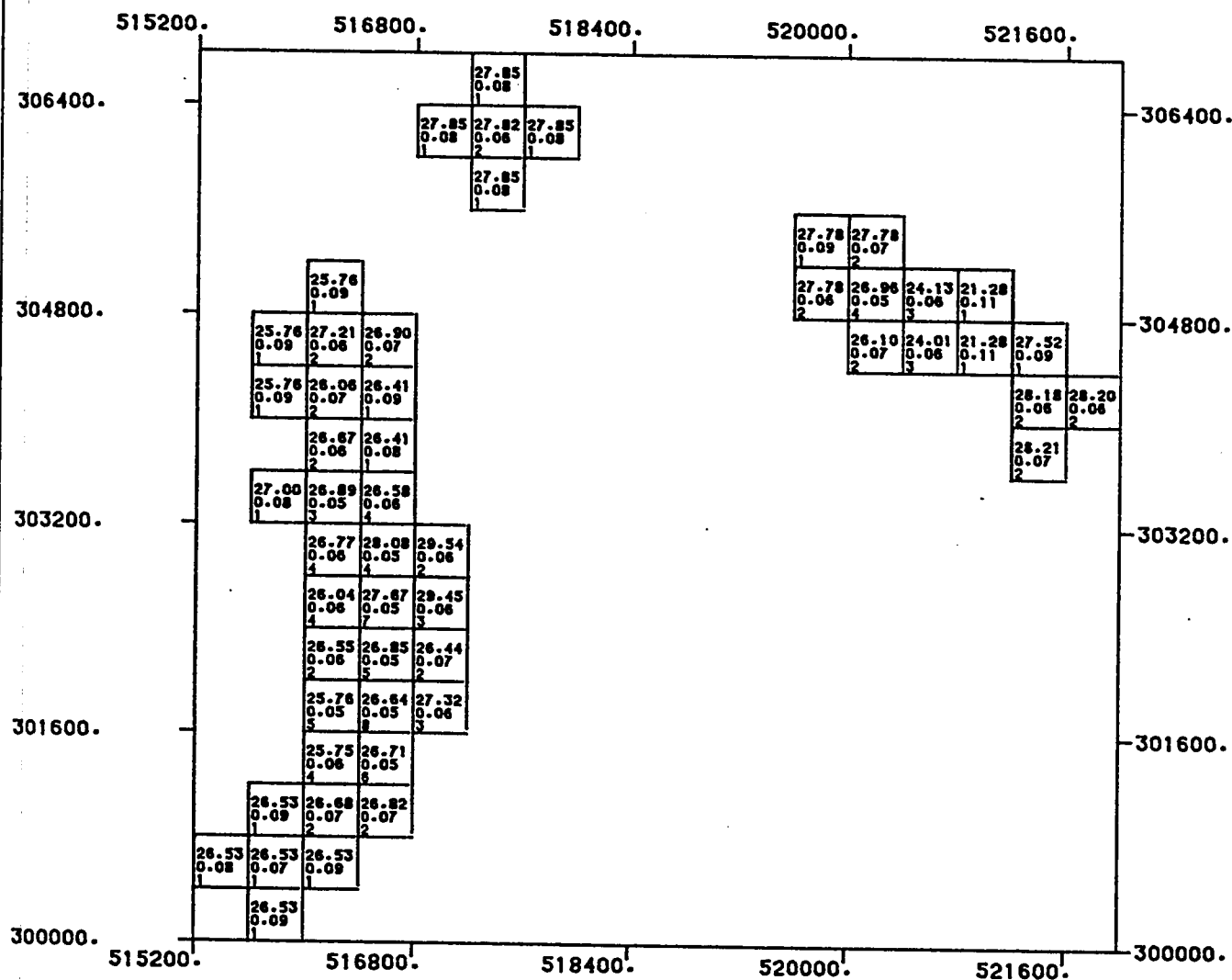


SCALE OF MAP

DATA PROCESSED AT: U P M - D P C , DHAHRAN
SOFTWARE BY : GEOSTAT SYSTEMS, MONTREAL

(D66)





ABU TARTUR PHOSPHATE DEPOSIT
RESULTS OF BLOCK KRIGING

(Z = 374.5)

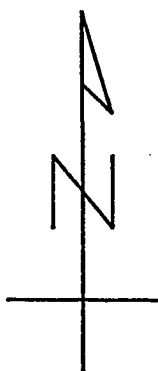
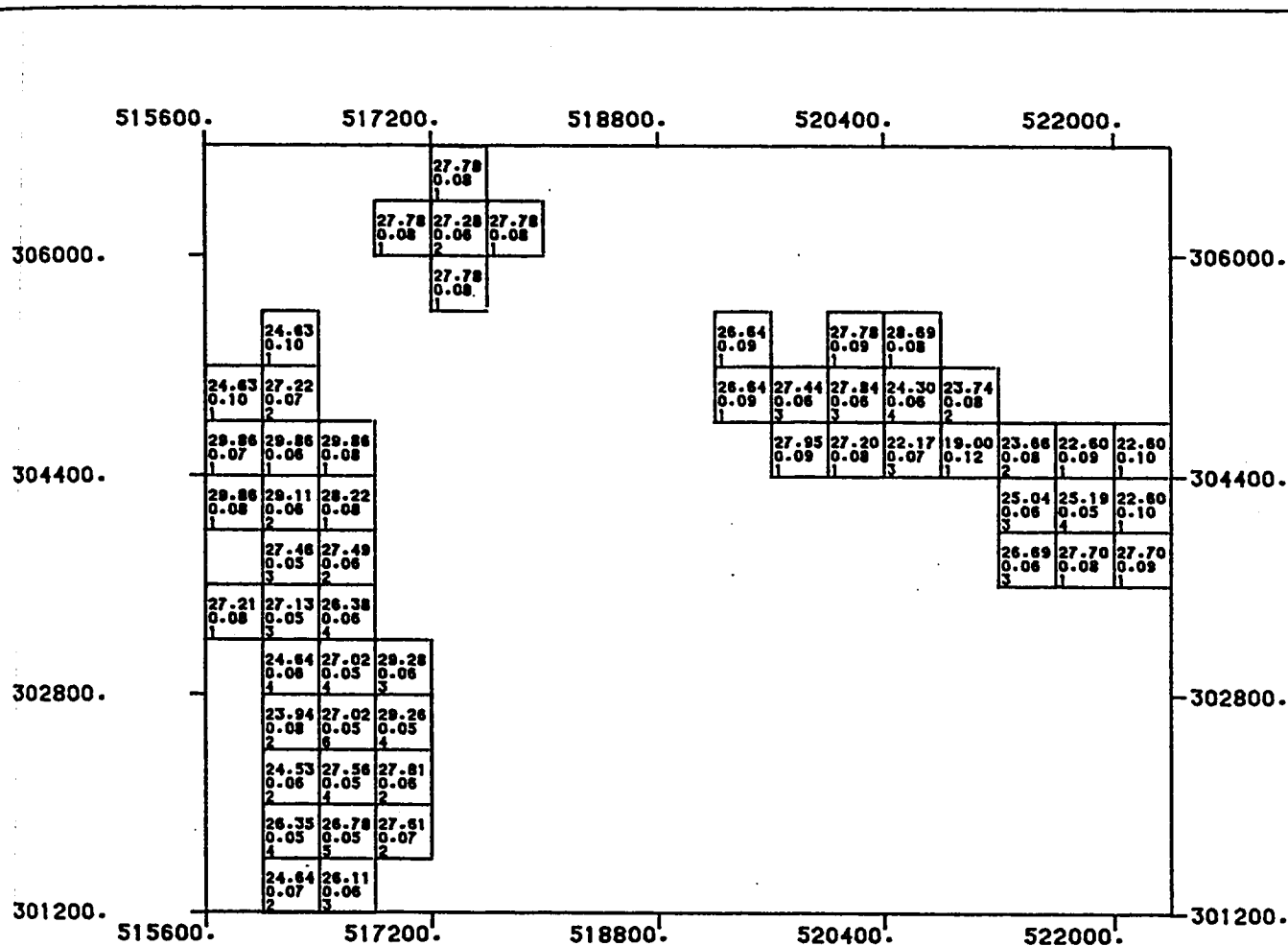
LEVEL NUMBER : 103

800.0 0.0 800.0 1600.0



SCALE OF MAP

DATA PROCESSED AT: U P M - D P C , DHARAN
SOFTWARE BY : GEOSTAT SYSTEMS, MONTREAL



ABU TARTUR PHOSPHATE DEPOSIT

RESULTS OF BLOCK KRIGING

(Z = 375.5)

LEVEL NUMBER : 104

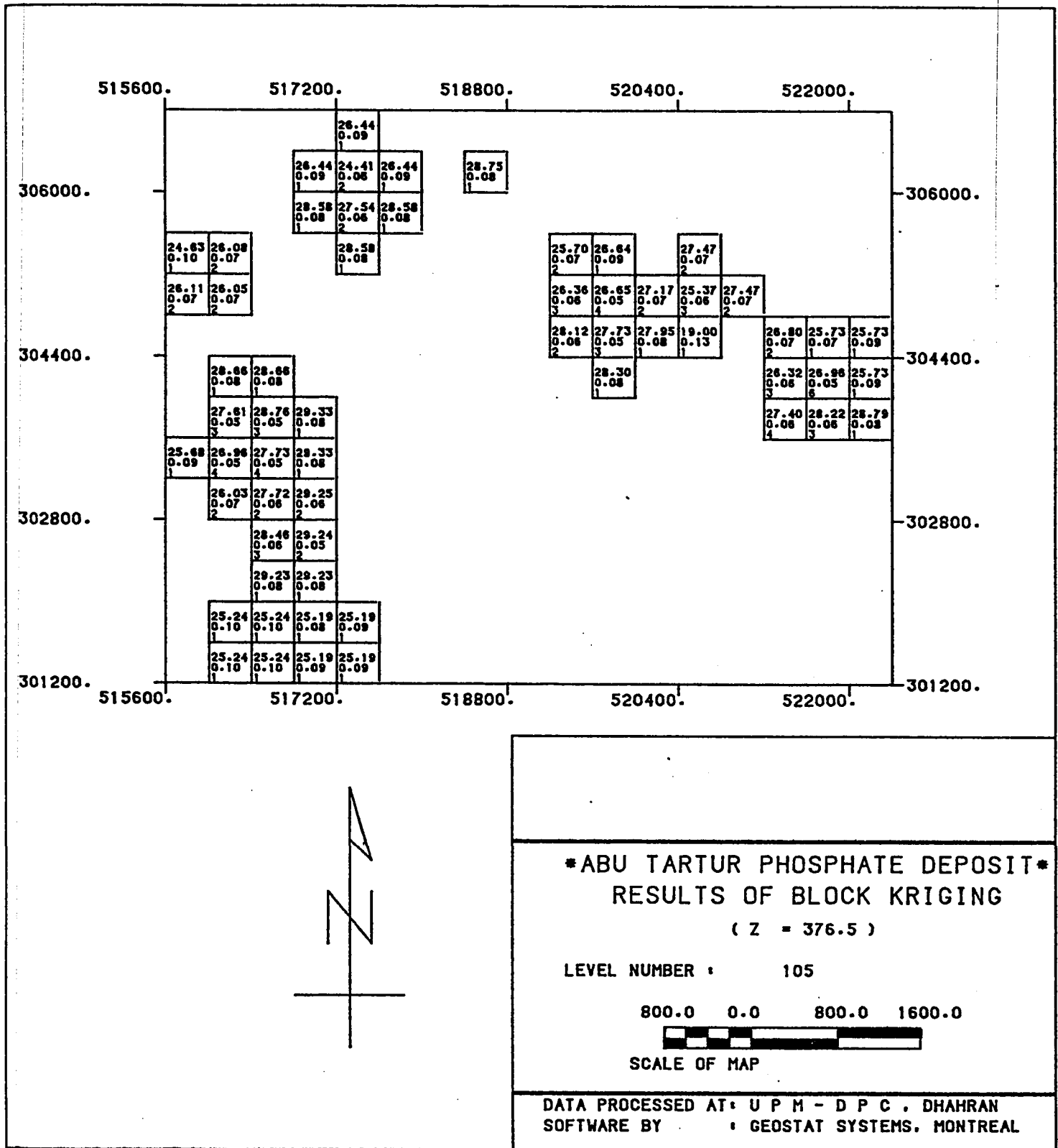
800.0 0.0 800.0 1600.0



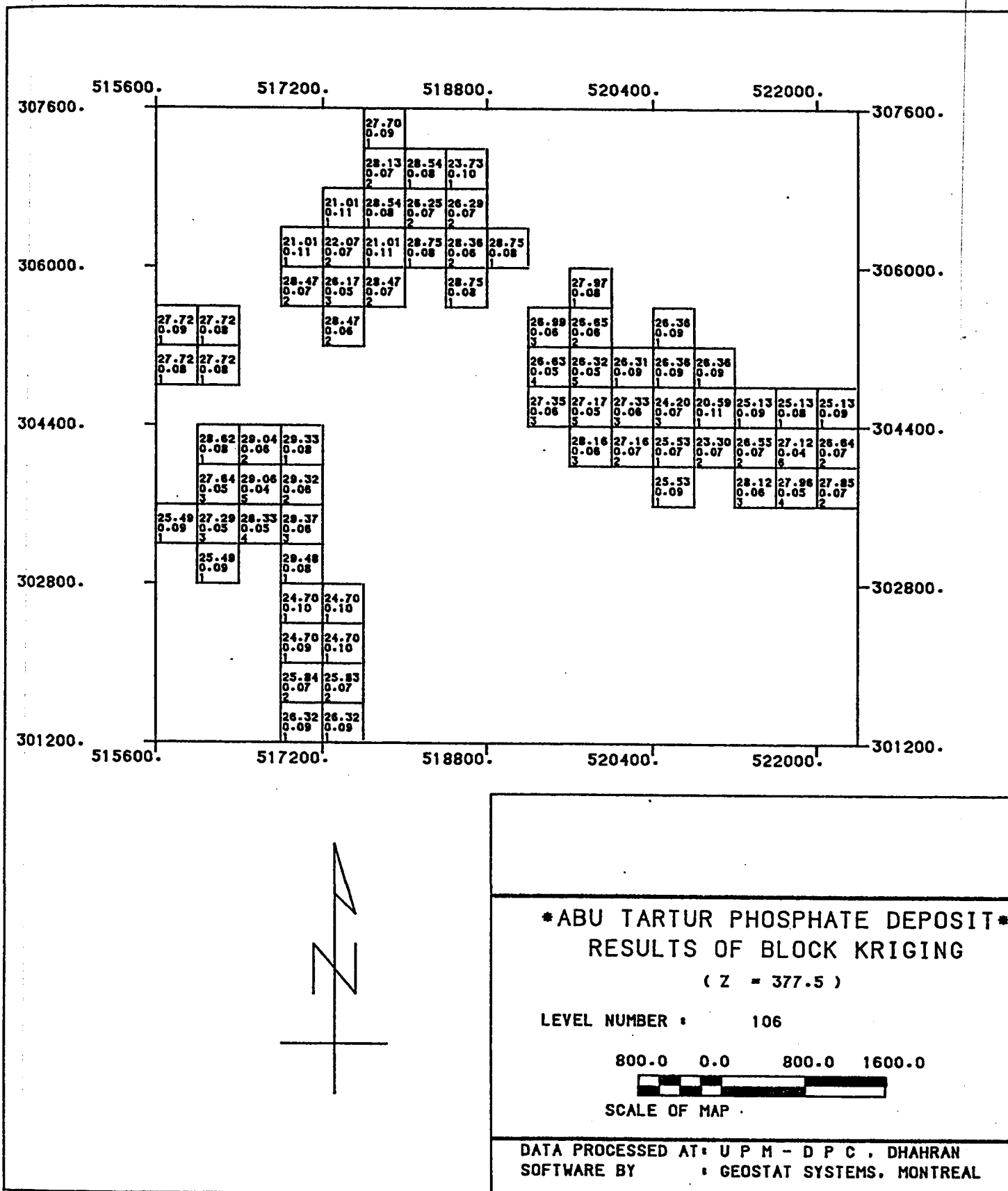
SCALE OF MAP

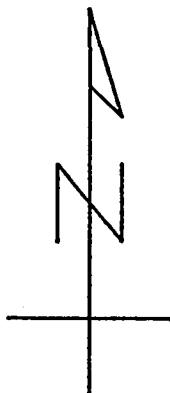
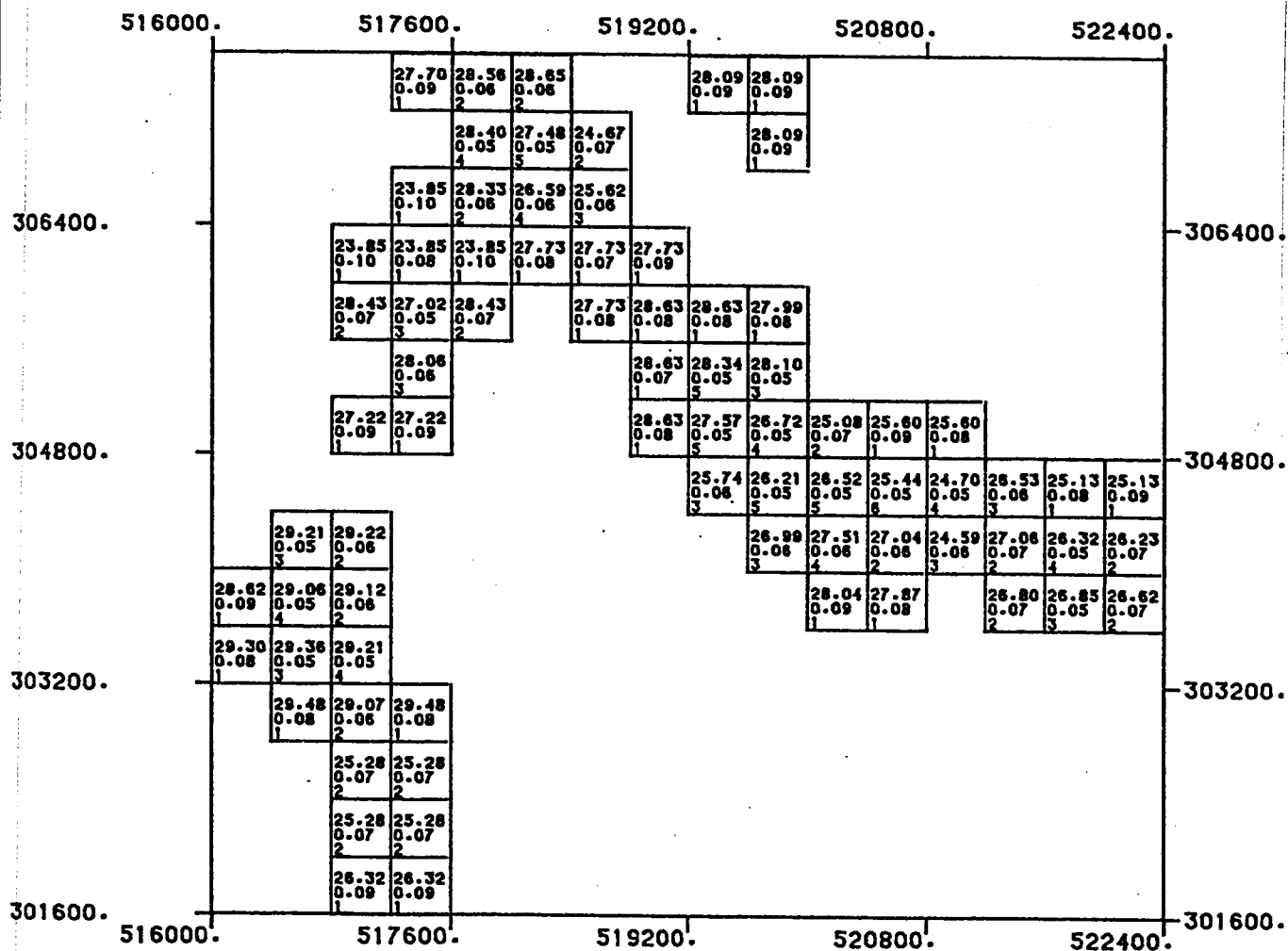
DATA PROCESSED AT: U P M - D P C , DHAHRAN
SOFTWARE BY : GEOSTAT SYSTEMS, MONTREAL

(D69)



(D70)





ABU TARTUR PHOSPHATE DEPOSIT
RESULTS OF BLOCK KRIGING

(Z = 378.5)

LEVEL NUMBER : 107

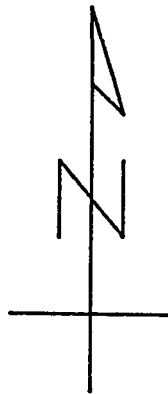
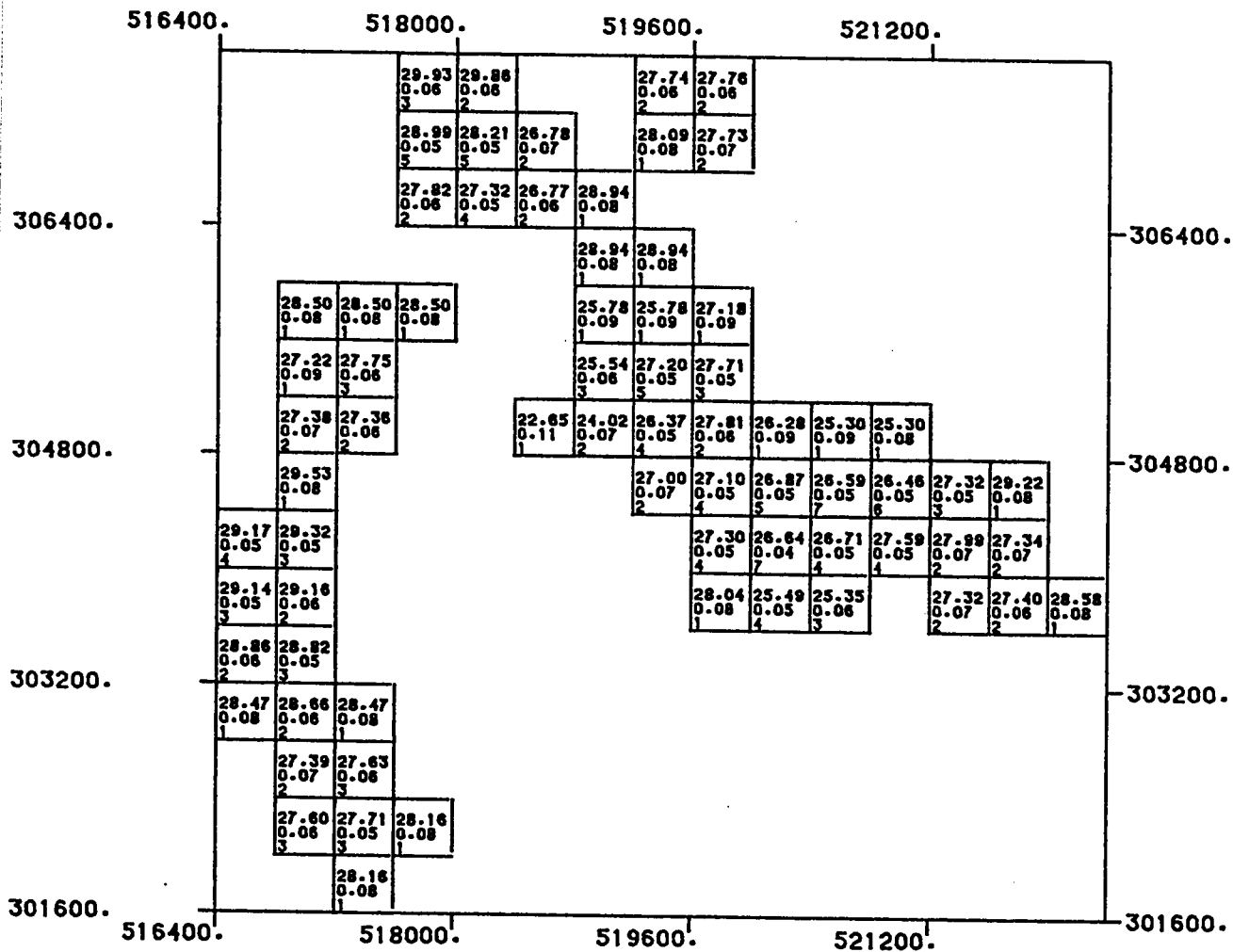
800.0 0.0 800.0 1600.0



SCALE OF MAP

DATA PROCESSED AT: U P M - D P C , DHAHRAN
SOFTWARE BY : GEOSTAT SYSTEMS, MONTREAL

(D72)



ABU TARTUR PHOSPHATE DEPOSIT
RESULTS OF BLOCK KRIGING

(Z = 379.5)

LEVEL NUMBER : 108

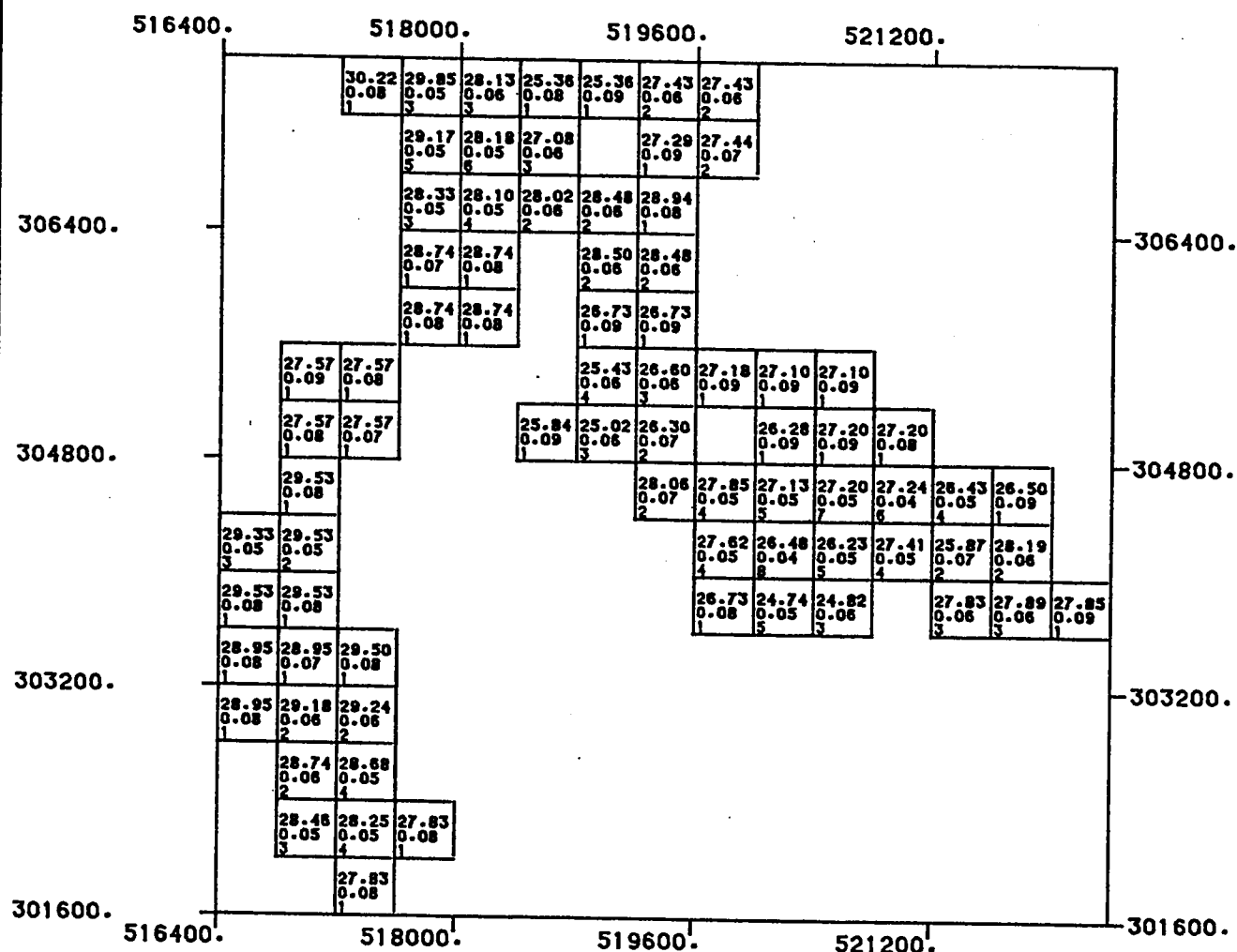
800.0 0.0 800.0 1600.0



SCALE OF MAP

DATA PROCESSED AT: U P M - D P C , DHAHRAN
SOFTWARE BY : GEOSTAT SYSTEMS, MONTREAL

(D73)



ABU TARTUR PHOSPHATE DEPOSIT
RESULTS OF BLOCK KRIGING

(Z = 380.5)

LEVEL NUMBER : 109

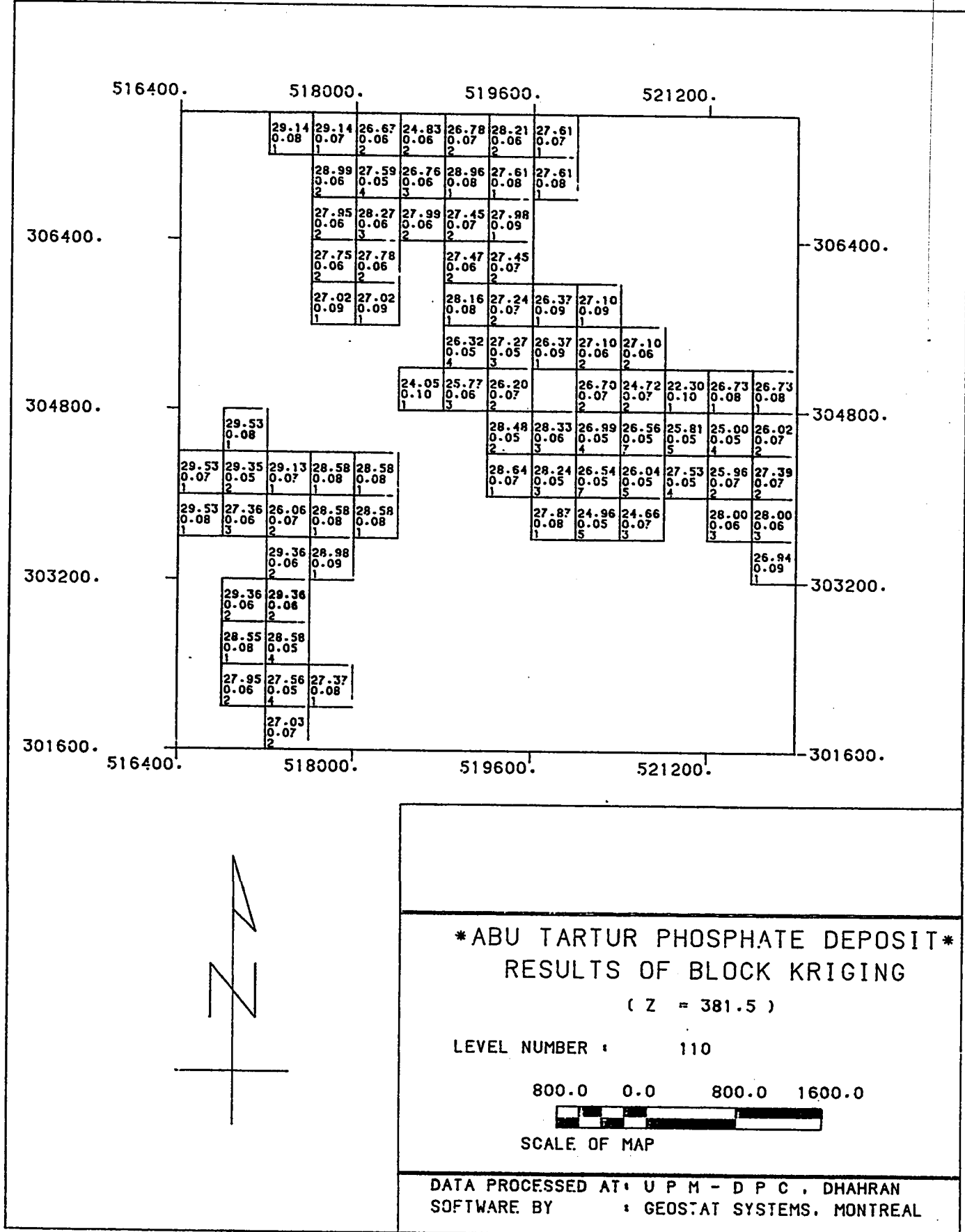
800.0 0.0 800.0 1600.0

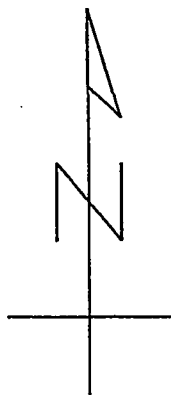
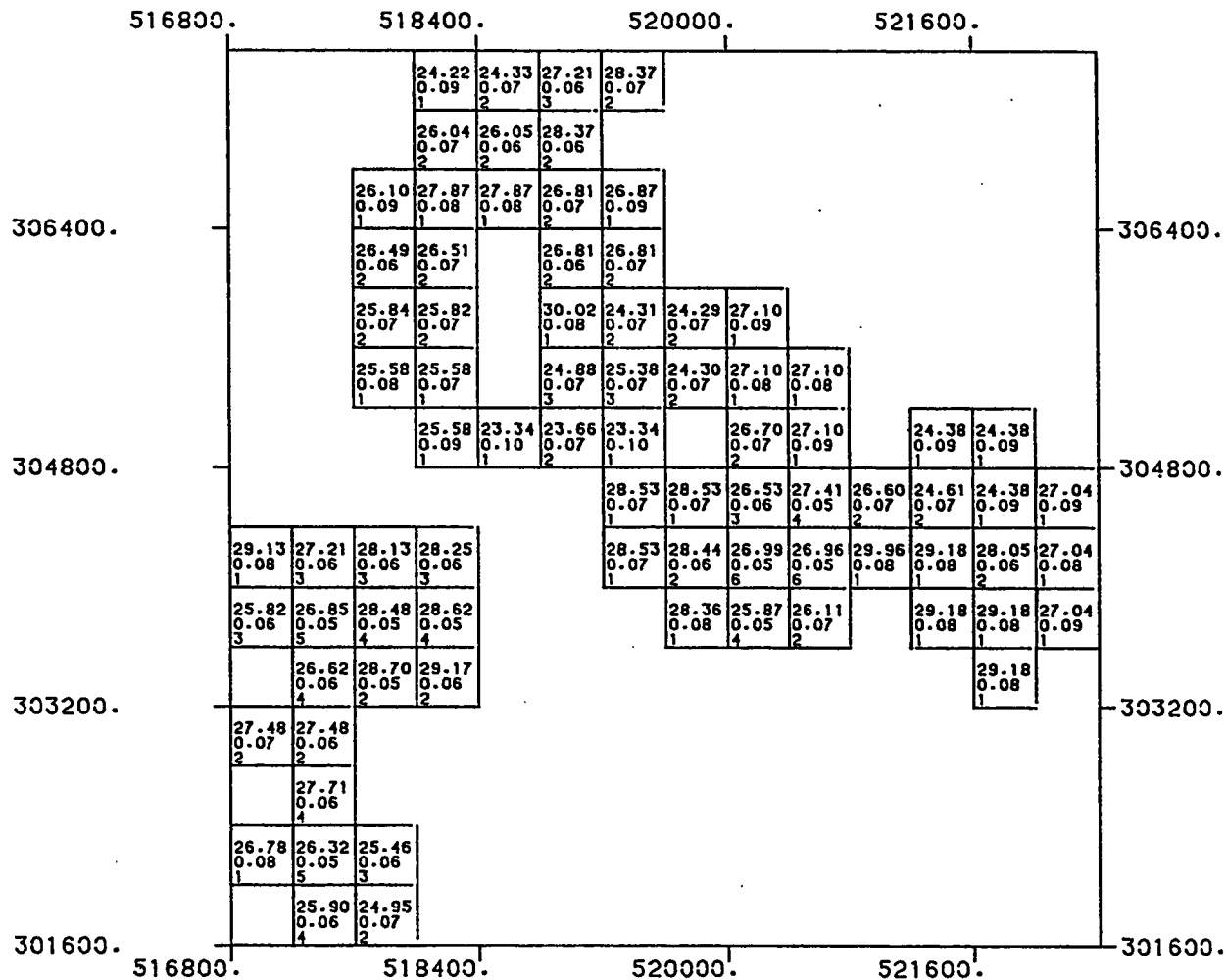


SCALE OF MAP

DATA PROCESSED AT: U P M - D P C , DHAHRAN
SOFTWARE BY : GEOSTAT SYSTEMS, MONTREAL

(D74)





ABU TARTUR PHOSPHATE DEPOSIT
RESULTS OF BLOCK KRIGING

(Z = 382.5)

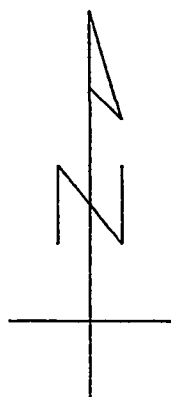
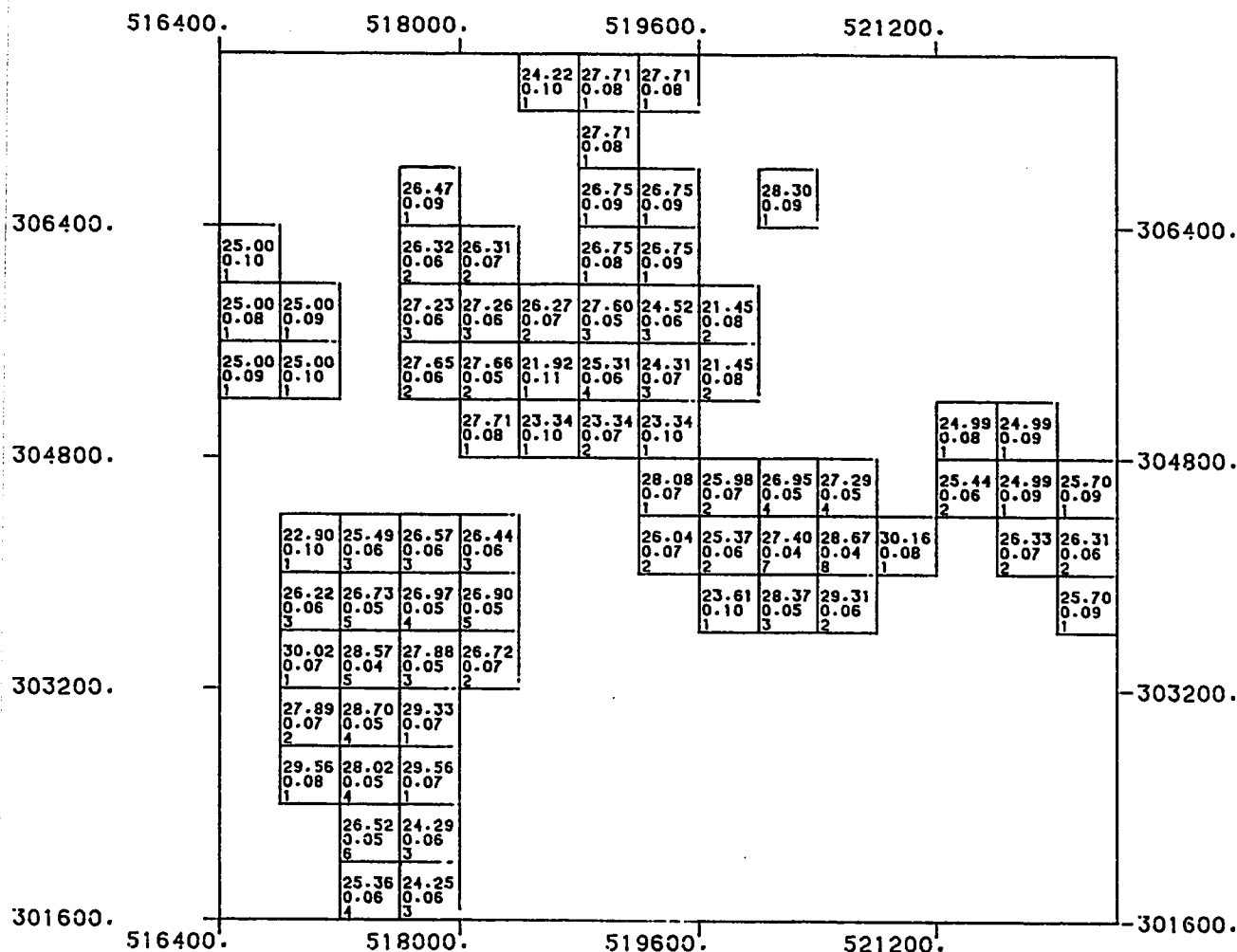
LEVEL NUMBER : 111

800.0 0.0 800.0 1600.0



SCALE OF MAP

DATA PROCESSED AT: U P M - D P C , DHAHRAN
SOFTWARE BY : GEOSTAT SYSTEMS, MONTREAL



ABU TARTUR PHOSPHATE DEPOSIT
RESULTS OF BLOCK KRIGING

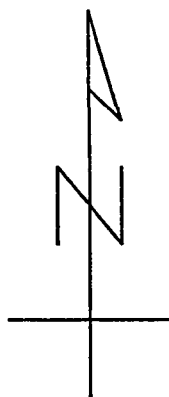
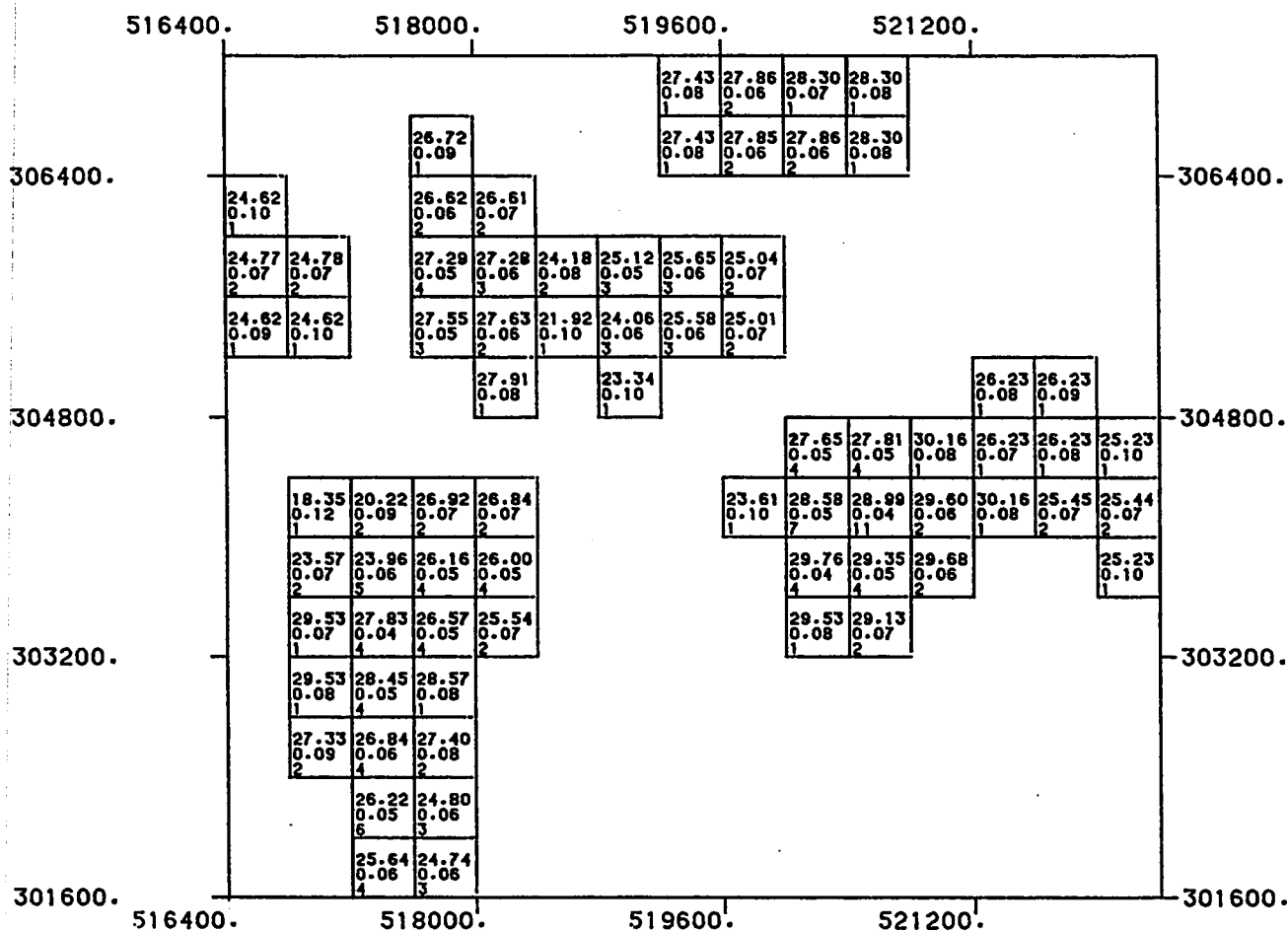
(Z = 383.5)

LEVEL NUMBER : 112

800.0	0.0	800.0	1600.0
-------	-----	-------	--------

SCALE OF MAP

DATA PROCESSED AT: U P M - D P C , DHAHRAN
SOFTWARE BY : GEOSTAT SYSTEMS, MONTREAL



ABU TARTUR PHOSPHATE DEPOSIT
RESULTS OF BLOCK KRIGING

(Z = 384.5)

LEVEL NUMBER : 113

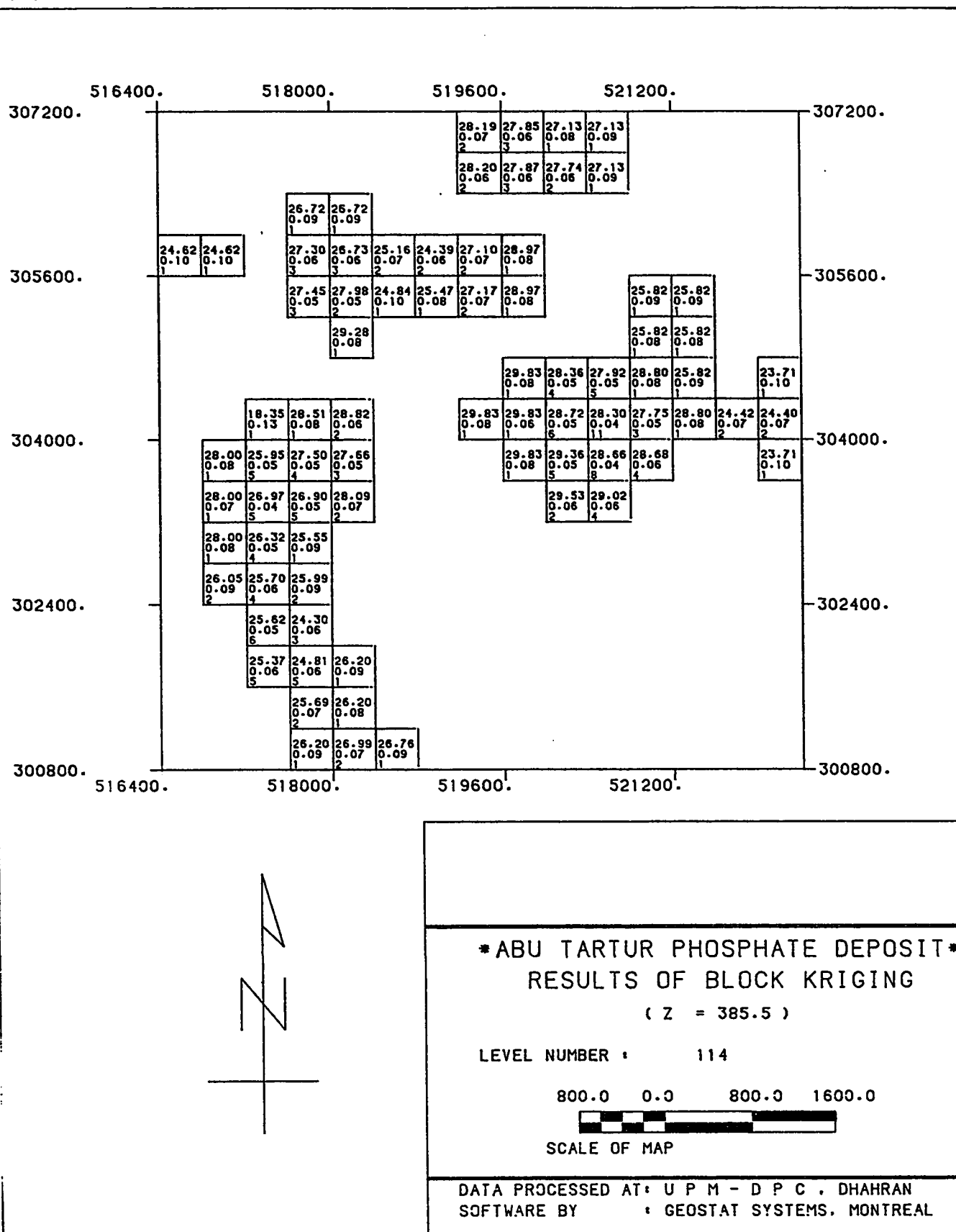
800.0 0.0 800.0 1600.0



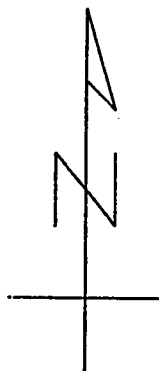
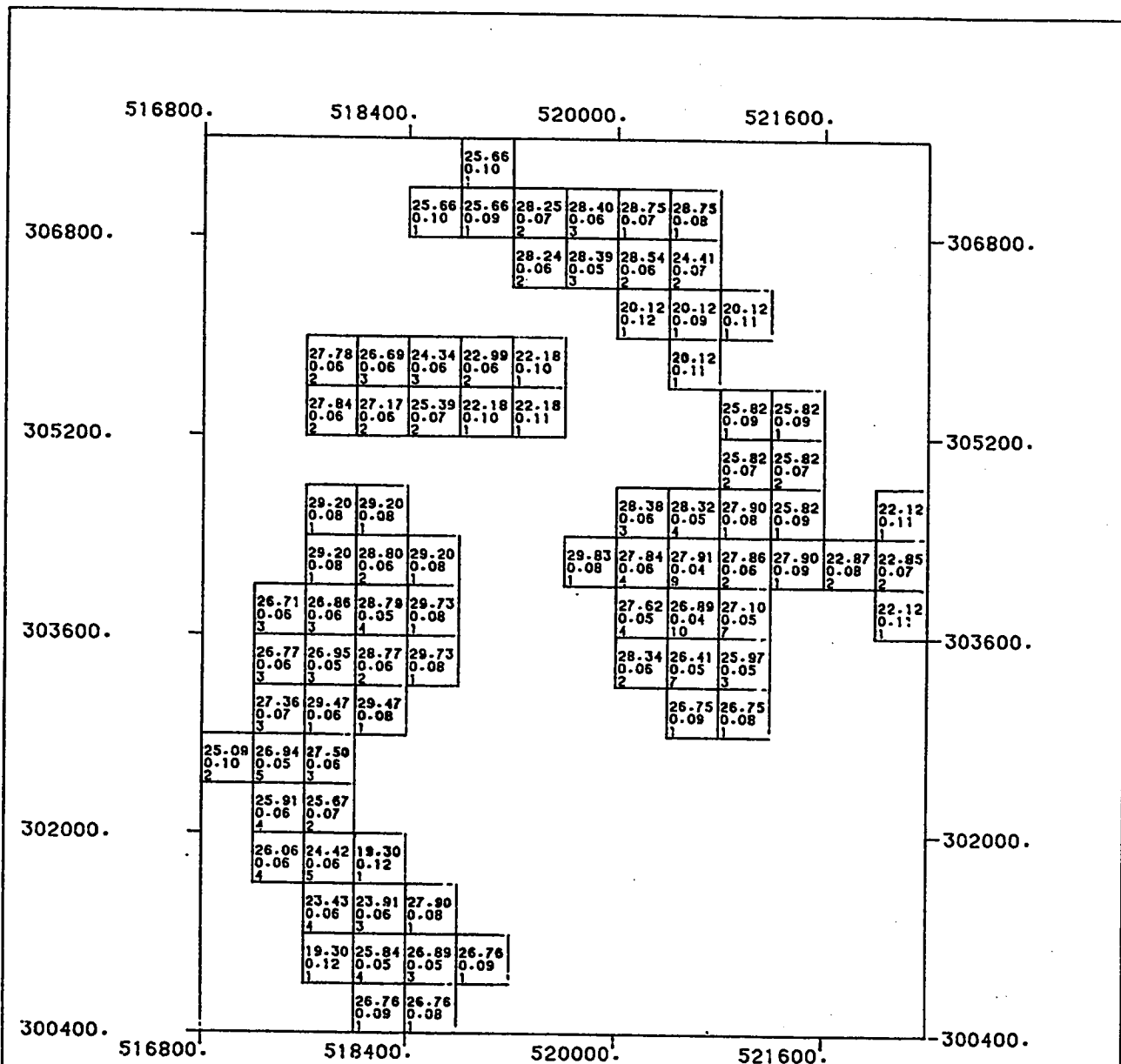
SCALE OF MAP 1:50,000

DATA PROCESSED AT: U P M - D P C , DHAHRAN
SOFTWARE BY : GEOSTAT SYSTEMS, MONTREAL

(078)



(D79)



ABU TARTUR PHOSPHATE DEPOSIT
RESULTS OF BLOCK KRIGING

(Z = 386.5)

LEVEL NUMBER : 115

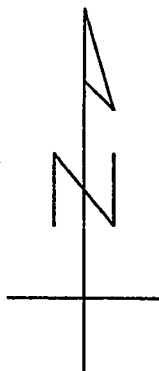
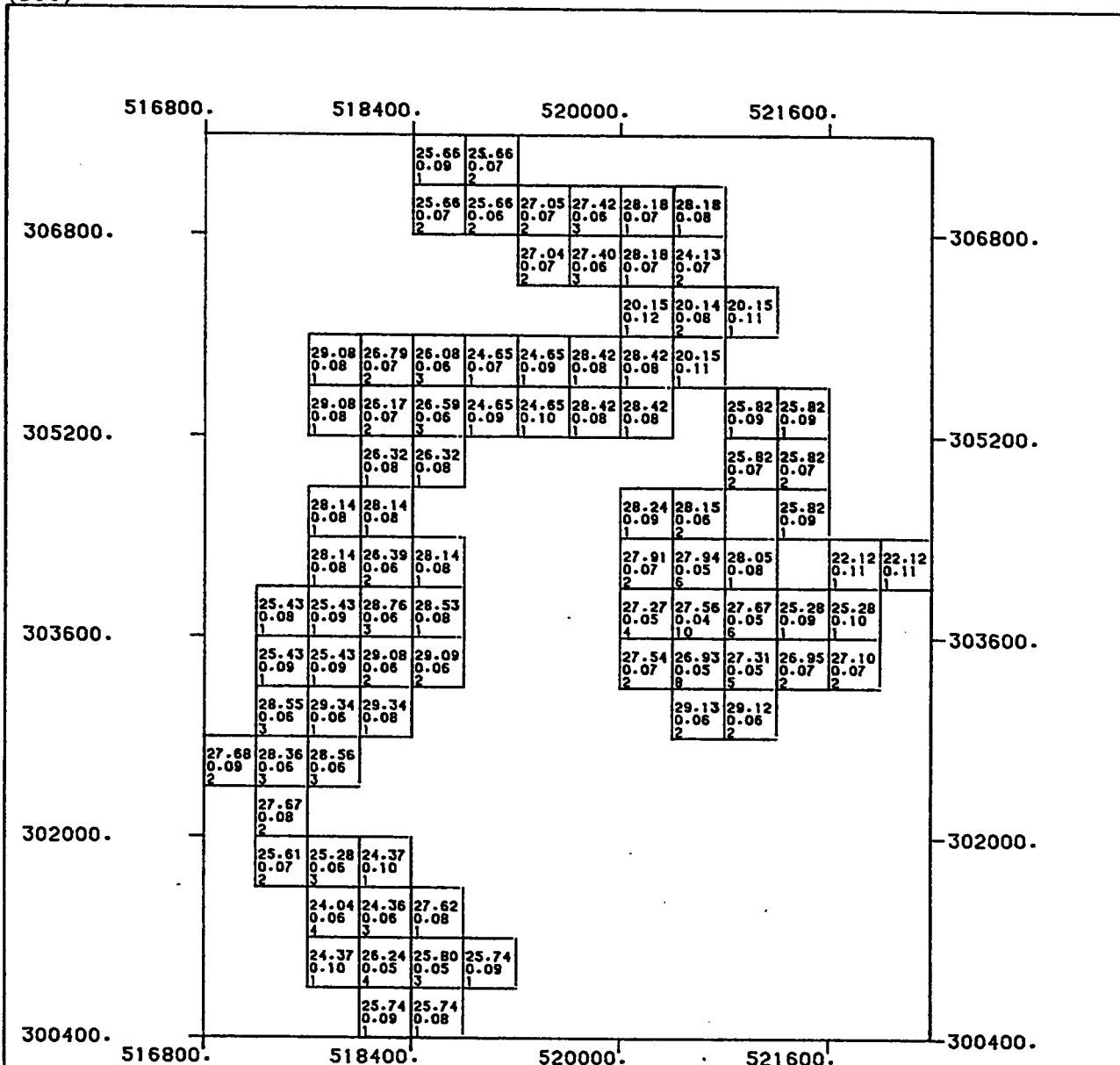
800.0 0.0 800.0 1600.0



SCALE OF MAP

DATA PROCESSED AT: U P M - D P C , DHAHRAN
SOFTWARE BY : GEOSTAT SYSTEMS, MONTREAL

(D80)



ABU TARTUR PHOSPHATE DEPOSIT
RESULTS OF BLOCK KRIGING

(Z = 387.5)

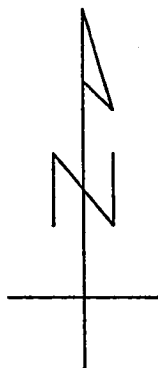
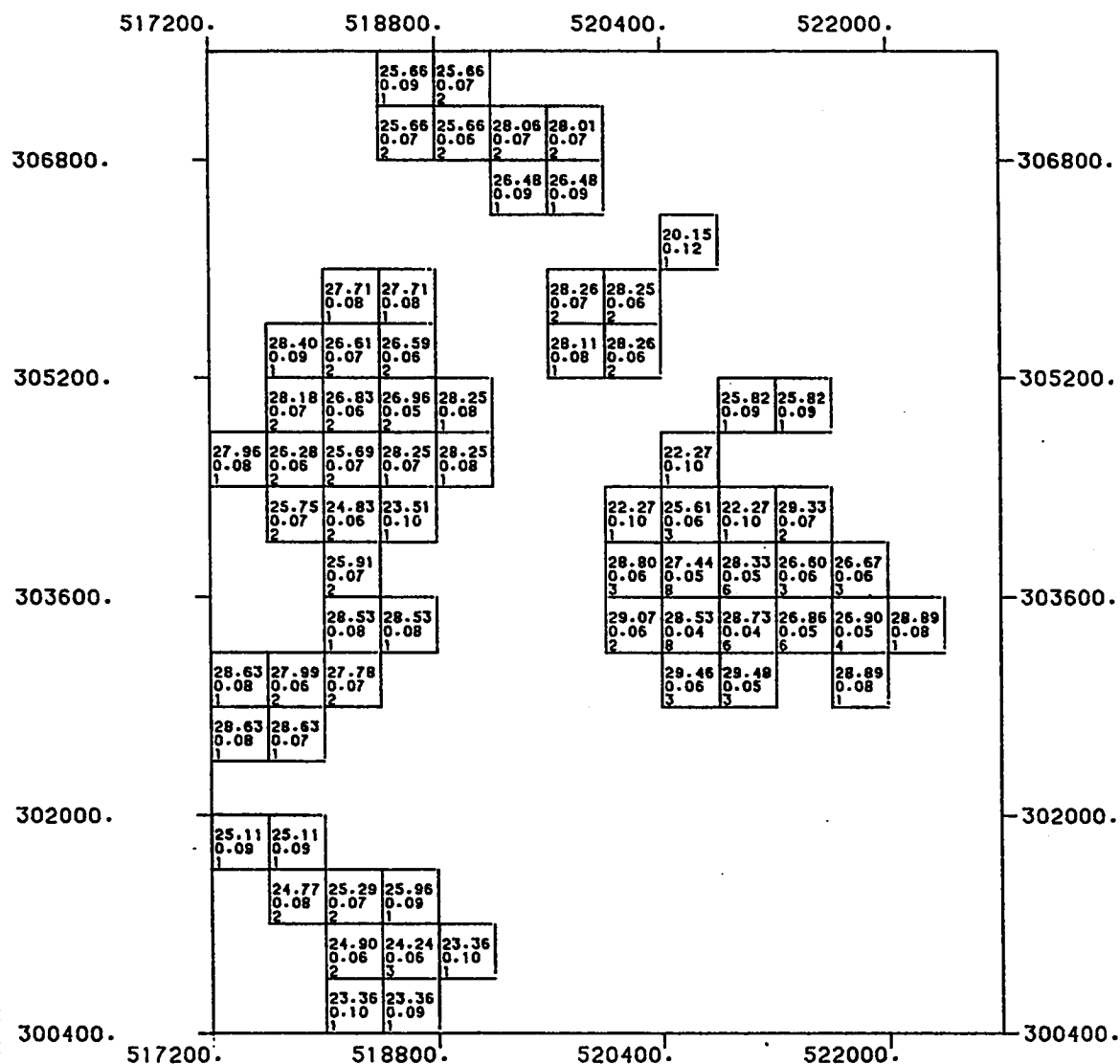
LEVEL NUMBER : 116

800.0 0.0 800.0 1600.0



SCALE OF MAP

DATA PROCESSED AT: U P M - D P C , DHAHRAN
SOFTWARE BY : GEOSTAT SYSTEMS, MONTREAL



ABU TARTUR PHOSPHATE DEPOSIT
RESULTS OF BLOCK KRIGING

(Z = 388.5)

LEVEL NUMBER : 117

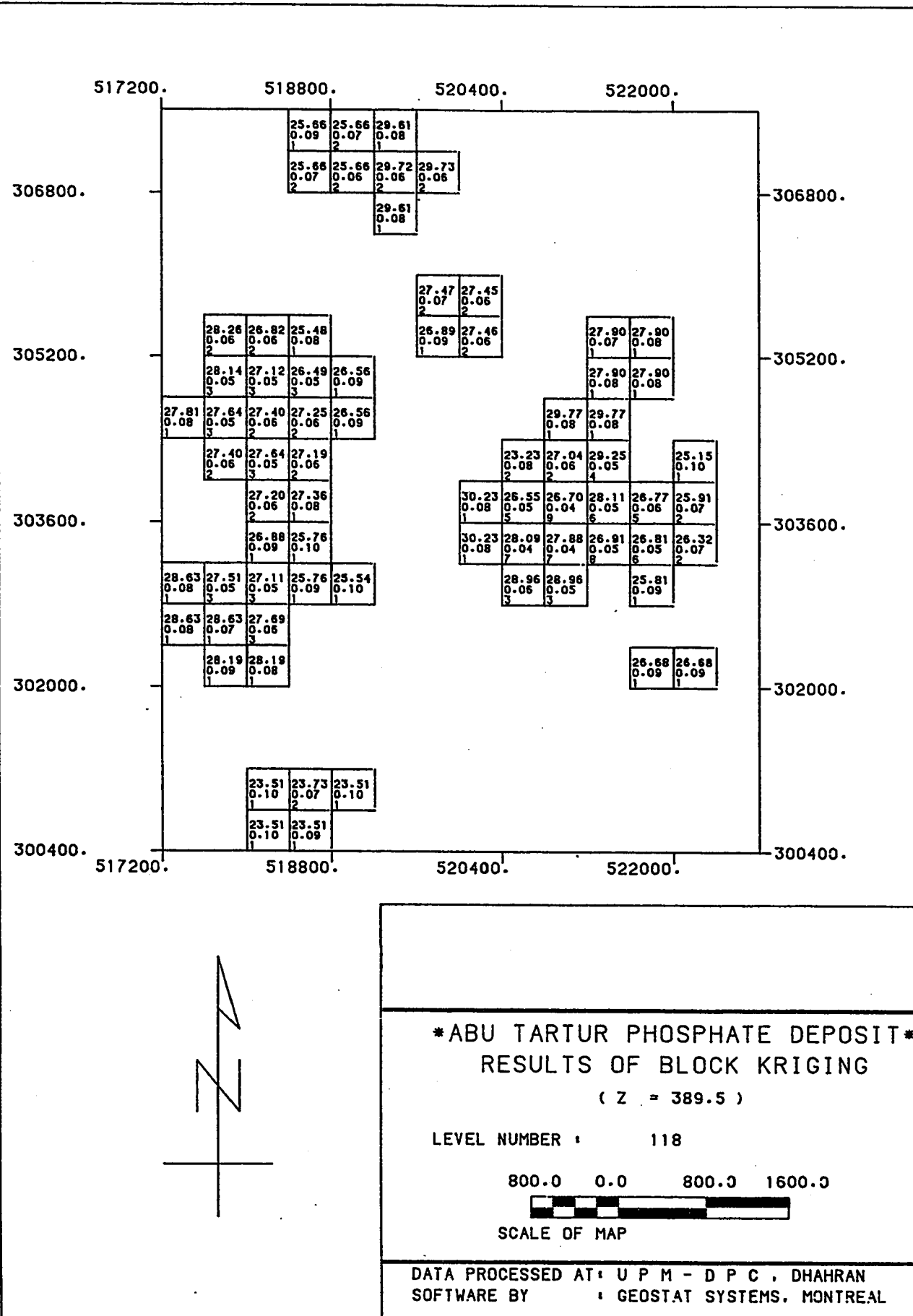
800.0 0.0 800.0 1600.0



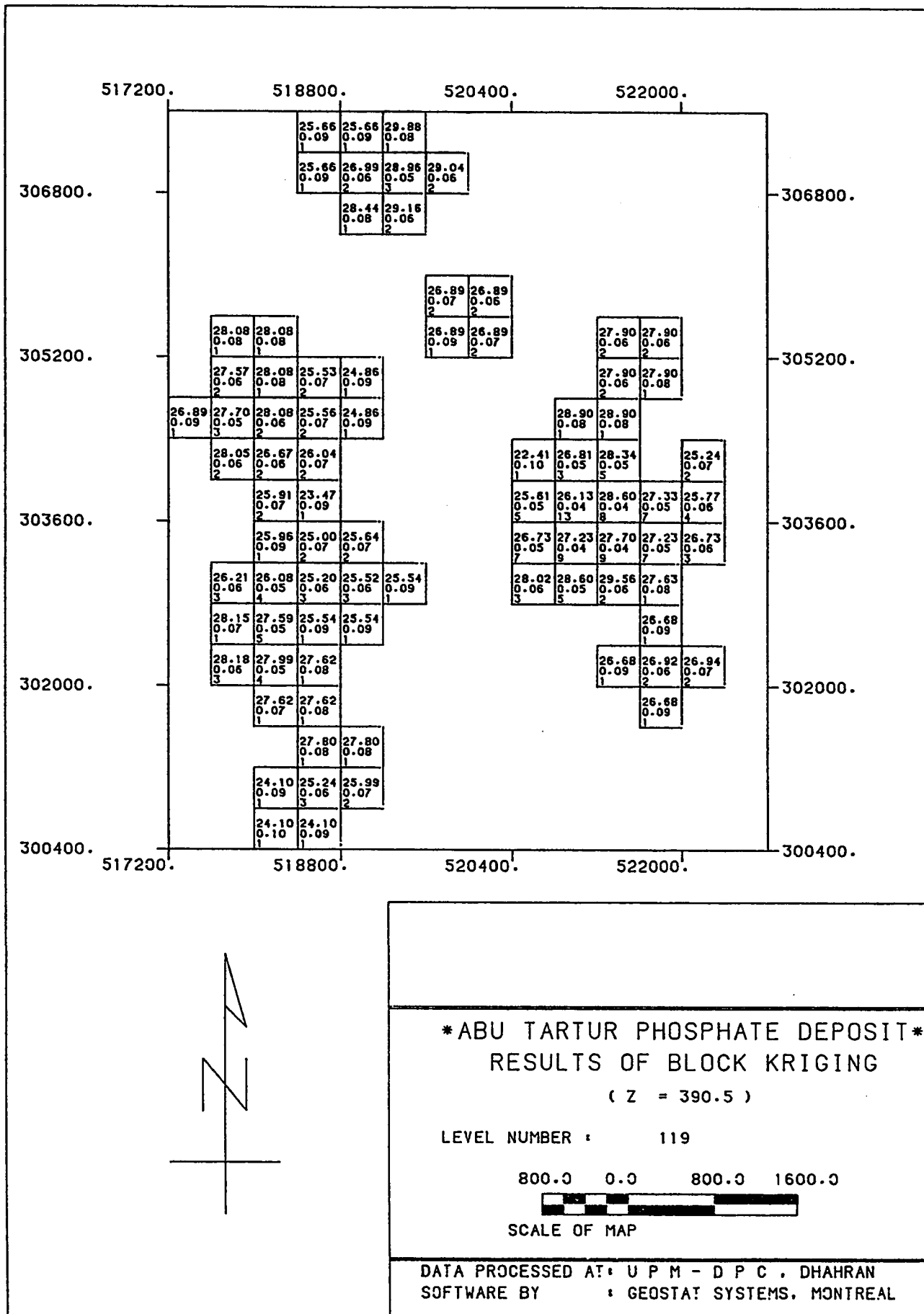
SCALE OF MAP

DATA PROCESSED AT: U P M - D P C , DHAHRAN
SOFTWARE BY : GEOSTAT SYSTEMS, MONTREAL

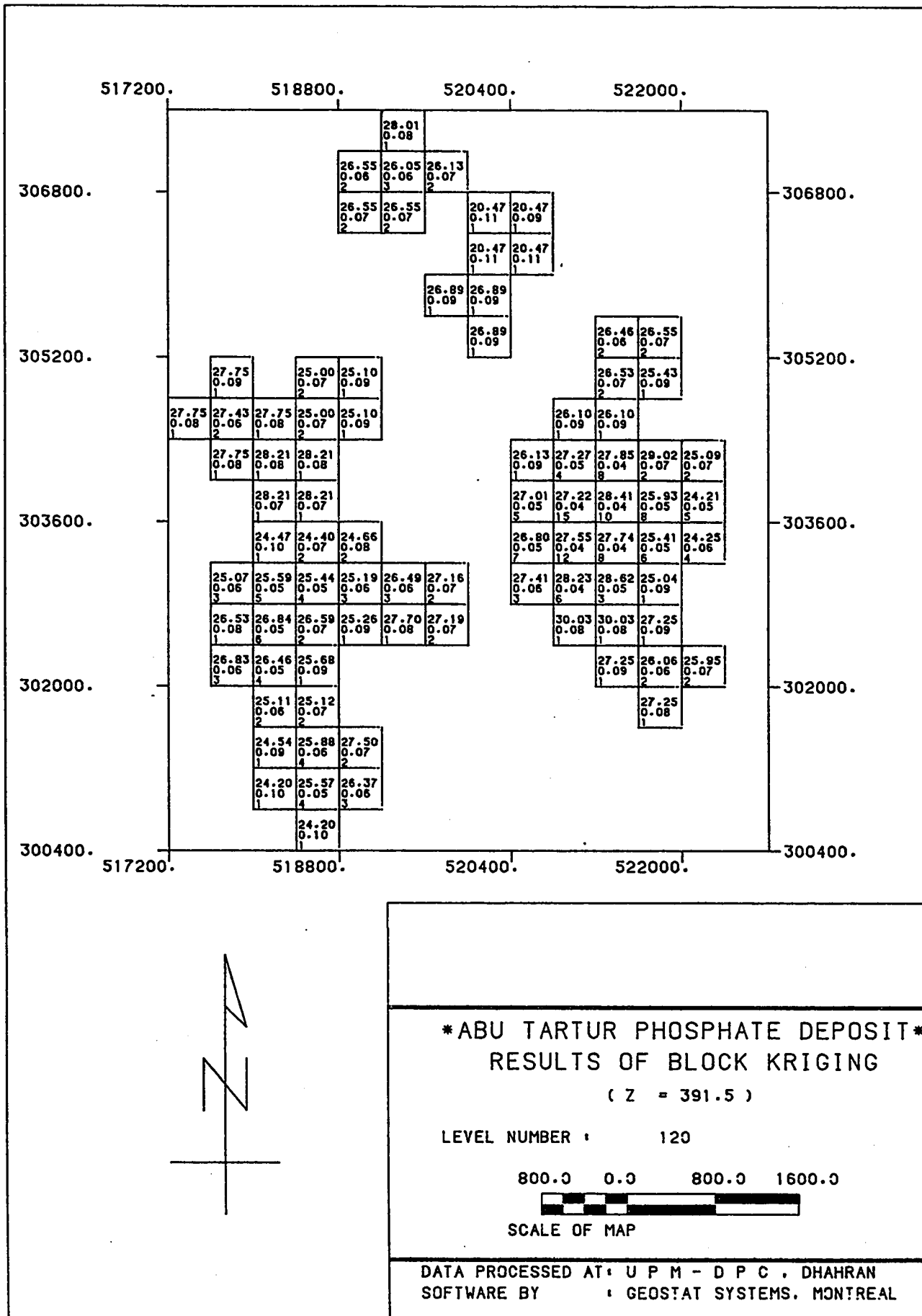
(D82)

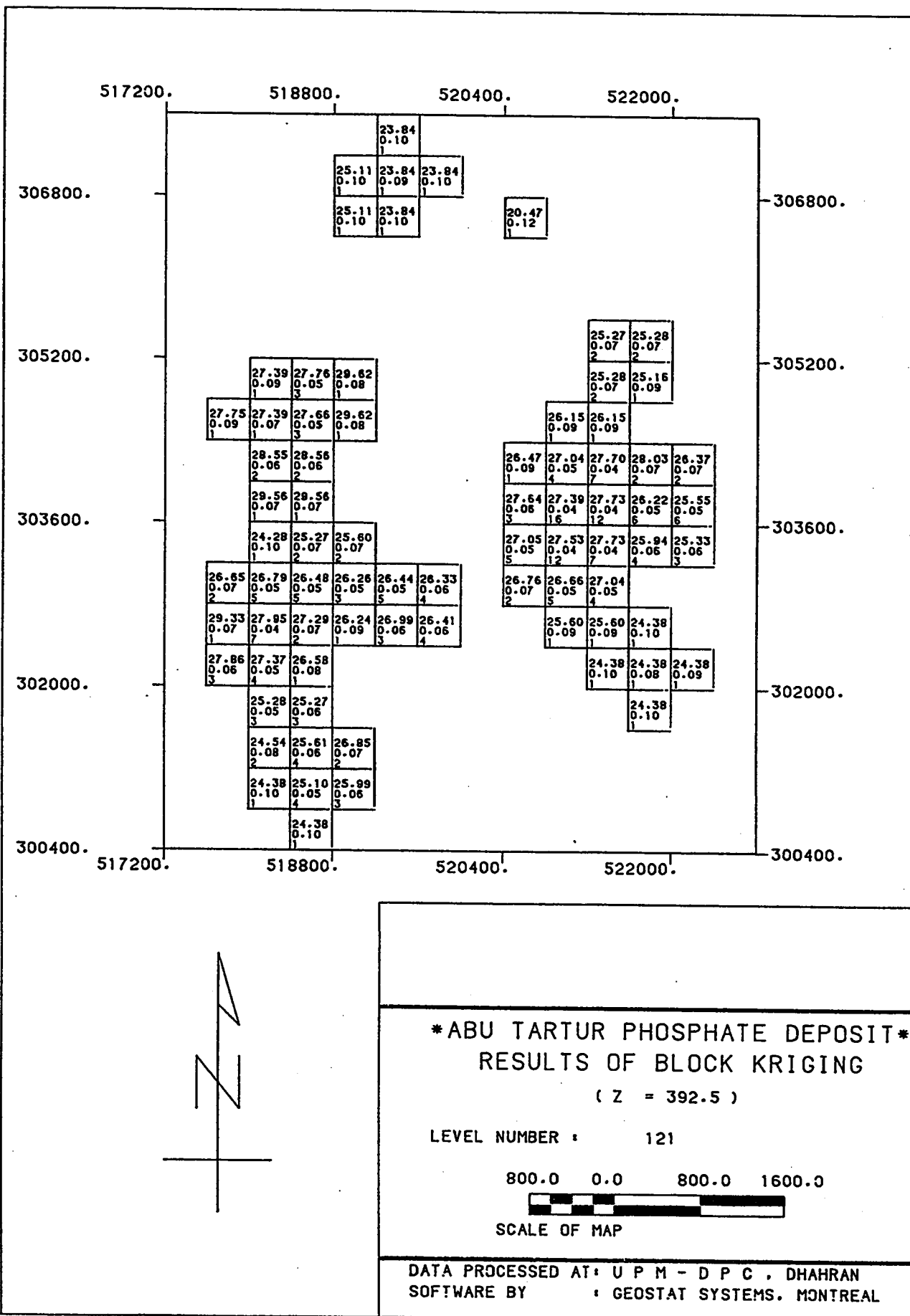


(D83)

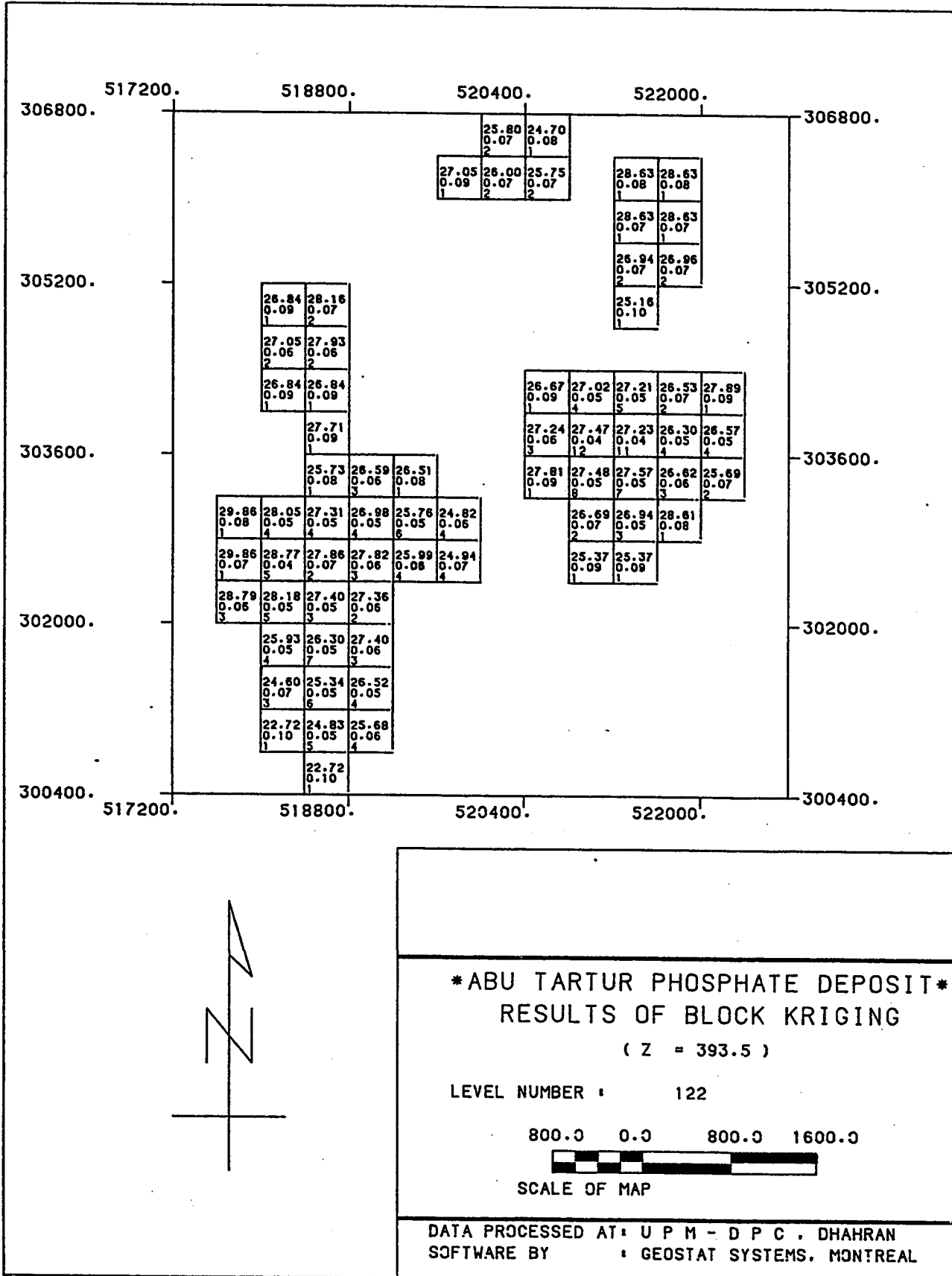


(D84)

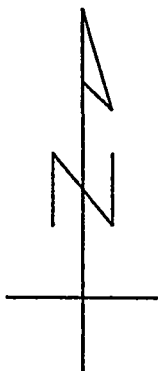
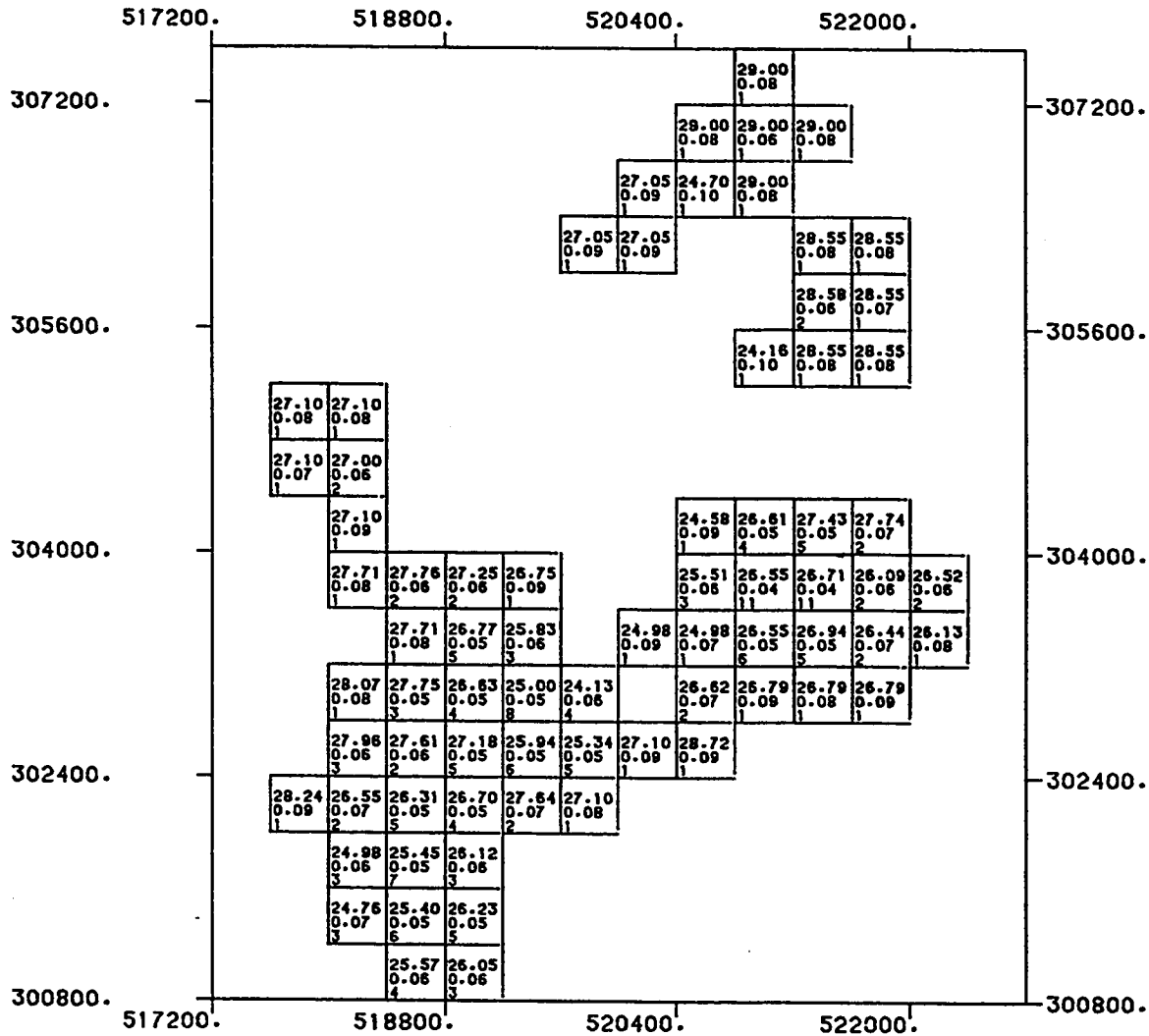




(D86)



(D87)



ABU TARTUR PHOSPHATE DEPOSIT
RESULTS OF BLOCK KRIGING

(Z = 394.5)

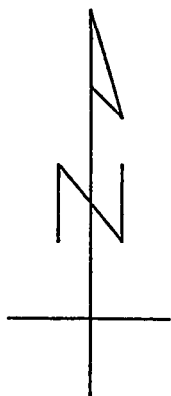
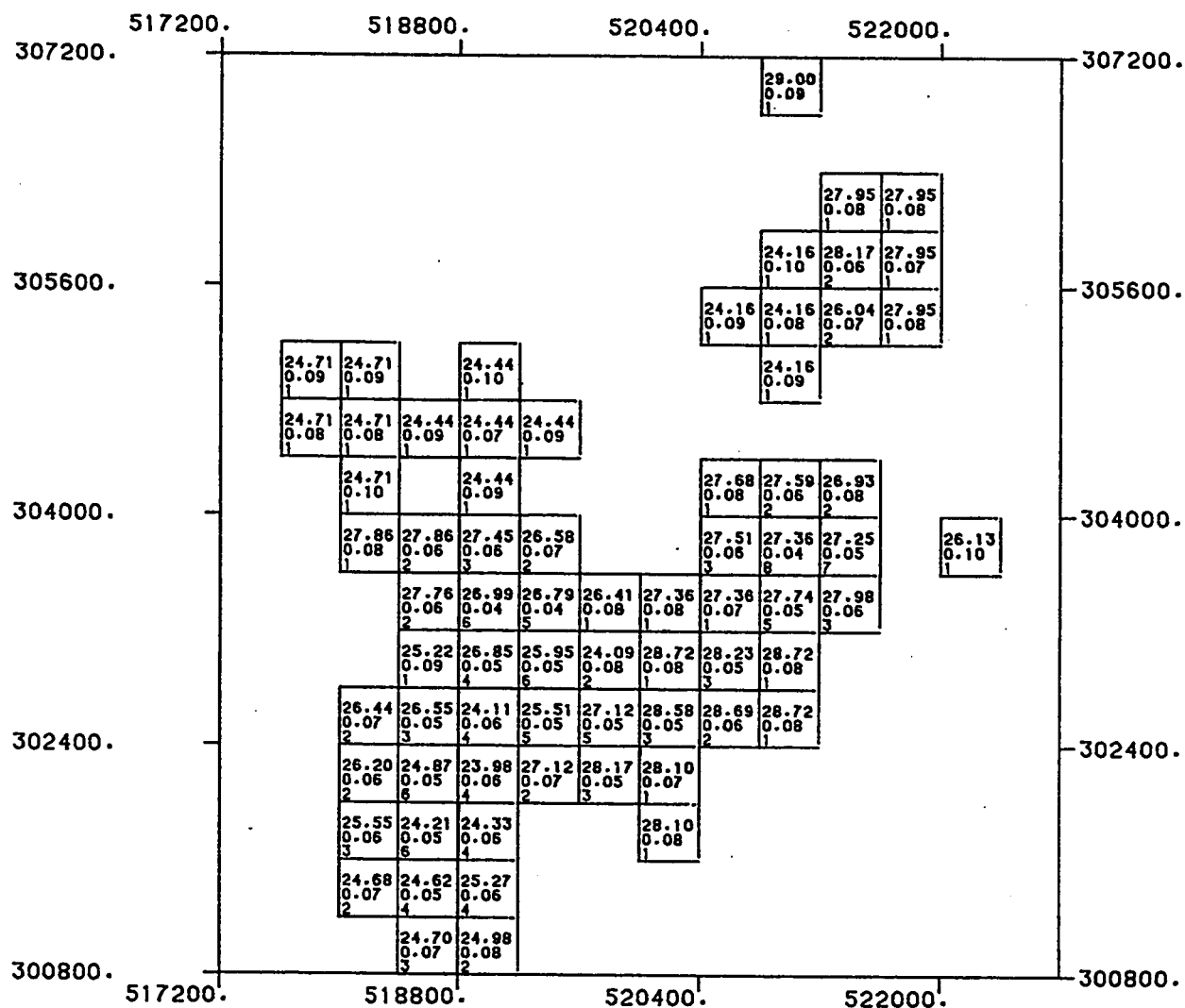
LEVEL NUMBER : 123

800.0 0.0 800.0 1600.0



SCALE OF MAP

DATA PROCESSED AT: U P M - D P C , DHAHRAN
SOFTWARE BY : GEOSTAT SYSTEMS, MONTREAL



ABU TARTUR PHOSPHATE DEPOSIT
RESULTS OF BLOCK KRIGING

(Z = 395.5)

LEVEL NUMBER : 124

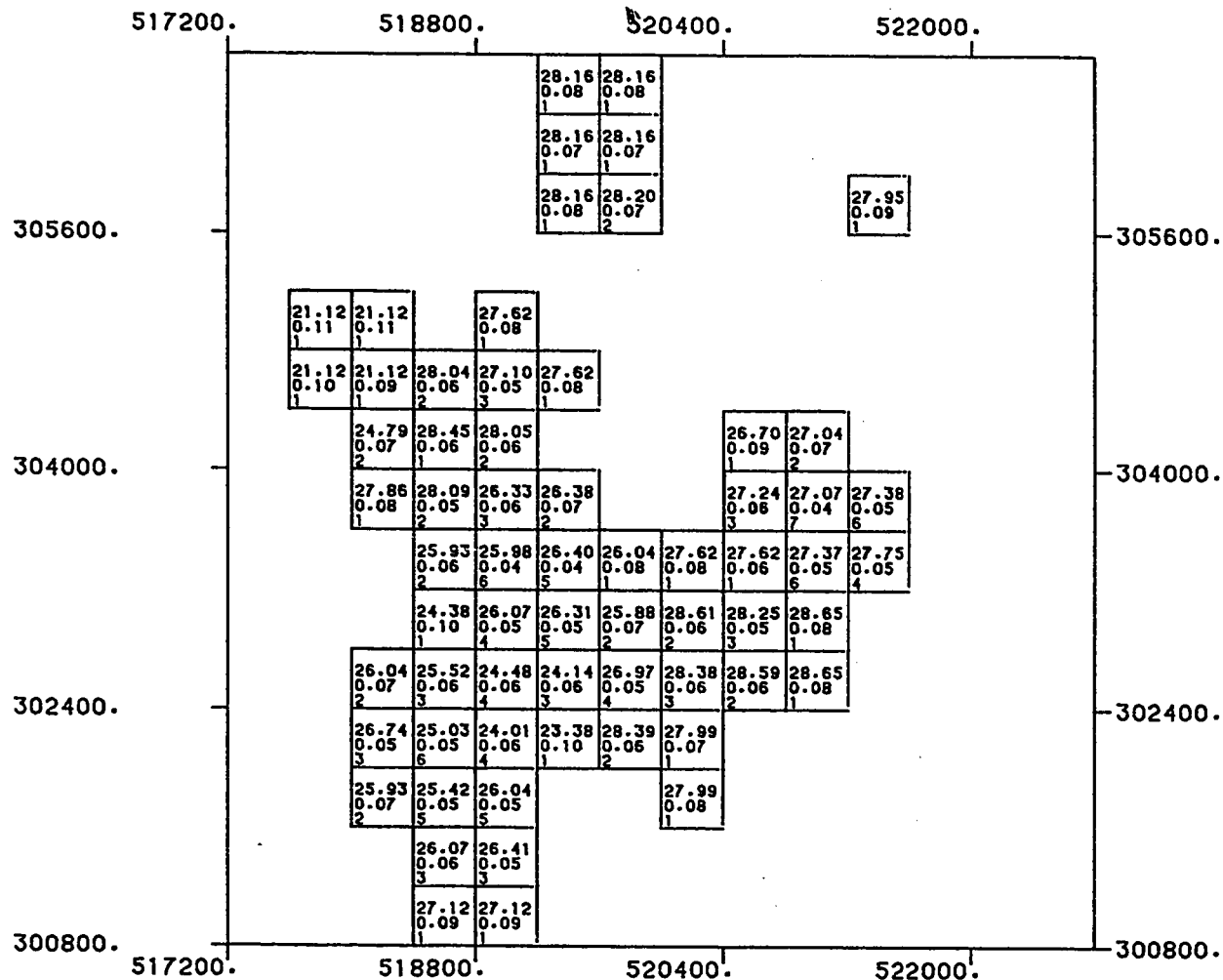
800.0 0.0 800.0 1600.0



SCALE OF MAP

DATA PROCESSED AT: U P M - D P C , DHAHRAN
SOFTWARE BY : GEOSTAT SYSTEMS, MONTREAL

(D89)



ABU TARTUR PHOSPHATE DEPOSIT
RESULTS OF BLOCK KRIGING

(Z = 396.5)

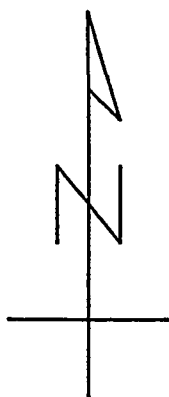
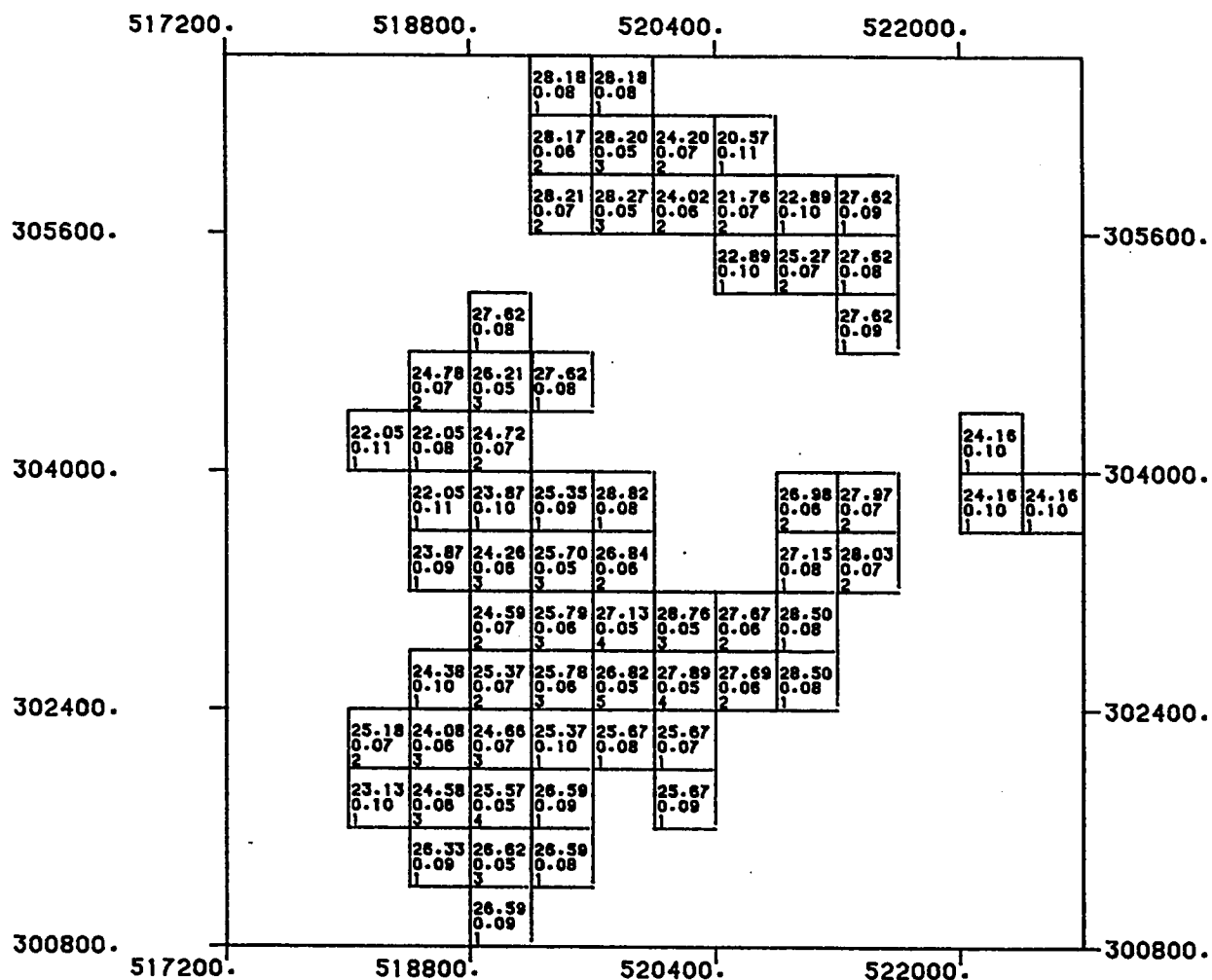
LEVEL NUMBER : 125

800.0 0.0 800.0 1600.0

SCALE OF MAP

DATA PROCESSED AT: U P M - D P C , DHAHRAN
SOFTWARE BY : GEOSTAT SYSTEMS. MONTREAL

(D90)



ABU TARTUR PHOSPHATE DEPOSIT
RESULTS OF BLOCK KRIGING

(Z = 397.5)

LEVEL NUMBER : 126

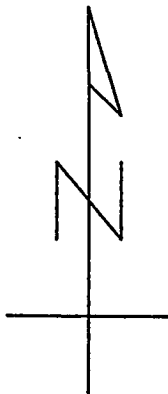
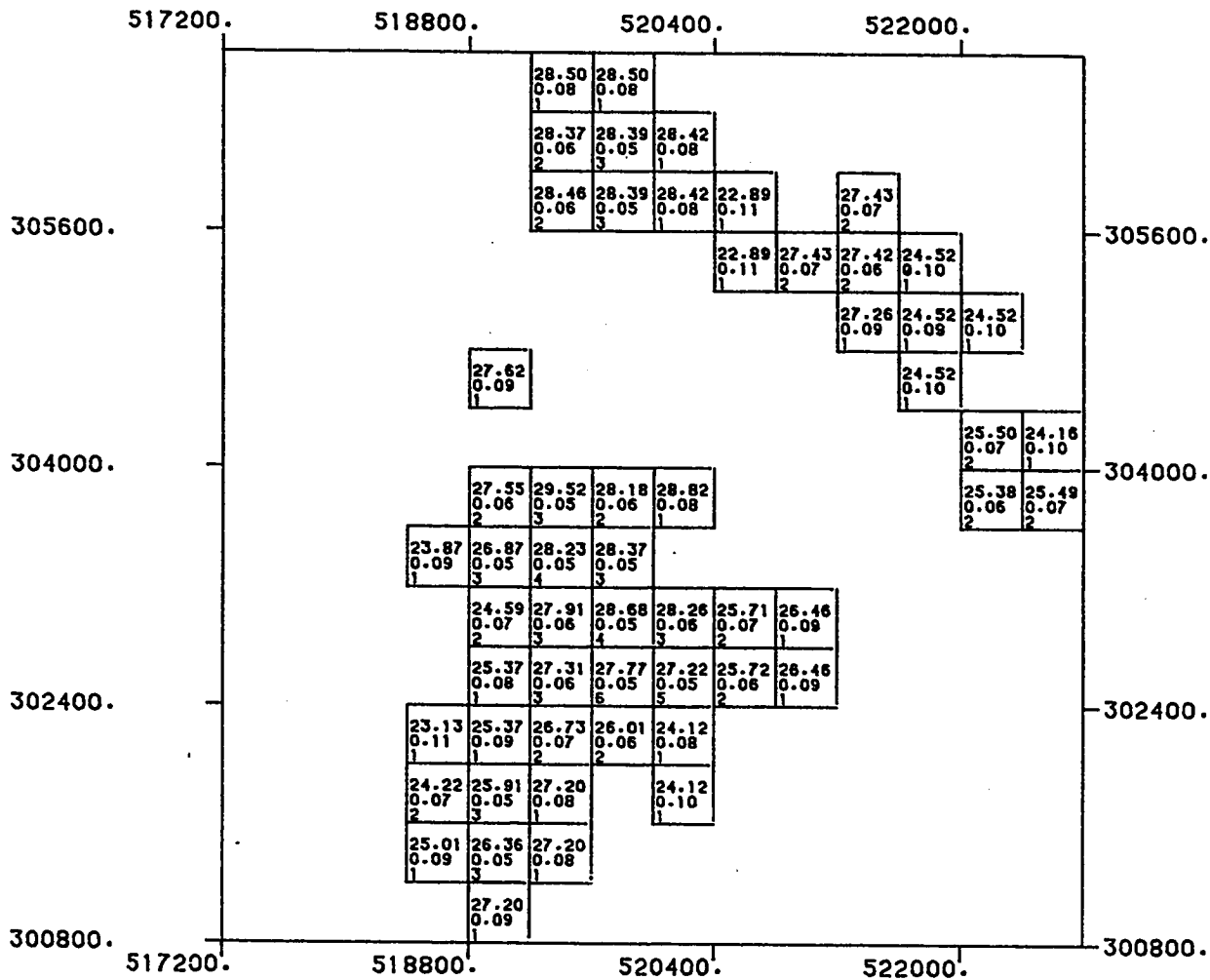
800.0 0.0 800.0 1600.0



SCALE OF MAP

DATA PROCESSED AT: U P M - D P C , DHAHRAN
 SOFTWARE BY : GEOSTAT SYSTEMS, MONTREAL

(D91)



ABU TARTUR PHOSPHATE DEPOSIT
RESULTS OF BLOCK KRIGING

(Z = 398.5)

LEVEL NUMBER : 127

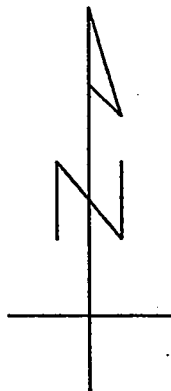
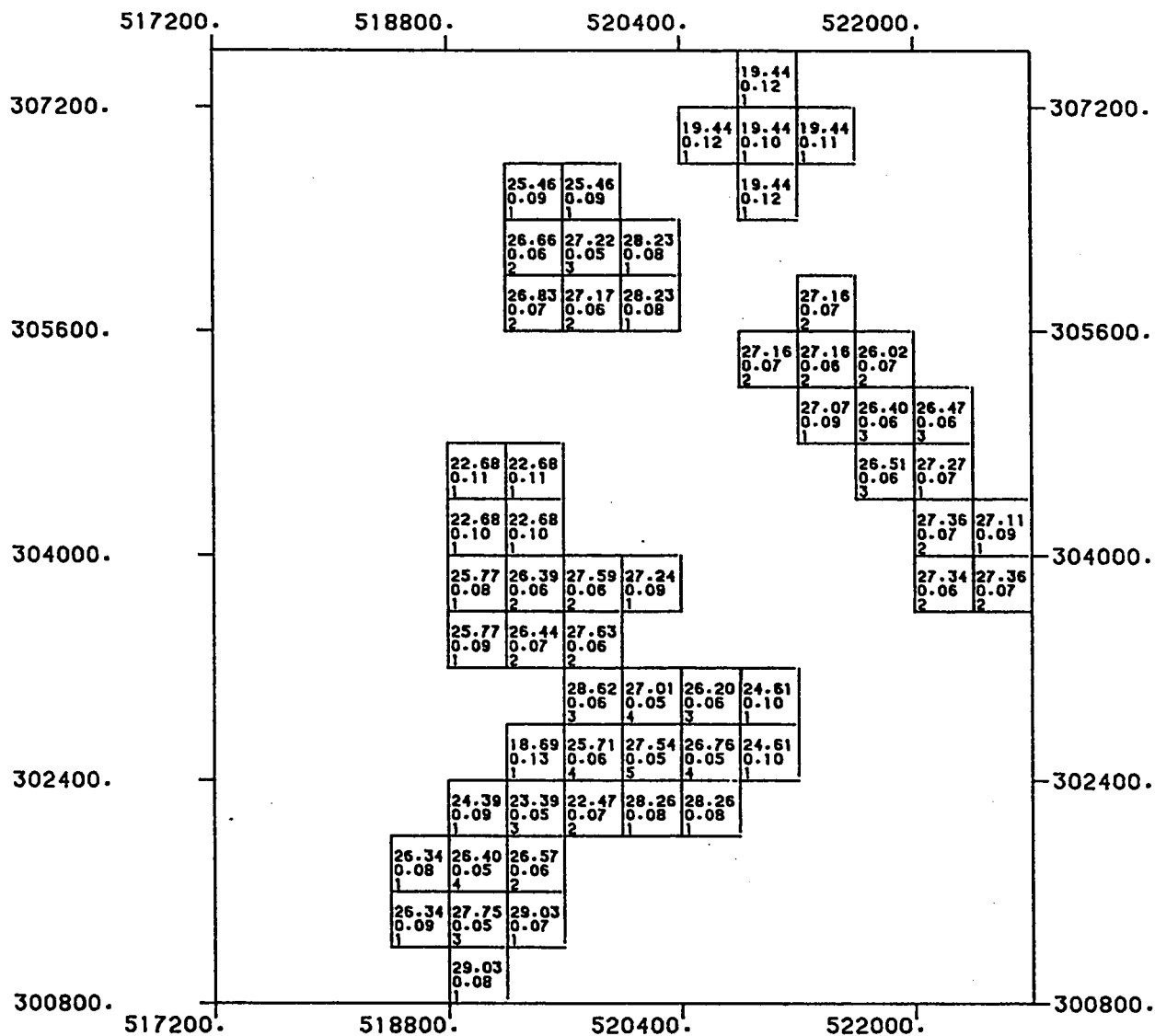
800.0 0.0 800.0 1600.0



SCALE OF MAP

DATA PROCESSED AT: U P M - D P C , DHAHRAN
SOFTWARE BY : GEOSTAT SYSTEMS, MONTREAL

(D92)



ABU TARTUR PHOSPHATE DEPOSIT
RESULTS OF BLOCK KRIGING

(Z = 399.5)

LEVEL NUMBER : 128

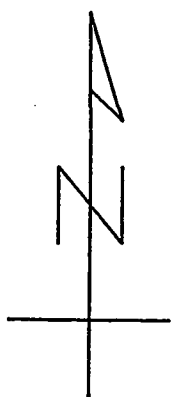
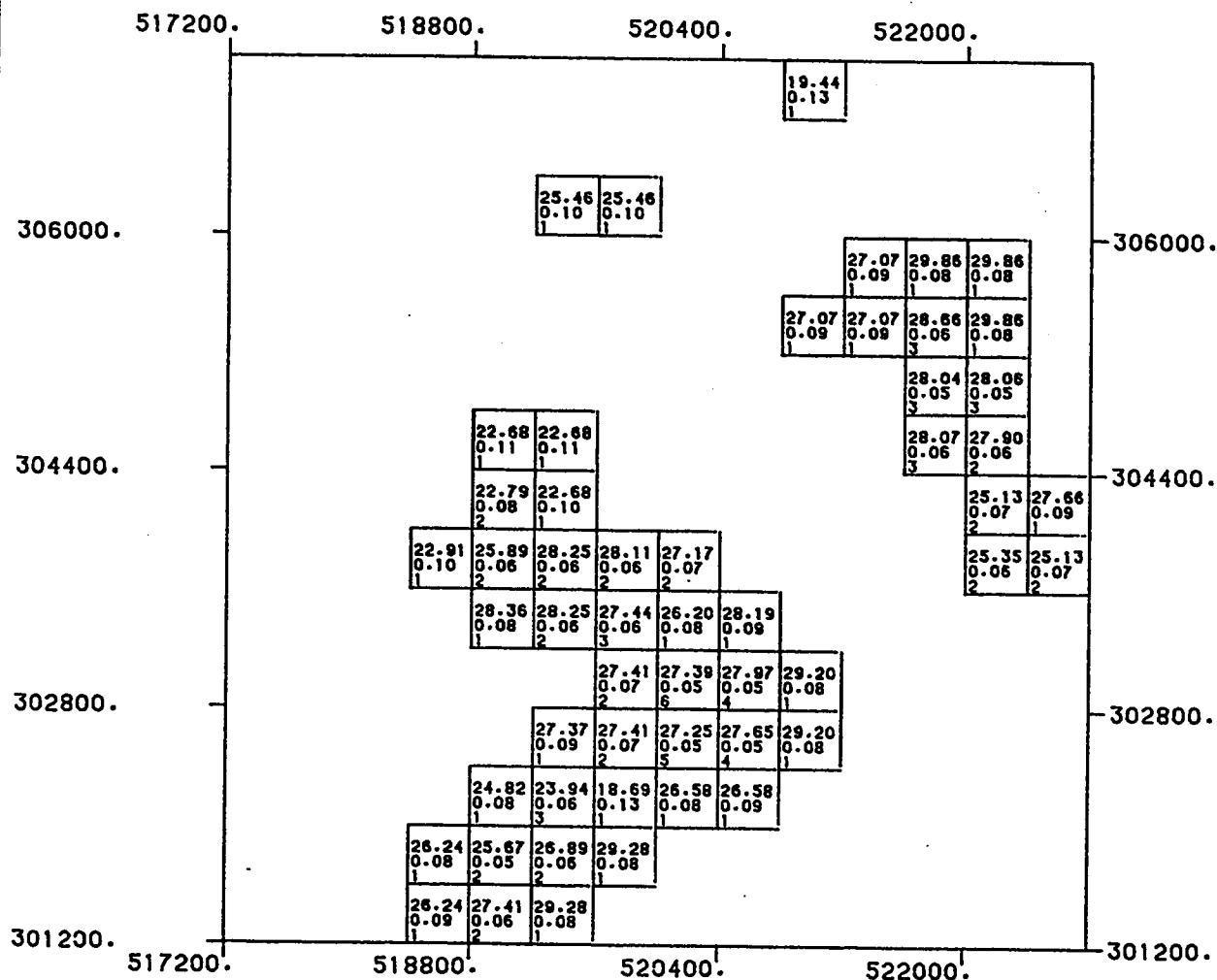
800.0 0.0 800.0 1600.0



SCALE OF MAP

DATA PROCESSED AT: U P M - D P C , DHAHRAN
 SOFTWARE BY : GEOSTAT SYSTEMS, MONTREAL

(D93)



ABU TARTUR PHOSPHATE DEPOSIT
RESULTS OF BLOCK KRIGING

(Z = 400.5)

LEVEL NUMBER : 129

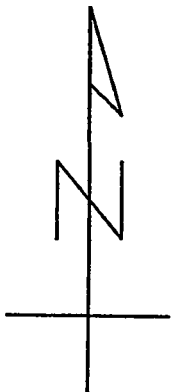
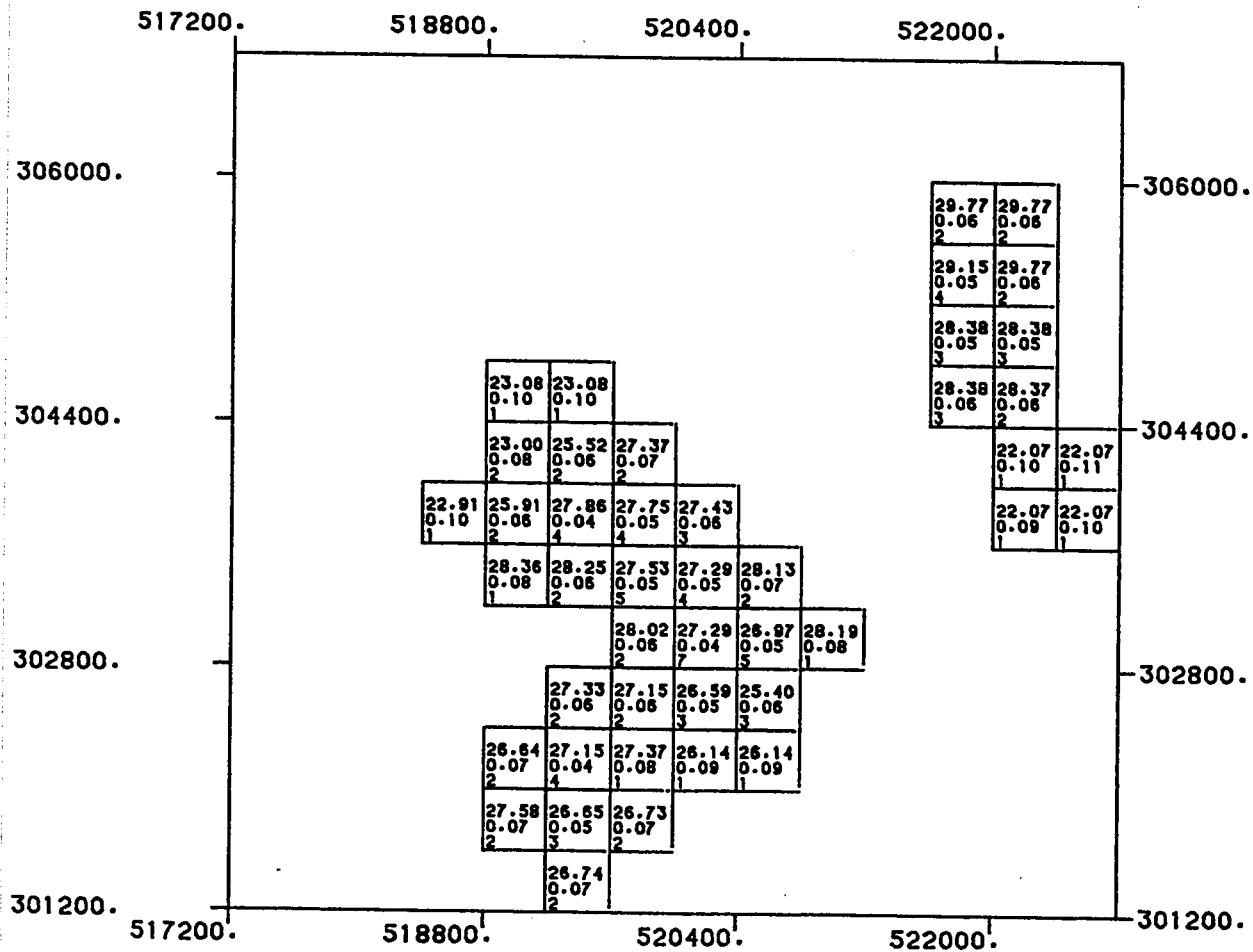
800.0 0.0 800.0 1600.0



SCALE OF MAP

DATA PROCESSED AT: U P M - D P C . DHAHRAN
SOFTWARE BY : GEOSTAT SYSTEMS, MONTREAL

(D94)



ABU TARTUR PHOSPHATE DEPOSIT

RESULTS OF BLOCK KRIGING

(Z = 401.5)

LEVEL NUMBER : 130

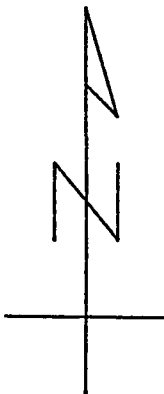
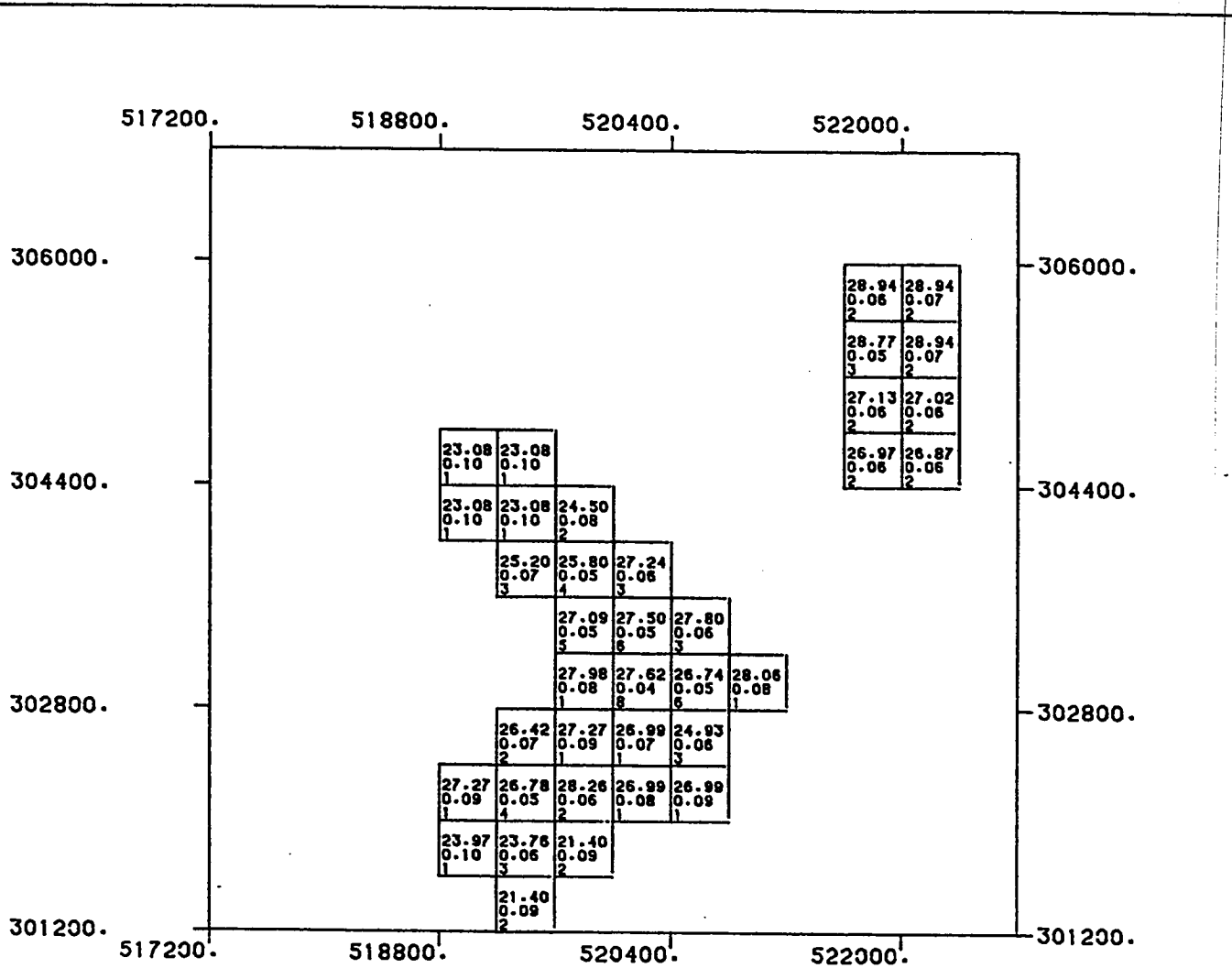
800.0 0.0 800.0 1600.0



SCALE OF MAP

DATA PROCESSED AT: U P M - D P C , DHAHRAN
SOFTWARE BY : GEOSTAT SYSTEMS. MONTREAL

(D95)



ABU TARTUR PHOSPHATE DEPOSIT
RESULTS OF BLOCK KRIGING

(Z = 402.5)

LEVEL NUMBER : 131

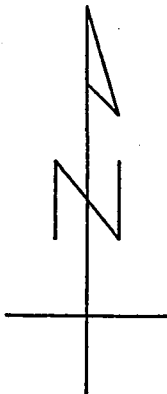
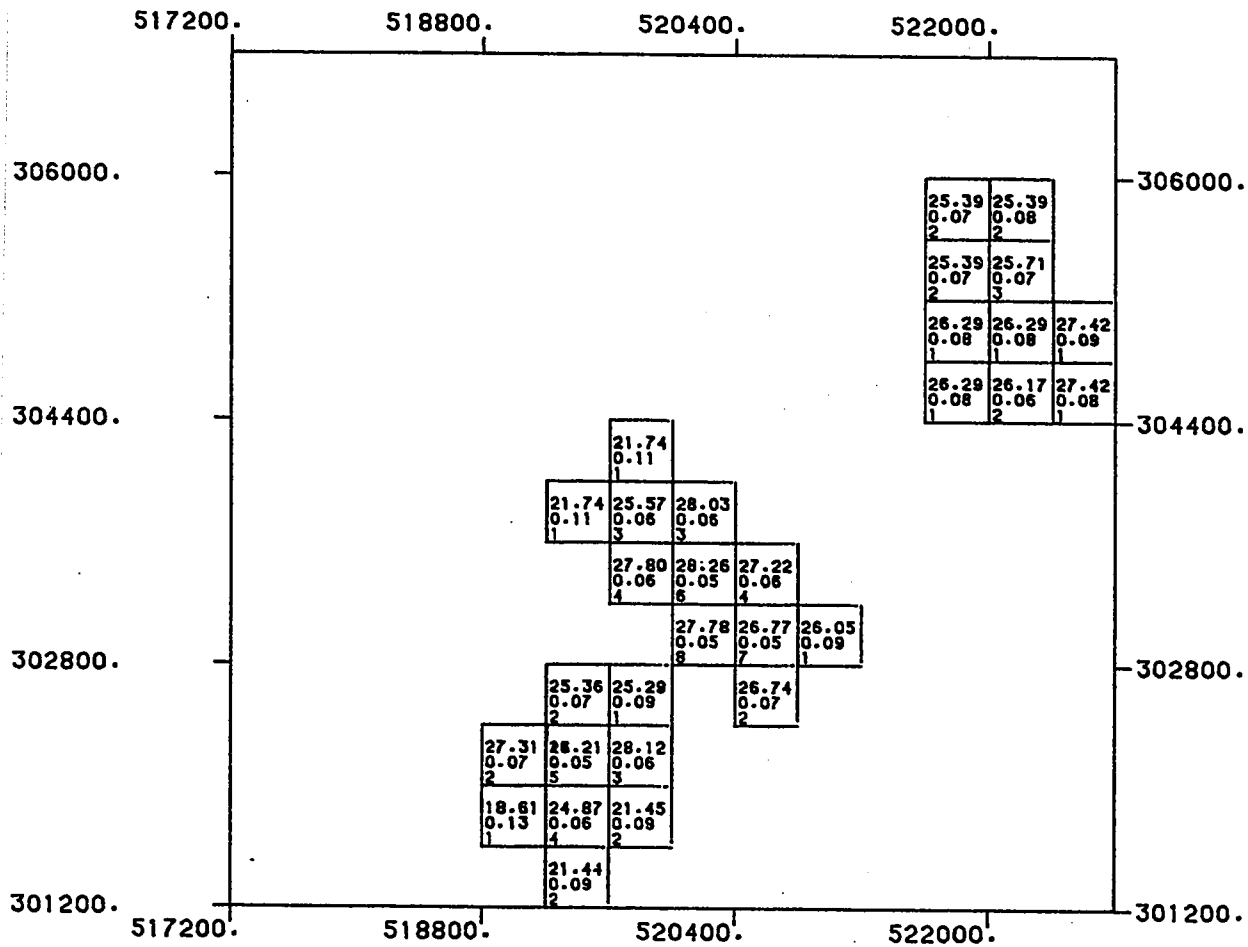
800.0 0.0 800.0 1600.0



SCALE OF MAP

DATA PROCESSED AT: U P M - D P C , DHAHRAN
SOFTWARE BY : GEOSTAT SYSTEMS, MONTREAL

(D96)



ABU TARTUR PHOSPHATE DEPOSIT
RESULTS OF BLOCK KRIGING

(Z = 403.5)

LEVEL NUMBER : 132

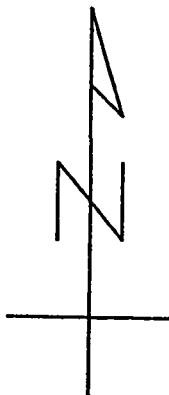
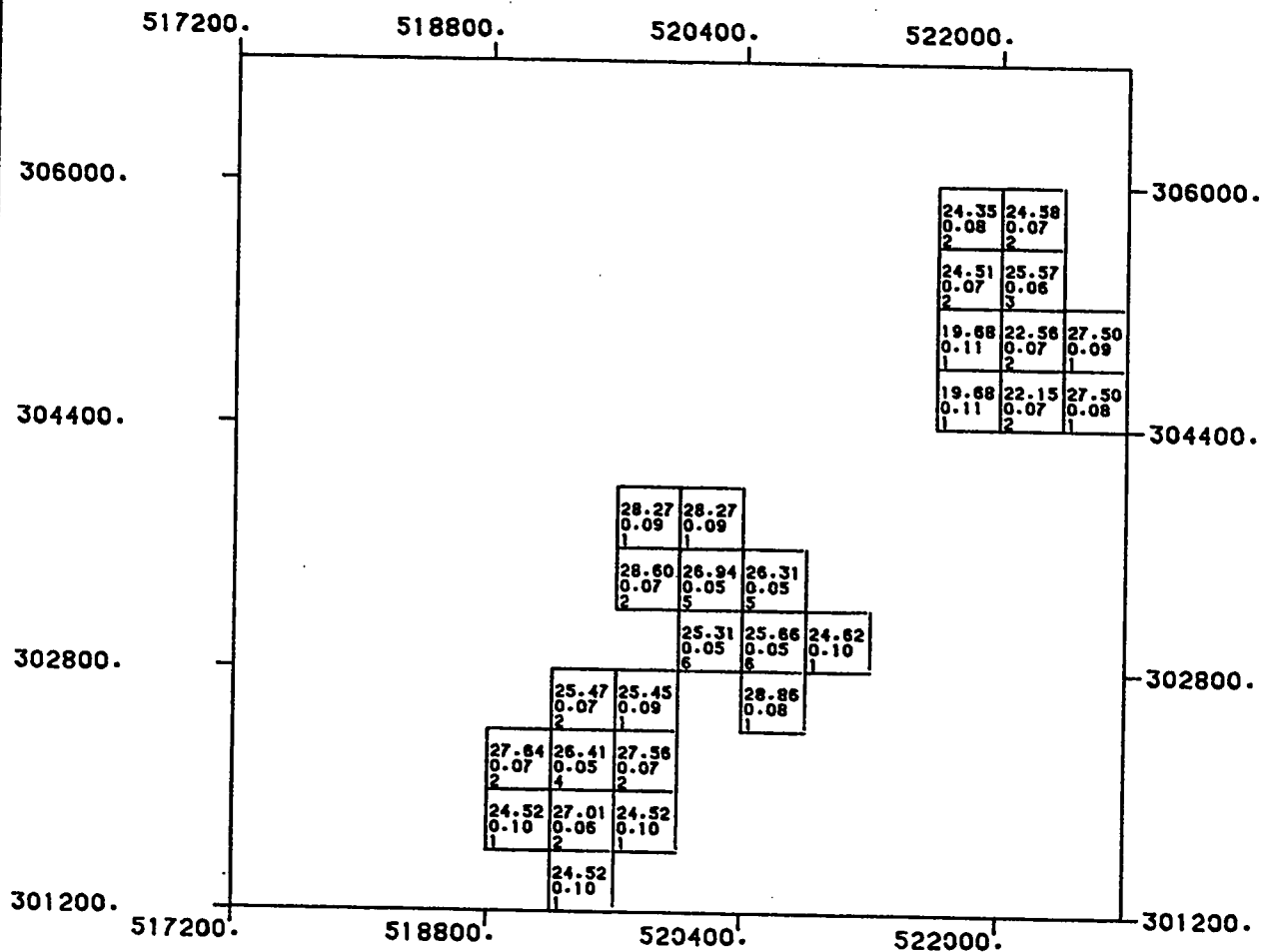
800.0 0.0 800.0 1600.0



SCALE OF MAP

DATA PROCESSED AT: U P M - D P C , DHAHRAN
SOFTWARE BY : GEOSTAT SYSTEMS, MONTREAL

(D97)



ABU TARTUR PHOSPHATE DEPOSIT
RESULTS OF BLOCK KRIGING

(Z = 404.5)

LEVEL NUMBER : 133

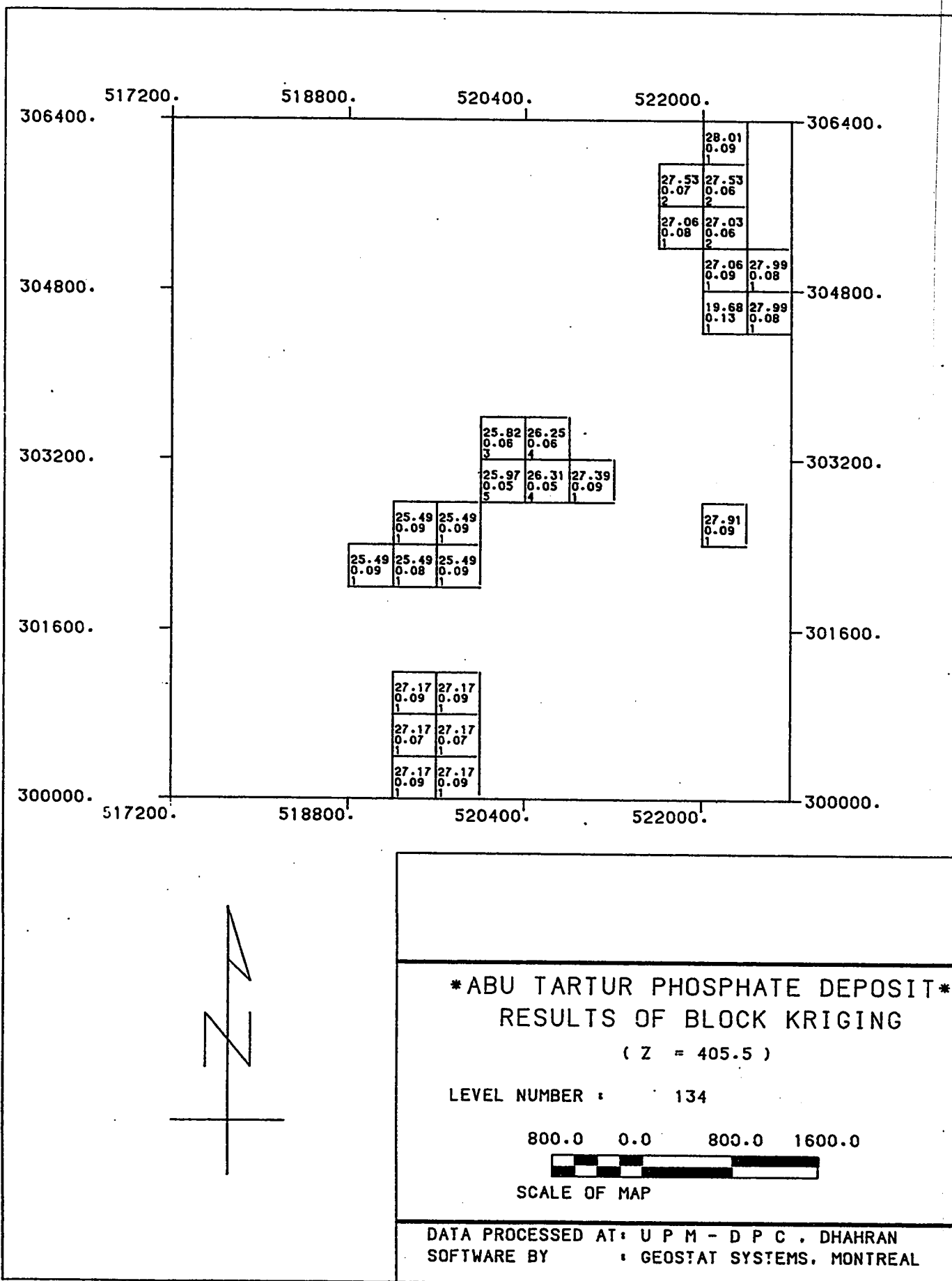
800.0 0.0 800.0 1600.0

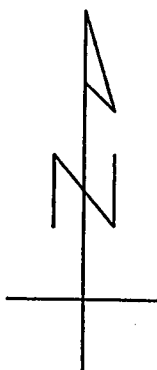


SCALE OF MAP

DATA PROCESSED AT: U P M - D P C , DHAHRAN
SOFTWARE BY : GEOSTAT SYSTEMS. MONTREAL

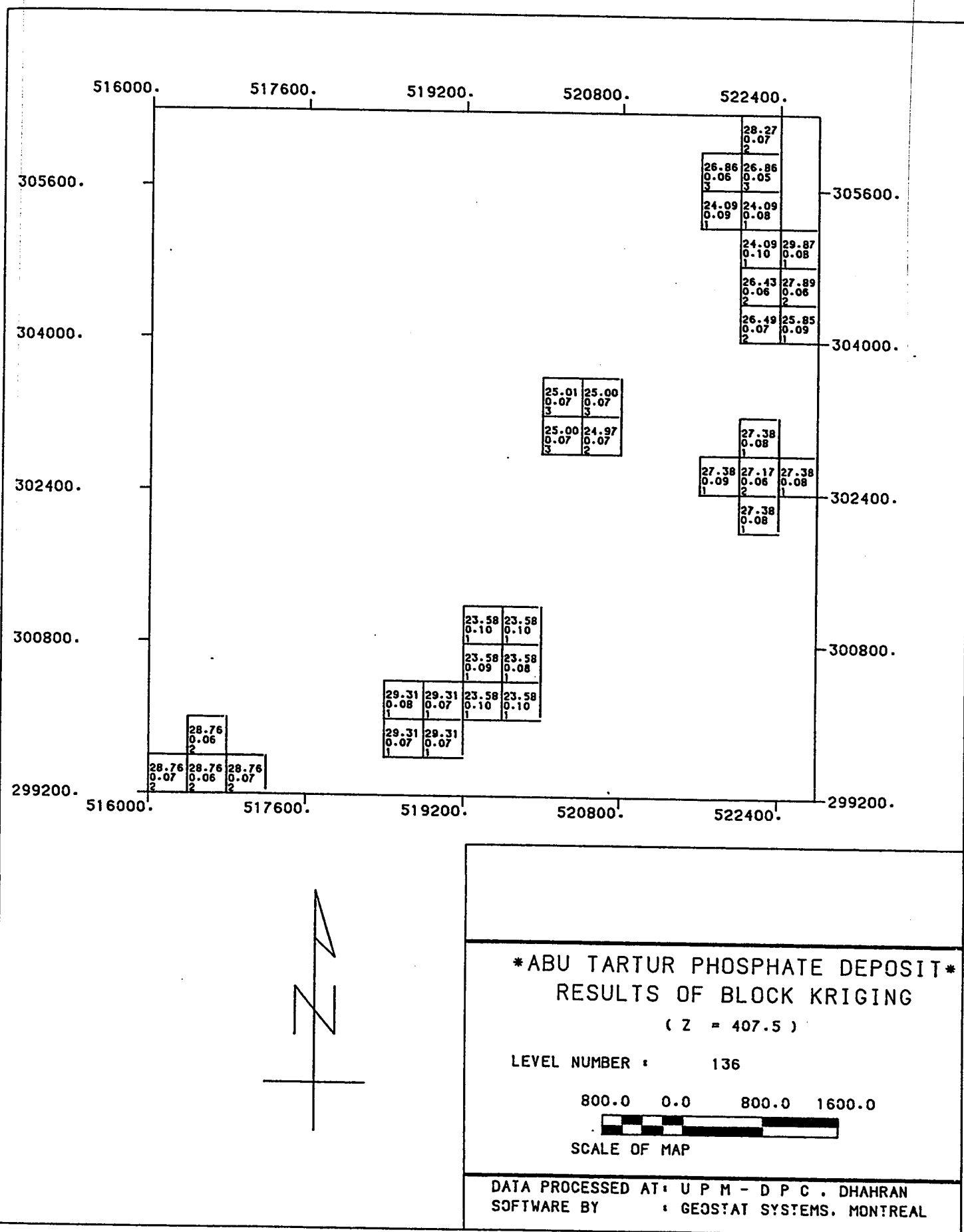
(D98)



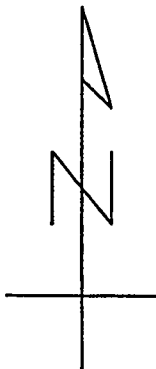
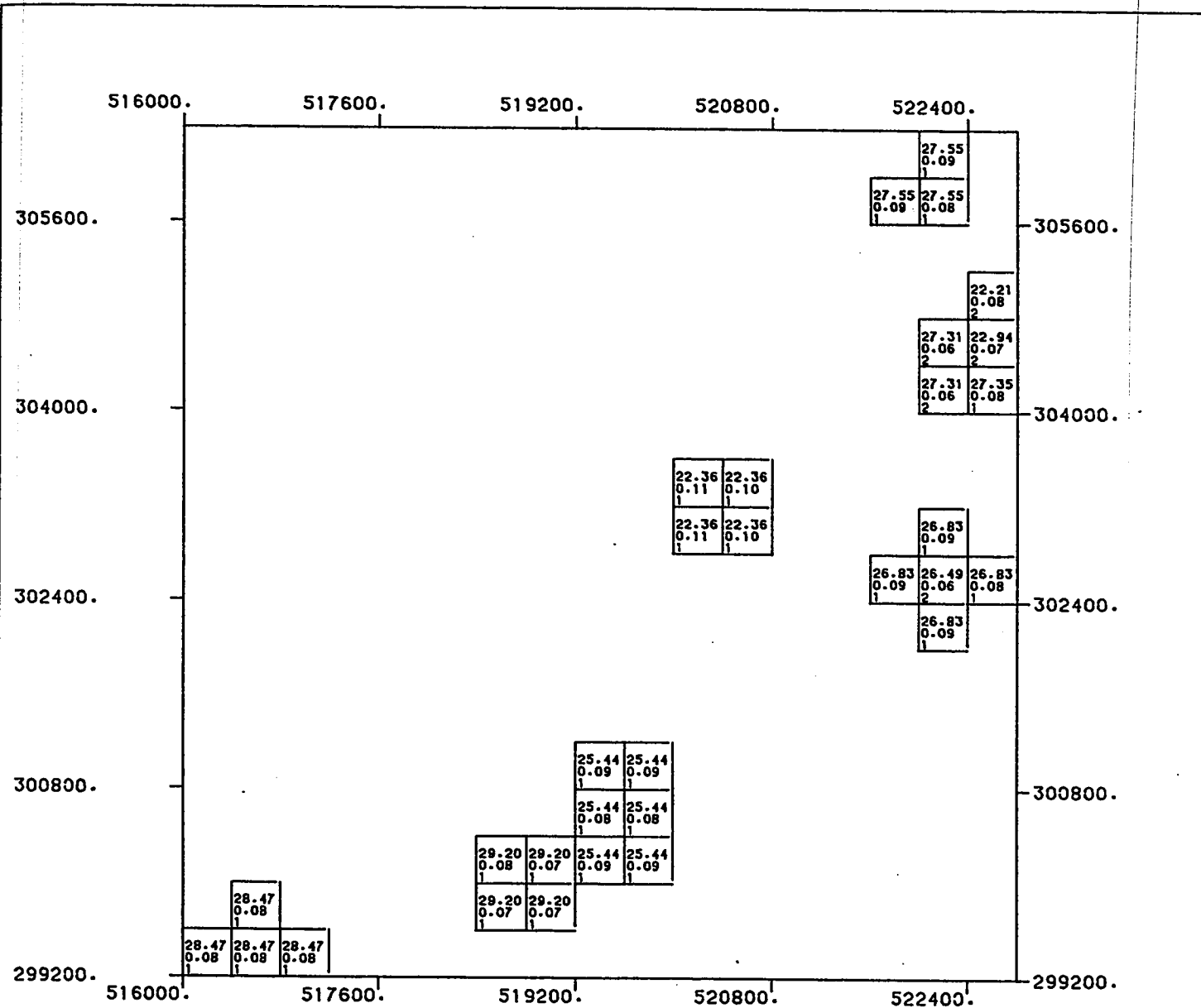


SCALE OF MAP

DATA PROCESSED AT: U P M - D P C , DHAHRAN
SOFTWARE BY : GEOSTAT SYSTEMS, MONTREAL



(D101)



ABU TARTUR PHOSPHATE DEPOSIT
RESULTS OF BLOCK KRIGING

(Z = 408.5)

LEVEL NUMBER : 137

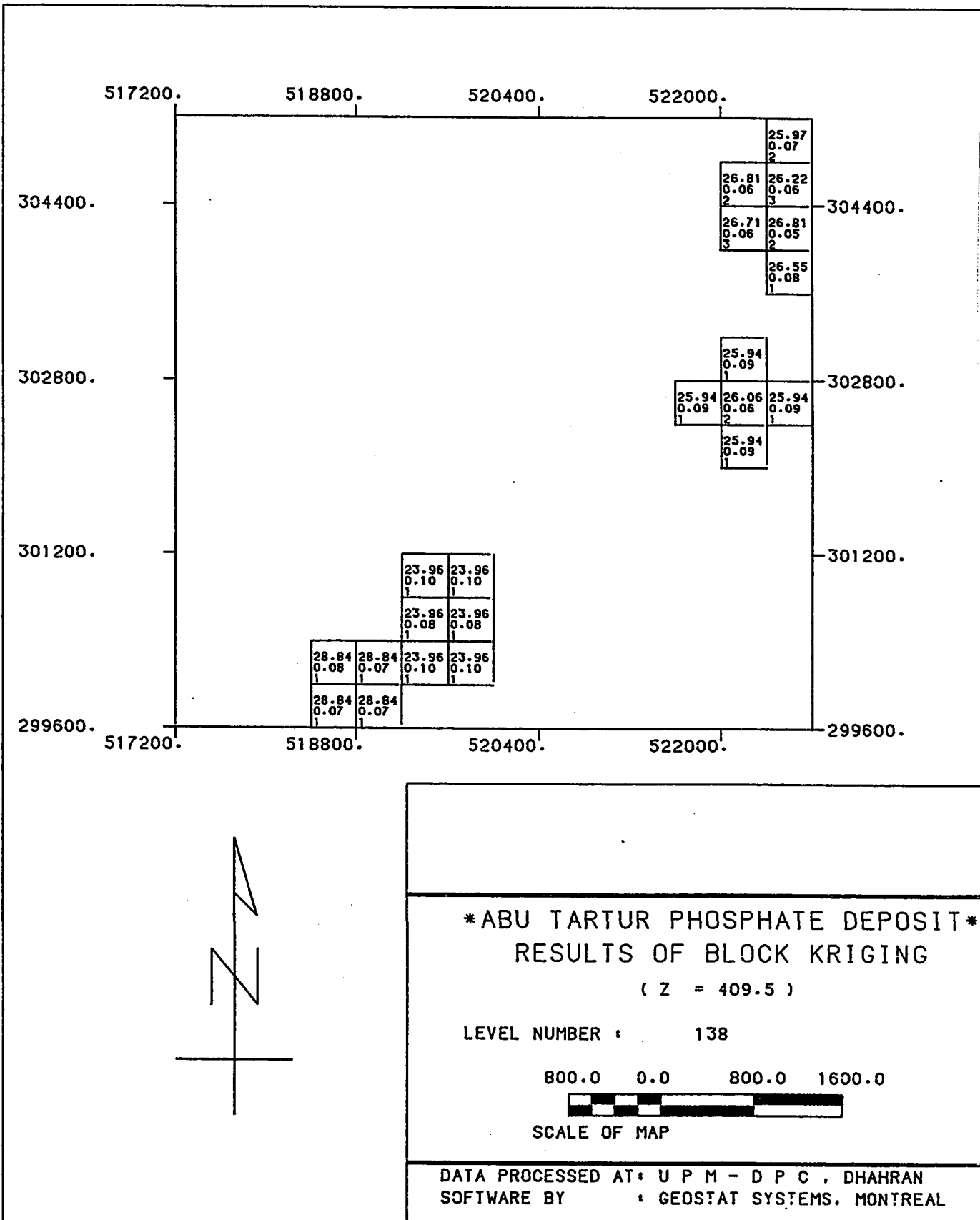
800.0 0.0 800.0 1600.0



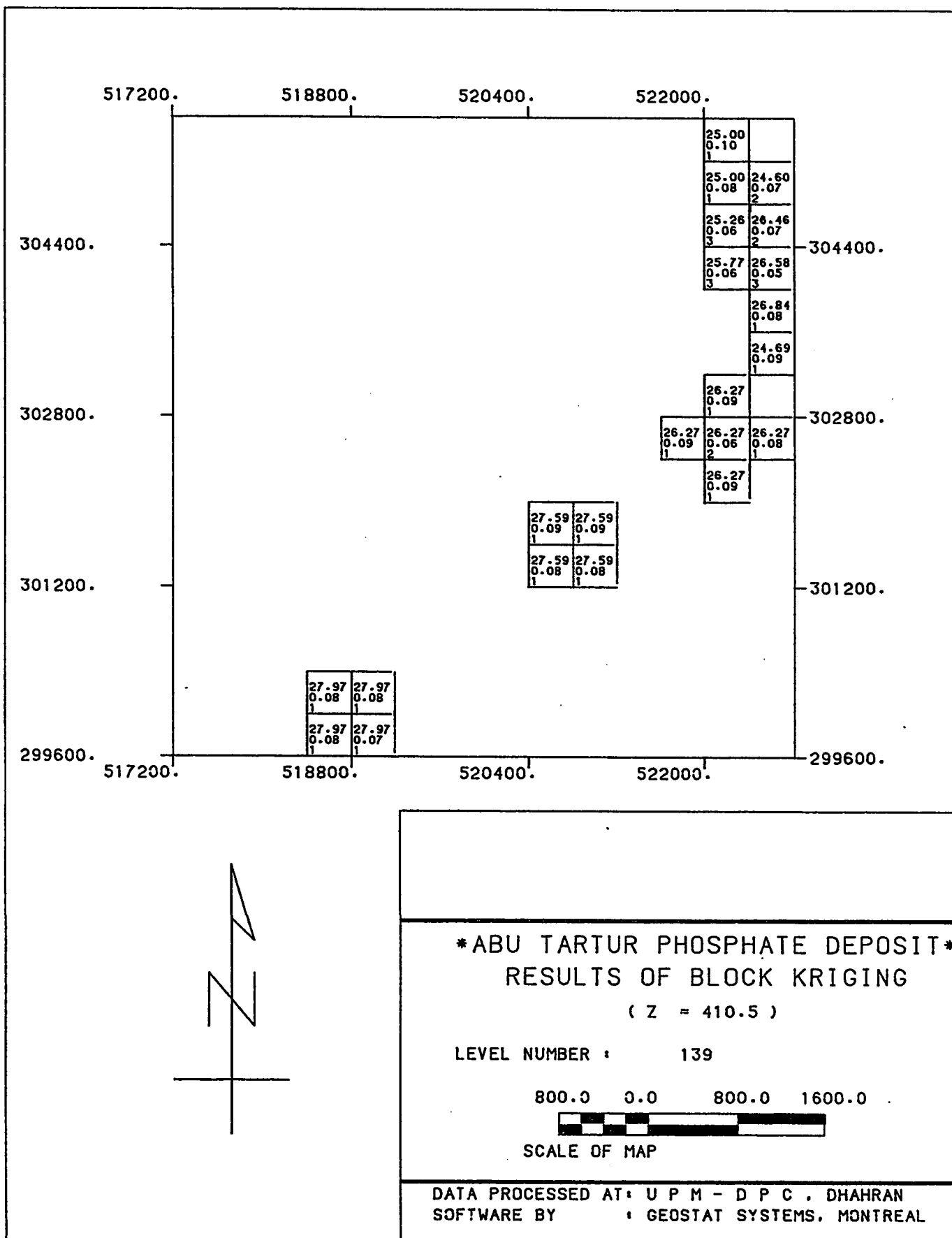
SCALE OF MAP

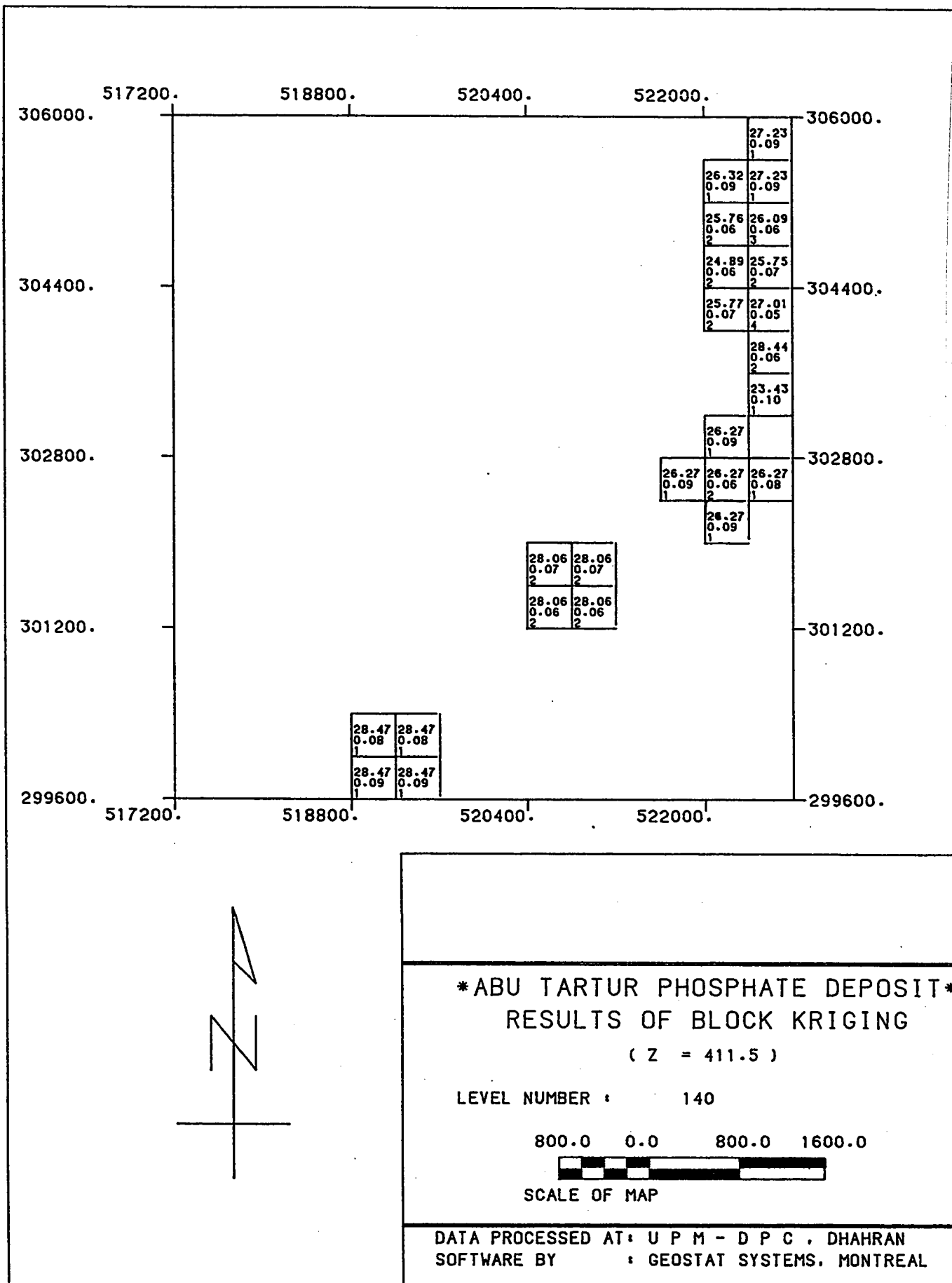
DATA PROCESSED AT: U P M - D P C , DHAHRAN
SOFTWARE BY : GEOSTAT SYSTEMS, MONTREAL

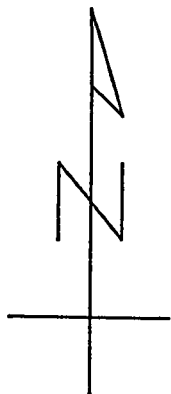
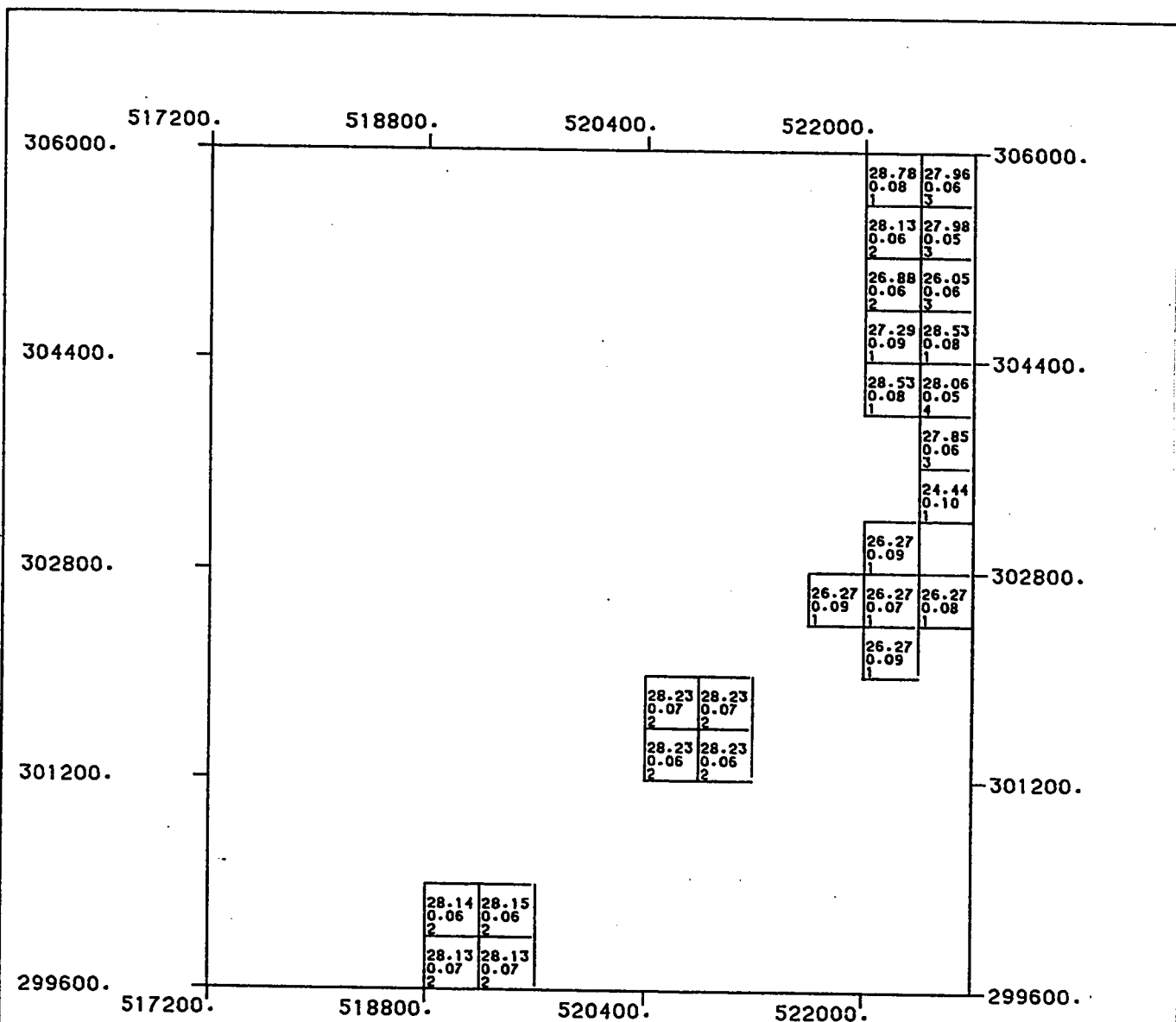
(D102)



(D103)







ABU TARTUR PHOSPHATE DEPOSIT
RESULTS OF BLOCK KRIGING

(Z = 412.5)

LEVEL NUMBER : 141

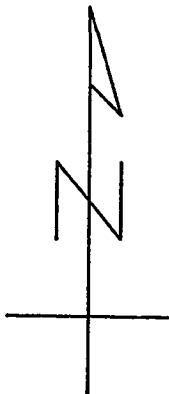
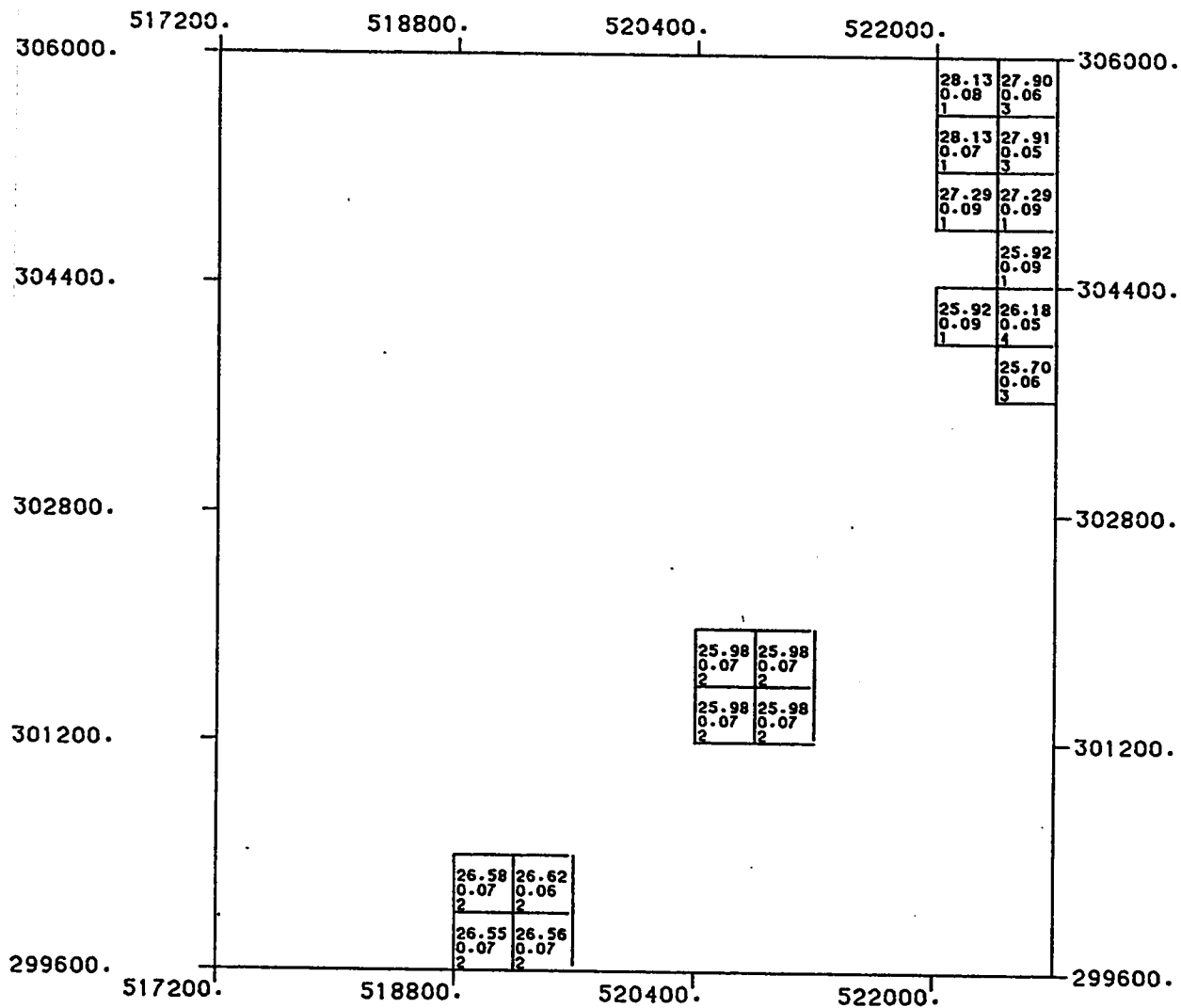
800.0 0.0 800.0 1600.0



SCALE OF MAP

DATA PROCESSED AT: U P M - D P C , DHAHRAN
SOFTWARE BY : GEOSTAT SYSTEMS, MONTREAL

(D106)



ABU TARTUR PHOSPHATE DEPOSIT
RESULTS OF BLOCK KRIGING

(Z = 413.5)

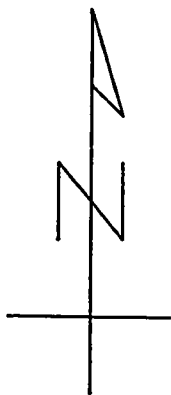
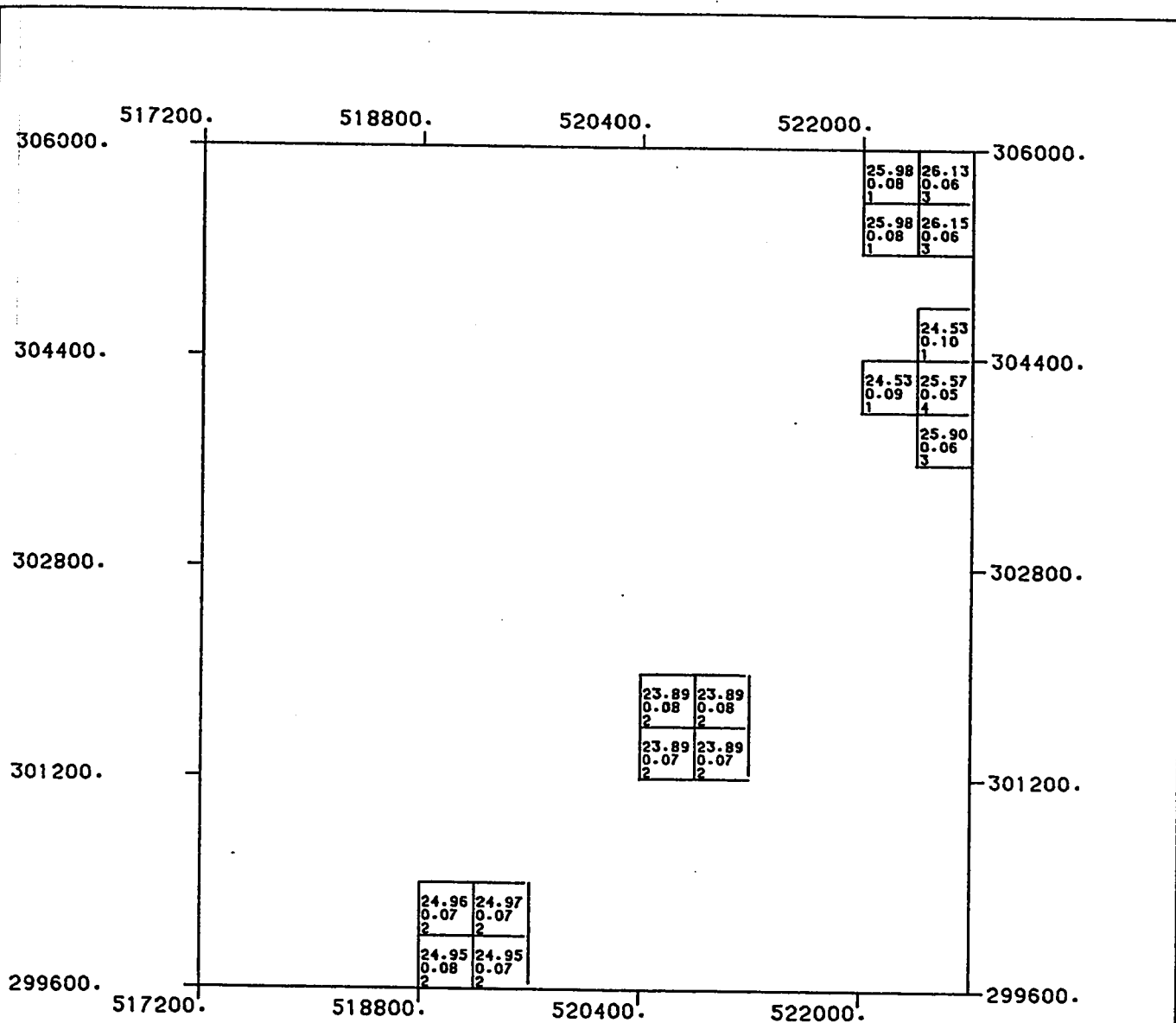
LEVEL NUMBER : 142

800.0 0.0 800.0 1600.0



SCALE OF MAP

DATA PROCESSED AT: U P M - D P C , DHAHRAN
 SOFTWARE BY : GEOSTAT SYSTEMS, MONTREAL



ABU TARTUR PHOSPHATE DEPOSIT
RESULTS OF BLOCK KRIGING

(Z = 414.5)

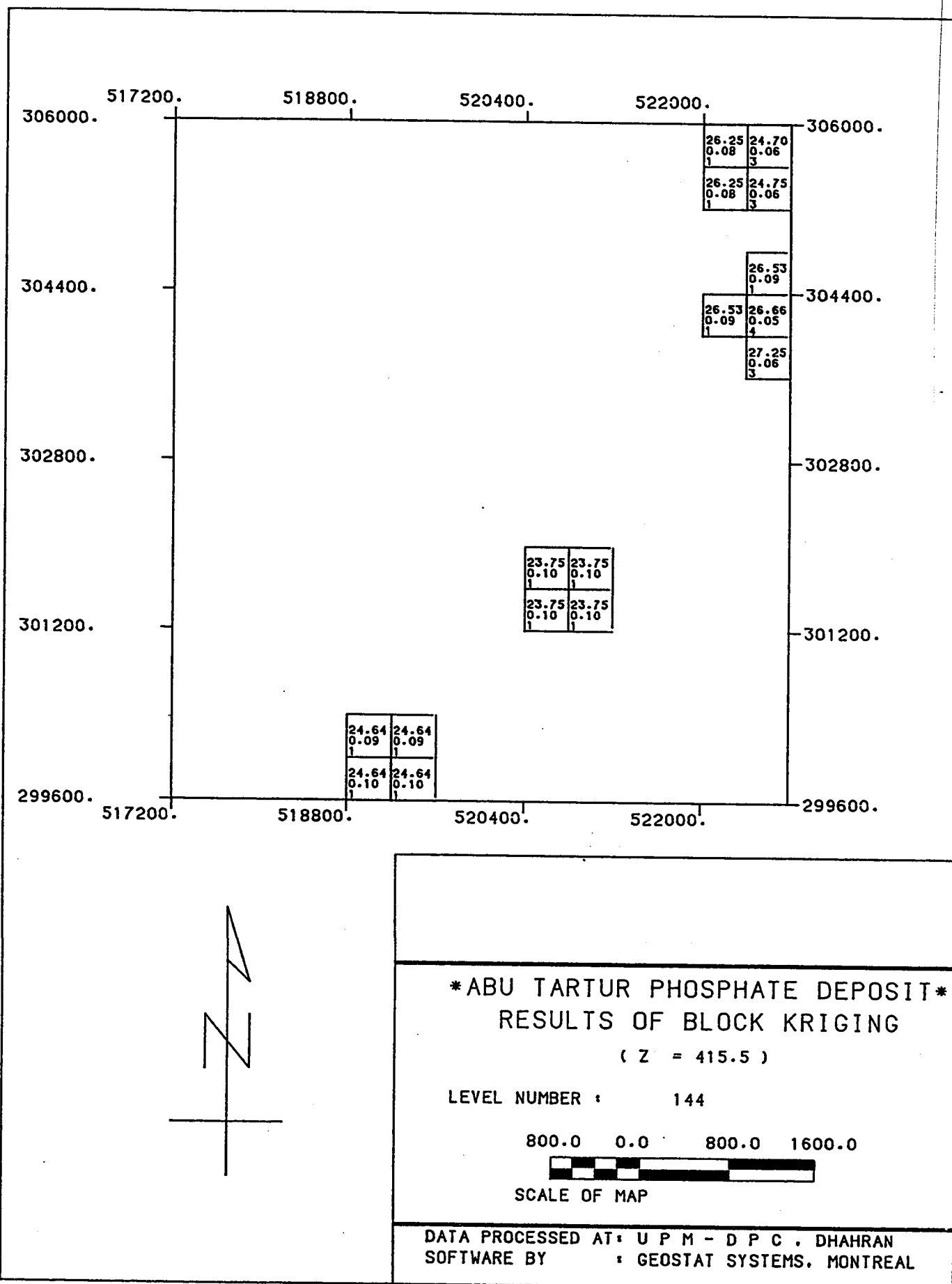
LEVEL NUMBER : 143

800.0 0.0 800.0 1600.0

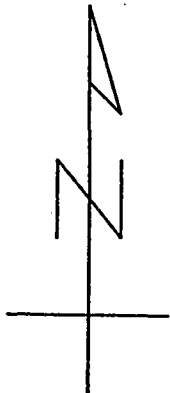
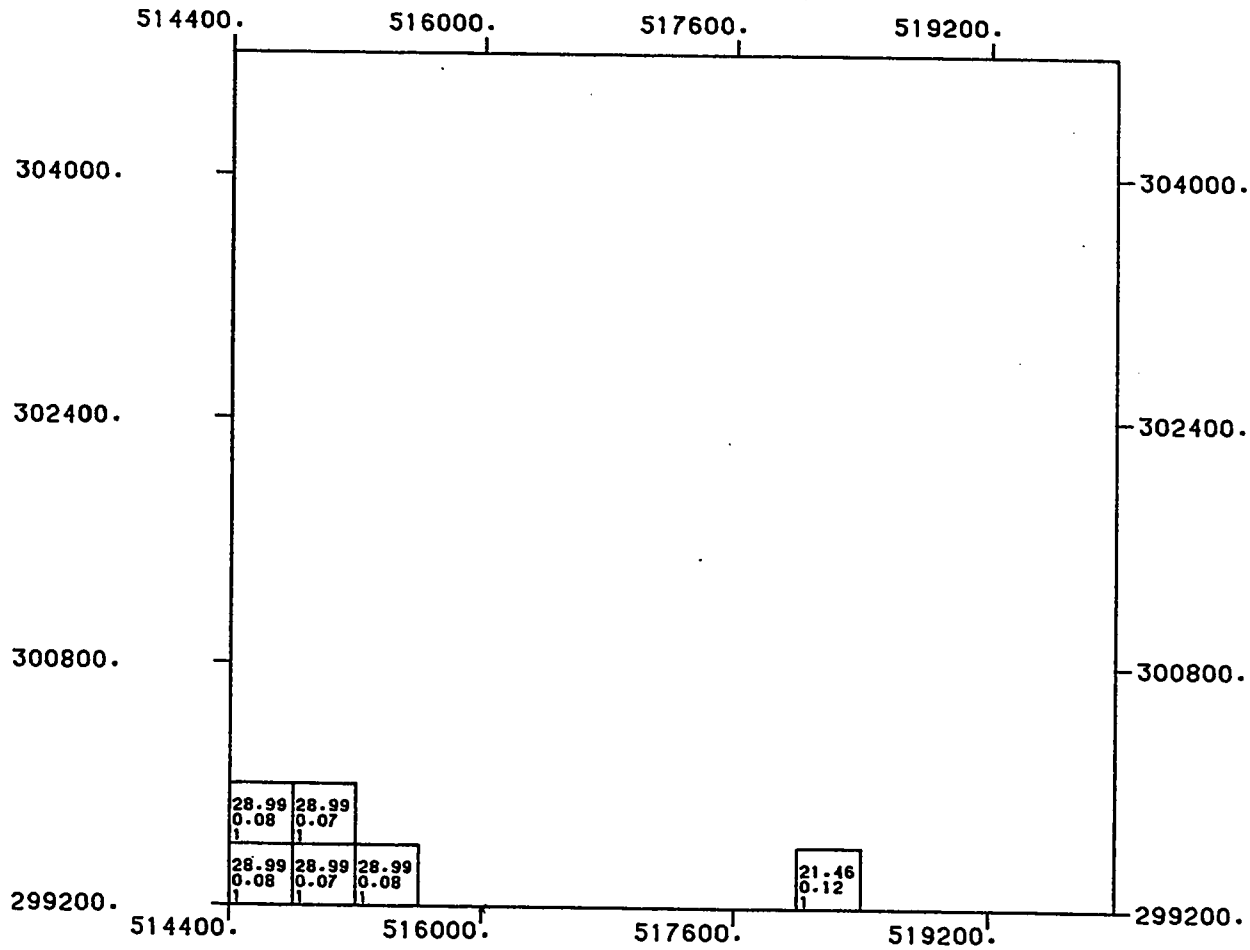


SCALE OF MAP

DATA PROCESSED AT: U P M - D P C , DHAHRAN
SOFTWARE BY : GEOSTAT SYSTEMS, MONTREAL



(D109)



ABU TARTUR PHOSPHATE DEPOSIT
RESULTS OF BLOCK KRIGING

(Z = 418.5)

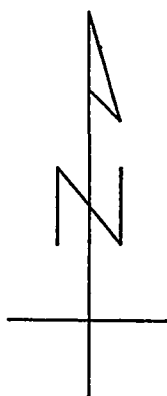
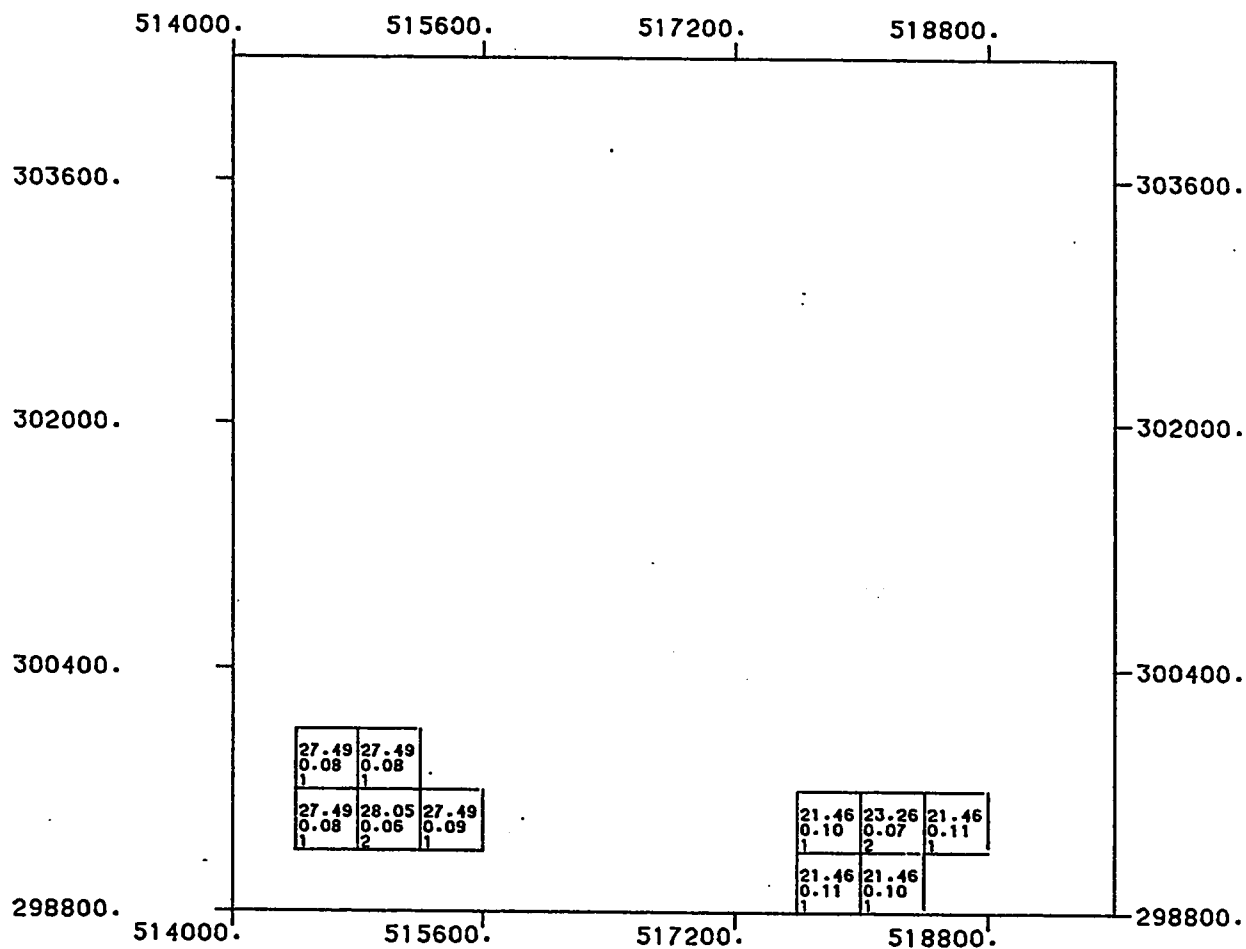
LEVEL NUMBER : 147

800.0 0.0 800.0 1600.0



SCALE OF MAP :

DATA PROCESSED AT : U P M - D P C , DHAHRAN
 SOFTWARE BY : GEOSTAT SYSTEMS, MONTREAL



ABU TARTUR PHOSPHATE DEPOSIT
RESULTS OF BLOCK KRIGING
 (Z = 419.5)

LEVEL NUMBER : 148

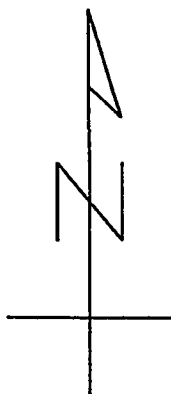
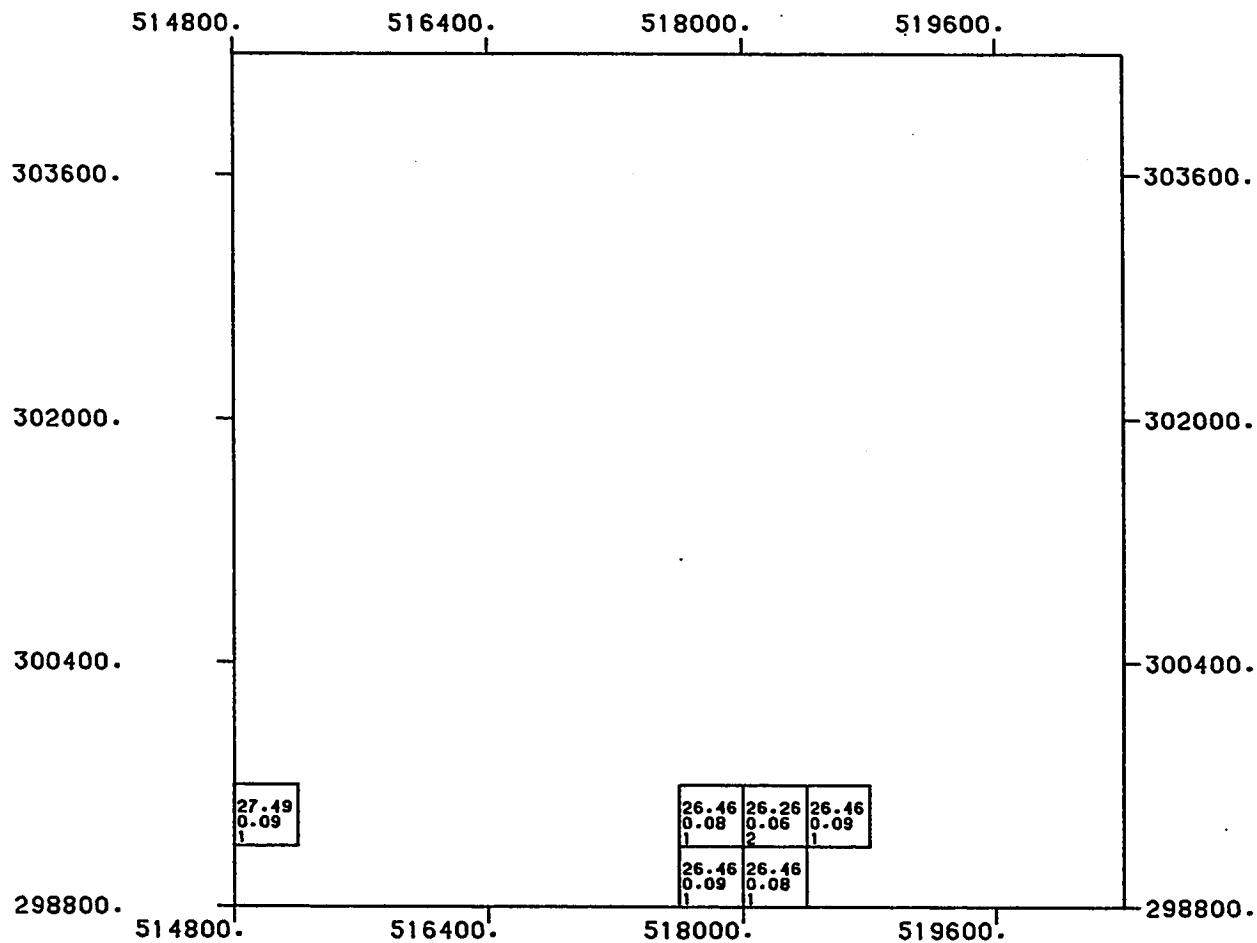
800.0 0.0 800.0 1600.0



SCALE OF MAP

DATA PROCESSED AT: U P M - D P C , DHAHRAN
 SOFTWARE BY : GEOSTAT SYSTEMS, MONTREAL

(D111)



ABU TARTUR PHOSPHATE DEPOSIT
RESULTS OF BLOCK KRIGING

(Z = 420.5)

LEVEL NUMBER : 149

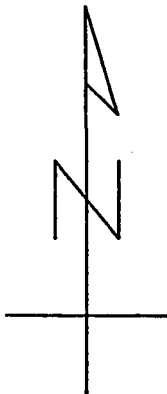
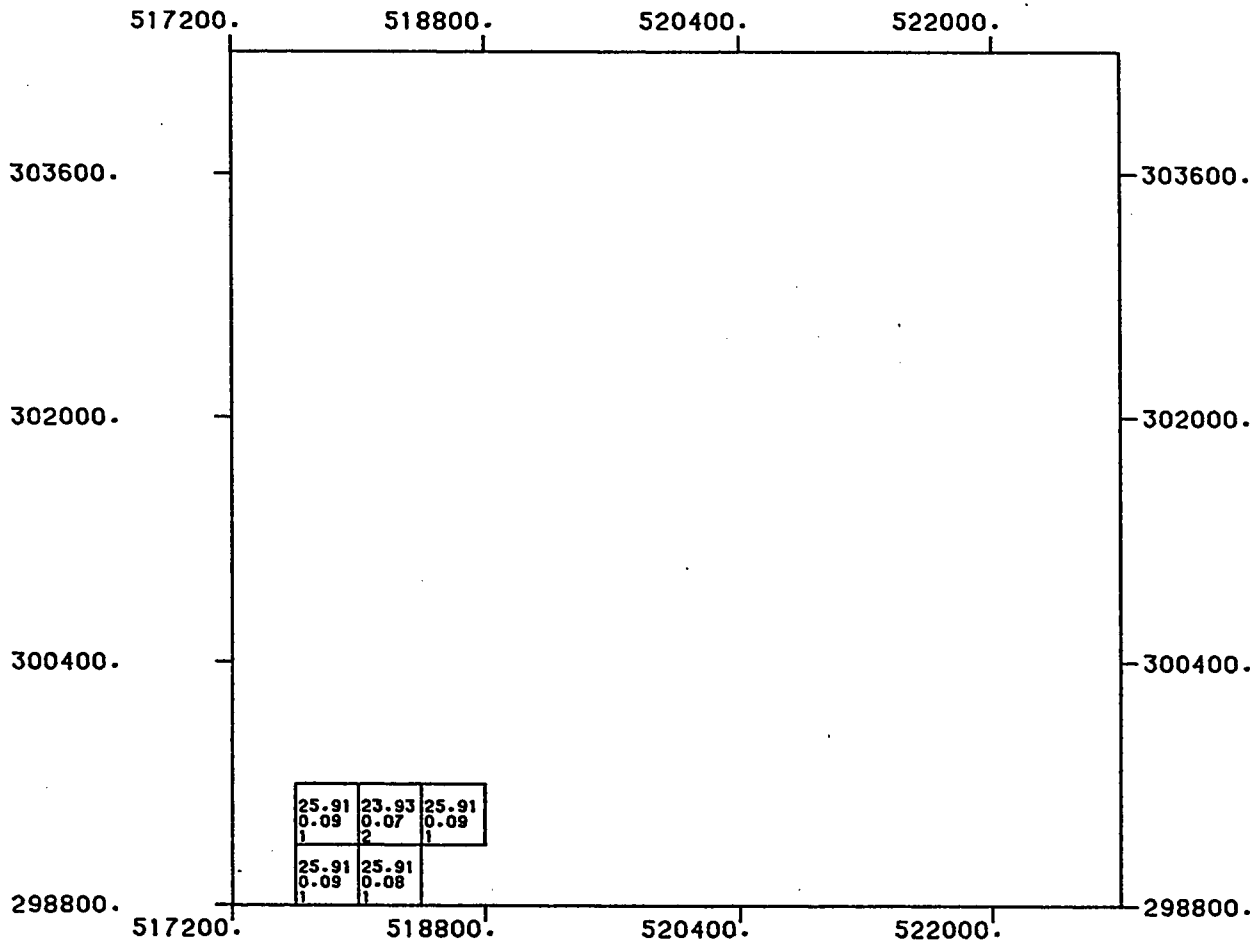
800.0 0.0 800.0 1600.0



SCALE OF MAP

DATA PROCESSED AT: U P M - D P C , DHAHRAN
SOFTWARE BY : GEOSTAT SYSTEMS, MONTREAL

(D112)



ABU TARTUR PHOSPHATE DEPOSIT
RESULTS OF BLOCK KRIGING

(Z = 421.5)

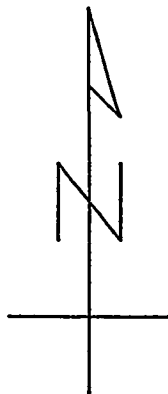
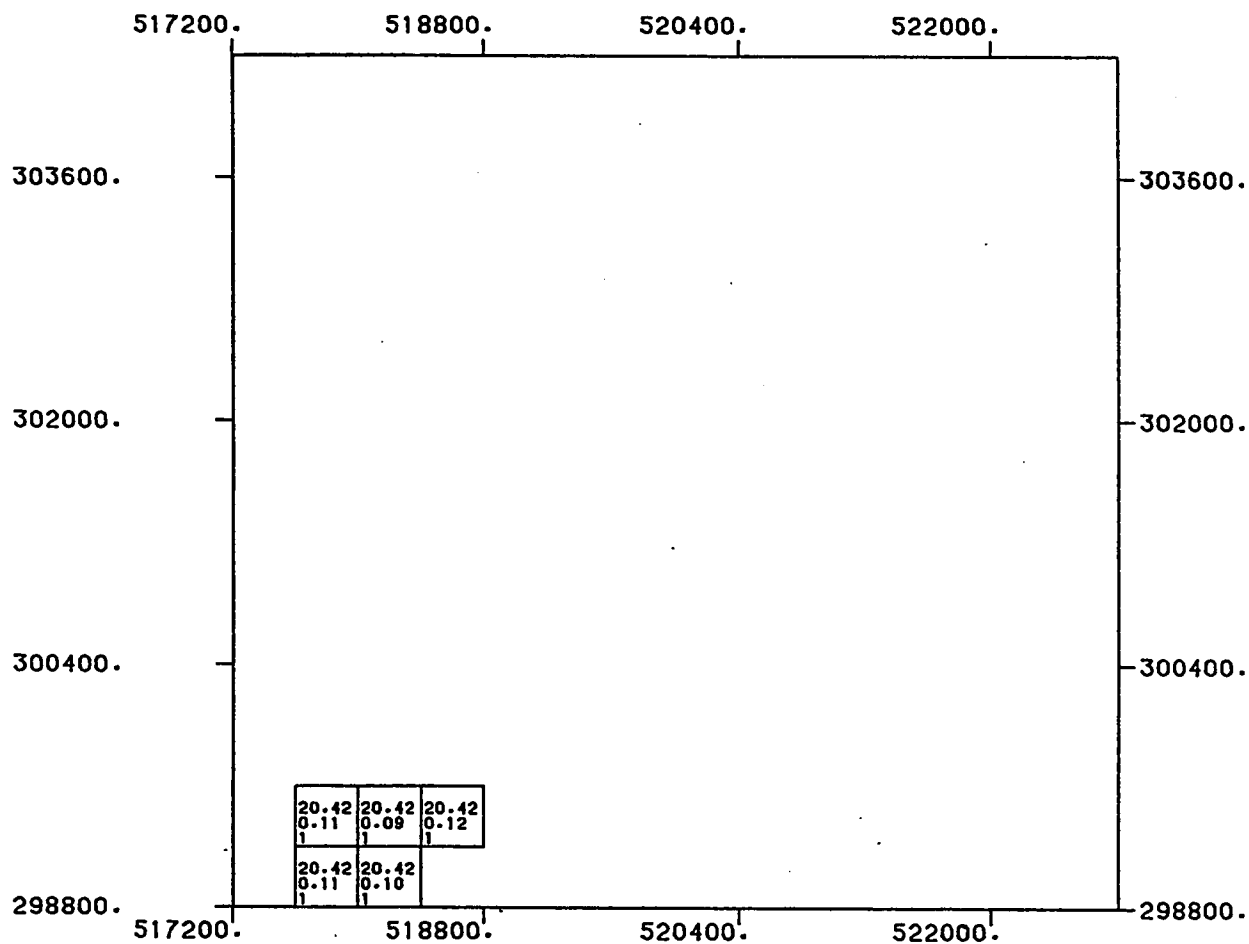
LEVEL NUMBER : 150

800.0 0.0 800.0 1600.0



SCALE OF MAP

DATA PROCESSED AT: U P M - D P C ; DHAHRAN
 SOFTWARE BY : GEOSTAT SYSTEMS, MONTREAL



ABU TARTUR PHOSPHATE DEPOSIT
RESULTS OF BLOCK KRIGING

(Z = 422.5)

LEVEL NUMBER : 151

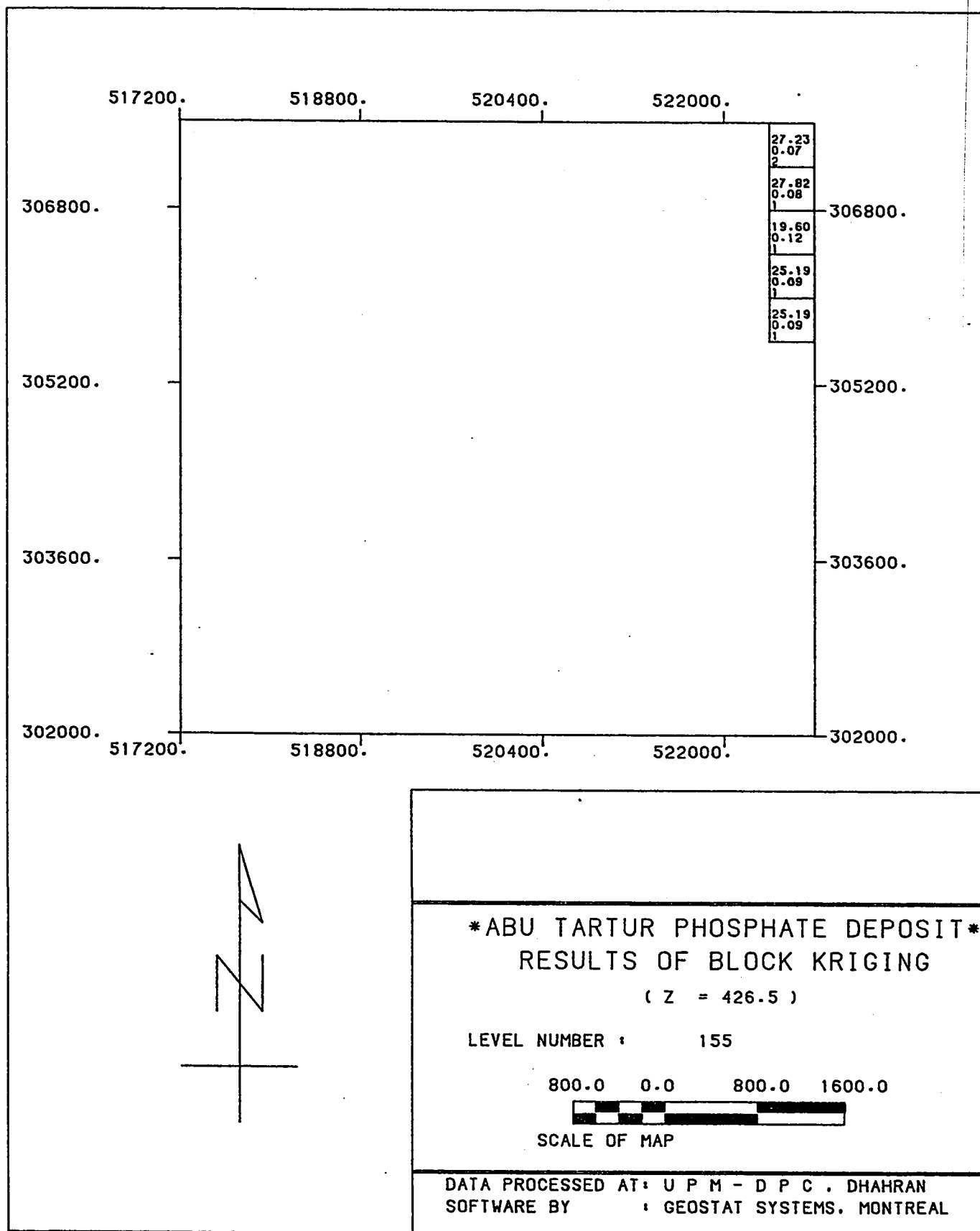
800.0 0.0 800.0 1600.0



SCALE OF MAP

DATA PROCESSED AT: U P M - D P C , DHAHRAN
SOFTWARE BY : GEOSTAT SYSTEMS, MONTREAL

(D114)



بِسْمِ اللَّهِ الرَّحْمَنِ الرَّحِيمِ

تقدير مخزون رواسب الفوسفات. بمنطقة
أبو طرطور بالصحراء الغربية بجمهورية مصر
العربية باستخدام طرق الإحصاء الإحيوي لوجي

رسالة مقدمة من:

علي أحمد عبد اللطيف

(بكالوريوس هندسة التعدين)

إلى

جامعة الملك فهد للبترول والمعادن
للحصول على درجة الماجستير في علوم الأرض

يناير ١٩٨٧ م

PLEASE NOTE:

Oversize maps and charts are filmed in sections in the following manner:

LEFT TO RIGHT, TOP TO BOTTOM, WITH SMALL OVERLAPS

The following map or chart has been refilmed in its entirety at the end of this dissertation (not available on microfiche). A xerographic reproduction has been provided for paper copies and is inserted into the inside of the back cover.

Black and white photographic prints (17" x 23") are available for an additional charge.

University Microfilms International

310999.9	509999.9	510999.9	511999.9	5
309999.9				
308999.9				
307999.9				
306999.9				

512999.9

513999.9

514999.9

515999.9

X111,

515999.9

516999.9

517999.9

518999.9

N1-

N111+

N1-9+

NG-9+

NG11+

NG-7+

T-20+

S-18+

S-22+

R-20+

Q-

T-24+
NE-9+

D-8 +

NE-7+

T-28+

S-26+

R-24+

Q-22+

P-2

8999.9	519999.9	520999.9	521999.9	522
--------	----------	----------	----------	-----

N1-7+

N1-5+

N1-3

J-10+

NC-7+

NC-5+

NC-3+

S-18+

D-9 +

R-20+

Q-18+

NE-7+

NE-5+

NE-3+

Q-22+

P-20+

Q-18+

N-18+

522999.9

523999.9

524999.9

525999.9

-310'

N1-3₊

N1-1₊

TN33₊

-309'

-308'

NG-3₊

-307'

D-9₊

L-4₊

K-6₊

NE-3₊

-306'

TN-6₊

J-8₊

999.9

523999.9

524999.9

525999.9

-310999.9

N1-1+

-309999.9

TN33+

-308999.9

-307999.9

L-4 +

-306999.9

TN-6+

K-6 +

J-8 +

306999.9

305999.9

304999.9

303999.9

302999.9

301999.9

A-1 +

A-17+

SB16+

SC17+

x

T

NC13+

T-40+

S-

NB15+

NB14+

NB13+

NB12+

R-

T-48+

S-46+

R-44+

Q-

A-15+

A-14+

A-13+

A-12+

T-52+

S-50+

R-48+

Q-46+

P-4

SB16+

SB15+

SB14+

R-52+

SB13+

SB12+

P-48+

Q-46

SC15+

SC14+

SC13+

Q-50+

N-48

SC12+

N-50+

N-52+

M-50+

D-8 + NE-7+
T-28+ S-26+ R-24+ Q-22+ P-
T-32+ S-30+ R-28+ Q-26+ P-24+ Q-2
T-36+ S-34+ R-32+ P-28+ Q-26+ NC-8+ N-26+
NC11+ Q-30+ NC-9+ N-28+ M-21
T-40+ S-38+ R-36+ Q-34+ P-32+ Q-30+ N-30+ M-28+
NB12+ NB11+ NB10+ NB-9+ N-32+ NB-8+ L-2
R-40+ Q-36+ N-34+ M-32+ L-30+
D-6 + Q-38+ N-36+ M-34+ A-8 + K-31
A-12+ A-11+ A-10+ A-9 + L-34+ K-32+
N-38+ M-38+ L-36+ K-34+ D-3 + J-31
Q-42+ P-40+ N-40+ N-42+ M-40+ K-36+ J-34+
SB12+ SB11+ SB10+ SB-9+ SB-8+ I-31
Q-46+ N-44+ L-40+ K-38+ J-36+ I-36+
N-46+ D-5 + M-44+ K-42+ K-40+ J-40+ SC-9+ G-36+
N-48+ L-44+ SC10+ J-42+ I-40+ SC-8+ G-38+ E-36+
SC12+ N-50+ M-48+ X-6 + L-46+ K-44+ D-4 + J-40+ I-40+ E-38+
X-5 +

NE-7+ NE-5+ NE-3+

Q-22+ P-20+ O-18+

X N-18+

P-24+ N-20+ M-18+

O-22+

N-22+ M-20+ L-18+ K-16+ J-14+

Q-26+ N-24+ M-22+ L-20+ J-16+ I-14+ NC-

-8+ NC-4+

N-26+ NC-7+ L-22+ K-20+ NC5A+ J-18+

N-28+ M-26+ L-24+ K-22+ J-20+ NC-5+ O-16+

M-28+ L-26+ K-24+ J-23+ J-22+ I-20+ O-18+

NB-8+ NB-7+ K-26+ D-1+ J-25+ NB-6+ I-23+ NB-5+ G-20+ E-18+

L-28+ PM-3+

L-30+ K-28+ J-26+ I-25+ I-24+ H-23+ G-22+ E-20+ C-18+

K-30+ J-28+ I-27+ I-26+ H-25+ A-5+ F-23+ E-22+ A-4+ C-20+

A-8+ A-7+ A-6+ D-2+ F-24+ E-23+ F-25A+ F-25+ E-24+ C-22+ B-HZ+

K-32+ J-30+ I-29+ I-28+ H-27+ G-26+ E-25+ PM-1+

G-27+

K-34+ D-3+ J-32+ I-30+ H-29+ G-28+ F-27+ E-26+ C-24+ BH28+

J-34+ H-31+ G-30+ F-29+ E-28+ C-26+

SB-8+ SB-7+ SB-6+ SB-5+

I-34+ H-33+ G-32+ E-30+ SB-4+

I-36+ O-34+ E-32+ TN-4+

G-36+ SC-7+ E-34+

G-38+ E-36+

E-38+

TN27+

TN-6+

-306

J-8 +

X

I-10+

TN31+

-305

I-14+

NC-3+

O-16+

E-14+

-304

NB-3+

TN-5+

E-18+

C-18+

A-3 +

-303

C-20+

BH28+ TN28+

TN29+

-302

SB-4+

TN-4+

-301

TN-6,

-306999.9

-8 +

10,

TN31,

-305999.9

14,

-304999.9

3,

TN-5,

-303999.9

28,

TN29,

-302999.9

-301999.9

301999.9

300999.9

299999.9

298999.9

297999.9

509999.9

510999.9

511999.9

SC12₊

N-50₊

N-52₊

M-50₊

x

SD14₊

SD13₊

SD12₊ X-12₊ X-11₊

L-52₊

SE15₊

SE13₊

SE12₊

D-12₊

SF12₊

K-62₊

L-66₊

L-70₊

.9

512999.9

513999.9

514999.9

515999.9

SC12+ SC11+ SC10+ SC-8+ G-38+E-3
 N-50+ M-48+ X-6 + L-46+ K-44+ D-4 + J-42+ I-40+
 N-52+ M-50+ X-5 + L-48+ K-46+ J-44+ I-42+ G-40+ E-3
 X-4 +
 SD12+ X-12+ X-11+ X-10+ SD11+ X-9 + X-8 K-48+ X-7 + SD10+ SD-9+ G-42+ SD-8+ E-40+
 L-52+ X-3 + K-50+ J-48+ I-6 + G-44+ E-42+
 X-2 + E-43+
 K-52+ X-1 + J-50+ I-48+ G-46+ E-44+
 SE12+ SE11+ J-52+ I-50+ SE10+ G-48+ SE-9+ E-46+
 I-52+ G-50+ E-48+
 I-54+ G-52+ E-50+ TN-3+
 SF12+ SF11+ G-54+ SF10+ TN-2+
 G-56+ TN-1+
 TN23+
 TN22+

515999.9

516999.9

517999.9

518999.9

G-38, E-36,

TN27,

E-38,

G-40,

x

D-8,

E-40,

TN26,

2,

TN25,

TN-3,

TN-2,

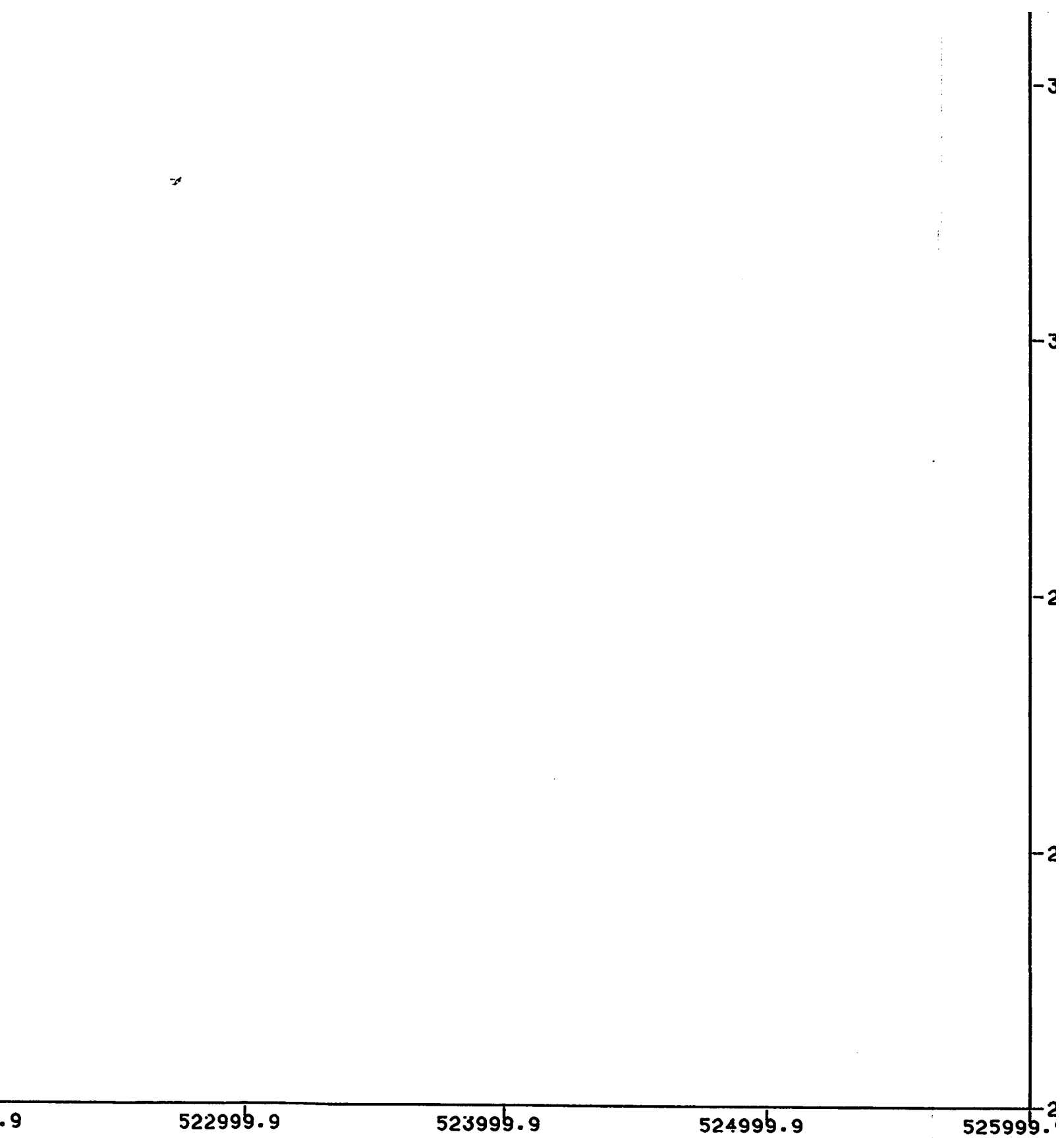
518999.9

519999.9

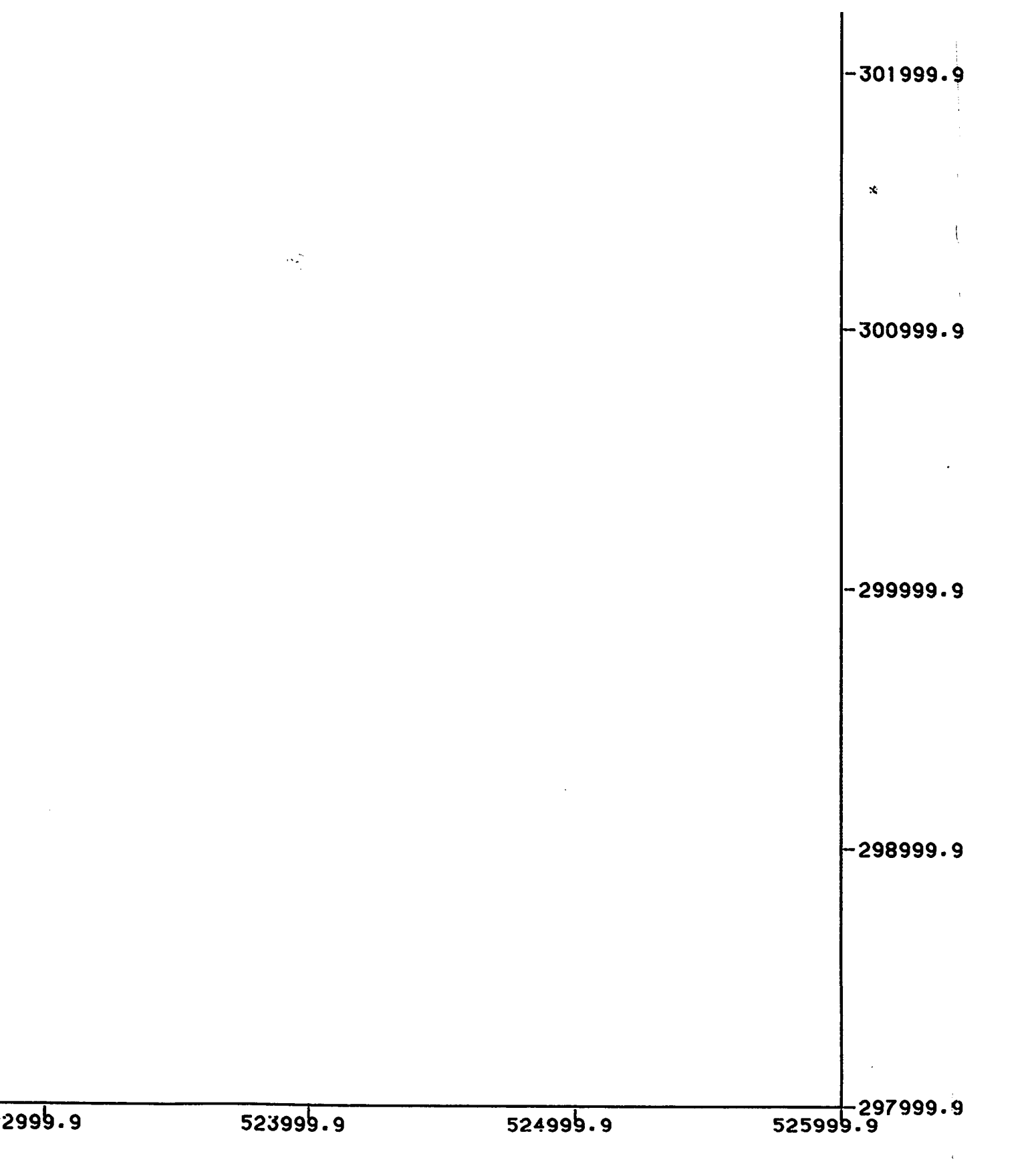
520999.9

521999.9

5



*** ABU TARTUR PHOSPHATE DEPC
PLATE (1) MAP OF DRILL HOLE COLLAI



*** ABU TARTUR PHOSPHATE DEPOSIT ***

PLATE (1) MAP OF DRILL HOLE COLLARS

299999.9

298999.9

297999.9

509999.9

510999.9

511999.9

5

D-12,

SF12+

K-62+

L-66+

L-70+

9.9

512999.9

513999.9

514999.9

51 5996

I-52₊

G-50₊

E-48₊

I-54₊

G-52₊

E-50₊

TN-3₊

TN-2₊

SF12₊

SF11₊

G-54₊

SF10₊

TN-1₊

G-56₊

TN23₊

TN22₊

515999.9

516999.9

517999.9

518999.9

TN25.

TN-3.

TN-2.

518999.9

519999.9

520999.9

521999.9

x

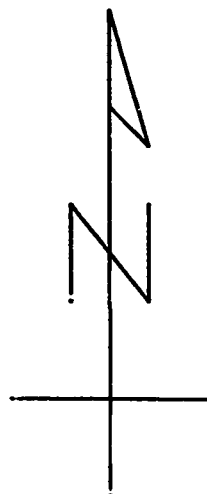
99.9

522999.9


523999.9

524999.9

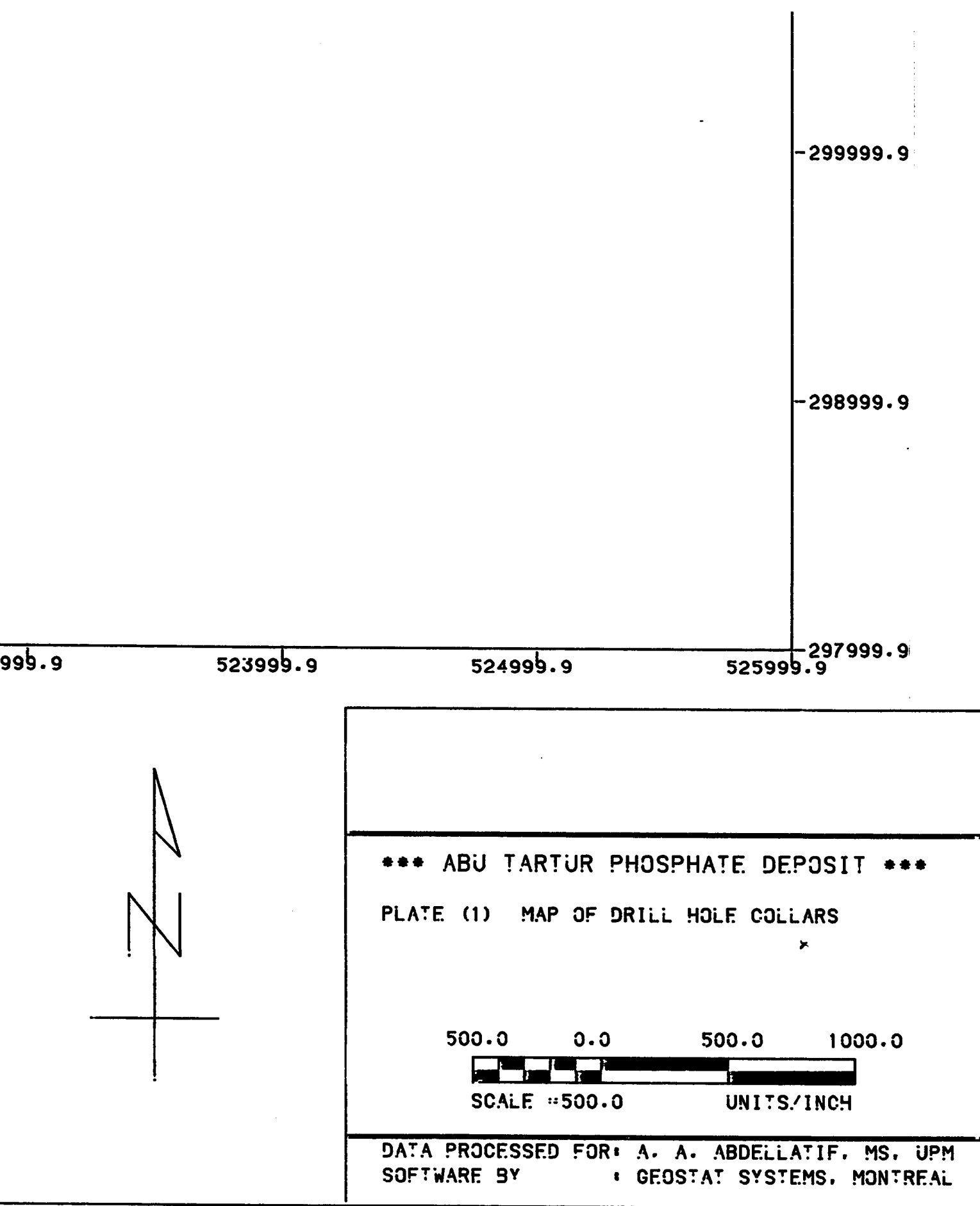
525999.9



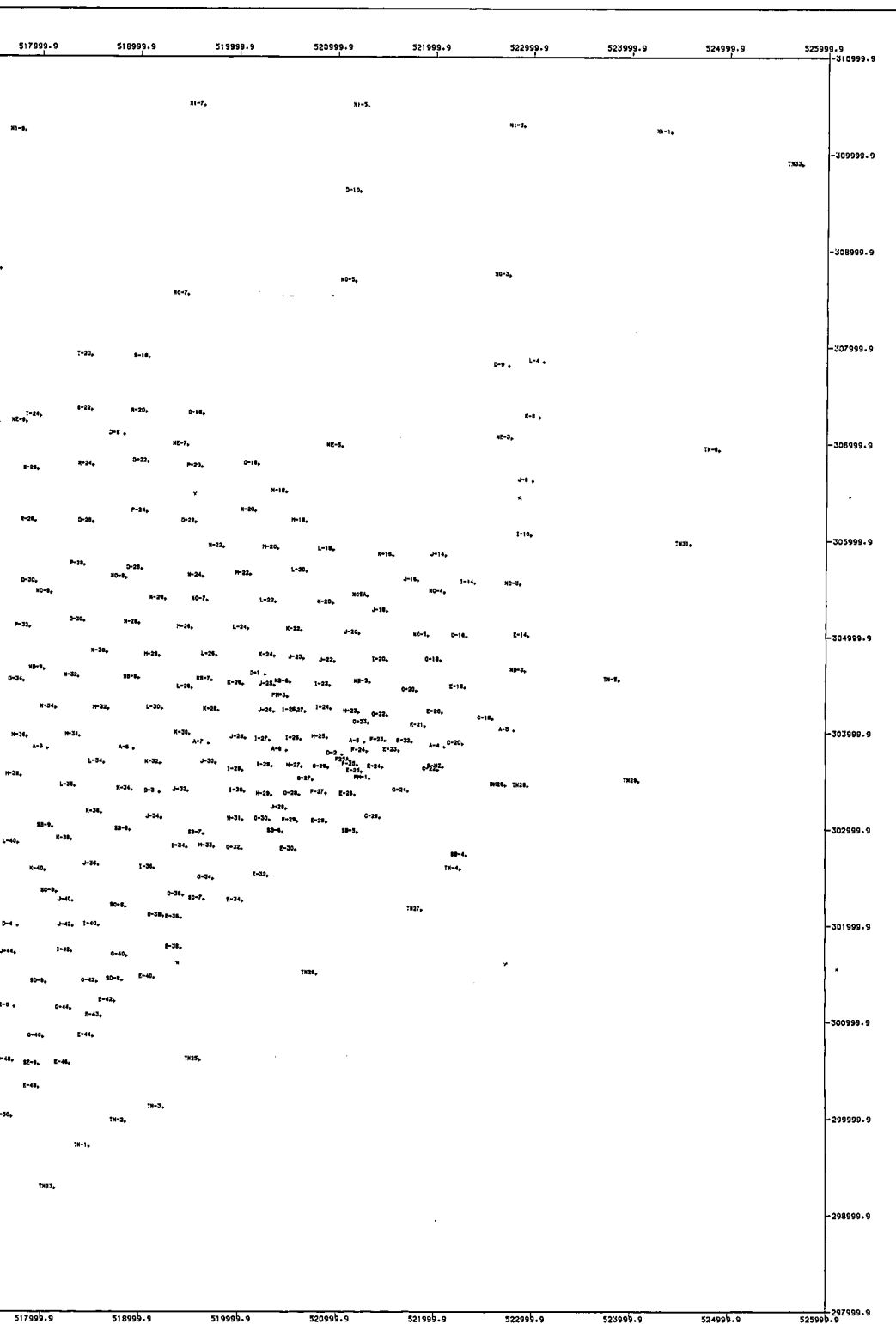
*** ABU TARTUR PHOSPHATE DE
PLATE (1) MAP OF DRILL HOLE COLI

500.0 0.0 500.0

SCALE =500.0 UNITS.

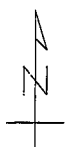
DATA PROCESSED FOR: A. A. ABDELL.
SOFTWARE BY : GEOSTAT SYSTI



[illegible]



ABDUL-LATIF ALIAHMED
1355693 c 1994



*** ABU TARTUR PHOSPHATE DEPOSIT ***
PLATE (1) MAP OF DRILL HOLE COLLARS

500.0 0.0 500.0 1000.0
SCALE 1:500.0 UNITS/FINCH

DATA PROCESSED FOR: A. A. ABDELLATIF, MS. UPM
SOFTWARE BY: GEDSTAT SYSTEMS, MONTREAL